

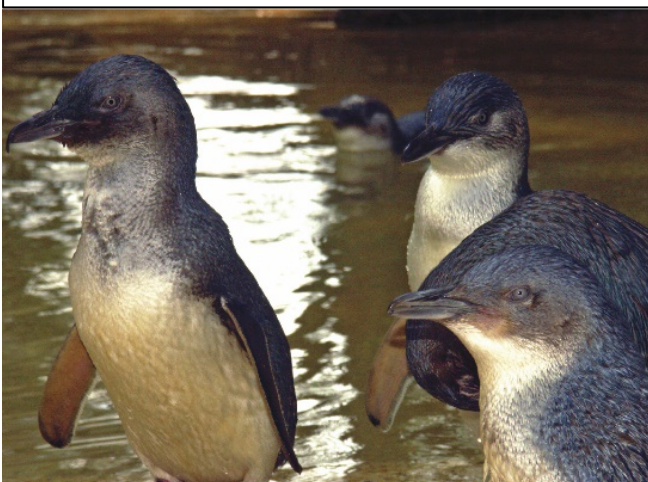


**Asian Biophysics Association Symposium**  
in conjunction with the  
**Australian Society for Biophysics Meeting**

**Melbourne Dec 2-6, 2018**



# Abstract Book



**DELEGATE HANDOUT: Asian Biophysics Association Symposium *in conjunction with the* Australian Society for Biophysics**

Dec 2 - 6, 2018. RMIT University, Melbourne, Australia

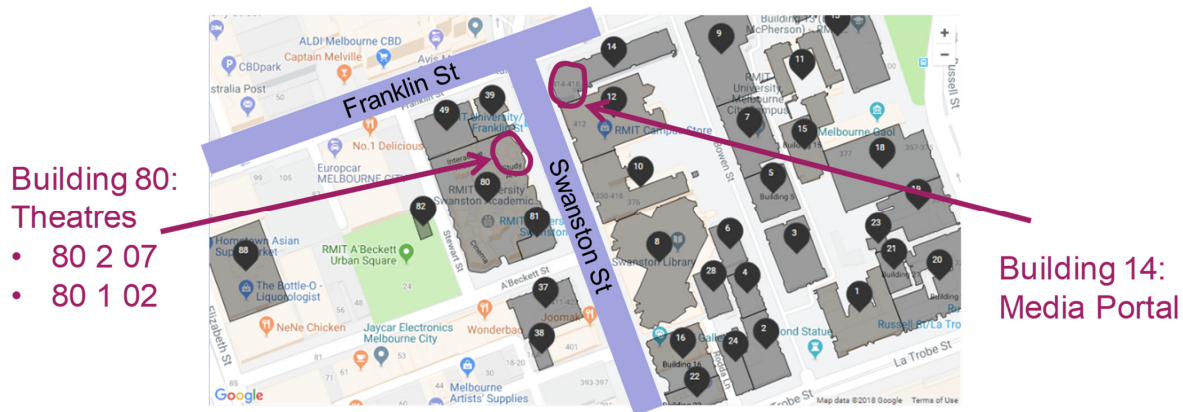


**1. Orientation**

**Oral sessions.** Oral sessions will be held in Building 80. Stream 1 will be held in theatre 80 2 07 and stream 2 in theatre 80 1 02. The joint sessions will run in theatre 80 2 07.

**Registration, welcome function, all meal breaks and posters.** Will be held in the Media Portal (Building 14) which is directly across the road from Building 80.

**Getting around inner Melbourne.** The trams within the central business district are free and require no ticket. This includes getting to the conference dinner. Note that travel outside the central business district requires buying a prepaid Myki ticket (<https://www.ptv.vic.gov.au/tickets/myki>).



**2. Registration**

The registration desk in the Media Portal (Building 14) will be staffed by volunteers from Sunday 4 pm to 7 pm, on Monday 8 am to 8:45 am, and at the morning tea breaks from Monday to Thursday. Please be sure to wear your name tag at all times during the conference including the dinner.

**3. Internet**

Attendees can use the Wi-Fi "RMIT Guest" network. To access it, click on "Event" and enter the password "637562".

**4. Speakers**

We have a PC & Mac onsite for talks and associated pointers and microphones. You can also connect your computer and if so, please ensure you have the appropriate display adapter with you. Please upload your talk at least 30 min prior to the session. We have volunteers (Evelyn Deplazes, Toby Allen and Kate Poole) to help with audiovisual support.

**5. Chairs**

Please be at your session 30 min prior to the start of the session to meet the speakers and help get familiar with the audiovisual setup. We ask chairs to be diligent in prompting speakers to stick to allocated times and we ask that speaker order is not changed (since people may switch streams between talks). If a speaker does not turn up, we ask that their time slot be maintained as a free break.

**6. Posters**

We have two poster sessions. Posters with Abstract ID 1-99 will be in Session A on Monday. Posters with Abstract ID 100-203 will be in Session B on Wednesday. Please keep your poster up for only the day you are presenting (i.e. put the poster up in the morning and take down in the afternoon). Velcro pads or pins will be provided to attach your poster to the board. Students will have a "red dot" for judging and please be at your poster for judging. Poster prizes will be announced in the closing session.

**7. Morning tea, lunch and afternoon tea**

Will be held in the Media Portal (Building 14). Please only take the special meals (e.g. vegetarian, halal, allergy) if you pre-ordered this in registration. If you forgot to pre-order a special meal, you will need to purchase your meal at a local restaurant (there are many nearby).

### 8. Conference dinner

The conference dinner will be held at the Melbourne Sealife Aquarium on Wednesday at 7 pm. We will have guides to help you get there. To take advantage of this, please meet in front of the Media Portal (Building 14) at 6:30 pm. The directions are as follows. You can walk there (~30 min), take the tram (~20 min) or take an Uber or taxi.

### 9. Australian Society for Biophysics Annual General Meeting

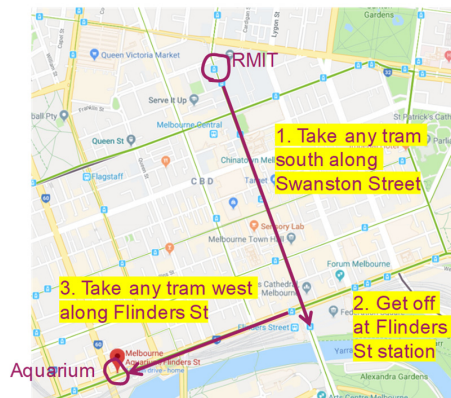
The meeting will occur immediately after the McAuley Hope Lecture at 12:30 pm Tuesday in theatre 80 2 07. All ASB members are welcome and encouraged to attend.

### 10. Asian Biophysics Association (ABA) Steering Committee meeting

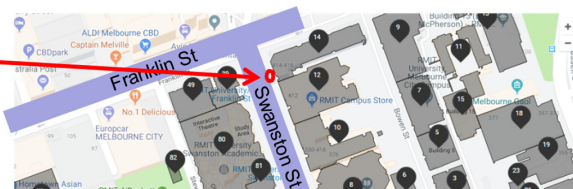
The ABA Steering Committee meeting will be held on Monday December 3 and is open to the steering committee and those invited. The meeting will take place in 2 sessions. The formal part of the meeting will commence at 6:30 pm in room 080.03.010 (Building 80 on level 3), immediately after the scientific sessions conclude that evening. At 7:30 pm, the dinner will be held at BBQ Brothers 10, 589 Elizabeth St, Melbourne VIC 3000. [www.bbqbrothers10.com](http://www.bbqbrothers10.com)

### 11. Trip to Healesville Sanctuary

You need to have pre-purchased a ticket to go on this tour. Tickets can be bought via our website up until Monday 3<sup>rd</sup> Dec 9 am. The tour will leave the conference venue at 1 pm sharp on Tuesday. Please meet at the location on the map. Note that you cannot eat food on the bus, so please eat your lunch in the prior scientific session. Meals will be available early on Tuesday for delegates on the tour. The bus trip home will depart Healesville Sanctuary at 5.15 pm and arrive back in Melbourne between 6.30 and 7.15 pm (depending on traffic). The tour is run by 'Wild Wombat Winery tours'.



Meet here in front of the Media Portal (Building 14)

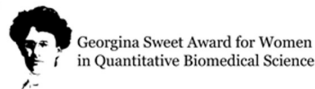


### 12. Code of Conduct

Our meeting follows the "London Code of Conduct", which is expanded upon on our website.

<https://events01.synchrotron.org.au/event/55/page/84-code-of-conduct> In essence, the organisers are committed to making this meeting productive and enjoyable for everyone, regardless of gender, sexual orientation, disability, physical appearance, body size, race, nationality or religion. We will not tolerate harassment of participants in any form. Attendees violating these rules may be asked to leave the event at the sole discretion of the organisers without a refund of any charge. Any participant who wishes to report a violation of this policy is asked to speak, in confidence, to Danny Hatters or Renae Ryan (Organising Committee co-chairs).

13. A special thankyou to our sponsors. Please visit their displays at our meeting and support their businesses.



Sunday 2/12/18	
Stream 1	Stream 2
16.00-19.00	Registration
17.00-19.00	Welcome reception

**Session themes and chairs**

Monday 3/12/18		Tuesday 4/12/18		Wednesday 5/12/18		Thursday 6/12/18	
Stream 1		Stream 1		Stream 1		Stream 1	
8.45-9.00	Welcome and introduction	8.30-9.00	Nanobiophysics	9.00-9.30	Superres microscopy	8.45-9.45	Plenary 3 : Chair Marc Kvaisanskul
9.00-10.00	Plenary 1 - Chair: Margaret Sunde	9.00-9.30	Chair: Boris Martinac	9.30-10.00	Chair: Till Boecking	9.45-10.00	Neuroscience
10.00-10.30	Morning Tea	9.30-10.00		10.00-10.15		10.15-10.45	Chair: Tiemin Liu
10.30-11.00	Bioinformatics	10.00-10.30	Morning Tea	10.15-10.45	Morning Tea	10.45-11.15	Morning Tea
11.00-11.30	Chair: Megan O'Mara	10.30-11.00	Membrane Biophysics	10.45-11.15	Superres microscopy	11.15-11.45	Neuroscience
11.30-12.00	Chair: David Stroud	11.00-11.30	Chair: Xiyun Yan	11.15-11.45	Chair: Tao Xu	11.45-12.15	Chair: Danny Hatters
12.00-13.30	Lunch and Posters	11.30-11.45		11.45-12.00	Co-Chair: Donna Whelan	12.15-12.30	Chair: Liz Hinde
13.30-14.00	Omic	11.45-12.30	Macauly-Hope Lecture	12.00-12.45	Lunch and Posters	12.30-13.30	Lunch
14.00-14.30	Chair: David Stroud	12.30-18.00	Chair: Adelle Coster	13.45-14.15	Structural Biology		
14.30-14.45		ASB AGM		14.15-14.45	Chair:Ray Norton		
14.45-15.15	Afternoon Tea	12.30-13.30		14.45-15.15	Shannon Mostyn		
15.15-15.45	Biophysics and Medicine			15.15-15.45	Afternoon Tea		
15.45-16.15	Chair: Matt Baker			15.45-16.15	Neuroscience		
16.15-16.30				16.15-16.45	Chair: Takayuki Nishizaka		
16.30-16.45	Coffee break			16.45-17.00	EMBO Plenary - Chair: Margaret Sunde		
16.45-17.15	Biophysics and Medicine			17.00-18.00			
17.15-17.45	Chair: Jamie Vandenberg			19.00-21.00	Conference dinner		
17.45-18.30							

**Session speakers**

Monday 3/12/18		Tuesday 4/12/18		Wednesday 5/12/18		Thursday 6/12/18	
Stream 1		Stream 1		Stream 1		Stream 1	
8.45-9.00	Welcome and introduction	8.30-9.00	Masahiro Sokabe	9.00-9.30	Yujie Sun	8.45-9.45	Plenary 3 - Jackie Ying
9.00-10.00	Plenary 1 - Zihao Rao	9.00-9.30	Kate Poole	9.30-10.00	Liz Hinde	9.45-10.00	Qianyi Wu
10.00-10.30	Morning Tea	9.30-9.45	Joyce Chiu	10.00-10.15	Jieqiong Lou	10.15-10.45	Ruby Chen
10.30-11.00	Carmay Lim	9.45-10.00	Artem Efremov	10.15-10.45	Morning Tea	10.45-11.15	Morning Tea
11.00-11.30	Satoru Itoh	10.00-10.30	Morning Tea	10.45-11.15	Olga Shimoni	11.15-11.45	Pingbo Huang
	Amanda Buyan				Niall Geoghegan	11.45-12.15	Rob Vandenberg
11.30-12.00	Shoba Ranganathan	10.30-11.00	Sara Baratchi		Max Baker	12.15-12.30	Danish Idrees
	Lunch and Posters		Takayuki Nishizaka		Donna Whelan	12.30-13.30	Lunch
12.00-13.30	Sihyun Ham	11.00-11.30	Kumiko Hayashi		Lunch and Posters		
	Lunch and Posters		Amani Alghalayini				
14.00-14.30	David Poger	11.30-11.45	Macauly-Hope Lecture				
	Nick Scott	11.45-12.30	Lunch (or Zoo Outing)				
14.30-14.45	Wataru Nemoto	12.30-13.30	ASB AGM				
14.45-15.15	Afternoon Tea						
15.15-15.45	Jia-Wei Wu						
15.45-16.15	Rob Salomon						
16.15-16.30	Mark Hulett						
16.30-16.45	Ewa Goldys						
	Hsash Okumura						
	Kenshiro Maruyama						
	Coffee break						
16.45-17.15	Michelle Dunstone						
	Hye Ran Koh						
17.15-17.45	Quan Hao						
	Lining Arnold Ju						
17.45-18.15	Midori Murakami						
	Zhihong Zhang						
18.15-18.30	Joseph Font						
	Sophie Hertel						
	Ashley M Rozario						

Speaker	Title	Session	Time
Zihe Rao	The atomic resolution structure of HSV capsids <b>*** SPONSORED BY Australian Research Council Center of Excellence in Advanced Molecular Imaging</b>	Mon morn. Plenary 1	9.00-10.00
Carmay Lim	Principles Governing Biological Processes	Mon morn. Bioinform.	10.30-11.00
Satoru Itoh	Oligomer formation of Abeta(29-42) by Coulomb replica-permutation molecular dynamics simulations	Mon morn. Bioinform.	11.00-11.15
Amanda Buyan	Understanding Piezo1's Relationship with Lipids	Mon morn. Bioinform. (YBA)	11.15-11.30
Shoba Ranganathan	Tracking missing human olfactory receptors	Mon morn. Bioinform.	11.30-12.00
Sihyun Ham	When computer meets Bio?	Mon morn. Bioinform.	13.30-14.00
David Poger	Tackling lipid diversity in membranes: the effect on membrane and protein functions	Mon morn. Bioinform.	14.00-14.30
Wataru Nemoto	Prediction of cancer-associated hotspot mutations that affect GPCR oligomerization	Mon morn. Bioinform.	14.30-14.45
Meng-Qiu Dong	Improving Mass-Spectrometry Analysis of Protein Structures with Arginine-Specific Chemical Cross-linkers.	Mon morn. Omics	10.30-11.00
David James	Precision Medicine and Metabolic Disease	Mon morn. Omics	11.00-11.30
Kristin Brown	Metabolic Reprogramming in Cancer	Mon morn. Omics	11.30-12.00
Traude Beilharz	Bringing the genome to life with transcriptome dynamics	Mon morn. Omics	13.30-14.00
Nicholas Scott	Insights on the drivers of tissue specific properties from a multi tissue interactome	Mon morn. Omics	14.00-14.30
Dezerae Cox	Quantifying Protein Foldedness at the Proteome-Wide Scale	Mon morn. Omics	14.30-14.45
Jia-Wei Wu	Structural and biochemical studies of lipid transfer protein ORPs	Mon aftern. Struct. Biol.	15.15-15.45
Mark Hulett	Structural lessons from defensins for membrane disruption by innate defense peptides.	Mon aftern. Struct. Biol.	15.45-16.15
Hisashi Okumura	Difference in structural and fluctuation difference between two ends of Aβ amyloid fibril revealed by molecular dynamics simulations	Mon aftern. Struct. Biol.	16.15-16.30
Michelle Dunstone	Protein conformation of C9 controls the final membrane complex assembly	Mon aftern. Struct. Biol.	16.45-17.15
Quan Hao	Structural studies of new post-translational modification erasers/readers	Mon aftern. Struct. Biol.	17.15-17.45
Midori Murakami	Structure of the photo-activated acid-meta state of squid rhodopsin	Mon aftern. Struct. Biol.	17.45-18.00
Josep Font	Visualising the Cl <sup>-</sup> permeation pathway of glutamate transporters	Mon aftern. Struct. Biol.	18.00-18.15
Sophie Hertel	Artificial assembly of the bacterial flagella motor protein FLIG on DNA scaffolds	Mon aftern. Struct. Biol.	18.15-18.30
Rob Salomon	Hitting the dimensionality limit in single cell characterisation using fluorescence and Genomic Cytometry	Mon aftern. Biophys. & Med.	15.15-15.45
Ewa M. Goldys	Light on a nanoscale for probing and interacting with biological systems	Mon aftern. Biophys. & Med.	15.45-16.15
Kenshiro Maruyama	Migration of Endoderm and Mesoderm Derived from Human Induced Pluripotent Stem Cells during Human Gastrulation Stage	Mon aftern. Biophys. & Med.	15.15-15.30
Hye Ran Koh	Investigation of RNA interference by single mRNA imaging at the single-cell level.	Mon aftern. Biophys. & Med.	16.45-17.15
Lining Arnold Ju	Compression Force Sensing Regulates Integrin αIIbβ3 Biomechanical Adhesive Function on Diabetic Platelets	Mon aftern. Biophys. & Med. (YBA)	17.15-17.30
Satoru Kidoaki	Modulation of APC expression in mesenchymal stem cell during nomadic culture on heterogeneous field of elasticity	Mon aftern. Biophys. & Med.	17.30-17.45
Zhihong Zhang	In Vivo Immuno-Optical Imaging the Behaviour and Function of Immunocytes in the Complex Microenvironment	Mon aftern. Biophys. & Med.	17.45-18.15
Ashley M Rozario	Subdiffraction Imaging to Characterize Live-Cell Dynamics of Microtubule-Affecting Anticancer Compounds	Mon aftern. Biophys. & Med.	18.15-18.30
Masahiro Sokabe	How can cells detect substrate rigidity?	Tues morn. Nanobiophys.	8.30-9.00
Kate Poole	Mechanical activation of ion channels at the cell-substrate interface	Tues morn. Nanobiophys.	9.00-9.30
Joyce Chiu	Mechano-redox control of integrin de-adhesion	Tues morn. Nanobiophys.	9.30-9.45
Artem Efremov	Force-dependent Ca <sup>2+</sup> signalling in cell filopodia	Tues morn. Nanobiophys.	9.45-10.00
Sara Baratchi	Towards Understanding Mechanotransduction of Blood Flow	Tues morn. Nanobiophys.	10.30-11.00
Takayuki Nishizaka	Insights into the mechanism of archaeal motor rotation from observation of unexpectedly high torque	Tues morn. Nanobiophys.	11.00-11.30
Kumiko Hayashi	Abstract Investigation of multiple-dynein transport of melanosomes by non-invasive force measurement using the fluctuation theorem	Tues morn. Nanobiophys.	11.30-11.45
Masahito Yamazaki	Single GUV studies on mode of action of antimicrobial peptides and cell-penetrating peptides	Tues morn. Memb. Biophys.	8.30-9.00
Diba Sheipouri	Control of glycine receptor activation by glycine transporters co-expressed in Xenopus oocytes	Tues morn. Memb. Biophys.	9.00-9.15
Anton Le Brun	Using Neutron Reflectometry to Understand Antibiotic Resistance in Gram-negative Bacteria at the Outer Membrane	Tues morn. Memb. Biophys.	9.15-9.30
Katherine Davies	Studying the effect of membrane curvature and composition on MLKL binding and permeabilisation using model membrane systems	Tues morn. Memb. Biophys.	9.30-9.45
Katrina Black	Investigating the role of conformational change in gating and conduction of KIR K <sup>+</sup> channels	Tues morn. Memb. Biophys.	9.45-10.00
Isabelle Rouiller	Study of Membrane Proteins by Single Particle Cryo-Electron Microscopy <b>***SPONSORED BY ThermoFisher Scientific (FE)</b>	Tues morn. Memb. Biophys.	10.30-11.00
Sudipta Maiti	Ordered and Disordered Segments of Amyloid-β Drive Sequential Steps of the Toxic Pathway	Tues morn. Memb. Biophys.	11.00-11.30
Amani Alghalayini	Study of heat transfer from laser-irradiated gold nanoparticles using tethered bilayer lipid membranes	Tues morn. Memb. Biophys.	11.30-11.45
Mibel Aguilar		Tues morn. <b>***Macaulay-Hope ASB Awardee Lecture</b>	
Yujie Sun	Super-resolution study of nuclear structure and dynamics	Wed morn. Super-Res & Imag.	9.00-9.30
Liz Hinde	Quantitative imaging of the architectural organisation of the cell nucleus	Wed morn. Super-Res & Imag.	9.30-10.00
Jieqiong Lou		Wed morn. Super-Res & Imag.	10.00-10.15
Olga Shimoni	Intracellular trafficking of single fluorescent nanoparticles	Wed morn. Super-Res & Imag.	10.45-11.15
Niall Geoghegan	4D microscopy of red blood cell membrane biophysics during Plasmodium falciparum invasion	Wed morn. Super-Res & Imag.	11.15-11.30
Max Baker	RHIM-based functional amyloid assemblies in viral evasion of host cell death	Wed morn. Super-Res & Imag.	11.30-11.45
Donna Whelan	Detecting DNA Damage Using Correlative Synchrotron Infrared Spectroscopy and Super-Resolution Fluorescence Microscopy	Wed morn. Super-Res & Imag.	11.45-12.00
Fan Bai	Single-molecule fluorescent imaging and single-cell sequencing in bacteria	Wed morn. Biophys. & Med.	9.00-9.30
Gangadhara Gangadhara	Highly selective PI3Kγ active state inhibitors and its mode of action	Wed morn. Biophys. & Med.	9.30-9.45
Yun Zhu	Rational improvement of gp41-targeting HIV-1 fusion inhibitors	Wed morn. Biophys. & Med.	9.45-10.00
Derrick Lau	In vitro reconstitution of HIV capsid lattices as interaction platforms to study host protein binding dynamics	Wed morn. Biophys. & Med.	10.00-10.15
N.R. Jagannathan	Study of Cancer Metabolism by MRI and in-vivo MR Spectroscopy	Wed morn. MRI & PET	10.45-11.15
Leigh Johnston	Pathways to contrast in sodium MRI	Wed morn. MRI & PET	11.15-11.45
Viswanath P. Sudarshan	TBC	Wed morn. MRI & PET	11.45-12.00
Hanna S Yuan	Structural insights into mitochondrial DNA maintenance by nucleases	Wed aftern. Struct. Biol.	13.45-14.15
Brett Collins	The architecture of the membrane associated retromer-sorting nexin complex revealed by cryo-electron tomography	Wed aftern. Struct. Biol.	14.15-14.45
Nirukshan Shanmugam	The role of amyloid formation in human necroptosis cascade and its modulation by viruses	Wed aftern. Struct. Biol.	14.45-15.00
Sofia Caria	A Grouper Iridovirus GIV66: a Bcl-2 protein that inhibits apoptosis by exclusively sequestering Bim	Wed aftern. Struct. Biol.	15.00-15.15
Ichio Shimada	NMR methodologies for studying larger protein complexes	Wed aftern. Struct. Biol.	15.45-16.15
Jacqui Matthews	Kinetic regulation of a transcription factor complex	Wed aftern. Struct. Biol.	16.15-16.45
Chris MacRaid	Antibody Interactions of Disordered Malaria Antigens	Wed aftern. Struct. Biol.	16.45-17.00
Pek-Lan Khong	Diffusion tensor MR imaging of treatment-induced white matter injury in childhood cancer survivors: clinical and translational studies	Wed aftern. MRI & PET	13.45-14.15
Ian Harding	MR-PET Imaging of Neuroinflammation in the Human Brain	Wed aftern. MRI & PET	14.15-14.45
Jarryd Pla	Superconducting micro-resonators for high-sensitivity and high-resolution spectroscopy	Wed aftern. MRI & PET	14.45-15.15
Won Do Heo	Optogenetic control of diverse molecular and cellular processes in the mouse brain	Wed aftern. Neuroscience	15.45-16.15
Nick Spencer	Optogenetic activation of the Enteric Nervous System and induction of colonic transit in conscious mice	Wed aftern. Neuroscience	16.15-16.45
Guang Zhu	G-quadruplex Structures Formed by Human Telomeric DNA and C9orf72 Hexanucleotide Repeats	Wed aftern. Neuroscience	16.45-17.00
Satyajit Mayor		Wed aftern. <b>***EMBO Keynote Lecture</b>	
Jackie Ying		Thur <b>***Georgina Sweet Awardee</b> Plenary 2	
Qianyi Wu	Characterisation of Mutations in the Excitatory Amino Acid Transporter SLC1A3 Linked to Episodic Ataxia Type 6 (EA6)	Thur morn. Neuroscience	9.45-10.00
Ruby Chen	Protein misfolding and therapeutics in neurodegenerative diseases	Thur morn. Neuroscience	10.15-10.45
Pingbo Huang	Mechanosensitive channels: from cell swelling to hearing	Thur morn. Neuroscience	11.15-11.45
Rob Vandenberg	Exploring Acyl-Amino Acids as Inhibitors of Glycine Transporters for the Treatment of Chronic Pain.	Thur morn. Neuroscience	11.45-12.15
Danish Idrees	Delineation of the phenotypic heterogeneity observed in the aggregation of Cu, Zn Superoxide Dismutase1	Thur morn. Neuroscience	12.15-12.30
Noritaka Kato	Nonlinear Optical Assay for Sensitive Detection of Cell Membrane Damage	Thur morn. Memb. Biophys.	9.45-10.00
Yoshitaka Nakayama	"Force-From-Lipids" gating of Corynebacterium glutamicum mechanosensitive channels specialized in glutamate export	Thur morn. Memb. Biophys.	10.00-10.15
Qian Su	Single-Molecule and Super-Resolution Microscopy for Intracellular Membrane Dynamics	Thur morn. Memb. Biophys.	10.15-10.45
Keng-hui Lin	Investigating apical constriction force of Madin-Darby Canine Kidney Cells by laser ablations.	Thur morn. Super-Res & Imag.	11.15-11.45
Nagaraj Moily	A biosensor based FLIM-FRET phasor approach to measure proteostasis capacity in cells	Thur morn. Super-Res & Imag.	11.45-12.00
Toby Bell	'Next Generation' Super-resolution Microscopy: going live with SOFI and large with Expansion.	Thur morn. Super-Res & Imag.	12.00-12.15
Till Boecking	Single-molecule analysis of HIV-1 capsid uncoating	Thur morn. Super-Res & Imag.	12.15-12.30

# ABSTRACTS

# Contents

Biomembrane Plasticity – what, how and why of membrane structure and function . . .	1
Multi-site competitive exchange on DNA origami . . . . .	1
Study of heat transfer from laser-irradiated gold nanoparticles using tethered bilayer lipid membranes . . . . .	2
Electrostatic repulsion is required for efficient assembly of the transmembrane domain of a trimeric autotransporter . . . . .	2
Single-cell imaging study of bacterial antibiotic tolerance . . . . .	3
Biophysical and structural characterization of a putative K <sup>+</sup> channel from Mycobacterium tuberculosis - a potential drug target . . . . .	4
RHIM-based functional amyloid assemblies in viral evasion of host cell death . . . . .	4
Development of small molecule inhibitors of pathogenic and functional amyloid associated with human and plant diseases. . . . .	5
Towards understanding the mechanotransduction of blood flow . . . . .	6
A thermo-responsive plasmid-magnetic hybrid nanostructure as an active platform for photothermal therapy and targeted drug delivery . . . . .	6
Superparamagnetic Nanoparticles as Stimuli-Responsive Co-Delivery System for Chemophotothermal Therapy . . . . .	7
Computational studies on mechanism of amyloid $\beta$ -protein inhibition by Hexapeptide amide . . . . .	8
Measurement of the Elastic Properties of Proteins Using a Fast and Robust Molecular Mechanics Approach . . . . .	9
The molecular identity of Chara OH <sup>-</sup> channel . . . . .	10
The integration of core metabolism with RNA processing . . . . .	10
‘Next Generation’ Super-resolution Microscopy: going live with SOFI and large with Expansion. . . . .	11
PolyBrick: A Polymerising DNA Origami Nanobot with Tuneable Polymer Length Distributions Due to Strain Accumulation . . . . .	11

Identifying the lipid bilayer interactions of the antimicrobial peptide melimine and its derivatives . . . . .	12
Investigating the role of conformational change in gating and conduction of KIR K <sup>+</sup> channels . . . . .	13
Single-molecule analysis of HIV-1 capsid uncoating . . . . .	13
Metabolic reprogramming in Cancer . . . . .	14
Understanding Piezo1's Relationship with Lipids . . . . .	15
Solvation Free Energy Prediction of Alzheimer's Proteins Using Deep Learning . . . . .	15
A Grouper Iridovirus GIV66: a Bcl-2 protein that inhibits apoptosis by exclusively sequestering Bim . . . . .	16
Measuring height-dependant nanopillar bending stiffness . . . . .	16
A crystallographic study into the structural basis of chloride permeation in the archaeal aspartate transporter, GltPh . . . . .	17
Using bacterial biosensor proteins to evaluate SAXS-based screening . . . . .	18
TDP-43 aggregation and therapeutic development in neurodegenerative diseases . . . . .	18
Mechano-redox control of integrin de-adhesion . . . . .	19
The architecture of the membrane associated retromer-sorting nexin complex revealed by cryo-electron tomography . . . . .	20
Quantifying Protein Foldedness at the Proteome-Wide Scale . . . . .	20
Studying the effect of membrane curvature and composition on MLKL binding and permeabilisation using model membrane systems . . . . .	21
The Effect of H <sub>3</sub> O <sup>+</sup> on the Structure and Dynamics of Interfacial Water in Phospholipid Bilayers . . . . .	22
Characterization of Amyloid Formation by Somatostatin-14: Role of Protofilaments in Heparin-Mediated Aggregation . . . . .	22
Effects of Metal Ions on the Conformational Equilibria of the Na <sup>+</sup> /K <sup>+</sup> - and H <sup>+</sup> /K <sup>+</sup> - ATPases . . . . .	23
Intra- and intermolecular interactions studied by synchrotron far-IR spectroscopy . . . . .	24
Protein labelling strategies at the National Deuteration Facility: isotopic labelling for NMR (2H/13C/15N) and neutron (2H) scattering . . . . .	24
Protein conformation of C9 controls the final membrane complex assembly . . . . .	25
Free energy simulations of general anaesthetic binding to a pentameric ligand-gated channel. . . . .	26
Force-dependent Ca <sup>2+</sup> signalling in cell filopodia . . . . .	27



Structural characterisation of a novel peptide from the Australian sea anemone <i>Actinia tenebrosa</i> . . . . .	27
Medicinal Chemistry Studies into 6-Substituted Hexamethylene Amiloride (HMA) Analogues as Inhibitors of the Human and Murine Urokinase Plasminogen Activators . . . . .	28
Cholesterol Distribution Mapping of Red Blood Cell Membrane during Malaria Parasite Invasion . . . . .	29
Spatially mapping brain metabolism in a mouse model of Huntington's disease . . . . .	29
Visualising retrovirus capsid uncoating using RNA-binding proteins . . . . .	30
Molecular dynamics simulations of inactivation and drug binding in the hERG ion channel . . . . .	31
Visualising the Cl <sup>-</sup> permeation pathway of glutamate transporters . . . . .	31
A Functional and Pharmacological Comparison of hGlyT2 and zGlyT2 . . . . .	32
Investigating the mechanism of the glutamine transporter ASCT2 and its potential as a molecular target in cancer therapy . . . . .	32
Development of classification method of protein-protein interfaces based on their secondary structures . . . . .	33
$\beta$ -strand twisting/bending in soluble and transmembrane $\beta$ -barrel structures . . . . .	33
Hypotonic Stress Induced-ATP Release is via Volume-regulated Anion Channels in Undifferentiated Breast Cell Lines . . . . .	34
Drug repurposing approach to identify novel inhibitors for targeting DNA gyrase in <i>Mycobacterium tuberculosis</i> : insights into mechanism and drug action . . . . .	35
Synergistic relationship between zinc and positive allosteric modulators of glycine receptors . . . . .	35
Highly selective PI3K $\gamma$ active state inhibitors and its mode of action . . . . .	36
Esters selectively modulate the interaction of physiologically relevant mono- and divalent cations with phospholipid bilayers. . . . .	36
4D microscopy of red blood cell membrane biophysics during <i>Plasmodium falciparum</i> invasion . . . . .	37
Light on a nanoscale for probing and interacting with biological systems . . . . .	38
The effect of cholesterol on Na <sup>+</sup> , K <sup>+</sup> -ATPase activity . . . . .	38
The downstream signalling motifs of Akt . . . . .	39
The response of mechanosensitive ion channels in cardiac cell stretching stimulation . . . . .	40
When Computer Meets Bio? . . . . .	40
A study on the interaction of lubricin with different substrates . . . . .	41

Structural studies of new post-translational modification erasers/readers . . . . .	41
MR-PET Imaging of Neuroinflammation in the Human Brain . . . . .	42
Correlative Super-Resolution/AFM for Investigating Cellular Ultrastructure . . . . .	43
test contribution . . . . .	43
Abstract Investigation of multiple-dynein transport of melanosomes by non-invasive force measurement using the fluctuation theorem . . . . .	43
Optogenetic control of diverse molecular and cellular processes in the mouse brain . . . .	44
Optogenetic control of diverse molecular and cellular processes in the mouse brain . . . .	45
ARTIFICIAL ASSEMBLY OF THE BACTERIAL FLAGELLA MOTOR PROTEIN FLIG ON DNA SCAFFOLDS . . . . .	45
Mapping DNA target search in live cell chromatin organisation by fluorescence fluctuation analysis . . . . .	46
Probing the Interfacial Structure of Nanoemulsions . . . . .	47
Energetics of Lipid Membrane Surface Deformation . . . . .	47
Membrane disrupting action of Caerin 1.1 . . . . .	48
Mechanosensitive Channels: From Osmosensing to Hearing . . . . .	48
Structural definition of phospholipid-mediated oligomerization of defensins in fungal and tumour cell lysis . . . . .	49
Delineation of the phenotypic heterogeneity observed in the aggregation of Cu, Zn Superoxide Dismutase1 . . . . .	50
A Thermodynamic Model of Amyloid- $\beta$ Protein Oligomerization on Negatively Charged Lipid Bilayers with High Curvatures . . . . .	50
Ferritin Assembly Mechanism Studied by Time-resolved Small-angle X-ray Scattering . . . .	50
Oligomer formation of A $\beta$ (29-42) by Coulomb replica-permutation molecular dynamics simulations . . . . .	51
Dynamic behaviour of DNA-binding proteins characterized by single-molecule fluorescence microscopy . . . . .	52
Study of Breast Cancer Metabolism by MRI and in-vivo MR Spectroscopy . . . . .	53
Precision Medicine Approaches in Metabolic Disease . . . . .	53
Pathways to Contrast in Sodium MRI . . . . .	54
Improving Mass Spectrometry Analysis of Protein Structures with Arginine-Specific Chemical Cross-linkers . . . . .	54
Compression Force Sensing Regulates Integrin $\alpha$ IIb $\beta$ 3 Biomechanical Adhesive Function on Diabetic Platelets . . . . .	54

Tracking phosphorylation induced conformational change in cardiac Troponin: an EPR and PRE-NMR study . . . . .	55
Binding Mechanism of Synthesized 5 $\beta$ -dihydrocortisol and 5 $\beta$ -dihydrocortisol acetate with Human Serum Albumin to understand their Role in Breast Cancer . . . . .	56
Binding Mechanism of Synthesized 5 $\beta$ -dihydrocortisol and 5 $\beta$ -dihydrocortisol acetate with Human Serum Albumin to understand their Role in Breast Cancer . . . . .	56
Physicochemical and Computational Analysis for S100A4-MetAP2 peptide Interaction . . . . .	57
Spectroscopic study of UV-absorbing microbial rhodopsin . . . . .	57
Nonlinear Optical Assay for Sensitive Detection of Cell Membrane Damage . . . . .	58
Experimental and Theoretical Spectroscopic Study of the Tyrosine Kinase Inhibitor PD-153035 . . . . .	59
Diffusion tensor MR imaging of treatment-induced white matter injury in childhood cancer survivors: clinical and translational studies . . . . .	59
Modulation of APC expression in mesenchymal stem cell during nomadic culture on heterogeneous field of elasticity . . . . .	60
Subcellular Localization Factors of Type II Membrane Proteins . . . . .	61
Structural features determining cardiotoxic steroid-induced Na <sup>+</sup> -K <sup>+</sup> pump stimulation – a journey back to the future in the management of new-onset atrial fibrillation? . . . . .	61
Structure-Property-Energetics Relationships in Deriving Guidelines for Rational Drug Design: Thermodynamic Approach . . . . .	62
Unveiling the molecular mechanism of RNA interference by single molecule approaches . . . . .	63
Molecular dynamics study on the mechanism of voltage dependent inactivation in a mutant of the voltage-gated potassium channel . . . . .	63
Analysis of functional and structural properties of a neuroferritinopathy-related ferritin light chain variant A96T . . . . .	64
Structure and Assembly Mechanism of the Type III Secretion System Needle Tip Complex . . . . .	65
In vitro reconstitution of HIV capsid lattices as interaction platforms to study host protein binding dynamics . . . . .	65
Using Neutron Reflectometry to Understand Antibiotic Resistance in Gram-negative Bacteria at the Outer Membrane . . . . .	66
Computational Study on the Amyloid-beta peptides in Explicit Water . . . . .	67
Computational Drug Design to Target Human MDM2 Protein . . . . .	67
Biomembrane Dynamics at Cell-Surface Interfaces: A Role in Multi-Drug Resistance Mechanism . . . . .	67
General anaesthetic modulation of pentameric ligand-gated ion channel function . . . . .	68

N-linked glycosylation determines the membrane trafficking of human Piezo1 ion channels . . . . .	69
Principles Governing Biological Processes . . . . .	69
Investigating apical constriction force of Madin-Darby Canine Kidney cells by laser ablation . . . . .	69
Tuning the antimicrobial properties of biomimetic microstructured titanium surfaces towards efficient killing of Staphylococcus aureus . . . . .	70
Entropic Contribution to Enhanced Thermal Stability in the Thermostable P450 CYP119 . . . . .	70
Direct characterization of contributions of self-motion of hydrogen and interatomic motion of heavy atoms to protein anharmonicity . . . . .	71
Phasor analysis and image correlation spectroscopy of histone FLIM/FRET reveals spatiotemporal regulation of chromatin organization by the DNA damage response. . . . .	71
Regulatory effect of the N-terminus in Na,K-ATPase . . . . .	72
Antibody Interactions of Disordered Malaria Antigens . . . . .	73
Ordered and Disordered Segments of Amyloid- $\beta$ Drive Sequential Steps of the Toxic Pathway . . . . .	73
Multi-scale molecular dynamics simulation of spheroidal high-density lipoprotein subpopulations . . . . .	74
A new, flexible enhanced sampling method to predict binding free energy of small molecules – membrane systems . . . . .	75
Migration of Endoderm and Mesoderm Derived from Human Induced Pluripotent Stem Cells during Human Gastrulation Stage . . . . .	75
Run-time and velocity distributions of human KIF1A mutants in hippocampal neurons in relation to hereditary spastic paraplegia . . . . .	76
Kinetic regulation of a transcription factor complex . . . . .	77
The Aminopeptidase N: domain motions and species complexity in the M1 family . . . . .	77
The role of the C-terminal chemistry in the membrane disrupting activity of the antimicrobial peptide aurein 1.2 . . . . .	78
Super-resolution imaging of DNA at low damage levels . . . . .	78
Stability of Fatty Acid Binding Protein by Molecular Simulation . . . . .	79
A biosensor based FLIM-FRET phasor approach to measure proteostasis capacity in cells . . . . .	79
N-acyl amino acid analgesics bind at an allosteric site to selectively inhibit the glycine transporter, GlyT2 . . . . .	80
Structure of the photo-activated acid-meta state of squid rhodopsin . . . . .	81

“Force-From-Lipids” gating of <i>Corynebacterium glutamicum</i> mechanosensitive channels specialized in glutamate export . . . . .	81
Prediction of cancer-associated hotspot mutations that affect GPCR oligomerization . . . . .	82
Looking for dominant-negative effect of hERG channel mutations . . . . .	83
Influence of wrinkled surface topologies on the colonisation of <i>Pseudomonas aeruginosa</i> . . . . .	83
Insights into the mechanism of archaeellar motor rotation from observation of unexpectedly high torque . . . . .	84
Intrinsic diversities of catalytic activity among single enzyme molecules and virus particles revealed with femtoliter reactor array . . . . .	84
Gene expression from a single large DNA encapsulated in artificial cell device . . . . .	85
Interaction of RecA proteins and DNA-wrapped carbon nanotubes using various carbon nanotube powders . . . . .	86
Difference in structural and fluctuation difference between two ends of A $\beta$ amyloid fibril revealed by molecular dynamics simulations . . . . .	86
Membrane bound states of melittin form distinct phases in DMPC . . . . .	87
Response of pheochromocytoma (PC 12) cells following exposure to electromagnetic fields of 18 GHz . . . . .	88
Conformational switching of the MLKL pseudokinase domain controls cell death by necroptosis. . . . .	88
Spin resonance at the quantum limit using superconducting microwave resonators . . . . .	89
Effect of Lipid Diversity on Membrane and Protein Functions . . . . .	90
Mechanoelectrical transduction at the cell-substrate interface . . . . .	90
The arginine-rich dipeptide repeats proteins of C9ORF72-associated Motor Neuron Disease cause the ribosome to stall during synthesis . . . . .	91
Insights on the impact of mitochondrial organisation on bioenergetics in high-resolution computational models of cardiac cell architecture . . . . .	92
Interactions of cryoprotectants with model membranes- The Langmuir monolayer study . . . . .	92
Broken Force Dispersal Network in Tip-links induces Hearing-Loss . . . . .	93
Tracking missing human olfactory receptors . . . . .	93
Structures of the Herpes simplex virus type 2 B-capsid & C-capsid with capsid-vertex-specific component . . . . .	94
PIEZO1 Can be Modulated by Substrate Mechanics Alone . . . . .	94
Cholesterol-dependent PIEZO1 clusters are essential for efficient cellular mechanotransduction . . . . .	95

Separately Measuring Photosynthesis of Oxygenic and Anoxygenic Photosynthetic Organisms using Pulse Amplitude Modulation (PAM) Fluorometry . . . . .	95
Study of Membrane Proteins by Single Particle Cryo-Electron Microscopy . . . . .	96
Subdiffraction Imaging to Characterize Live-Cell Dynamics of Microtubule-Affecting Anti-cancer Compounds . . . . .	96
FTIR study of hydrogen bonding environment in different FAD redox states of photolyase/cryptochrome family . . . . .	97
Hitting the dimensionality limit in single cell characterisation using fluorescence and Genomic Cytometry. . . . .	98
Aggregation kinetics in the presence of brain lipids of A $\beta$ 40 peptides cleaved from a soluble fusion protein . . . . .	98
DNA amplification from single molecule in micro-sized droplet . . . . .	99
An atlas of protein-protein interactions across mouse tissues . . . . .	100
The role of amyloid formation in human necroptosis cascade and its modulation by viruses . . . . .	100
Control of glycine receptor activation by glycine transporters co-expressed in <i>Xenopus</i> oocytes . . . . .	101
Function-related Dynamics of High Molecular Proteins . . . . .	102
Tracking of Single Nanoparticles in Living Cells . . . . .	102
Testing . . . . .	103
Active Mechanosensing at Cell-Substrate and Cell-Cell Adhesions . . . . .	103
Optogenetic activation of the Enteric Nervous System and induction of colonic transit in conscious mice . . . . .	104
Single-Molecule and Super-Resolution Microscopy for Intracellular Membrane Dynamics	104
Bayesian PET reconstruction using a joint PET-MR patch based dictionary prior . . . . .	105
Effect of Magnetic Field on Stimulation of Young Para Rubber Trees ( <i>Hevea brasiliensis</i> Müll. Arg.) . . . . .	105
Quantitative analysis of Sec14-mediated lipid transfer by using small-angle neutron scattering . . . . .	106
The impact of proteostasis imbalance on proteome solubility . . . . .	107
Super-resolution study of nuclear structure and dynamics . . . . .	107
Near-infrared spectroscopy of DNA wrapped single-walled carbon nanotubes with fluorescent dyes . . . . .	108
Statistical and quantum-chemical analysis of the effect of heme porphyrin distortion in heme proteins: differences between oxidoreductases and oxygen carrier proteins . . .	109

A Potent Inhibitor for Mitotic Kinesin Eg5 . . . . .	109
Molecular dynamics study of structural fluctuations in CDR-H3 of anti-HIV antibodies PG9 and PG16 . . . . .	110
DNA-Templated Assembly of the Type III Secretion System Tip Complex . . . . .	110
Lipids can disperse clusters of BAK dimers after formation of the apoptotic pore . . . . .	111
Allosteric Inhibitors of Glycine Transport for the Treatment of Pain . . . . .	112
A fluorescent protein-tagged peptide toxin as a tool for KV1.3 visualisation . . . . .	112
The apo structure of Dehydrodihydrocholesterol Desaturase and the co-crystal structure with inhibitors . . . . .	113
Comparison of biomolecular force fields on simulation P-glycoprotein . . . . .	114
Structure of a prokaryotic SEFIR domain reveals two novel SEFIR-SEFIR interaction modes . . . . .	114
The Effect of DNA Backbone on The Triplet Mechanism of UV-Induced Thymine-Thymine (6-4) Dimer Formation . . . . .	115
Detecting DNA Damage Using Correlative Synchrotron Infrared Spectroscopy and Super-Resolution Fluorescence Microscopy . . . . .	115
Molecular mechanisms of lipid transfer by ORP family . . . . .	116
Characterisation of Mutations in the Excitatory Amino Acid Transporter SLC1A3 Linked to Episodic Ataxia Type 6 (EA6) . . . . .	117
NDM-1 with cadmium substitution reveals initiate state of beta-lactam hydrolysis . . . . .	117
Building biology: a new method for understanding subunit interactions in protein super-structures . . . . .	118
Membrane stiffness is a key determinant of EcMscS activity . . . . .	118
Nano-ZnO interface stimulates the insulin fibrillation and cytotoxicity at physiological pH . . . . .	119
The (6-4) Photolyase Reaction ~Role of the Important Residues in Active Center~ . . . . .	119
Single particle analysis for membrane fusion of liposomes . . . . .	120
Development of isothermal-isobaric replica-permutation method and its application to the $\beta$ -hairpin mini protein . . . . .	121
Single GUV Studies on Mode of Action of Antimicrobial Peptides and Cell-Penetrating Peptides . . . . .	122
Thermotropic Phase Transition Behavior and Structural Properties of Partially Fluorinated Dipalmitoylphosphatidylcholine Bilayer . . . . .	123
Nanosystems for Food, Drug and Biomedical Applications . . . . .	123

Structural insights into mitochondrial DNA maintenance by nucleases . . . . .	124
Evolutionary and Taxonomic Analyses of Luciferases, Photoproteins and Luciferins . . .	124
Using cryo-electron microscopy maps for X-ray structure determination . . . . .	125
In Vivo Immuno-Optical Imaging the Behaviour and Function of Immunocytes in the Complex Microenvironment . . . . .	126
Castration modulates electrophysiological properties of HVC neurons in adult male zebra finches . . . . .	127
G-quadruplex Structures Formed by Human Telomeric DNA and C9orf72 Hexanucleotide Repeats . . . . .	127
DNP-NMR studies of the antimicrobial peptide maculatin in bacteria . . . . .	128
Rational improvement of gp41-targeting HIV-1 fusion inhibitors . . . . .	128



28

## Biomembrane Plasticity – what, how and why of membrane structure and function

Mibel Aguilar<sup>1</sup><sup>1</sup> Monash University

Corresponding Author(s): mibel.aguilar@monash.edu

Biomolecular-membrane interactions play a critical role in the regulation of many important biological processes such as protein trafficking, cellular signalling and ion channel formation. Peptide/protein-membrane interactions can also destabilise and damage the membrane which can lead to cell death. Characterisation of the molecular details of these binding-mediated membrane destabilisation processes is therefore central to understanding cellular events such as antimicrobial action, membrane-mediated amyloid aggregation, and apoptotic protein induced mitochondrial membrane permeabilization. Optical biosensors have provided a unique approach to characterising membrane interactions allowing quantitation of binding events and new insight into the kinetic mechanism of these interactions. We have developed dual polarisation interferometry (DPI) techniques to allow biophysical analysis of membrane structure changes [1]. The unique advantage of DPI is that it allows real-time measurement of bilayer structure changes during peptide binding and results demonstrate that the mechanisms of bilayer disturbance differ significantly between different classes of peptides and proteins. The combination of DPI with other biophysical techniques now opens the door to redefining molecular mechanism of biomolecular interactions in which the membrane bilayer is a key player.

[1] Lee TH, et al, 'Exploring Molecular-Biomembrane Interactions with Surface Plasmon Resonance and Dual Polarization Interferometry Technology: Expanding the Spotlight onto Biomembrane Structure', *Chemical Reviews*, 118 (2018) 5392-5487.

76

## Multi-site competitive exchange on DNA origami

Rokiah Alford<sup>1</sup>; Lisanne Spenklink<sup>2</sup>; James Walsh<sup>1</sup>; Jonathan Berengut<sup>1</sup>; Sophie Hertel<sup>1</sup>; Till Boecking<sup>1</sup>; Antoine van Oijen<sup>2</sup>; Lawrence Lee<sup>1</sup><sup>1</sup> EMBL node for Single Molecule Sciences, UNSW<sup>2</sup> School of Chemistry, University of Wollongong

Corresponding Author(s): rokiah.alford@unsw.edu.au

Through weak, non-covalent interactions between their subunits macromolecular protein complexes self-assemble into ordered, stable structures. One such protein complex is the replisome, which needs its polymerase subunits to be able to bind and function stably, but also to exchange with other subunits in solution when required. This paradox of stability and exchange can be explained by a mechanistic model known as 'multi-site competitive exchange' [1] which allows for a subunit to remain part of the complex when there are no competing subunits, but for exchange to occur in a concentration dependent manner when competitors are present. To better understand this model in nature and to harness the concept for nanotechnology, we designed and synthesised an artificial multi-site competitive exchange system using DNA origami (figure 1). The structure was imaged with electron microscopy and competitive exchange was observed with total internal reflection fluorescence microscopy (TIRFM). Using this system, in conjunction with computer simulations, we found different variables that can be used to tune the rates and concentrations at which subunit exchange occurs. This allows for the rational design of synthetic DNA nanostructures that can switch configurations in response to external stimuli. In summary, this research used DNA nanostructures

to probe a previously untested hypotheses about an important biological mechanism, while simultaneously broadening the design space in DNA nanotechnology.

[1] Åberg C, Duderstadt KE, van Oijen AM. Stability versus exchange: a paradox in DNA replication. *Nucleic Acids Research*. 2016;44(10):4846-4854. doi:10.1093/nar/gkw296.

78

## Study of heat transfer from laser-irradiated gold nanoparticles using tethered bilayer lipid membranes

**Author(s):** Amani Alghalayini<sup>1</sup>

**Co-author(s):** Cranfield Charles<sup>1</sup> ; Cronell Bruce<sup>2</sup> ; Guan Yeoh<sup>3</sup> ; Jiang Lele<sup>1</sup> ; Victoria Timchenko<sup>3</sup> ; Xi Gub<sup>3</sup> ; Valenzuela Stella<sup>1</sup>

<sup>1</sup> *School of Life Sciences, University of Technology Sydney, Sydney, NSW 2007, Australia*

<sup>2</sup> *Surgical Diagnostics, Roseville, Sydney, NSW 2069, Australia*

<sup>3</sup> *School of Mechanical and Manufacturing Engineering, University of New South Wales, Sydney 2052, Australia*

**Corresponding Author(s):** amani.alghalayini@student.uts.edu.au

There is growing interest in understanding the heat transfer characteristics of laser irradiated gold nanoparticles (GNPs) embedded in biological tissues. Laser-induced GNP hyperthermia can provide a minimally invasive, targeted treatment for infections, tumors and for the controlled release of drugs in situ [1]. However, assessing the direct consequences of the laser-induced heating phenomena of embedded GNPs in biological tissues is problematic. Here, we demonstrate how an innovative nanomaterial-electrode interface that mimics the membranes of cells, can provide insights into the heat transfer characteristics of laser irradiated GNPs within biological systems.

By transversal focusing of a laser of the appropriate wavelength, we have developed a real-time dynamic non-invasive method to record the heat production of nanoparticles added to the liquid phase located directly above the tethered bilayer lipid membranes (tBLMs). Nanoscale heating was manipulated by irradiating gold nanoparticles in solution located above and/or directly attached to the t-BLMs with a laser of set wavelength coupled to the GNPs plasmon resonance frequency. Electrical impedance spectroscopy was then used to evaluate the heating effects on the tBLMs via a thermally induced change in basal membrane ionic conduction [2]. The ability of the nanoparticles to induced localized hyperthermia was further tested against differing tBLM lipid and sterol compositions. Localized tBLM-GNP intimate contact and communication were optimized by functionalization of the tBLM using biotinylated cholesterol in combination with streptavidin coated gold nanoparticles (Figure 1).

The techniques presented here provide a novel approach for future refining GNP-laser-induced hyperthermia for clinical treatments.

[1] Pissuwan, D., S.M. Valenzuela, and M.B. Cortie, *TRENDS in Biotechnology*, 2006. 24(2): p. 62-67.  
Cornell, B. F., Braach-Maksvytis, V., King, L. G., Osman, P. D. J., Raguse, B. & Wieckzorek, L. (1997) *Nature (London)* 387, 580–583.

72

## Electrostatic repulsion is required for efficient assembly of the transmembrane domain of a trimeric autotransporter

Eriko Aoki<sup>1</sup> ; Daisuke Sato<sup>1</sup> ; Kazuo Fujiwara<sup>2</sup> ; Masamichi Ikeguchi<sup>1</sup>

<sup>1</sup> *Soka University*

<sup>2</sup> Soka university**Corresponding Author(s):** eaoki@soka.ac.jp

Haemophilus Influenzae adhesin (Hia) belongs to the trimeric autotransporter family and mediate the adhesion to host cell. Hia contains two functional domains: a passenger domain is a virulence factor, and the transmembrane domain anchors Hia into the outer membrane. The transmembrane domain forms a 12-stranded  $\beta$ -barrel in which four strands are provided by each subunit [1]. The  $\beta$ -barrel has a pore that is traversed by three  $\alpha$ -helices, one of which are provided from each subunit. The domain has a unique arrangement of the arginine 1077 stemming from each subunit (Fig. 1). Three Arg1077 side chains protrude into the pore of the  $\beta$ -barrel and are close to each other. The arrangement seems to be unfavorable for trimer assembly because of repulsion between the positive charges of these residues. In this study, we investigated the assembly of the transmembrane domain using two fragments corresponding to residues 992-1098 and 1022-1098 and found that they could reassemble in detergent. The reassembly reaction was monitored by SDS-PAGE analysis. The result showed that the reassembly kinetics and rate constants of two fragments were similar. Moreover, the reassembly kinetics of Hia1022-1098 was also monitored by fluorescence spectroscopy and circular dichroism. The results indicated that the folding and assembly of Hia1022-1098 occur in a concerted manner. To investigate the role of Arg1077 in trimer assembly, we replaced this arginine with a neutral amino acid, methionine (R1077M), or a positively charged amino acid, lysine (R1077K), and properties of these mutants were investigated. The reassembly kinetics of R1077M mutant was clearly different from that of the wild-type protein, although the reassembly kinetics of R1077K mutant was similar to that of the wild-type protein. The Far-UV CD spectrum of the reassembled R1077M mutant showed that a portion of R1077M molecules forms a misassembled oligomer. These results show that the electric repulsion between the positive charges of Arg1077 is important for preventing the formation of misassembled oligomers in vitro [2].

[1] G. Meng, J. W. St Geme, 3rd, and G. Waksman, EMBO J. 25, 2297 (2006)  
E. Aoki, D. Sato, K. Fujiwara, and M. Ikeguchi, Biochemistry, 56, 2139 (2017)

217

## Single-cell imaging study of bacterial antibiotic tolerance

Fan Bai<sup>1</sup><sup>1</sup> Biomedical Pioneering Innovation Center (BIOPIC), School of Life Sciences, Peking University**Corresponding Author(s):**

In this talk, I will present our recent works on studying bacterial antibiotic tolerance using single-cell imaging. Natural variations in gene expression provide a mechanism for multiple phenotypes to arise in an isogenic bacterial population. In particular, a sub-group termed persisters show high tolerance to antibiotics. Previously, their formation has been attributed to cell dormancy. Here we demonstrate that bacterial persisters, under  $\beta$ -lactam antibiotic treatment, show less cytoplasmic drug accumulation as a result of enhanced efflux activity. Consistently, a number of multi-drug efflux genes, particularly the central component TolC, show higher expression in persisters. Time-lapse imaging and mutagenesis studies further establish a positive correlation between tolC expression and bacterial persistence. The key role of efflux systems, among multiple biological pathways involved in persister formation, indicates that persisters implement a positive defense against antibiotics prior to a passive defense via dormancy. On the other hand, we also monitored the process of bacterial regrowth after surviving antibiotic attack at the single-cell level and found that each individual survival cell shows different 'dormancy depth', which in return regulates the lag time for cell resuscitation after removal of antibiotic. We established that protein aggresome - a collection of endogenous protein aggregates - is an important indicator of bacterial dormancy depth, whose formation is promoted by decreased cellular ATP level. For cells to leave the dormant state and re-suscitate, clearance of protein aggresome and recovery of proteostasis are required. We revealed the ability to recruit functional DnaK-ClpB machineries, which facilitate protein disaggregation in an ATP-dependent manner, determines the lag time for bacterial regrowth.

109

## Biophysical and structural characterization of a putative K<sup>+</sup> channel from *Mycobacterium tuberculosis* - a potential drug target

**Author(s):** Saumya Bajaj<sup>1</sup>

**Co-author(s):** Abbas El Sahili<sup>2</sup>; Shih Chieh Chang<sup>3</sup>; Jeremy Ng Jun Heng<sup>1</sup>; Ming Wei Chen<sup>4</sup>; Bee Ting Lim<sup>4</sup>; Julien Lescar<sup>2</sup>; K George Chandy<sup>1</sup>

<sup>1</sup> Lee Kong Chian School of Medicine, Nanyang Technological University, Singapore

<sup>2</sup> Nanyang Institute of Structural Biology, School of Biological Sciences, Nanyang Technological University, Singapore

<sup>3</sup> Lee Kong Chian School of Medicine, Nanyang Technological University, Singapore

<sup>4</sup> Protein Production Platform, School of Biological Sciences, Nanyang Technological University, Singapore

**Corresponding Author(s):** saumya.bajaj@ntu.edu.sg

Tuberculosis (TB) is a global public health burden; in 2017, 10 million people were affected with TB, with 1.6 million resultant deaths [1]. *Mycobacterium tuberculosis*, the etiologic agent of TB, has evolved to evade antibiotics and this has resulted in multidrug-resistant (MDR-TB) and extensively drug-resistant (XDR-TB) MTb strains. An additional survival strategy seems to be organization into biofilms. MTb has a strong propensity to grow in biofilms that exhibit high resistance to common anti-TB drugs [2]. Bacteria within biofilm communities communicate via potassium waves coupled to metabolic signals [3]. MTb has a network of K<sup>+</sup> channels and transporters that may underlie such metabolic-electrical coupling. Better understanding of metabolic-sensing and electrical communication in MTb biofilms may lead to novel therapeutics to counter the global scourge of antibiotic resistance. We have identified a putative K<sup>+</sup> channel (gene: Rv3200c) in MTb with a potential role in metabolic-electrical coupling. Rv3200c has an N-terminal transmembrane region (Ion\_Trans\_2 domain: Pfam PF07885) comprising two TM segments and a putative pore-segment containing the signature GYGD pore motif. Rv3200c has a C-terminal cytoplasmic region containing a proximal TrkA\_N domain (Pfam PF02254) followed by a unique sequence. The TrkA\_N domain has a nucleotide-binding site (GXGXXG) that could potentially couple metabolism to channel gating. We purified the C-terminus of Rv3200c (CTD) and used isothermal calorimetry to demonstrate that it binds nucleotides in the following order of affinity: AMP>cAMP>ADP>ATP>NAD<sup>+</sup>. The CTD has been crystallized and efforts are underway to determine its structure using X-ray diffraction data. We also purified the full-length Rv3200c protein in the presence of detergent n-Dodecyl-β-D-maltoside by nickel-chelate and size-exclusion chromatography. Negative-stain electron microscopy revealed tetrameric structures (10nmx10nm), with a stain-permeable pore vestibule, consistent with K<sup>+</sup> channels. We are optimizing protein sample preparation for structure determination via cryo-electron microscopy.

[1] Global tuberculosis report 2018. Geneva: World Health Organization (2018).

K. Kulka, G. Hatfull and A.K. Ojha, J Vis Exp. 60, 3820 (2012).

A. Prindle, J. Liu, M. Asally, S. Ly, J. Garcia-Ojalvo and G.M. Süel, Nature. 527, 59 (2015).

155

## RHIM-based functional amyloid assemblies in viral evasion of host cell death

**Author(s):** Max Baker<sup>1</sup>

**Co-author(s):** Chi L. L. Pham; Nirukshan Shanmugam; Thu Vu; Emma Sierecki; Yann Gambin; Megan Steain; Margaret Sunde

<sup>1</sup> University of Sydney

**Corresponding Author(s):** mbak3566@uni.sydney.edu.au

The Receptor Homotypic Interaction Motif (RHIM) is a conserved amino acid sequence, found in four human proteins, which mediates the assembly of a heteromeric signalling complex known as the necrosome that is required for certain types of programmed cell death [1]. The necrosome has a fibrillar amyloid structure. This RHIM-mediated amyloid structure is primarily responsible for the induction of cell death by programmed necrosis, termed necroptosis, but recent findings indicate that it may also play a role in the induction of other cell death pathways, including apoptosis and pyroptosis.

Herpesviruses, highly seropositive DNA viruses that impose significant medical and economic burden, require living host cells to function. To this end, they have evolved multiple mechanisms to counteract host cell death pathways [2]. Herpesviruses express proteins which contain RHIM sequences and which interact with human RHIM proteins to form heteromeric, interspecies amyloid complexes that abrogate the signalling capabilities of the human proteins. Here we report the characterisation of a novel RHIM-containing protein from Varicella Zoster virus known as ORF20. Using a range of biophysical techniques, including fluorescence, electron microscopy and single molecule spectroscopy, we have shown that the ORF20 RHIM drives formation of homomeric amyloid fibrils and that it interacts with human RHIM proteins to form heteromeric complexes. In parallel, we have demonstrated the ability of this virus to inhibit cell death through the activity of ORF20 protein but find that unlike other viral RHIM proteins, ORF20 inhibits apoptosis, not necroptosis, and this activity is not solely dependent on RHIM interactions. The characterisation of this novel RHIM demonstrates the importance of RHIM-based signalling in multiple human cell death pathways, as well as the diversity of viral strategies to overcome the complexity of signalling driving these processes.

[1] Li J, McQuade T, Siemer AB, Nepstschmig J, Moriwaki K, Hsaio YS, et al. *Cell* 159, 339-350 (2012).  
Kaiser WJ, Upton JW and Mocarski ES. *Curr Opin Virol* 3, 296-306 (2013).

153

## Development of small molecule inhibitors of pathogenic and functional amyloid associated with human and plant diseases.

Sarah Ball<sup>None</sup> ; Chi Pham<sup>1</sup> ; Julius Adamson<sup>2</sup> ; Victor Lo<sup>1</sup> ; Hannah Nicholas<sup>2</sup> ; Ann Kwan<sup>None</sup> ; Matthew Todd<sup>None</sup> ; Rutledge Peter<sup>2</sup> ; Margaret Sunde<sup>3</sup>

<sup>1</sup> *The University of Sydney*

<sup>2</sup> *The University of Sydney*

<sup>3</sup> *The University of Australia*

**Corresponding Author(s):** sbal5807@uni.sydney.edu.au

Amyloid is a fibrillar protein structure characterised by the presence of a stable, cross- $\beta$ -sheet conformation. It is known for its pathogenic role in diseases such as Alzheimer's disease, Type II diabetes and isolated atrial amyloidosis where the presence of amyloid is unwanted. However, amyloid has also been shown to have a functional role in many organisms, including mammals, bacteria and fungi. In fungi, amyloid is utilized to increase the infectivity of the fungus. Fungi such as *Aspergillus fumigatus* and *Magnaporthe oryzae*, responsible for invasive aspergillosis and rice blast disease respectively, both produce small proteins called hydrophobins. Hydrophobins form amyloid rodlet structures that aid in the fungal life cycle and facilitate infection of hosts.

Given the involvement of amyloid in human and plant diseases, prevention of amyloid fibril formation may provide an avenue for combating these diseases. We have tested a series of new small-molecule compounds that target the cross- $\beta$ -sheet structure of amyloid. The effectiveness of the inhibitors has been assessed by thioflavin T fluorescence assays and verified by electron microscopy. A *Caenorhabditis elegans* model of Alzheimer's disease has also been implemented to assess the efficacy of these small-molecules in vitro and results will be shown. We find that some of these small molecules are able to prevent assembly of a range of amyloids, both functional and pathogenic. This

is likely because the small molecules are active against the cross- $\beta$  conformation, which is a generic element of amyloid fibrils.

159

## Towards understanding the mechanotransduction of blood flow

**Author(s):** Sara Baratchi<sup>1</sup>

**Co-author(s):** Yung Chih Chen ; Khashayar Khoshmanesh ; Peter McIntyre ; Karlheinz Peter

<sup>1</sup> *RMIT University*

**Corresponding Author(s):** sara.baratchi@rmit.edu.au

Hemodynamic forces associated with blood flow have a pivotal role in the function of the vascular endothelium in health and disease. In this context, in humans, the earliest lesions of atherosclerosis characteristically develop where the flow is disturbed, and shear stress is relatively low, such as in arterial branches or where vessels bend [1, 2]. Atherosclerosis is a major pathology with limited treatment options. Understanding the mechanosensory complexes that govern atherosclerotic plaque formation and growth is essential to design effective therapeutic approaches. Mechanosensitive ion channels such as TRPV4 play an important role in the physiological function of endothelial cells [3, 4]. Membrane translocation has been shown to control the response of several members of the transient receptor potential (TRP) family of ion channels to different stimuli including TRPV4 [5-8]. We have used novel microfluidic methodologies, animal models of atherosclerosis and different imaging techniques to understand how shear stress controls the distribution and function of mechanosensitive ion channels in endothelium.

1. Baratchi, S., et al., Molecular Sensors of Blood Flow in Endothelial Cells. *Trends Mol Med*, 2017. 23(9): p. 850-868.
2. Chiu, J.J. and S. Chien, Effects of disturbed flow on vascular endothelium: pathophysiological basis and clinical perspectives. *Physiol Rev*, 2011. 91(1): p. 327-87.
3. Martinac, B., Mechanosensitive ion channels: an evolutionary and scientific tour de force in mechanobiology. *Channels (Austin)*, 2012. 6(4): p. 211-3.
4. Martinac, B., et al., Tuning ion channel mechanosensitivity by asymmetry of the transbilayer pressure profile. *Biophys Rev*, 2018.
5. Boycott, H.E., et al., Shear stress triggers insertion of voltage-gated potassium channels from intracellular compartments in atrial myocytes. *Proc Natl Acad Sci U S A*, 2013. 110(41): p. E3955-64.
6. Baratchi, S., et al., Shear stress mediates exocytosis of functional TRPV4 channels in endothelial cells. *Cell Mol Life Sci*, 2016. 73(3): p. 649-66.
7. Baratchi, S., et al., Shear Stress Regulates TRPV4 Channel Clustering and Translocation from Adherens Junctions to the Basal Membrane. *Sci Rep*, 2017. 7(1): p. 15942.
8. Numata, T., T. Shimizu, and Y. Okada, Direct mechano-stress sensitivity of TRPM7 channel. *Cell Physiol Biochem*, 2007. 19(1-4): p. 1-8.

203

## A thermo-responsive plasmo-magnetic hybrid nanostructure as an active platform for photothermal therapy and targeted drug delivery

Mona Khafaji<sup>1</sup> ; Omid Bavi<sup>2</sup> ; Manouchehr Vossoughi<sup>3</sup> ; Azam Irajizad<sup>4</sup>

<sup>1</sup> *Institute for Nanoscience and Nanotechnology, Sharif University of Technology, Tehran 14588, Iran*

<sup>2</sup> *Department of Mechanical and Aerospace Engineering, Shiraz University of Technology*

<sup>3</sup> *Department of Chemical and Petroleum Engineering, Sharif University of Technology*

<sup>4</sup> *Department of Physics, Sharif University of Technology*

**Corresponding Author(s):** o.bavi@sutech.ac.ir

Cancer treatment is one of the most challenging issues of recent years. Extensive researches have been conducted in various fields of medicine, pharmacy, and medical physics in this regard. Today, considering nanotechnology developments, researchers believe that full cancer treatment is possible through the use of nanosystems designed with scientific background to overcome the defects of previous methods [1-2]. Synthesis of novel nanohybrid structures is one of the methods which some researches have recently attempted. Among all nanoparticles for synthesis of hybrid structures, gold nanorods and superparamagnetic iron oxide nanoparticles are good candidates because of their special properties. Combining nanoparticles with surface plasmon resonance properties and superparamagnetic properties into one single structure can lead to a development of new functional and efficient techniques in therapeutic, bioimaging and biosensing [3-4].

Herein, hybrid nanostructures were synthesized from the bonding of gold nanorods and iron oxide nanoparticles. The effectiveness of gold nanorods as a photothermal treatment agent has already been confirmed. The presence of iron oxide nanoparticles within the structure allows the magnetic targeting. Through nanostructure coating by PNIPAM, it is possible to load several types of drugs. So there will be a possibility to combination chemotherapy. The release of the drug results from a phase change in the PNIPAM under high temperatures, as well as a breakdown of the hydrogen bonding of the drug and polymer molecules at a low pHs. This condition causes the maximum release of the drug to occur simultaneously with photothermal treatment and in cancerous cells. The results of in vitro studies indicate that the combination of therapeutic methods through synthesized nanostructures is better than any of them. Therefore, it can be concluded that the new nanostructure is a good candidate for the integration of therapeutic methods, due to its bio- and hemo-compatibility and multiple capabilities in treatment and drug delivery.

[1] Li, N. et al. Multiple gold nanorods@hierarchically porous silica nanospheres for efficient multi-drug delivery and photothermal therapy. *J. Mater. Chem. B*, 2017. 5: p. 1642–1649.

Wu, H. et al. Synergistic Cisplatin/Doxorubicin Combination Chemotherapy for Multidrug-Resistant Cancer via Polymeric Nanogels Targeting Delivery. *ACS Appl. Mater. Interfaces*. 2017. 9: p. 9426–9436.

Štarha P., et al., Efficient Synthesis of a Maghemite/Gold Hybrid Nanoparticle System as a Magnetic Carrier for the Transport of Platinum-Based Metallotherapeutics. *International Journal of Molecular Sciences*, 2015. 16(1): p. 2034.

Khafaji, M., Vossoughi, M., Hormozi-nezhad, M. R. & Dinarvand, R. A new bifunctional hybrid nanostructure as an active platform for photothermal therapy and MR imaging. *Scientific Reports*. 2016. 6: p. 1–12

202

## Superparamagnetic Nanoparticles as Stimuli-Responsive Co-Delivery System for Chemo-Photothermal Therapy

Mona Khafaji<sup>1</sup> ; Omid Bavi<sup>2</sup> ; Manouchehr Vossoughi<sup>3</sup>

<sup>1</sup> *Institute for Nanoscience and Nanotechnology, Sharif University of Technology*

<sup>2</sup> *Department of Mechanical and Aerospace Engineering, Shiraz University of Technology*

<sup>3</sup> *Department of Chemical and Petroleum Engineering, Sharif University of Technology*

**Corresponding Author(s):** o.bavi@sutech.ac.ir

Most of the chemotherapeutic drugs act non-specifically so they have effect not only on cancer cells but also on healthy cells. Therefore drug delivery systems have been designed to decrease the drug's side effects and increase the influence of chemotherapy. Many different drug nanocarriers were proposed but among of them, magnetic nanoparticles attract more attention [1,2]. Magnetic iron oxide nanoparticles hold much promise for biomedical applications, including diagnosis by magnetic resonance imaging (MRI), targeted drug delivery and hyperthermia. However some factors such as size, shape and surface charge can determine the biological behaviour of nanoparticles but chemical stability, biocompatibility, strong magnetization with low coercivity are the requirements for any biological application of magnetic colloids. Silica coated magnetic iron oxide nanoparticles have been complied with the requirements. The outer shell of silica protects the inner magnetic core from oxidation, in addition to provide sites for surface functionalization [2-5].

In this work, PEG modified silica coated superparamagnetic iron oxide nanoparticles (PSIONs) were synthesized as multifunctional cancer treatment agents. Magnetic behaviour of this nanostructure remains superparamagnetic with enhanced magnetic saturation compared to the previous reports even after complete shielding by silica and PEG. PEG modification increased the stability, biocompatibility and drug loading capacity of the mentioned nanostructure. Therefore, in addition to T2-weighted magnetic resonance contrast agent, PSIONs could act as magnetically-targeted drug carriers. Drug molecules have been attached to the terminal carboxylic acid groups of PEG chains. Results showed that the drug release have been pH and thermo-sensitive. Using the drug loaded nanoparticles, only 2.7% of human breast adenocarcinoma cells (MCF7) could survive. Therefore, the synthesized nanostructure would be a good candidate for magnetic targeting MRI and dual-drug chemotherapy.

[1] Benyettou F. et al., Mesoporous  $\gamma$ -Iron oxide nanoparticles for magnetically triggered release of doxorubicin and hyperthermia treatment. *Chemistry A European Journal*, 2016. 22(47): p. 17020-17028.

Erdem M., Yalcin S. & Gunduz, U. Folic acid-conjugated polyethylene glycol-coated magnetic nanoparticles for doxorubicin delivery in cancer chemotherapy: Preparation, characterization and cytotoxicity on HeLa cell line. *Hum. Exp. Toxicol.*, 2017. 36: p. 833-845.

Thapa B., Diaz-Diestra D., Beltran-Huarac J., Weiner B. R. & Morell G. Enhanced MRI T2 relaxivity in contrast-probed anchor-free PEGylated iron oxide nanoparticles. *Nanoscale Res. Lett.*, 2017. 12: p.1-13.

Lee S. et al. Near-infrared heptamethine cyanine based iron oxide nanoparticles for tumor targeted multimodal imaging and photothermal therapy. *Sci. Rep.* 2017. 7: p. 1-14.

Sivakumar B. et al. Highly versatile SPION encapsulated PLGA nanoparticles as photothermal ablaters of cancer cells and as multimodal imaging agents. *Biomater. Sci.*, 2017. 5: p. 432-443.

22

## Computational studies on mechanism of amyloid $\beta$ -protein inhibition by Hexapeptide amide

Safura Jokar<sup>1</sup> ; Omid Bavi<sup>None</sup> ; Amir Shamloo<sup>2</sup> ; Davood Beiki<sup>3</sup>

<sup>1</sup> *Department of Pharmacy, Tehran University of Medical Sciences*

<sup>2</sup> *Department of Mechanical Engineering, Sharif University of Technology*

<sup>3</sup> *Research Center of Nuclear Medicine, Tehran University of Medical Sciences*

**Corresponding Author(s):** o.bavi@sutech.ac.ir

Alzheimer's disease (AD) is one of the most common chronic neurodegenerative disease that is characterized by misfolding and aggregation of amyloid  $\beta$  peptide (A $\beta$ ) in brains. Amyloid- $\beta$  (1-42) is a major fragment of the amyloid precursor protein (APP) which tends to aggregate into amyloid fibrils that forms the main part of the amyloid beta plaques [1]. Hexapeptide amide has been derived from the C-terminal segment of the amyloid  $\beta$  peptide (1-42) by screening a randomized library by phage display. Previous in vitro studies have suggested that this peptide can bind to A $\beta$  and inhibit the aggregation of amyloid  $\beta$  peptide (A $\beta$ ) [2]. However, the mechanism and the pathway that this peptide binds to A $\beta$  as well as protein-ligand interactions are unclear. Here, we have adopted molecular



docking and molecular dynamics simulations to model and explore of the exact mechanism involved in the interaction between hexapeptide amide and amyloid  $\beta$  peptide [3, 4].

The initial conformation for MD simulations was obtained by AutoDock Vina software. Then, MD simulations on Amyloid- $\beta$  (1-42) and hexapeptide-A $\beta$  (1-42) complex in water were carried out by Gromacs 5.0.4. These findings demonstrated that hexapeptide amide has suitable affinity binding to A $\beta$  peptide which can inhibit the process of  $\alpha$ -helix conformation to  $\beta$ -sheet structure in amyloid  $\beta$  peptide.

[1] S.Aileen Funke, D.Willbold, *Curr Pharm Des.* 18, 6 (2012).

L.Larbanoux, C. Burtea, E.Anciaux, S.Laurent, I.Mahieu, L.Vander Elst, R.N. Muller, *Peptides.* 32, 6 (2011).

C.Yang, X.Zhu, J. Li, R. Shi, *J Mol Model.*16, 4 (2010).

C. Hetényi, Z. Szabó, É. Klement, Z. Datki, T. Körtvélyesi M. Zarándi, B. Penke, *Biochem Biophys Res Commun.* 292, 4 (2002).

20

## Measurement of the Elastic Properties of Proteins Using a Fast and Robust Molecular Mechanics Approach

Omid Bavi<sup>1</sup> ; Navid Bavi<sup>2</sup> ; Pouria Beydaghi<sup>3</sup> ; Reza Naghdabadi<sup>3</sup> ; S. Mehdi Vaez Allaei<sup>4</sup>

<sup>1</sup> *Department of Mechanical and Aerospace Engineering, Shiraz University of Technology*

<sup>2</sup> *Institute for Biophysical Dynamics, University of Chicago, Chicago, USA*

<sup>3</sup> *Department of Mechanical Engineering, Sharif University of Technology, Tehran, Iran*

<sup>4</sup> *Department of Physics, University of Tehran*

**Corresponding Author(s):** o.bavi@sutech.ac.ir

Proteins in living cells are constantly subjected to a wide spectrum of mechanical forces, such as the forces that stem from the lipid bilayer (specific to membrane proteins), other proteins or intra/extracellular ligands [1-3]. Given the key role that mechanical properties of transmembrane helices play in proteins' structural integrity and function [4], it is therefore essential to develop computational tools that are precise and at the same time fast in describing proteins' behaviour under different mechanical loading. We have developed a molecular mechanics (MM) approach that accounts for the atomic as well as molecular interactions in proteins by modelling the bonded and non-bonded interactions as physical springs, while using finite element method for solving the governing differential equations. In this study we have used the helices of a mechanosensitive ion channel MscL as a prototype protein. This method is used to measure the mechanical properties and study the behaviour of different transmembrane helices of MscL under various types of mechanical forces such as stretch, torsion and bending. We compared our results with those estimated using molecular dynamics (MD) simulation. For instance, the Young's modulus of TM1 helix in mycobacterium tuberculosis (MtMscL) has been estimated to be  $E = 8.5 \pm 0.1$  GPa using the MM approach, which is in good agreement with that obtained by MD simulation [5]. Compared to techniques such as all-atom MD simulations, by utilizing this approach, excessive computation costs and simulation time can be avoided. Our method has several implications for modelling macro biological molecules such as large membrane proteins complexes and cytoskeletal elements [6].

[1] Bavi, N., et al., Structural Dynamics of the MscL C-terminal Domain. *Scientific reports*, 2017. 7(1): p. 17229.

Martinac, B., et al., Tuning ion channel mechanosensitivity by asymmetry of the transbilayer pressure profile. *Biophysical reviews*, 2018: p. 1-8.

Schönfelder, J., et al., The life of proteins under mechanical force. *Chemical Society Reviews*, 2018. 47(10): p. 3558-3573.

Martinac, A.D., et al., Pulling MscL open via N-terminal and TM1 helices: A computational study towards engineering an MscL nanovalve. *PloS one*, 2017. 12(8): p. e0183822.

Bavi, N., et al., Nanomechanical properties of MscL  $\alpha$  helices: A steered molecular dynamics study.

Channels, 2017. 11(3): p. 209-223.

Anishkin, A. and S. Sukharev, Channel disassembled: Pick, tweak, and soak parts to soften. Channels, 2017. 11(3): p. 173-175.

95

## The molecular identity of Chara OH<sup>-</sup> channel

Mark Parker<sup>1</sup> ; Marion Hoepflinger<sup>2</sup> ; Shaunna Phipps<sup>1</sup> ; Mary Bisson<sup>3</sup> ; Ilse Foissner<sup>2</sup> ; Mary Beilby<sup>4</sup>

<sup>1</sup> *The State University of New York at Buffalo*

<sup>2</sup> *University of Salzburg*

<sup>3</sup> *State University of New York at Buffalo*

<sup>4</sup> *The University of NSW*

**Corresponding Author(s):** m.j.beilby@unsw.edu.au

The recent sequencing of *Chara braunii* genome (Nishiyama et al. 2018, Cell 174, 448–464) facilitates finding molecular identities of channels important in the characean electrophysiology. Closely related *Chara australis* enhances photosynthetic efficiency by carbon concentrating mechanism of pH banding. The proton pump-mediated acid bands aid diffusion of CO<sub>2</sub> across plasma membrane, while the alkaline bands remove excess OH<sup>-</sup>, created by the carbon transport into the chloroplasts. The postulated mechanism in the alkaline band is a H<sup>+</sup>/OH<sup>-</sup> channel. However, the sequence data of *Chara* and, indeed, of higher plants lack the homologies to animal H<sup>+</sup> channels. There are several putative plant voltage-gated hydrogen channel sequences available in public databases, but again no homologous forms were detected in *Chara*. However, we found CL5060.2, a homology to the mammalian Slc4 family of transporters. The murine Slc4a11 transporter is almost perfectly selective for H<sup>+</sup>/OH<sup>-</sup>. These channels are found in the eye and ear with mutations responsible for blindness and deafness. In early experiments the *Chara* CL5060.2 channels were put into suitable expression vector and inserted into *Xenopus* eggs. They behaved similarly to mouse OH<sup>-</sup> channels by being activated by the rise in pHo/pHi. Intact *Chara* cells respond to pH above 9 by transforming their electrophysiology into “high pH state” dominated by OH<sup>-</sup> channels, where the membrane potential difference follows EH/OH.

199

## The integration of core metabolism with RNA processing

Traude Beilharz<sup>1</sup>

<sup>1</sup> *Monash University*

**Corresponding Author(s):** traude.beilharz@monash.edu

My team seeks to understand how mRNA metabolism is integrated within multiple regulatory systems to maintain cellular homeostasis. Specifically, we study the role of 3'-UTR dynamics to better understand the regulation of mRNA translation in space and time. For example, the 3'-UTR is an important platform for regulation of mRNA fate. Through the binding of regulatory elements, it can influence the stability, localisation and translatability of mRNA. Moreover, up to 80% of genes are expressed as 3'-UTR length-isoforms by encoding multiple locations for cleavage in a process known as alternative polyadenylation. I will discuss unpublished data that describes how steady-state 3'-UTR choice is the product of a balance between transcriptional rate and the available concentration of the cleavage and polyadenylation machinery. This conclusion stems from findings from custom RNA-seq, proteomics and metabolomics. Treating yeast cells with the naturally occurring adenosine analogue, cordycepin has the unexpected consequence of bulk transcriptome lengthening by increased usage of distal polyadenylation sites. This is due to a switch in core metabolism to favour nucleotide biosynthesis with a subsequent increase in transcriptional rate. Disabling transcription

with a 'slow' polymerase mutant attenuates 3'-UTR lengthening. Yeast strains with defective cleave and polyadenylation machinery induce similar 3'-end lengthening of the transcriptome suggesting that with limited cleavage-machinery, transcription runs-on as though it were going too fast for the nascent transcript to be cut and matured normally. The transcript is then terminated at the next available position at which the polymerase slows down. Approximately 1/3 of the transcriptome undergoes alternative polyadenylation when transcription and cleavage are out of balance. The genes for which this occurs have an inherently wider nucleosome-depleted region at the 3'-end suggesting that higher-order chromatin structure plays a role in alternative polyadenylation. In the context of aberrant adenylation-site choice, such as that induced by cordycepin, these nucleosome boundaries then create the transcriptional pause-sites necessary to engage the machinery to make and mature a functional 3'-end.

175

## 'Next Generation' Super-resolution Microscopy: going live with SOFI and large with Expansion.

Toby Bell<sup>1</sup> ; Ashley Rozario<sup>2</sup> ; Riley Hargreaves<sup>3</sup> ; Sam Duwe<sup>4</sup> ; Peter Dedecker<sup>4</sup> ; Fabian Zwettler<sup>5</sup> ; Markus Sauer<sup>5</sup> ; Gregory Moseley<sup>2</sup> ; Donna Whelan<sup>6</sup>

<sup>1</sup> School of Chemistry, Monash University, Victoria 3800, Australia

<sup>2</sup> Monash University

<sup>3</sup> Monash University

<sup>4</sup> University of Leuven

<sup>5</sup> Wuerzburg University

<sup>6</sup> Department of Pharmacy and Applied Science, La Trobe University, Bendigo, Victoria 3552, Australia

### Corresponding Author(s):

Microscopy methods that can circumvent the diffraction limit of light to achieve super-resolution imaging are increasingly finding application, especially in visualising sub-cellular detail. Approaches which are founded on the detection and localization of single fluorophores yield the best resolution gains – up to an order of magnitude – and are the most widely applied. Preparation of biological samples usually involves chemical fixation and (bio)chemical labelling (e.g. immunolabelling, 'click' labelling), processes which affect the biological context and along with the high photon flux required to drive fluorophore 'blinking', reduces relevance and potentially lead to image artifacts and misinterpretation.

Stochastic optical fluctuation imaging (SOFI), which can achieve resolution gains of ~2 – 4x and requires only minimal excitation power, is well-suited to perform super-resolution imaging in live cells.[1] In an alternative approach to improving resolution, Expansion microscopy (ExM) physically expands the sample (the 'fluorophore network' that remains following digestion) by up to 4x in each direction to reveal sub-diffraction detail.[2] Here we report on recent progress in applying both SOFI and ExM to our on-going study of the modification of the host-cell microtubule (MT) network by viral proteins.[3] We show that MT bundles are present in live cells expressing rabies P3 protein and that these bundles can be expanded and imaged using modified ExM protocols.

Figure 1: live cell SOFI (left) and expansion microscopy (right) of microtubule bundles in cells expressing rabies virus P3 protein. Scale bars 5 µm.

[1] P. Dedecker, G. Mo, T. Dertinger, J. Zhang, Proc. Natl. Acad. Sci., 109:10909 (2012).

F. Chen, P.W. Tillberg, E.S. Boyden, Science, 347:543-548 (2015).

A. Brice, D.R. Whelan, N. Ito, K. Shimizu, L. Wiltzer-Bach, C.Y. Lo, D. Blondel, D. A. Jans, T.D.M. Bell, G.W. Moseley, Scientific Reports, 6:33494 (2016)

110

## PolyBrick: A Polymerising DNA Origami Nanobot with Tuneable Polymer Length Distributions Due to Strain Accumulation

**Author(s):** Jonathan Berengut<sup>1</sup> ; Lawrence Lee<sup>1</sup>

**Co-author(s):** Julian Berengut<sup>1</sup> ; Jonathan Doye<sup>2</sup> ; Thomas Ouldridge<sup>3</sup>

<sup>1</sup> *UNSW Sydney*

<sup>2</sup> *Oxford University*

<sup>3</sup> *Imperial College London*

**Corresponding Author(s):** jberengut@gmail.com

In the field of DNA nanotechnology, we can assemble hundreds of synthetic DNA strands into complex, precise “nanobots” capable of nanoscale tasks such as targeted drug delivery and biosensing. To increase the scale and complexity of the tasks that these nanobots can perform, it is necessary to program them to assemble into larger formations. Here we present the PolyBrick, a DNA origami nanobot (see fig. a, b, c) that assembles into homopolymers with tuneable equilibrium length distributions. We achieved this by equipping the PolyBricks with a combination of hybridising ‘sticky’ domains (fig. e) and poly-thymine passivated ‘repulsion’ domains (fig. f). The domains are linked with flexible connectors (fig. d), allowing deformation as the PolyBricks join together (fig. g) and strain accumulation as the polymers lengthen (fig. h, i). We demonstrate these principles through mathematical modelling, coarse-grain simulation and direct measurement of assembled nanostructures.

16

## Identifying the lipid bilayer interactions of the antimicrobial peptide melimine and its derivatives

**Author(s):** Thomas Berry<sup>None</sup> ; Bruce Corenell<sup>1</sup> ; Charles Cranfield<sup>2</sup>

**Co-author(s):** Andrea Leong ; Debarun Dutta ; Huixin Wang ; Mark Willcox ; Maryam Parviz ; Naresh Kumar ; Renxun Chen ; William Donald

<sup>1</sup> *Surgical Diagnostics pty. ltd.*

<sup>2</sup> *University of Technology Sydney*

**Corresponding Author(s):** thomas.berry@student.uts.edu.au

The bespoke peptide melimine and its derivatives are a chimera of two natural antimicrobial peptides (AMPs), melittin and protamine. They have been shown to exhibit broad spectrum activity across both gram negative and gram positive bacteria.[1] Melimine consists of a sequence of 28 amino acids which contain 13 arginine residues. This gives the peptide a net charge of positive 16. A derivative designated cys-melimine, containing a cysteine on N-terminus, allows for substrate binding via the sulphur moiety of the cysteine while still maintaining its antimicrobial effectiveness. Electrical impedance spectroscopy was used to study the conduction changes and ionic permeability as a result of peptide-lipid interactions in tethered bilayer lipid membranes (tBLMs) of varying lipid composition. Dynamic light scattering (DLS) was employed to study changes in lipid assembly as a result of interactions with the melimine derivatives. Differential scanning calorimetry (DSC) was also used to examine the influence of the peptides on the lipid phase transition of DPPC bilayers. The results from each technique were correlated with the antimicrobial potency for various strains of Gram positive and Gram negative bacteria. It was found that the effect of the peptides on the membrane conductivity correlated with the hydrophobicity of constituent amino acid residues (Figure 1). A similar correlation was found with the antimicrobial potency. A simple model for the effect of these peptides on lipid bilayers is proposed based on their steric packing in the membrane.[2]

[1] Willcox, M. D.; Hume, E. B.; Aliwarga, Y.; Kumar, N.; Cole, N., A novel cationic-peptide coating for the prevention of microbial colonization on contact lenses. *Journal of Applied Microbiology* 2008,

105 (6), 1817-25.

Cranfield, C. G.; Berry, T.; Holt, S. A.; Hossain, K. R.; Le Brun, A. P.; Carne, S.; Al Khamici, H.; Coster, H.; Valenzuela, S. M.; Cornell, B., Evidence of the Key Role of H<sub>3</sub>O<sup>+</sup> in Phospholipid Membrane Morphology. *Langmuir* 2016, 32 (41), 10725-10734.

117

## Investigating the role of conformational change in gating and conduction of KIR K<sup>+</sup> channels

Jacqui Gulbis<sup>1</sup> ; Katrina Black<sup>2</sup> ; David Miller<sup>3</sup> ; Brian Smith<sup>4</sup> ; Derek Laver<sup>5</sup> ; Jani Bolla<sup>6</sup> ; Paul Johnson<sup>5</sup> ; Carol Robinson<sup>6</sup> ; Adam Hill<sup>7</sup>

<sup>1</sup> *The Walter and Eliza Hall Institute*

<sup>2</sup> *Walter and Eliza Hall Institute*

<sup>3</sup> *WEHI*

<sup>4</sup> *LaTrobe University*

<sup>5</sup> *The University of Newcastle*

<sup>6</sup> *The University of Oxford*

<sup>7</sup> *Victor Chang Cardiac Research Institute*

**Corresponding Author(s):** black@wehi.edu.au

It is essential that potassium (K<sup>+</sup>) levels within cells be finely controlled for normal behaviour of cells, tissues and organisms. Potassium channels are highly selective pores that allow K<sup>+</sup> diffusion across cell membranes and so control K<sup>+</sup> levels in a highly regulated process. Channels rapidly switch between permissive and restrictive states in a process known as ‘gating’. Conventionally, it is thought that K<sup>+</sup> channels gate by undergoing a conformational change, with ‘open’ channels containing a wide pore mouth, and ‘closed’ channels a constricted mouth, such that a fully hydrated K<sup>+</sup> ion (~8 Å) cannot transit through the channel.

The Gulbis lab has investigated the gating phenomenon in the KIR subfamily of potassium channels. By covalently linking adjacent subunits together, movement at the pore mouth could be constrained, limiting the channel to its narrow or ‘closed’ state. Crosslinking was inspected by a variety of biophysical techniques, including X-ray crystallography, SDS-PAGE and native mass spectrometry. The functional capacity of locked relative to non-locked channels was then assessed by means of a bulk fluorometric liposomal flux assay.

Unexpectedly, it was found that pore-aperture limited KIR channels were able to conduct potassium readily. This result questions the conventional understanding of KIR channel gating and implies that gating may not be due to simple steric effects.

140

## Single-molecule analysis of HIV-1 capsid uncoating

Till Boecking<sup>None</sup>

**Corresponding Author(s):** till.boecking@unsw.edu.au

HIV-1 uses its capsid to evade immune detection while it initiates reverse transcription of its RNA genome en route from the cell periphery to the nucleus. The capsid is assembled from 1000-1500 copies of a single viral protein, CA, into a conical fullerene structure composed of CA hexamers and pentamers. Disassembly or “uncoating” of the metastable capsid releases the viral DNA prior to import into the nucleus. Current models postulate that uncoating initiates either in the cytoplasm

or after the capsid has docked at the nuclear pore. In either scenario, the initiation and propagation of disassembly are thought to be controlled by host proteins and small molecules that are recruited to the capsid at different stages after cell entry.

To understand the intrinsic capsid disassembly pathway and how it can be modulated, we recently developed a single-particle fluorescence microscopy method to follow the real-time uncoating kinetics of authentic HIV capsids *in vitro* immediately after permeabilising the viral membrane. Our assay allows us to track the dynamic interactions of proteins with the capsid, pinpoint the precise moment at which the capsid develops its first defect, and visualise the kinetics of lattice disassembly thereafter.

Here we report the effect of small capsid-binding molecules on the kinetics of uncoating. The small molecule PF74 is a potent inhibitor of HIV replication, which binds in a pocket between CA subunits in a hexamer. It has been reported to stabilise self-assembled CA tubes *in vitro* but destabilises HIV cores in cells. In our single-particle imaging assay, PF74 uncoupled the step of capsid opening from lattice disassembly. PF74 accelerated capsid opening but prevented disassembly of the ruptured lattice. This observation reconciles the previous ambiguity regarding the mode of action of PF74. It stabilises CA lattices, but in a manner that makes it incompatible with a closed structure. Binding rapidly leads to capsid rupture in a manner that releases little CA but removes the barrier for free diffusion of proteins. The small molecule hexacarboxybenzene binds to a conserved arginine cluster in the central pore of the CA hexamer. In our assay, addition of hexacarboxybenzene dramatically slowed down the removal of the first capsomer but did not prevent subsequent lattice disassembly. This observation suggests that polyanions bound to the central pore enhance the lifetime of the closed core as it travels through the cytoplasm.

Taken together, our observations suggest that different stages of uncoating can be controlled independently with the interplay between different capsid-binding regulators likely to determine the overall uncoating kinetics.

201

## Metabolic reprogramming in Cancer

Kristin Brown<sup>1</sup>

<sup>1</sup> *Peter MacCallum Cancer Centre*

**Corresponding Author(s):** kristin.brown@petermac.org

Metabolic reprogramming is a hallmark of cancer now widely recognised to play a critical role in transformation and tumour progression. In recent years, there has been growing interest in developing strategies to exploit the metabolic vulnerabilities of cancer cells for therapeutic gain. However, our ability to do this is dependent on a thorough understanding of the ways in which cancer cell metabolism is influenced by cell-intrinsic and cell-extrinsic factors.

In cancer cells, signalling networks downstream of oncogenes affect metabolic pathways. Our recent studies have focussed on the oncogenic transcriptional co-activator YAP, a master regulator of organ size and tumourigenesis. Aberrant activation of YAP is widespread in human cancers yet, there is little knowledge regarding mechanisms by which YAP drives tumourigenesis. We find that YAP overexpression induces *de novo* lipogenesis *in vitro* and *in vivo*. Mechanistically, this phenomenon is dependent on the ability of YAP to induce transcriptional upregulation of serum- and glucocorticoid-regulated kinase 1 (SGK1), an effector of the oncogenic phosphoinositide 3-kinase (PI3K) pathway. Downstream of YAP, SGK1 promotes mTORC1 signalling leading to activation of the sterol regulatory element-binding proteins (SREBP1/2), master regulators of lipid metabolism. Importantly, we find that inhibition of key enzymes in the *de novo* lipogenesis pathway blocks the uncontrolled proliferation associated with YAP-driven transformation *in vitro* and *in vivo*. Our data reveal a mechanism of crosstalk between two important oncogenic signalling pathways and reveal a metabolic vulnerability that can be targeted to disrupt oncogenic YAP/PI3K pathway activity.

The environment also has a major influence on cancer cell metabolism. Our studies have focussed on characterising metabolic reprogramming events triggered upon chemotherapy exposure. Using *in vitro* and *in vivo* metabolomic profiling of triple-negative breast cancer (TNBC) cells, we find that an increase in the abundance of pyrimidine nucleotides occurs in response to chemotherapy exposure. Mechanistically, the increase in pyrimidine nucleotides induced by chemotherapy is dependent on enhanced activity of the *de novo* pyrimidine synthesis pathway. We find that pharmacological inhibition of *de novo* pyrimidine synthesis sensitizes TNBC cells to genotoxic chemotherapy agents by exacerbating DNA damage. Moreover, combined treatment with doxorubicin and leflunomide, a clinically approved inhibitor of the *de novo* pyrimidine synthesis pathway, induces regression of TNBC xenografts. Our studies provide pre-clinical evidence to demonstrate that adaptive reprogramming of *de novo* pyrimidine synthesis represents a metabolic vulnerability that can be exploited to improve the anti-cancer activity of genotoxic chemotherapy agents for the treatment of TNBC.

29

## Understanding Piezo1's Relationship with Lipids

**Author(s):** Amanda Buyan<sup>1</sup>

**Co-author(s):** Charles Cox<sup>2</sup>; Jonathan Barnoud<sup>3</sup>; Boris Martinac<sup>2</sup>; Siewert-Jan Marrink<sup>3</sup>; Ben Corry<sup>1</sup>

<sup>1</sup> *Australian National University*

<sup>2</sup> *Victor Chang Cardiac Institute*

<sup>3</sup> *University of Groningen*

**Corresponding Author(s):** amanda.buyan@anu.edu.au

The sensations of touch and hearing, along with many other physiological processes, require cells to be able to sense and react to mechanical stimuli. One way this is done is via membrane embedded mechanically gated channels. These channels can detect forces through deformation of the lipid bilayer, deemed the “force-from-lipids” principle. Bacterial homologues, such as MscL and MscS, exemplify this principle and have been studied for the past couple of decades, and have contributed greatly to our understanding of mechanically gated channels. However, understanding the underlying molecular force sensing mechanisms, and how similar bacterial and eukaryotic mechanosensitive channels are in terms of their gating mechanisms, remains an open question.

The recent discovery and structure elucidation of the first eukaryotic mechanically gated channels, named the PIEZO family, allows for the mechanisms of mechanical gating to be studied in higher organisms. Since their discovery, PIEZO channels have been implicated in many cellular processes, but the gating mechanism and the role that lipids play in PIEZO's mechanics remain elusive. To this end, we are using a combination of electrophysiology and molecular simulations to understand protein-lipid interactions between Piezo1 and relevant lipids in model mammalian bilayers, and ultimately the role that lipids have on Piezo1's activation. We are able to show that piezo has specific interactions with a number of membrane components that likely play a role in mediating the bilayer-protein interaction.

Amanda Buyan has been nominated for the Young Biophysicist Award.

34

## Solvation Free Energy Prediction of Alzheimer's Proteins Using Deep Learning

**Author(s):** SeoungHee Byen<sup>1</sup>

**Co-author(s):** Sihyun Ham<sup>1</sup>

<sup>1</sup> Sookmyung Women's University

**Corresponding Author(s):** qusj711@naver.com

Alzheimer's disease is known to be associated with the aggregation of A $\beta$ 42 and Tau43 proteins which are intrinsically disordered proteins (IDPs). Solvation free energies and internal energies of proteins reflect the free energy landscape of the proteins in water, and solvation free energy is also a key parameter to understand protein aggregation. In this study, we utilized the deep learning technique to develop machines predicting the solvation free energy of the proteins. We compared two machines using deep neural network (DNN) and convolution neural network (CNN), in which the contact maps of proteins are used directly or pre-processed by convolution. We report that the correlation coefficients between predicted and reference values of all the energies are greater than 0.90, and DNN predicts slightly better than CNN. This study also shows that protein contact maps are important input features for predicting solvation free energy. We believe that our result is useful in studying the thermodynamic properties of the proteins.

47

## **A Grouper Iridovirus GIV66: a Bcl-2 protein that inhibits apoptosis by exclusively sequestering Bim**

Sofia Caria<sup>1</sup> ; Suresh Banjara<sup>2</sup> ; Tim Ryan<sup>3</sup> ; Marc Kvansakul<sup>1</sup>

<sup>1</sup> La Trobe University

<sup>2</sup> LaTrobe University

<sup>3</sup> Australian Synchrotron

**Corresponding Author(s):** s.caria@latrobe.edu.au

Programmed cell death or apoptosis is a critical mechanism for the controlled removal of damaged or infected cells, and proteins of the Bcl-2 family are important arbiters of this process. Viruses have been shown to encode for functional and structural homologues of Bcl-2 to counter premature host cell apoptosis to ensure viral proliferation and/or survival. Grouper iridovirus (GIV) is a large DNA virus belonging to the iridoviridae family that harbors GIV66, a putative Bcl-2 like protein. GIV66 is a mitochondrially localized inhibitor of apoptosis, however the molecular and structural basis of apoptosis inhibition is currently not understood. Apoptosis occurs through the perforation of the mitochondria outer membrane by Bak and Bax that will lead to the activation of the caspase cascade. To gain insight into the mechanism of action through which GIV66 blocks this mitochondria outer membrane permeabilization, we systematically evaluated the ability of GIV66 to bind peptides spanning the BH3 domain of proapoptotic Bcl-2 family members. Our data reveal that GIV66 harbours an unusually high level of specificity for pro-apoptotic Bcl-2, and only engages with Bim. We then determined crystal structures of both GIV66 on its own as well as bound to Bim BH3. Unexpectedly, GIV66 forms dimers via a novel interface that occludes access to the canonical Bcl-2 ligand binding groove, which break apart upon Bim binding. These data suggest that GIV66 dimerisation impacts on the ability of GIV66 to bind and select host pro-death Bcl-2 protein. Our findings provide a mechanistic understanding for the potent anti-apoptotic activity of GIV66 by identifying it as the first single specificity pro-survival Bcl2 protein and demonstrating the pivotal role of Bim for GIV mediated inhibition of apoptosis.

135

## **Measuring height-dependant nanopillar bending stiffness**

Vi Khanh Truong<sup>1</sup> ; Jason Wandiyanto<sup>2</sup> ; Andrew S. M. Ang<sup>3</sup> ; Samuel Cheeseman<sup>4</sup> ; Aaron Elbourne<sup>5</sup> ; Christopher C. Berndt<sup>5</sup> ; Shane MacLaughlin<sup>6</sup> ; XiuMei Xu<sup>7</sup> ; Russell Crawford<sup>8</sup> ; Elena Ivanova<sup>8</sup>

<sup>1</sup> School of Science, RMIT University



<sup>2</sup> Swinburne University of Technology

<sup>3</sup> School of Engineering, Faculty of Science, Engineering and Technology, Swinburne University of Technology, Hawthorn, Australia

<sup>4</sup> School of Science, RMIT

<sup>5</sup> School of Engineering, Faculty of Science, Engineering and Technology, Swinburne University of Technology, Hawthorn, Australia

<sup>6</sup> BlueScope Steel Research, Port Kembla, NSW, Australia

<sup>7</sup> IMEC, Kapeldreef 75, Leuven 3001, Belgium

<sup>8</sup> RMIT University

**Corresponding Author(s):** sam.cheeman@gmail.com

Recent advances in nanotechnology have led to the emerging field of nanobiotechnology [1, 2]. In particular, vertical nanopillar array platforms have been widely fabricated for a number of biotechnological applications, e.g. either supporting mammalian cell growth or killing bacterial cells. These mechano-responsive events happening at the interface between nanopillar and cell membrane of both mammalian and bacterial cells are strongly influenced by the mechanical characteristics of nanopillars, in particular bending stiffness. The mechanical characteristics of free standing nanopillars have been theoretically estimated [3]; however, there are limited studies on direct measurement of nanopillar bending stiffness. In this work, we had employed electron beam lithography to fabricate nanopillar arrays with various heights of 220, 360, 420, 480 and 590 nm in order to directly estimate exact bending stiffness values. Hysitron nanoindenter equipped with diamond Berkovich tip was used to record the indentation force curve of Berkovich tip interacting with nanopillared surfaces. The geometry of the tip and nanopillar allows monitoring the Berkovich tip bending a single nanopillar. Bending stiffness of 220, 360, 420, 480 and 590 nm nanopillars was estimated to be 1.65, 0.73, 0.66, 0.45 and 0.31 nN/nm, respectively. The experimental and theoretical values for the nanopillar with the defined heights are well correlated within 10% variation. This approach presented here informs the design parameters for next-generation, physical nanopillared materials for biomedical applications.

#### ACKNOWLEDGEMENTS

Funding from the Australian Research Council Industrial Transformation Research Hubs Scheme (Project Number IH130100017) is gratefully acknowledged.

#### REFERENCES

- M.A. Bucaro, Y. Vasquez, B.D. Hatton, J. Aizenberg, Fine-tuning the degree of stem cell polarization and alignment on ordered arrays of high-aspect-ratio nanopillars, *ACS Nano* 6(7) (2012) 6222-6230.
- V.K. Truong, N.M. Geeganagamage, V.A. Baulin, J. Vongsvivut, M.J. Tobin, P. Luque, R.J. Crawford, E.P. Ivanova, The susceptibility of *Staphylococcus aureus* CIP 65.8 and *Pseudomonas aeruginosa* ATCC 9721 cells to the bactericidal action of nanostructured *Calopteryx haemorrhoidalis* damselfly wing surfaces, *Applied Microbiology and Biotechnology* 101(11) (2017) 4683-4690.
- A.G.N. Sofiah, M. Samykano, K. Kadirgama, R.V. Mohan, N.A.C. Lah, Metallic nanowires: Mechanical properties – Theory and experiment, *Applied Materials Today* 11 (2018) 320-337.

151

## A crystallographic study into the structural basis of chloride permeation in the archaeal aspartate transporter, GltPh

Ichia Chen<sup>1</sup> ; Josep Font Sadurni<sup>2</sup> ; Robert Vandenberg<sup>2</sup> ; Renae Ryan<sup>2</sup>

<sup>1</sup> The University of Sydney

<sup>2</sup> University of Sydney

**Corresponding Author(s):** iche4489@uni.sydney.edu.au

The excitatory amino acid transporters (EAATs) play a paramount role in the maintenance of glutamatergic neurotransmission within the synapse. These secondary active transporters enable rapid

glutamate reuptake into glial cells and neurons, and in addition, possess a thermodynamically uncoupled, substrate-activated chloride channel function. Abnormal channel activity has been directly associated with the pathogenesis of episodic ataxia and epilepsy [1], however, its physiological roles in normal brain function remain poorly understood. Moreover, the structural and mechanistic basis for chloride channel activation are unclear as none of the existing crystal structures of EAAT1 or the archaeal homolog, GltPh display an open channel. Here, we investigated chloride permeation in GltPh, using X-ray crystallography. Crystal structures of GltPh have been previously solved in the outward-facing, intermediate outward-facing and inward-facing state, revealing an elevator-like mechanism of substrate transport. This requires a large downward movement of a substrate-containing transport domain along a scaffold domain which remains anchored to the membrane [2]. It is hypothesised that during the elevator movement of the transport domain, a continuous open pore of the channel will transiently form at the interface of the two domains. We employed a disulfide crosslinking strategy to trap the transporter in a chloride conducting conformation. This study presents several crystal structures at various stages of the substrate transport cycle, which were solved in an attempt to visualise the open channel state of the transporter.

[1] Parinejad N, Peco E, Ferreira T, Stacey SM, van Meyel DJ (2016). Disruption of an EAAT-Mediated Chloride Channel in a *Drosophila* Model of Ataxia. *J Neurosci* 36: 7640-7647.

Ryan RM, Vandenberg RJ (2016). Elevating the alternating-access model. *Nat Struct Mol Biol* 23: 187-189.

127

## Using bacterial biosensor proteins to evaluate SAXS-based screening

Po-chia Chen<sup>1</sup> ; Pawel Masiewicz<sup>1</sup> ; Kathryn Perez<sup>1</sup> ; Dmitri Svergun<sup>2</sup> ; Janosch Hennig<sup>1</sup>

<sup>1</sup> *EMBL Heidelberg*

<sup>2</sup> *EMBL Hamburg*

**Corresponding Author(s):** pchen@embl.de

The entire arsenal of biophysical tools are currently being employed as means discover potential pharmacological leads. In this context, small-angle X-ray scattering (SAXS) offers useful complementary information to initial high-throughput assays based on thermodynamics, protein function, and other modes. However, it has hitherto been under-utilised as a screening tool, and we believe one factor is a lack of an appropriate benchmark that can be tested across different beamlines and benchtop sources, and used to formulate expectations for prospective users on aspects of material consumption, throughput and precision.

We will report the state of progress in evaluating bacterial periplasmic binding proteins as a candidate for benchmarking. A set of amino-acid uptake proteins HisBP, DEBP, GlnBP, and LAOBP was chosen to cover affinities ranges between nM to mM, and screened at ESRF Grenoble at concentrations between 0.5-4 mg/ml. The twelve-point SAXS-titrations are used to predict the selectivity profile of respective proteins, and compared against values derived from ITC and NMR.

15

## TDP-43 aggregation and therapeutic development in neurodegenerative diseases

Yun-Ru Chen<sup>None</sup>

**Corresponding Author(s):** yrchen@gate.sinica.edu.tw

TDP-43 proteinopathies were found in several neurodegenerative diseases including frontotemporal lobar dementia (FTLD), amyotrophic lateral sclerosis (ALS), and Alzheimer's disease (AD). TDP-43 inclusion bodies are poly-ubiquitin positive and comprise hyperphosphorylated full-length and truncated TDP-43. In 2014, we demonstrated for the first time that full-length TDP-43 forms toxic and spherical oligomers in vitro and in vivo. The full-length TDP-43 forms spherical oligomers that share common epitopes with amyloid oligomers. The TDP-43 oligomers are neurotoxic and capable to transform Alzheimer's amyloid- $\beta$  ( $A\beta$ ) to  $A\beta$  oligomers. We further found TDP-43 interacts with  $A\beta$  in the early stage. Besides, hyperphosphorylated mimetics of TDP-43, S5D, was examined and the result showed that S5D TDP-43, but not WT, is prone to form amyloid fibrils. Meanwhile, we generated a TDP-43 oligomer specific antibody, TDP-O, and validated the species in FTLD-TDP, ALS, and AD patients. The TDP-O antibody has high specificity toward TDP-43 oligomers, but does not recognize native TDP-43 in the nucleus. Furthermore, we are able to rescue the motor function and pathology in ALS TDP-43 model mice upon intravenous administration of mTDP-O antibody. Therefore, this unique property provides the antibody a great potential for diagnostic and therapeutic development.

[1] Yu-Sheng Fang, Kuen-Jer Tsai, Yu-Jen Chang, Patricia Kao, Rima Woods, Pan-Hsien Kuo, Cheng-Chun Wu, Jih-Ying Liao, Shih-Chieh Chou, Vinson Lin, Lee-Way Jin, Hanna S. Yuan, Irene H Cheng, Pang-Hsien Tu, and Yun-Ru Chen. "Full-Length TDP-43 Forms Toxic Amyloid Oligomers that are Present in Frontotemporal Lobar Dementia-TDP Patients." (corresponding author) *Nature Communications*, 5:4824 (2014).

Patricia F. Kao, Yun-Ru Chen, Xiao-Bo Liu, Charles DeCarli, William W. Seeley, and Lee-Way Jin\*. Detection of TDP-43 oligomers in frontotemporal lobar degeneration-TDP. (2015) (*Annals of Neurology*, 78(2):211-21).

19

## Mechano-redox control of integrin de-adhesion

Joyce Chiu<sup>1</sup> ; Freda Passam<sup>2</sup> ; Lining Ju<sup>2</sup> ; Aster Pijning<sup>3</sup> ; Zeenat Jahan<sup>4</sup> ; Ronit Mor-Cohen<sup>5</sup> ; Adva Yeheskel<sup>5</sup> ; Katra Kolšek<sup>6</sup> ; Camilo Aponte-Santamaria<sup>6</sup> ; Frauke Gräter<sup>6</sup> ; Philip J. Hogg<sup>1</sup>

<sup>1</sup> *The University of Sydney*

<sup>2</sup> *Heart Research Institute*

<sup>3</sup> *The Centenary Institute*

<sup>4</sup> *St George Clinical School*

<sup>5</sup> *Tel Aviv University*

<sup>6</sup> *Heidelberg Institute of Theoretical Studies*

**Corresponding Author(s):** joyce.chiu@sydney.edu.au

Many proteins embedded in a cell's surface allow the cell to interact with its surroundings. Integrins are a group of cell surface proteins that have many uses in different cells. Integrins become activated when they come into contact with other specific proteins, which like other molecules that bind to proteins are referred to collectively as "ligands". Much research has focused on how ligands become attached to integrins and how this activates these cell surface proteins. Yet how integrins release ligands and become inactive has not been studied before. One type of integrin, called  $\alpha$ IIb $\beta$ 3, is involved in blood clotting. Found on the surface of blood platelets – the fragments of cells in the blood that play a central role in clotting, this integrin binds to a ligand called fibrinogen. Fibrinogen links platelets together to form clots by building bridges between integrins. Here we describe how ligand binding and force combine to trigger a chemical event which controls the adhesive properties of  $\alpha$ IIb $\beta$ 3 [1]. Our studies of the secreted platelet oxidoreductase, ERp5, have revealed that it mediates release of fibrinogen from activated platelet  $\alpha$ IIb $\beta$ 3 integrin. Protein chemical studies show that ligand binding to extended  $\alpha$ IIb $\beta$ 3 integrin renders the  $\beta$ I-domain Cys177-Cys184 disulphide bond cleavable by ERp5. Fluid shear and force spectroscopy assays indicate that disulphide cleavage is enhanced by mechanical force. Cell adhesion assays and molecular dynamics simulations demonstrate that cleavage of the disulphide induces long-range allosteric effects within the  $\beta$ I-domain, mainly affecting the metal-binding sites, that results in release of fibrinogen. This coupling of ligand binding,

force and redox events to control cell adhesion may be employed to regulate other protein-protein interactions.

[1] F. Passam, J. Chiu et al ELife. 7, e34843 (2018).

26

## The architecture of the membrane associated retromer-sorting nexin complex revealed by cryo-electron tomography

Brett Collins<sup>1</sup>

<sup>1</sup> *The University of Queensland*

**Corresponding Author(s):** b.collins@imb.uq.edu.au

Compartmentalisation is a defining feature of all eukaryotic cells, and we have evolved highly sophisticated protein machineries to control the flow of transmembrane molecules and membrane lipids between different organelles. The retromer protein complex is required for generating cargo-selective tubulovesicular carriers from endosomal membranes (1). Retromer-mediated trafficking is an essential process in all eukaryotes, controlling the cellular localisation and homeostasis of hundreds of transmembrane proteins, and its disruption is associated with major neurodegenerative disorders (2). However, how retromer is assembled and how it is recruited to form membrane tubules remains unknown. Here we describe the structure of the *Chaetomium thermophilum* trimeric retromer complex (Vps26-Vps29-Vps35) assembled on membrane tubules with the sorting nexin protein Vps5, using X-ray crystallography, molecular modelling and cryo-electron tomography with sub-tomogram averaging at sub-nanometre resolution (3). The structure reveals two interwoven layers where Vps5 forms a membrane-associated lattice, while the outer lattice consists of arches of retromer that extend away from the membrane surface. Vps35 forms the legs of these arches, Vps29 sits at the apex where it is free to interact with regulatory factors, and the feet of the arches connect to each other through Vps26. Vps26 also forms the primary interface with Vps5 via the same site previously shown to mediate Snx3 and cargo interactions (4), suggesting the existence of distinct retromer-sorting nexin complexes. The architecture of the tubulovesicular retromer coat revealed here provides key insights into the conserved mechanisms of retromer assembly and retromer-mediated endosomal trafficking.

### References

1. Seaman, M. N. The retromer complex - endosomal protein recycling and beyond. *Journal of cell science* 125, 4693-4702, (2012).
2. McMillan, K. J., Korswagen, H. C. & Cullen, P. J. The emerging role of retromer in neuroprotection. *Current opinion in cell biology* 47, 72-82, (2017).
3. Kovtun, O., Leneva, N., et al. Owen, D.J., Briggs, J.D. and Collins, B.M. Structure of the membrane-assembled retromer coat determined by cryo-electron tomography. *Nature*. ePub. (2018).
4. Lucas, M. et al. Structural Mechanism for Cargo Recognition by the Retromer Complex. *Cell* 167, 1623-1635 e1614, (2016).

38

## Quantifying Protein Foldedness at the Proteome-Wide Scale

**Author(s):** Dezeræe Cox<sup>1</sup>

**Co-author(s):** Gavin Reid ; Yuning Hong ; Danny Hatters

<sup>1</sup> *Department of Biochemistry and Molecular Biology, Bio21 Institute, University of Melbourne*

**Corresponding Author(s):** dezerae.cox@unimelb.edu.au

Cells have an extensive quality control network responsible for maintaining proteostasis. This network regulates protein synthesis, folding and transport. Proteostasis is often severely imbalanced in neurodegenerative diseases such as Alzheimer's and Motor Neuron diseases, permitting the characteristic aggregation and deposition of vulnerable proteins. After decades of dedicated examination, the folding and stability characteristics of many individual proteins are well understood in vitro. However, understanding the process of protein folding and unfolding in live cells remains a grand challenge. A key limitation to probing protein folding within a biological context is the capacity to quantitatively assess the folding status of individual proteins at the proteome-wide scale. We have recently developed a fluorogenic thiol-binding dye (TPE-MI) that can capture a snapshot of the balance of unfolded protein relative to folded states in intact live cells [1]. This approach does not require any expression of specific protein reporters, and has the potential to offer single-protein folding information for endogenous proteins at a proteome-wide scale. Here, we describe the development and application of this probe to determine proteome foldedness in cells following a variety of stressors. This represents an invaluable tool which will empower researchers to quantitatively probe proteome foldedness across diverse disease states in a variety of model organisms.

[1] M.Z. Chen, N.S. Moily, J.L. Bridgford, R.J. Wood, M. Radwan, T.A. Smith, et al., *Nature Communications*, 8, 474 (2017)

102

## Studying the effect of membrane curvature and composition on MLKL binding and permeabilisation using model membrane systems

Katherine Davies<sup>1</sup>; Jan Steinkuehler<sup>2</sup>; Eric Hanssen<sup>3</sup>; Rumiana Dimova<sup>2</sup>; Emma Petrie<sup>4</sup>; James Murphy<sup>5</sup>; Peter Czabotar<sup>5</sup>

<sup>1</sup> *Walter and Eliza Hall Institute of Medical Research, Parkville 3052, Australia*

<sup>2</sup> *Max Planck Institute of Colloids and Interfaces, Golm Science Park 14476, Germany*

<sup>3</sup> *Bio21 Molecular Science and Biotechnology Institute, The University of Melbourne, Parkville 3052, Australia*

<sup>4</sup> *The Walter and Eliza Hall Institute*

<sup>5</sup> *Walter and Eliza Hall Institute*

**Corresponding Author(s):** [davies.k@wehi.edu.au](mailto:davies.k@wehi.edu.au)

Necroptosis is a form of programmed cell death characterized by lack of caspase activity and a loss of plasma membrane integrity. Morphologically similar to necrosis, in the act of necroptosis, the plasma membrane is disrupted, causing release of cellular components to the extracellular fluid and an ensuing inflammatory response. Necroptosis proceeds via a regulated kinase cascade involving Receptor Interacting Protein Kinases RIPK1 and RIPK3. Mixed Lineage Kinase domain-Like protein (MLKL), a pseudokinase, is the final known obligate effector essential for the execution of necroptosis. Whilst the MLKL pseudokinase domain is incapable of catalysing phosphotransfer reactions, it is the site of RIPK3 phosphorylation. This phosphorylation event is thought to be integral to flipping a molecular switch regulated by the pseudokinase domain, resulting in activation of MLKL. Upon activation, MLKL oligomerises and translocates to the plasma membrane, and is there thought to play a destabilising role. Details of MLKL's molecular mechanism of action, such as the stoichiometry of oligomerisation and how it interacts with the plasma membrane, remain unknown.

To understand better how MLKL might disrupt the plasma membrane as the cell undergoes necroptosis, we have performed a study of MLKL's activity on a variety of model membrane systems: small unilamellar vesicles, giant unilamellar vesicles and floating supported bilayers. We also examined MLKL's activity on phase separated membranes. We have shown for the first time that MLKL preferentially binds to lipid disordered domains and is capable of forming higher order structures on the membrane. By using a range of techniques such as confocal and cryo-electron microscopy, dye release assays and neutron reflectometry, we are able to combine qualitative images of MLKL on membranes with binding and kinetic data to suggest how MLKL may interact with the plasma membrane and disrupt it, and how factors such as membrane curvature and lipid composition affect this process.

100

## The Effect of H<sub>3</sub>O<sup>+</sup> on the Structure and Dynamics of Interfacial Water in Phospholipid Bilayers

**Author(s):** Evelyne Deplazes<sup>1</sup>

**Co-author(s):** David Poger<sup>2</sup>

<sup>1</sup> Curtin University

<sup>2</sup> The University of Queensland

**Corresponding Author(s):** evelyne.deplazes@curtin.edu.au

The plasma cell membrane forms the physical boundary between the cell interior and its external environment. While the lipid bilayer forms the main component of the cell membrane, it is more than a 'low dielectric, planar slab'. The local composition, structure and dynamics of the cell membrane play an active role in many physiological process including the permeation of solutes, membrane fusion and the stability of membrane proteins. In addition, the water that sits at the water-lipid interface, the so called interfacial water, shows properties that deviate from 'bulk' water and it has been proposed this interfacial water should be treated as a structural and functional component of the membrane [1]. Both the membrane structure and the properties of interfacial water are affected by environmental factors such as temperature, ionic strengths and pH; of which the latter is poorly understood.

In a recent study [2], we used molecular dynamics (MD) simulations to show that in the presence of hydronium ions (H<sub>3</sub>O<sup>+</sup>) the phospholipid bilayers show increased membrane thickness and reduced area per lipid, in agreement with previous experimental data [3]. In the present study, we focus on how H<sub>3</sub>O<sup>+</sup> ions affect the structure and dynamics of interfacial water. For this, data from multiple  $\mu$ s-long unrestrained MD simulations of phospholipid bilayers as well as 'bulk' water in the presence and absence of H<sub>3</sub>O<sup>+</sup> were analysed. Consistent with previous studies, our data shows that compared to bulk, interfacial water has an increased survival probability, a preferred orientation of the water dipole and a reduced orientation relaxation. Furthermore, analysis from simulations in the presence of H<sub>3</sub>O<sup>+</sup> suggests that certain properties of interfacial water are unaffected by the H<sub>3</sub>O<sup>+</sup> ions while others show clear differences. For example, there appears to be no difference in the average survival probability, water orientation relaxation as well as the hydrogen bond lifetimes for interfacial water in the presence or absence of H<sub>3</sub>O<sup>+</sup>. In contrast, the dipole orientation of the interfacial water molecules change in the presence of H<sub>3</sub>O<sup>+</sup> ions. This is most likely a consequence of the changes in the P-N dipole vector of the lipid head groups that interact with the H<sub>3</sub>O<sup>+</sup> ions. In addition, the layer of interfacial water in which the dipole deviates from the random orientation in bulk is thicker in the presence of H<sub>3</sub>O<sup>+</sup>.

[1] Disalvo E.A. (ed.), Membrane Hydration - The Role of Water in the Structure and Function of Biological Membranes, (2015).

Deplazes, E.; Poger, D.; et. al, Physical Chemistry Chemical Physics, 1, 20, (2018).

Cranfield C.G., Berry T., et al., Langmuir, 32, (2016).

43

## Characterization of Amyloid Formation by Somatostatin-14: Role of Protofilaments in Heparin-Mediated Aggregation

Durga Dharmadana<sup>1</sup> ; Nicholas P. Reynolds<sup>2</sup> ; Charlotte E. Conn<sup>3</sup> ; Celine Valery<sup>1</sup>

<sup>1</sup> School of Health and Biomedical Sciences, RMIT University

<sup>2</sup> ARC Training Center for Biodevices, Swinburne University

<sup>3</sup> School of Science, RMIT University

**Corresponding Author(s):** durga.dharmadana@rmit.edu.au

Glycosaminoglycans (GAGs), such as heparin, have been reported to play a significant role in amyloid formation of a wide range of proteins/peptides either associated with diseases or native biological functions [1]. However, the specific mechanism by which GAGs promote amyloid formation and effects of GAGs on amyloid nanostructure are not fully understood. By combining microscopic, scattering and spectroscopic techniques we studied the influence of the GAG, heparin on the self-assembling kinetics, molecular structure, nanostructure morphology, and macroscopic phases of neuropeptide somatostatin-14 [2]. We show that two different types of assemblies are formed in the presence and absence of heparin, particulate precipitates, and liquid crystalline gels respectively. Despite the fact that both types of assemblies are reversible, heparin-peptide assembly showed slower release rate. Even though nanofibrils were observed for both types of assemblies, presence of heparin promotes the formation of unstructured aggregates. Thioflavin T assay results suggest that electrostatic interactions between positively charged peptide and negatively charged sulphate groups of heparin are the driving and limiting factor in the self-assembly process. According to infrared spectroscopic data, heparin hinders the formation of parallel  $\beta$ -sheet networks between protofilaments. Furthermore, SAXS data reveal that in the early stage of aggregation process, heparin promotes oligomer formation. Based on our results, we propose that, in the presence of heparin, the peptide rapidly precipitates into protofilaments intercalated by heparin which leads to relatively large and disordered precipitates in solution. Our findings provide insights into the nature of peptide-GAGs interactions and also highlight the danger of using GAGs in amyloid studies, particularly when concluding on structure-function relationships.

[1] D. Dharmadana, N.P. Reynolds, C.E. Conn and C. Valery, *Interface focus*. 7, 4 (2017).

D. Dharmadana, N.P. Reynolds, C. Dekiwardia, C.E. Conn and C. Valery, *Nanoscale*. (2018).

166

## Effects of Metal Ions on the Conformational Equilibria of the Na<sup>+</sup>/K<sup>+</sup>- and H<sup>+</sup>/K<sup>+</sup>- ATPases

Ronald Clarke<sup>1</sup> ; Dil Diaz<sup>1</sup> ; Flemming Cornelius<sup>2</sup>

<sup>1</sup> *University of Sydney*

<sup>2</sup> *University of Aarhus*

**Corresponding Author(s):**

The Na<sup>+</sup>/<sub>+</sub>K<sup>+</sup>- and H<sup>+</sup>/K<sup>+</sup>-ATPases are closely related ion pumps. The Na<sup>+</sup>/K<sup>+</sup>-ATPase is responsible for maintaining the electrochemical potential gradients for Na<sup>+</sup> and K<sup>+</sup> across the plasma membrane of all animal cells, which are crucial for numerous physiological functions. The H<sup>+</sup>/K<sup>+</sup>-ATPase is responsible for stomach acidification. Both enzymes exist in two main conformations, E1 and E2. The distribution of the enzymes between these two states determines their relative affinities for their substrate ions. Recent results [1] showed that the distribution of the Na<sup>+</sup>/K<sup>+</sup>-ATPase between the E1 and E2 states depends on the ionic strength of the solution. It was suggested that this is due to ionic strength screening of an electrostatic interaction stabilizing the E2 state relative to the E1. Because prior experiments have shown that the lysine-rich N-terminus of the Na<sup>+</sup>/K<sup>+</sup>-ATPase undergoes significant movement during the E2-E1 transition and it is known that the surrounding membrane contains a high content of negatively charged lipids, e.g. phosphatidylserine (PS), it was hypothesized that the electrostatic interaction could be between the N-terminus and the surrounding lipid membrane [1].

In this study we investigated the effect of mono-, di- and trivalent metal ions on the E2-E1 distribution of both the Na<sup>+</sup>/<sub>+</sub>K<sup>+</sup>-ATPase and H<sup>+</sup>/K<sup>+</sup>-ATPase. The E2-E1 distribution was quantified via a ratiometric fluorescence method utilising the probe eosin. Eosin binds to the ATP binding site of both proteins, but its binding affinity is dependent on the enzyme conformation. Hence the proportion of enzyme-bound and free eosin changes when the enzyme undergoes its E2-E1 transition. This is reflected in both a change in fluorescence intensity and a shift in the maximum excitation wavelength. The results obtained showed that the conformational equilibria of the Na<sup>+</sup>/<sub>+</sub>K<sup>+</sup>- and

H<sup>+</sup>/K<sup>+</sup>-ATPases are very sensitive to the presence of di- and trivalent metal ions. It is proposed that this could be due to specific binding of these ions to the negatively-charged headgroup of PS in the membrane around the proteins, thus causing release of the N-terminus from the membrane and stabilisation of the enzymes in the E1 conformation. Potentially such a mechanism could allow crosstalk between the Na<sup>+</sup>,K<sup>+</sup>-ATPase and the sarcoplasmic reticulum Ca<sup>2+</sup>-ATPase in muscle cells via the cytoplasmic Ca<sup>2+</sup> concentration and hence could play a role in the regulation of muscle contraction and relaxation.

[1] Jiang et al, *Biophys J* 112, 288-299 (2017).

180

## Intra- and intermolecular interactions studied by synchrotron far-IR spectroscopy

Annette Dowd<sup>1</sup> ; Rania Seoudi<sup>None</sup> ; Sara Pandidan<sup>None</sup> ; Adam Mechler<sup>2</sup>

<sup>1</sup> *UTS*

<sup>2</sup> *La Trobe University*

**Corresponding Author(s):** annette.dowd@uts.edu.au

Understanding folding and self assembly, such as in phospholipids forming a bilayer or peptide chains forming proteins, is key to understanding the way biological systems work. In these processes organisation of molecules takes place through weak non-covalent interactions, e.g. H-bonds and van der Waals interactions. The self assembly process is also dependent on environmental factors such as pH, salts and dielectric constant.

Unfortunately there still isn't a complete picture of how the many weak forces operate together to yield hierarchical structures or emergent behaviour such as phase transitions. For example, although calorimetric methods can identify the so-called main transition in phospholipid bilayers, they cannot identify the intermolecular interactions and changes in motion of different parts of the molecules which absorb the thermal energy. There is thus a need for experimental approaches to study these weak forces and the small structural changes they cause, particularly where standard crystallographic analysis is not available.

Infrared spectroscopy monitors molecular vibrations which depend on molecular configuration and packing. Mid-IR vibrational frequencies show only small shifts (typically < FWHM) when the moiety in question experiences a different conformational environment. In contrast, far-IR vibrational frequencies are known to be extremely sensitive to conformation and structural strain with modes shifting by more than 100 cm<sup>-1</sup>.

We have carried out measurements at the Australian Synchrotron Far-IR beamline on tripeptides, phospholipids and antimicrobial peptides using a cryostat with diamond liquid cell on both lyophilised and hydrated samples over a range of temperatures. Far-IR vibrational measurements show distinctly different spectra for isometric tripeptides, indicating the sensitivity of this technique to small conformational differences (Fig. 1b) [1].

In fact, the subtle differences in structure of a tripeptide simulated with and without intramolecular H-bonding (see Fig. 1a) result in dramatically different calculated far-IR spectra. We have correlated such DFT calculations with our experimental spectra to obtain information about the peptide conformation [1]. We have also shown that far-IR spectroscopy is sensitive to changes in tripeptide superstructure resulting from precipitation out of different solvents. We will also show changes in head group motion and chain motion in phospholipids in hydrated liposomes under different conditions.

[1] R. S. Seoudi, A. Dowd, B. J. Smith and A. Mechler, *Phys. Chem. Chem. Phys.* 18, 11467 (2016).

176



## Protein labelling strategies at the National Deuteration Facility: isotopic labelling for NMR ( $^2\text{H}/^{13}\text{C}/^{15}\text{N}$ ) and neutron ( $^2\text{H}$ ) scattering

Anthony P Duff<sup>1</sup> ; Karyn L Wilde<sup>1</sup> ; Agata Rekas<sup>1</sup> ; Natalia Davydova<sup>1</sup> ; Peter J Holden<sup>1</sup>

<sup>1</sup> ANSTO

**Corresponding Author(s):** anthony.duff@ansto.gov.au

The National Deuteration Facility (NDF) at the Australian Nuclear Science and Technology Organisation (ANSTO) has developed reliable and robust methods for the deuteration and multiple isotope labelling of a broad range of proteins by recombinant expression in *Escherichia coli* BL21, for the support of neutron scattering and solution or solid-state NMR studies of proteins [1]. Deuterium ( $^2\text{H}$ ) and the isotopes  $^{13}\text{C}$  and/or  $^{15}\text{N}$  are introduced into our minimal defined growth medium utilised for biomass production using NDF methods for high-yield recombinant protein expression [1]. Partially deuterated and perdeuterated protein is produced for small angle neutron scattering (SANS) and neutron crystallography investigations, with triple- ( $^2\text{H}/^{15}\text{N}/^{13}\text{C}$ ) and double-labelled ( $^2\text{H}/^{15}\text{N}$ ) protein produced for NMR studies. Selectively-labelled ( $^{15}\text{N}/^{13}\text{C}$ ) protein has also been produced for NMR studies, with further method development continually undertaken to expand NDF capabilities. For example, production of ILV- and AILV- $^{13}\text{C}$ -methyl labelled protein in a  $^2\text{H}$  background is currently being developed and demonstrated with collaborator proposals.

An overview of the NDF facility and labelling methods will be presented along with some brief examples of published research utilising deuterated and multiple-labelled protein produced by the NDF [2-6].

Access to the NDF is available through an externally refereed proposal scheme. For further detail and information refer to <http://www.ansto.gov.au/ndf>.

The National Deuteration Facility is partially funded by the National Collaborative Research Infrastructure Strategy (NCRIS) – an initiative of the Australian Government.

[1] Duff AP, Wilde KL, Rekas A, Lake V, Holden PJ. Robust high-yield methodologies for  $^2\text{H}$  and  $^2\text{H}/^{15}\text{N}/^{13}\text{C}$  labelling of proteins for structural investigations using neutron scattering and NMR Methods in Enzymology, 565, 3-25 (2015).

Morris VK, Linser R, Wilde KL, Duff AP, Sunde M, Kwan AH. Solid-state NMR spectroscopy of functional amyloid from a fungal hydrophobin: a well-ordered  $\beta$ -sheet core amidst structural heterogeneity *Angewandte Chemie Int Ed*, 51, 12621-12625 (2012).

Christie MP, Whitten AE, King GJ, Hu SH, Jarrott RJ, Chen KE, Duff AP, Callow P, Collins BM, James DE, Martin JL. Low-resolution solution structures of Munc18:Syntaxin protein complexes indicate an open binding mode driven by the Syntaxin N-peptide *PNAS*, 109, 9816-9821 (2012)

Taylor JE, Chow JYH, Jeffries CM, Kwan AH, Duff AP, Hamilton W, Trewhella J. Calmodulin binds a highly extended HIV-1 MA protein that refolds upon its release *Biophys. J.*, 103, 541-549 (2012).

Golden E, Attwood PV, Duff AP, Meilleur F, Vrielink A. Production and characterization of recombinant perdeuterated cholesterol oxidase *Anal Biochem*, 485, 102-108 (2015).

Chen X, Wilde KL, Wang H, Lake V, Holden PJ, Middelberg APJ, He L, Duff AP. High yield expression and efficient purification of deuterated human protein galectin-2 *Food and Bioprocess Processing*, 90, 563-572 (2012).

81

## Protein conformation of C9 controls the final membrane complex assembly

Bradley Spicer<sup>None</sup> ; Ruby Law<sup>None</sup> ; Charles Bayly-Jones<sup>None</sup> ; Paul Conroy<sup>None</sup> ; Tom Caradoc-Davies<sup>None</sup> ; James Whisstock<sup>None</sup> ; Michelle Dunstone<sup>1</sup>

<sup>1</sup> Monash University

**Corresponding Author(s):** michelle.dunstone@monash.edu

MACPF/CDC pore forming proteins show a unique ability to self-assemble from soluble monomeric proteins into oligomeric rings that change conformation and insert into the target cell membrane. The MACPF/CDC family has been shown to form giant beta-barrel pores that oligomerise, typically using the same unit, and are capable of passive transport of whole soluble proteins across lipid membranes.

The current hypothesis suggests that oligomer assembly is mediated by: 1) binding to a lipid membrane and, 2) planar diffusion upon the target membrane. However, to date, this model is only consistent with pore forming proteins, such as CDCs and perforin, that have dedicated membrane binding domains. In contrast, the proteins of the Membrane Attack Complex (MAC) lack any membrane binding region, but can target a wide range of eukaryotic and bacterial surfaces. However, this precludes the MAC using membrane binding for assembly.

Here we show the first X-ray structure of the soluble C9 component of the MAC and compare this to the near atomic single particle cryo-EM structure of the 22-subunit polyC9. Together these structures show that a 22 amino acid region within the TMH1 loop obstructs oligomer assembly at the oligomer interface. Disulphide trap mutants demonstrate that TMH1 obstructs elongation and need to move position prior to binding of the next C9 unit in the oligomer assembly pathway.

These results challenge the existing dogma in MACPF/CDC pore assembly—that assembly is dependent on membrane binding and requiring lateral diffusion. Instead, movements of the TMH1 and possibly TMH2 of C9 drive MAC assembly. Accordingly, these results explain how the C9 component is able to self-oligomerise into the MAC without the need for lateral diffusion on a membrane and may explain the MAC's role in assembling on highly variable chemistries at the membrane surface of invading pathogens.

123

## Free energy simulations of general anaesthetic binding to a pentameric ligand-gated channel.

**Author(s):** Adam Dymke<sup>1</sup>

**Co-author(s):** Bogdan Lev<sup>2</sup>; Toby W Allen<sup>2</sup>

<sup>1</sup> RMIT

<sup>2</sup> School of Science, RMIT University, Melbourne, VIC 3001, Australia

**Corresponding Author(s):** adam.dymke@gmail.com

General Anaesthetics (GAs) are known to target pentameric ligand-gated channels (pLGICs) that are responsible for synaptic signal propagation in the central nervous system, but the mechanisms have remained a mystery for over a century. Despite recent identification of the molecular targets, it is still not fully understood how select compounds are able to either inhibit or potentiate pLGIC function by targeting different binding sites. This project seeks to elucidate the free energy surface defining binding and diffusion of GAs to pLGICs, and to provide molecular-level descriptions of their effects on pLGIC functional states. We have used enhanced sampling molecular dynamics simulations to investigate the binding of GA propofol to a mutant of the structurally-defined GLIC channel from the bacterium *Gloeobacter violaceus*, as a model for the human GABAAR channel associated with general anaesthesia. The structure and function of the pLGIC family is known to be largely conserved, such that the insights obtained should be relevant to all pLGICs, improving our understanding of general anaesthesia. Using metadynamics, with the aid of well-tempering and multiple-walker approaches, these simulations have observed three major binding sites, consistent with experimental data, and have led to observations of the pathways for propofol binding to the protein from solution and the host membrane. Supplemental free energy simulations of propofol translocating lipid bilayers have been used to validate the model against experimental partition coefficients, using umbrella sampling. The calculated free energy surface for GLIC, both in its open and closed states, enables quantitative measures of channel modulation to parallel experimental functional measurements. Combined with site-by-site calculations of propofol dissociation constants, and analysis of

the resultant structural changes that may affect conduction, we aim to explain how specific binding events cause channel inhibition or potentiation. The understanding gained from these simulations promises to aid future research into safer general anaesthetic compounds and extend scientific understanding of the function of the central nervous system.

24

## Force-dependent Ca<sup>2+</sup> signalling in cell filopodia

Artem Efremov<sup>1</sup>; Mingxi Yao<sup>1</sup>; Naila Alieva<sup>1</sup>; Alexander Bershadsky<sup>2</sup>; Jie Yan<sup>1</sup>

<sup>1</sup> *Mechanobiology Institute, National University of Singapore*

<sup>2</sup> *Weizmann Institute of Science*

**Corresponding Author(s):** mbiay@nus.edu.sg

Ca<sup>2+</sup> is a universal mediator of a large number of signalling pathways that concert behaviour of myriads proteins and enzymes in living cells. Recent discovery of mechanosensing Ca<sup>2+</sup>-dependent membrane channels, such as Piezo1 and Piezo2, suggests that Ca<sup>2+</sup> signalling pathway may also be one of the key parts contributing to the cell ability to sense mechanical properties of surrounding microenvironment. As it has been previously shown that filopodia play the central role in cell environment sensing and guidance of cell migration, we have investigated the role of mechanical forces in filopodia-dependent generation of intracellular Ca<sup>2+</sup> signals. It has been found that application of small stretching forces (~1-2pN) to filopodia leads to appearance of strong intra-filopodial Ca<sup>2+</sup> signals that propagate towards the cell body, frequently resulting in activation of Ca<sup>2+</sup> oscillations in the cell body. It has been found that this process is Piezo1 channels-independent. Furthermore, activation forces required for the initiation of intra-filopodial Ca<sup>2+</sup> signalling appear to be much smaller than previously reported values for Piezo1 channels, indicating that to probe mechanical properties of surrounding environment, cells may employ alternative molecular mechanisms different from those based on Piezo1 channels. Discovery of high sensitivity of intra-filopodial Ca<sup>2+</sup> signalling to extracellular forces provides new important insights into the role of filopodia in guidance of cell migration.

165

## Structural characterisation of a novel peptide from the Australian sea anemone *Actinia tenebrosa*

**Author(s):** Khaled Elnahriry<sup>1</sup>

**Co-author(s):** Dorothy Wai<sup>1</sup>; Krishnarjunaa Bankala<sup>1</sup>; Balasubramanyam Chittoor<sup>1</sup>; Christopher A. MacRaidl<sup>2</sup>; Noha N. Badawy<sup>1</sup>; Joachim M. Surm<sup>3</sup>; Peter J. Prentis<sup>4</sup>; Ray Norton

<sup>1</sup> *Medicinal Chemistry, Monash Institute of Pharmaceutical Sciences*

<sup>2</sup> *Medicinal Chemistry, Monash Institute of Pharmaceutical Sciences, Monash University*

<sup>3</sup> *School of Biomedical Sciences, Faculty of Health, Queensland University of Technology*

<sup>4</sup> *School of Earth, Environmental and Biological Sciences, Science and Engineering Faculty, Queensland University of Technology*

**Corresponding Author(s):** khaled.elnahriry@monash.edu

Sea anemone venoms have long been recognized as a rich source of peptides with interesting pharmacological and structural properties [1,2]. Our recent transcriptomic and proteomic studies of various Australian sea anemones have identified several novel peptides. UAITx-Ate1, from *Actinia tenebrosa*, is a 13-residue peptide containing a single disulphide bridge, with no homology to any previously reported sequences from anemones or other species. We have produced UAITx-Ate1 using solid-phase peptide synthesis, followed by oxidative folding and purification of the folded peptide

using reversed-phase high performance liquid chromatography. The structure of UAITx-Ate1 was determined by means of two-dimensional solution nuclear magnetic resonance (NMR) spectroscopy. A final ensemble of 20 lowest energy structures from 100 structures refined in implicit solvent using XPLOR-NIH resulted in moderately well-defined structures, with backbone and heavy atom RMSD values over all amino acid residues of 1.62 Å and 2.4 Å, respectively. A number of minor peaks in the NMR spectra were observed, suggesting the presence of a minor conformer. Diffusion-ordered NMR spectroscopy revealed that UAITx-Ate1 was monomeric in solution and that there were no intermolecular interactions. Chemical shift perturbations in the NMR spectra of UAITx-Ate1 in the presence of dodecylphosphocholine micelles suggest an interaction of UAITx-Ate1 with lipid membranes mediated by the region Ile4 - Arg8. Functional studies are currently being undertaken to ascertain the biological activity of UAITx-Ate1.

#### References

- R. S. Norton, *Toxicon*, 54, 1075 (2009).  
 P. J. Prentis, A. Pavasovic, and R. S. Norton, *Toxins*, 10, 36 (2018).

93

## Medicinal Chemistry Studies into 6-Substituted Hexamethylene Amiloride (HMA) Analogues as Inhibitors of the Human and Murine Urokinase Plasminogen Activators

Nehad Elsalamouny<sup>1</sup> ; Michael Kelso<sup>1</sup> ; Haibo Yu<sup>1</sup>

<sup>1</sup> *Illawarra Health and Medical Research Institute, School of Chemistry, University of Wollongong, NSW 2522, Australia.*

**Corresponding Author(s):** nehadsolimanhassan@yahoo.com

Up-regulated activities of the serine protease urokinase plasminogen activator (uPA) [1] and sodium hydrogen exchanger isoform 1 (NHE1) [2] are intimately associated with tumor invasion and metastasis, especially in breast cancer. Amiloride is an oral potassium-sparing diuretic that exhibits moderate anticancer side activity arising from dual inhibition of uPA and NHE1 [3]. The 5-substituted derivative 5-N,N-hexamethylene(amiloride) (HMA) is a more potent dual inhibitor of uPA and NHE1 [3]. 6-Substituted HMA analogues showed significantly increased potency against uPA with IC<sub>50</sub> values in the nM range [4].

Anticancer therapies should target tumor and stromal cells as they both play an important role in tumor invasion and proliferation [5]. Many inhibitors developed to date display species specificity. Compounds that don't show species selectivity are more likely to show efficacy in human tumor xenograft and other models in mice.

In this work, we have used computational methodologies to understand the molecular mechanisms for activity and selectivity of the 6-substituted HMA analogues. Our binding free energy simulations reproduced the experimental measured trends in affinities and selectivities. Asp189, Ser195 and Gly219 in uPA are the key residues interacting with all analogues. The most potent 2-aminopyrimidiny derivative forms an extra hydrogen bond with the S1β Ser146.

[1] M. Ranson, N. M. Andronicos, *Front. Biosci.*, 1, s294 (2003).

S. R. Amith, L. Fliegel, *Cancer Res.*, 73, 1259 (2013).

H. Matthews, M. Ranson, J. D. A. Tyndall, M. J. Kelso, *Bioorg. Med. Chem. Lett.*, 21, 6760 (2011).

B. J. Buckley, A. Aboelela, E. Minaei, L. X. Jiang, Z. Xu, U. Ali, K. Fildes, C.-Y. Cheung, S.M. Cook, D. C. Johnson, D. A. Bachovchin, G. M. Cook, M. Apte, M. Huang, M. Ranson, M. J. Kelso, *J. Med. Chem.* 61, 8299 (2018).

R. Hildenbrand, A. Schaaf, A. Dorn-Beineke, H. Allgayer, M. Sutterlin, A. Marx, P. Stroebel, P., *Histol. Histopathol.*, 24, 869 (2009).

195

## Cholesterol Distribution Mapping of Red Blood Cell Membrane during Malaria Parasite Invasion

Cindy Evelyn<sup>1</sup> ; Niall Geoghegan<sup>1</sup> ; Lachlan Whitehead<sup>1</sup> ; Michal Pasternak<sup>1</sup> ; Jenny Thompson<sup>1</sup> ; Julie Healer<sup>1</sup> ; Alan Cowman<sup>1</sup> ; Kelly Rogers<sup>1</sup>

<sup>1</sup> *Walter Eliza Hall Institute of Medical Research*

**Corresponding Author(s):** evelyn.c@wehi.edu.au

Eradication of malaria, one of the deadliest infectious diseases, is hindered by poor understanding of red blood cell infection by Plasmodium parasites. Successful parasite invasion of red blood cells leads to the symptomatic stage of the disease and transmission to mosquito vectors. This process involves a series of ligand-receptor interactions which are crucial for conditioning the host cell for invasion, hence much focus has been set on blocking these interactions for drug or vaccine discovery. However, the effect of these treatments is often limited by high polymorphisms of the parasite ligands and the redundancy of some interactions. For this reason, it is necessary to understand the unique role of each interaction for successful invasion to occur.

Through systemised ligand-receptor interactions, the parasite induces molecular changes that alter the physical properties of the host cell membrane and the cytoskeleton organisation beneath the membrane [1]. Controlled host cell remodelling enables parasite penetration, membrane resealing, and parasitophorous vacuole formation. Earlier studies proposed a complete biophysical model of this process through theoretical simulation of red blood cell membrane-wrapping mechanisms [2]. However, experimental validation of this model has been challenging due instrumental limitation.

The molecular organisation of the red blood cell membrane is a key aspect to the membrane-wrapping mechanism. Cholesterol is the most abundant component of red blood cell membrane and the presence of cholesterol in a lipid region stabilises the lipid structure. Lipid regions enriched with cholesterol are associated with specific proteins that are known to be important for membrane trafficking and cell signalling [1]. To this end, we applied high-resolution 4D imaging using lattice-light sheet microscopy, which allowed us to obtain a real-time view of the membrane dynamics during parasite invasion. In addition, we map the relative cholesterol concentration within the host cell membrane during the invasion using a ratiometric membrane dye [3,4]. Our preliminary results point to cholesterol enrichment as an important factor for the formation of the parasitophorous vacuole following successful invasion.

138

## Spatially mapping brain metabolism in a mouse model of Huntington's disease

**Author(s):** Anthony Hannan<sup>1</sup> ; Danny Hatters<sup>2</sup> ; Farheen Farzana<sup>3</sup>

**Co-author(s):** Boughton Berin<sup>4</sup> ; Malcolm McConville<sup>4</sup>

<sup>1</sup> *Florey institute of Neuroscience & Mental health, University of Melbourne, Victoria 3010, Australia*

<sup>2</sup> *Bio21 Institute of Molecular Science and Biotechnology*

<sup>3</sup> *Florey Florey Institute of Neuroscience and Mental Health, Bio21 Institute of Molecular Science and Biotechnology*

<sup>4</sup> *Metabolomics Australia, University of Melbourne*

**Corresponding Author(s):** ffarheen@student.unimelb.edu.au

Background: Huntington disease (HD) is a fatal neurodegenerative disease caused by mutations in the huntingtin gene that result in an abnormally long polyglutamine (polyQ) tract. A key pathological signature is the formation of intracellular inclusions formed by polyQ-expanded huntingtin

protein [1]. Our lab has previously shown that the formation of huntingtin inclusions in cell culture models deactivates the trigger for apoptosis emanating from the soluble mutant huntingtin protein. This correlates with the cells becoming functionally quiescent and undergoing a slow death by necrosis [2].

Hypothesis: We hypothesize that neuronal dysfunction in vivo is driven primarily by an induced quiescent state as huntingtin inclusions form and that this happens far earlier than cell death.

Aim: Our goal is to assess the extent to which neurons in vivo are metabolically quiescent and how this relates to the presence of inclusions in a transgenic mouse model of HD.

Methods: We have conducted a spatial metabolomics experiment to perform a steady state analysis of brain metabolites (lipids) between wild-type and R6/1, a mouse model of Huntington's disease. 24-week-old wild-type (WT) and HD mice were fed with deuterated water and culled at different time points to track metabolic turnover. The left hemisphere of the brain was cryo-sectioned and reserved for determining the spatial distribution and the relative abundance of the brain metabolites (lipids) using MALDI-TOF imaging mass spectrometry (MALDI-IMS). The right hemisphere was dissected to obtain the frontal cortex, striatum and hippocampus that were reserved for a GC-MS analysis.

Results: Our results represent the first stage of an ongoing project. To date, we have optimized collection of metabolites spatially in WT and HD mouse brains by MALDI-IMS. Our preliminary data points towards a change in the lipid distribution of the mouse cortex, striatum and the hippocampal dentate gyrus, regions that have been found to have dense population of inclusions using EM48-immunohistochemistry directed to the inclusions.

#### References

Macdonald, M. A Novel Gene Containing a Trinucleotide Repeat That Is Expanded and Unstable on Huntington's Disease Chromosomes. 1993. *Cell* 72(6): 971–983.

92

## Visualising retrovirus capsid uncoating using RNA-binding proteins

K. M. Rifat Faysal<sup>1</sup> ; Miro Janco<sup>1</sup> ; Chantal L. Marquez<sup>1</sup> ; Vaibhav Shah<sup>None</sup> ; James Walsh<sup>1</sup> ; David A. Jacques<sup>1</sup> ; Till Boecking<sup>1</sup>

<sup>1</sup> UNSW

**Corresponding Author(s):** k.faysal@student.unsw.edu.au

Timely disassembly of HIV-1 capsid, the protein shell that houses viral RNA, is essential for successful replication in cells. The disassembly of the capsid shell into its constituent capsid proteins, a process also known as uncoating, is poorly understood. Various biochemical and biophysical uncoating assays have been established to gain insight into the mechanisms governing viral uncoating [1]. Recently, we reported an in vitro single molecule fluorescence imaging assay to investigate the uncoating kinetics of viral particles, whereby the precise time of capsid opening is detected by the release of GFP packaged as a solution phase marker inside the capsid [2]. The assay requires engineering of proviral plasmids to contain sequences encoding the desired fluorescent tag at a suitable location of the viral genome, which can be cumbersome when working with different viral strains or capsid mutants. Additionally, the encapsidation of GFP inside the viral particle could compromise viral maturation and/or the intrinsic stability of the capsid.

In order to expand the applicability of our uncoating assay to a range of RNA viruses without the need for encapsidation of GFP, we utilize a fluorescently labelled RNA-binding protein as a probe to visualize capsid uncoating. As a proof of principle, we used HIV-1 nucleocapsid (NC) protein, which binds to multiple binding sites on viral RNA inside the capsid. We immobilised viral particles containing GFP on the coverslip as in our previous approach and added fluorescently labelled NC (F-NC) to the solution. Using total internal reflection fluorescence microscopy, we then followed the fluorescence intensity of GFP and of F-NC at the single-particle level. Release of the encapsidated GFP measured at individual viral particles correlated with an increase of the corresponding F-NC

signal. This observation suggests that capsid opening is detectable by the binding of F-NC to the viral RNA inside the capsid, i.e. upon capsid opening, F-NC can diffuse into the capsid and exchange with the endogenous (unlabelled) NC bound to viral RNA, leading to a signal increase. Furthermore, we observed that the concentration of F-NC needs to be carefully chosen to maximise the signal-to-noise ratio of RNA-bound F-NC. When the concentration was too high, the F-NC signal decayed. This signal decrease was attributed to F-NC saturating binding sites on viral RNA that are in close proximity to each other, leading to fluorescence quenching.

Our preliminary data suggest that fluorescently labelled RNA-binding proteins (such as F-NC) could be a generic probe for imaging-based detection of capsid opening that can be adapted to study viral uncoating of various retroviruses and their mutants. The new approach could therefore provide valuable insights into the early retroviral lifecycle.

Campbell EM, Hope TJ. HIV-1 capsid: The multifaceted key player in HIV-1 infection. *Nat Rev Microbiol*; 2015;13:471–83.

Márquez CL, Lau D, Walsh J, Shah V, McGuinness C, Wong A, et al. Kinetics of HIV-1 capsid uncoating revealed by single-molecule analysis. *Elife*; 2018;7:e34772.

66

## Molecular dynamics simulations of inactivation and drug binding in the hERG ion channel

Emelie Flood<sup>1</sup> ; Celine Boiteux<sup>2</sup> ; Chai Ng<sup>3</sup> ; Delin Sun<sup>4</sup> ; Ben Corry<sup>5</sup> ; Jamie Vanderberg<sup>3</sup> ; Toby W Allen<sup>6</sup>

<sup>1</sup> RMIT Univeristy

<sup>2</sup> School of Science, RMIT University, Melbourne, Australia

<sup>3</sup> Victor Chang Cardiac Research Institute, Sydney, Australia

<sup>4</sup> Lawrence Livermore National Laboratory, USA

<sup>5</sup> Australian National University

<sup>6</sup> School of Science, RMIT University, Melbourne, VIC 3001, Australia

**Corresponding Author(s):** emelie.flood@rmit.edu.au

147

## Visualising the Cl<sup>-</sup> permeation pathway of glutamate transporters

Josep Font Sadurni<sup>1</sup> ; Ichia Chen<sup>2</sup> ; Qianyi Wu<sup>1</sup> ; Rosemary Cater<sup>1</sup> ; Robert Vandenberg<sup>1</sup> ; Renae Ryan<sup>1</sup>

<sup>1</sup> University of Sydney

<sup>2</sup> The University of Sydney

**Corresponding Author(s):** josep.font@sydney.edu.au

The excitatory amino acid transporters (EAATs) facilitate efficient neurotransmission within the glutamatergic synapse by rapidly eliminating excess glutamate into the surrounding glial cells and neurons. In addition to clearing glutamate from the extracellular space, EAATs also function as Cl<sup>-</sup> channels. However, the structural basis for this Cl<sup>-</sup> channel is unknown and there is a limited understanding of the physiological role of this function. An altered channel activity has been associated with the pathogenesis of debilitating neurological disorders such as episodic ataxia and epilepsy [1]. Structures of EAAT1, ASCT2 and their archaeal homolog, GltPh have revealed significant insights to the mode of substrate transport of this family [2]. Yet, none of them provide sufficient information on the function and location of the Cl<sup>-</sup> permeation pathway, which is likely to form at the interface of the scaffold and transport domains during the substrate transport cycle. We have investigated

the functional and structural basis of the Cl<sup>-</sup> channel in EAATs and GltPh using a combination of techniques such as electrophysiology and X-ray crystallography.

[1] Parinejad N, Peco E, Ferreira T, Stacey SM, van Meyel DJ (2016). Disruption of an EAAT-Mediated Chloride Channel in a *Drosophila* Model of Ataxia. *J Neurosci* 36: 7640-7647.

Ryan RM, Vandenberg RJ (2016). Elevating the alternating-access model. *Nat Struct Mol Biol* 23: 187-189.

67

## A Functional and Pharmacological Comparison of hGlyT2 and zGlyT2

**Author(s):** Zachary Frangos<sup>1</sup>

**Co-author(s):** Robert Vandenberg<sup>1</sup> ; Renae Ryan<sup>1</sup> ; Robert Harvey<sup>2</sup>

<sup>1</sup> *University of Sydney*

<sup>2</sup> *University of the Sunshine Coast*

**Corresponding Author(s):** zfra6675@uni.sydney.edu.au

Glycine transporters (GlyTs) regulate glycine concentrations in the brainstem and spinal cord. Impaired glycinergic neurotransmission has been implicated in chronic neuropathic pain, therefore it follows that GlyTs may be possible therapeutic targets. A series of bioactive lipids have been developed that demonstrate potent inhibition of hGlyT2. Preliminary *in vivo* studies have shown these bioactive lipids are capable of crossing the blood brain barrier and generate analgesia in rat and mice models of neuropathic pain. These results prompted investigation into other animal models that could allow a more high-throughput examination of the *in vivo* activity of these compounds. *Danio rerio* (zebrafish) may be a viable alternative as glycinergic neurotransmission is important in locomotion, and perturbation of this network produces bilateral muscle contractions in GlyT2 morphants. Therefore this study aimed to assess the viability of zebrafish as an alternative *in vivo* model by comparing the functional and pharmacological properties of hGlyT2 and zGlyT2. Functionally, hGlyT2 and zGlyT2 are similar as both are specific glycine transporters, however zGlyT2 demonstrates a lower apparent glycine affinity. Pharmacologically, zGlyT2 is less sensitive than hGlyT2 to inhibition by bioactive lipids. These results suggest it would be beneficial to use transgenic zebrafish expressing hGlyT2 to examine the *in vivo* activity of these compounds rather than wild-type zebrafish. The results of this study will aid the development of a medium-throughput *in vivo* activity assay capable of identifying lead compounds in this class of inhibitors. The analgesic efficacy of these lead compounds can then be examined in rodent models of chronic pain.

114

## Investigating the mechanism of the glutamine transporter ASCT2 and its potential as a molecular target in cancer therapy

Natasha Freidman<sup>1</sup> ; Qian Wang<sup>2</sup> ; Robert Vandenberg<sup>1</sup> ; Jeff Holst<sup>2</sup> ; Renae Ryan<sup>1</sup>

<sup>1</sup> *University of Sydney*

<sup>2</sup> *University of New South Wales*

**Corresponding Author(s):** natasha.j.freidman@gmail.com

As triple-negative breast cancers (TNBC) are insensitive to hormone therapies, targetable markers are highly sought after to treat this subtype of breast cancer. TNBC cell lines are known to be glutamine dependent, and the glutamine transporter ASCT2 holds promise as a potential molecular



target. Although its selectivity for glutamine may be critical to the cell, it is also possible that transport of other substrates (alanine, serine, cysteine, threonine or asparagine) plays a role. Introduction of ASCT mutants with varied glutamine transport capacities has the potential to reveal whether it is the glutamine-transporting functionality of ASCT2 that accounts for its importance in TNBC, or if other substrates are involved.

In this study, the two ASCT isoforms – ASCT2 and ASCT1 were expressed and characterised in *Xenopus laevis* oocytes. In accordance with previous studies [1], it was shown that ASCT2 transports glutamine while ASCT1 does not. We selectively modulated glutamine transport in both ASCTs by introducing double mutations in the substrate binding sites [2]. Each ASCT variant was tested in two ASCT2 *-/-* breast cancer cell lines (HCC1806 and MCF-7). Our results show that glutamine uptake in TNBC is reduced upon ASCT2 knockout, and is restored following introduction of glutamine-transporting ASCT variants.

ASCT2 knockout has been shown to attenuate cell growth [3]. The ability of the four constructs to rescue this impaired cell growth is being examined. This system isolates the effects of glutamine transport specifically mediated by ASCT2. Hence, it may constitute a valuable tool in understanding the role of ASCT2 in TNBC, and its potential as a therapeutic target.

[1] P. Pingitore, L. Pochini, M. Scalise, M. Galluccio, K. Hedfalk, and C. Indiveri. *Biochimica et biophysica acta*. 1828, 2238-2246 (2013).

A. J. Scopelliti, J. Font, R.J. Vandenberg, O. Boudker and R.M. Ryan. *Nat Commun*. 9, 38 (2018)

A Broer, S Fairweather and S Broer. *Frontiers in pharmacology*. 9 (2018)

115

## Development of classification method of protein-protein interfaces based on their secondary structures

**Author(s):** Takashi Fujii<sup>None</sup>

**Co-author(s):** Kazuo Fujiwara ; Masamichi Ikeguchi

**Corresponding Author(s):** e18m5607@soka-u.jp

Protein-protein interactions play crucial roles in many biological functions. There are many studies on protein interfaces, and it is also known that structurally unrelated complexes have occasionally similar interfaces (Fig.1). Although the interior of protein is almost occupied by secondary structures, structures other than  $\alpha$ -helix or  $\beta$ -sheet are often found on the interface. As a tool for evaluating the similarity of the interface structures, we developed a new method based on the number of contacting residues included in various secondary structure pairs such as helix-helix, helix-sheet, etc. Contact residues were defined as residues that lost  $> 1\text{\AA}^2$  of ASA upon complex formation. If each contact surface of two subunits has  $> 10$  contact residues, the contact surface was defined as an interface. If two contact residues from each protein have at least one-atom pair of which distance is less than  $4.5\text{\AA}$ , the residue pair was defined as a contact pair. We extracted 5592 PDB entries of homodimer with a single domain from OLIGAMI (our web database) and CATH. Based on the hierarchical information of CATH, entries with similar tertiary structure were grouped. The group was further divided into sub groups by the similarity of the positions of interface residues in the aligned sequences. First, we compared features of interface structures of homologous proteins, and developed a similarity evaluation method applicable to a pair of complexes having different structures. We counted the number of contact pairs depending on the secondary structure to which contact residues are included. Based on the distribution of contact numbers in the homologous proteins, we developed an evaluation method of interface similarity and searched for similar interface structures from structurally unrelated complexes. As a search result of the similar interfaces among 5592 PDB entries, similarities were found in 65,640 entry pairs with different CATH Class. We concluded that the similar interface could be detected by a method based on the number of secondary structure contact pairs.

134

## **$\beta$ -strand twisting/bending in soluble and transmembrane $\beta$ -barrel structures**

Nobuaki Kikuchi<sup>1</sup> ; Kazuo Fujiwara<sup>1</sup> ; Masamichi Ikeguchi<sup>1</sup>

<sup>1</sup> *Soka University*

**Corresponding Author(s):** fujiwara@soka.ac.jp

The majority of  $\beta$ -strands in globular proteins have a right-handed twist and bend. The dominant driving force for  $\beta$ -strand twisting is thought to be inter-strand hydrogen bonds. We previously demonstrated that, for water-soluble proteins, both the twisting and bending of  $\beta$ -strand are suppressed by the polar side chains of serine, threonine, and asparagine residues [1]. To determine whether this also holds for transmembrane  $\beta$ -strands, we calculated and statistically analyzed the twist and bend angles of four-residue frames of  $\beta$ -strands in both transmembrane and water-soluble  $\beta$ -barrel proteins with known three-dimensional structures. We found that twisting was suppressed even for frames not containing serine, threonine, or asparagine residues in the case of transmembrane  $\beta$ -strands. The suppression of twisting in transmembrane  $\beta$ -strands could be attributed to the propagation of the suppressive effect of serine, threonine, and asparagine residues within a frame to the neighboring, hydrogen-bonded strands under the restriction that all strands in the closed barrel structure must have similar twist angles. A similar tendency was also observed for water-soluble  $\beta$ -barrel proteins. We previously showed that the dominant driving force for  $\beta$ -strand bending is hydrophobic interactions involving aromatic residues within and outside the strand. Transmembrane  $\beta$ -barrels have no hydrophobic core, however; rather, hydrophilic residues predominate inside the barrel, and the  $\beta$ -strands of transmembrane  $\beta$ -barrels have larger bend angles than those of water-soluble  $\beta$ -barrels. Our results reveal that, in transmembrane  $\beta$ -barrel proteins, the glycine-aromatic ring motif is important for generating the  $\beta$ -strand bending necessary for barrel formation.

[1] K. Fujiwara, S. Ebisawa, Y. Watanabe, H. Toda, and M. Ikeguchi, *Proteins*. 82, 1484 (2014)

158

## **Hypotonic Stress Induced-ATP Release is via Volume-regulated Anion Channels in Undifferentiated Breast Cell Lines**

Kishio Furuya<sup>1</sup> ; Yuko Takahashi<sup>2</sup> ; Masahiro Sokabe<sup>2</sup>

<sup>1</sup> *Nagoya University*

<sup>2</sup> *Nagoya University Graduate School of Medicine*

**Corresponding Author(s):** furuya@med.nagoya-u.ac.jp

The high interstitial ATP concentration in the cancer microenvironment plays a wide range of roles in cancer and is a major source of adenosine which acts as a strong immune suppressor. However, the source of ATP, which must be continuously released from cancer cells, has not yet been elucidated. We measured the ATP release during hypotonic stress using a real-time ATP luminescence imaging system and found that two completely different releasing manners exist in primary cultured mammary cells and in breast cell lines. In primary cultured cells, ATP was intermittently released with transient-sharp peaks, while in breast cell lines ATP was released with a slowly rising diffuse pattern that maintained a large and long-lasting ATP environment. DCPIB, an inhibitor of volume-regulated anion channels (VRACs), only suppressed the diffuse pattern. Cholera toxin treatment of breast cell lines changed the ATP response from the diffuse to the transient-sharp pattern. The inflammatory mediator sphingosine-1-phosphate induced ATP release with a diffuse pattern isovolumetrically in breast cell lines. In addition, treatment with transforming growth factor (TGF) $\beta$  changed the ATP release pattern from transient-sharp to diffuse in the primary cultured cells and enhanced the diffuse pattern in breast cell lines. A real-time PCR analysis indicated that among the isoforms of leucine-rich repeat-containing protein 8 (LRRC8), the molecular entities of VRAC, LRRC8A and 8C were expressed substantially in breast cell lines, and the expression increased with TGF $\beta$ . These results suggest that abundantly expressed VRACs are a conduit of ATP in undifferentiated cells including cancer cells

85

## Drug repurposing approach to identify novel inhibitors for targeting DNA gyrase in *Mycobacterium tuberculosis*: insights into mechanism and drug action

**Author(s):** Balasubramani G L<sup>1</sup>

**Co-author(s):** Rinky Rajput<sup>1</sup> ; Manish Gupta<sup>1</sup> ; Rakesh Bhatnagar<sup>1</sup> ; Abhinav Grover<sup>1</sup>

<sup>1</sup> JNU

**Corresponding Author(s):** glbala87@gmail.com

Drug repurposing has gained momentum globally and become an alternative avenue for drug discovery. Though tuberculosis (TB) can be cured with the use of currently available anti-tubercular drugs, emergence of drug resistant strains of *Mycobacterium tuberculosis* H37Rv (Mtb) and the huge death toll globally, together necessitate urgently newer and effective drugs for TB. To address this problem, we screened FDA-approved drugs by virtual screening and binding free energy calculations to identify novel inhibitors that target two active sites of Mtb DNA gyrase (i) dimer interface of gyraseA subunit, (ii) a active site region of ATP binding (N-terminal domain) pocket on gyrase B subunit overlapping the site targeted by coumarin drugs. Here, we identified total of 4 compounds tightly binds to ATPase binding pocket of N-terminal domain of gyrase B. Results obtained from biochemical and biophysical studies shows strong binding of screened compounds and inhibits gyrase catalytic cycle. Our evidence strongly suggests that these compounds bind to the N-terminal domain of gyrase B. Furthermore, we performed drug susceptibility test using screened compounds on Mtb and showed less MICs as compared to reported drugs. This finding indicates all the identified compounds represents potential scaffolds for further optimization of novel antibacterial agents that can act on drug-resistant strains.

### References

1. Agrawal A, Roué M, Spitzfaden C, Petrella S, Aubry A, Hann M, Bax B, Mayer C. *Biochem J*. 2013 Dec 1;456(2):263-73
2. Piton J1, Petrella S, Delarue M, André-Leroux G, Jarlier V, Aubry A, Mayer C. *PLoS One*. 2010 Aug 18;5(8):e12245

164

## Synergistic relationship between zinc and positive allosteric modulators of glycine receptors

**Author(s):** Casey Gallagher<sup>1</sup>

**Co-author(s):** Robert Vandenberg<sup>1</sup> ; Renae Ryan<sup>1</sup>

<sup>1</sup> University of Sydney

**Corresponding Author(s):** cgal2547@uni.sydney.edu.au

Glycine receptors are emerging as a key target for chronic pain therapies due to their role in nociceptive signalling within the spinal cord. Zinc is an endogenous biphasic modulator of glycine receptors that induces potentiation at low concentrations. It co-localises with glycine within vesicles at glycinergic synapses and reaches low micro-molar concentrations within the synapse during neurotransmission [1]. Zinc has previously been shown to enhance the activity of ethanol at glycine receptors through an unknown interaction [2], and may therefore enhance the activity of glycine receptor modulators. The aim of this study was to assess the interaction between zinc and N-oleoyl glycine, which is a positive allosteric modulator of glycine receptors. Zinc at physiological concentrations was found to have a synergistic interaction with N-oleoyl glycine, causing a level of potentiation that was greater than the effects of zinc and N-oleoyl glycine applied independently. These

results support previous evidence that suggest zinc can enhance the activity of positive allosteric modulators of glycine receptors. This synergism should be considered when developing glycine receptors modulators for therapeutic application, with the possibility of developing therapeutics that utilise this synergism to achieve greater efficacy.

[1] Y. Zhang, A. Keramidas and J.W. Lynch (2018). The free zinc concentration in the synaptic cleft of artificial glycinergic synapses rises to at least 1  $\mu$ M. *Neuroscience*. 9:88

L. M. McCracken, J.R. Trudell, M.L. McCracken and R.A.D Harris (2013). Zinc-dependent modulation of  $\alpha$ 2 and  $\alpha$ 3-glycine receptor subunits by ethanol. *Alcohol Clin. Exp. Res.* 37:12

80

## Highly selective PI3K $\gamma$ active state inhibitors and its mode of action

**Author(s):** Gangadhara Gangadhara<sup>None</sup>

**Co-author(s):** Göran Dahl ; Jens Petersen

**Corresponding Author(s):** gangadhara.gangadhara@astrazeneca.com

The class I phosphoinositide 3-kinases (PI3Ks) belong to the family of lipid kinases that phosphorylates Phosphatidyl 4,5 Phosphate (PIP2) to the second messenger, Phosphatidyl 3,4,5 Phosphate (PIP3). The PI3K signaling has been shown to be a key pathway in a signal transduction system linking multiple receptor classes to many essential cellular functions including growth, proliferation, and migration. PI3K $\gamma$  inhibitors might provide new avenues in treating respiratory & inflammation, metabolic disorder and cancer. For that reason, PI3K $\gamma$  has been an attractive target for the pharmaceutical industry. Unfortunately, it has been difficult to identify truly isoform selective compounds due to the high sequence homology between the four PI3K isoforms (PI3K $\alpha$ , PI3K $\beta$  & PI3K $\delta$ ). In the present study, we report our discovery of highly selective PI3K $\gamma$  inhibitors exhibiting 1000-fold selectivity over PI3K $\alpha$  & PI3K $\beta$ . We have characterized these inhibitors using Hydrogen-Deuterium Exchange Mass spectrometry (HDX-MS), Surface Plasmon Resonance (SPR) and X-ray crystallography. Characterization using X-ray crystallography reveals that inhibitor binds in a part of the ATP binding pocket that is completely conserved between isoforms but induces a new pocket leading to conformational changes around the DFG-motif. HDX-MS reveals that the compound induces a massive conformational change in PI3K $\gamma$  most likely involving the DFG-loop, activation-loop, helical domain and C-terminal helix via an allosteric mechanism, exploring an activation mechanism that is unique for PI3K $\gamma$ . SPR assay reveals that the binding kinetics involves a two-step binding mechanism. The conformational and kinetic differences are only observed in PI3K $\gamma$ . Site directed mutagenesis support and elucidates the binding mechanism and its conformational changes. The novel mode of action translates into highly selective inhibitors in relevant cellular system. This is the first example of a Class I PI3K inhibitor to achieve its selectivity by impacting the DFG motif in a manner that bears similarities to DFG in/out in type II protein kinase inhibitors.

90

## Esters selectively modulate the interaction of physiologically relevant mono- and divalent cations with phospholipid bilayers.

Beatriu Domingo Tafalla<sup>1</sup> ; Amani Alghalayini<sup>None</sup> ; Bruce Cornell<sup>2</sup> ; Charles Cranfield<sup>3</sup> ; Alvaro Garcia<sup>1</sup>

<sup>1</sup> *University of Technology, Sydney*

<sup>2</sup> *Surgical Diagnostics pty. ltd.*

<sup>3</sup> *University of Technology Sydney*

**Corresponding Author(s):** alvaro.garcia@uts.edu.au

Despite the many reported studies of mono and divalent ion interactions with phospholipid bilayers, the structure of the phospholipid-water interface and its modulation by ions remains to be clearly elucidated. To determine the effect of the ester linkage on ion interactions with phospholipids we studied tethered bilayer lipid membranes (tBLMs) formed from 1,2-dioleoyl-sn-glycero-3-phosphocholine (DOPC) or 1,2-di-O-(9Z-octadecenyl)-sn-glycero-3-phosphocholine (Diether DOPC) (Figure 1). Using electrical impedance spectroscopy, we report the potassium and sodium concentration dependence of the conductance across tethered bilayer lipid membranes (tBLMs) formed using ester or ether-linked phospholipids. We observed a reduced sodium ion conductance in the presence of ester-linked phospholipid tBLMs as opposed to ether-linked phospholipids. This difference was absent with experiments repeated with potassium ions (Figure 2). Experiments were repeated in the presence of divalent cations, magnesium and calcium, a smaller increase in conduction is reported. However, when the divalent cations were titrated on a background of sodium or potassium ions, there was reduced overall membrane conductivity (Figure 3). Calcium ions are able to modulate the ionic permeability of lipid bilayers in ester-linked phospholipid tBLMs to a greater degree than ether-linked phospholipid tBLMs. The effect of magnesium ions, however, demonstrated no discernible difference between ester and ether-linked phospholipid tBLMs. These data suggest that the interactions of mono and divalent cations with the ester moiety can selectively modulate the packing and conductivity of zwitterionic phospholipid bilayers.

133

## 4D microscopy of red blood cell membrane biophysics during Plasmodium falciparum invasion

Niall Geoghegan<sup>1</sup> ; Cindy Evelyn<sup>1</sup> ; Michal Pasternak<sup>1</sup> ; Julie Healer<sup>1</sup> ; Jenny Thompson<sup>1</sup> ; Lachlan Whitehead<sup>1</sup> ; Alan Cowman<sup>1</sup> ; Kelly Rogers<sup>1</sup>

<sup>1</sup> *Walter and Eliza Hall Institute of Medical Research*

**Corresponding Author(s):** geoghegan.n@wehi.edu.au

The symptoms of malaria are manifested during asexual blood stage of Plasmodium parasites, at the time of rapid multiplication of the parasite. This time window is a common target for the development of antimalarial therapies and potential vaccines. Difficulties in the development of efficient anti-malaria vaccines lie, in part, due to a fundamental lack of insight into the molecular processes and biophysical mechanisms which govern host-pathogen interactions at this stage. To this end, the distribution of important associated molecules during invasion of the red blood cell, has been studied by various microscopy techniques at fixed points in time [1, 2, 3]. The biophysical mechanisms for invasion have also been suggested through combined experimentation and modelling [4]. However, these studies lack the necessary temporal resolution to fully understand the molecular and biophysical basis for invasion in real time.

An important part of the invasion process is the formation of the parasitophorous vacuole membrane (PVM) at the point of entry to the host red blood cell. This membrane provides a physical barrier and an exchange surface between the parasite and the host cell. The formation of the PVM and subsequent remodelling of the host membrane during invasion are incredibly dynamic events and are very challenging to study in real time [5].

Presented in this study is a high-speed functional imaging method using lattice light sheet microscopy to determine the role of lipid order and cholesterol within parasite associated membranes during invasion. Using ratio metric fluorescence imaging we show, for the first time, temporal changes in the physical properties of various membrane structures formed by the invading parasite. The combined spatial and temporal resolution of the imaging techniques used offers unprecedented insights into the dynamic processes of Plasmodium invasion of red blood cells.

### References

- [1] J. C. Volz, "Essential role of the PfRh5/PfRipr/CyRPA complex during Plasmodium Falciparum invasion of Erythrocytes," *Cell Host and Microbiome*, vol. 20, pp. 60-71, 2016.
- G. E. Weiss, "Revealing the Sequence and Resulting Cellular Morphology of Receptor-Ligand Interactions during Plasmodium falciparum Invasion of Erythrocytes," *Plos Pathogens*, vol. 11, no. 2, 201.
- D. T. Riglar, "Super-resolution dissection of coordinated events during malaria parasite invasion of

the human erythrocyte," Cell host and microbiome, vol. 9, no. 1, pp. 9-20, 2011.

S. Dasgupta, "Membrane-wrapping contributions of the malaria parasite invasion of the human erythrocyte," Biophysical Journal, vol. 107, pp. 43-54, 2014.

C. Gruring, "Development and host cell modifications of Plasmodium Falciparum blood stages in four dimensions," Nature Communications, vol. 2, no. 165, 2011.

209

## Light on a nanoscale for probing and interacting with biological systems

Ewa Goldys<sup>1</sup>

<sup>1</sup> ARC Centre of Excellence for Nanoscale Biophotonics, Macquarie University, Sydney, Australia

### Corresponding Author(s):

The Australian Research Council Centre of Excellence for Nanoscale Biophotonics draws on key advances of the 21st century, nanoscience, and photonics to help understand life at the molecular level. This talk will focus on next-generation nanotechnologies developed in our Centre for probing, imaging and interacting with the living systems. These address the key challenges of ultrasensitive detection of key analytes in real environments, molecular complexity, and the requirement for interventions in deep tissue.

Fluorescence labeling is of the key detection methods in cell biology, genomics, proteomics and biomedical diagnostics. Bright and stable fluorescent nanoparticles offer key advantages in these applications. Long fluorescence lifetimes are desirable for ultrasensitive detection; such bioprobes can be used in a time-gating mode that offers exceptionally high background rejection. I will show how such nanoparticles can be used to image cell-surface receptors at a single particle level.

Fluorescent nanoparticles can be endowed with a variety of molecular functionalities. This versatile design makes it possible to sense chemical processes in the living organisms. We introduced a suite of nanoparticle sensors for imaging and probing trace levels of secreted molecules called cytokines, which are central to cellular communication and immunity. The complexity of the cytokine network requires high level of multiplexing, and to address this, we developed a nanoparticle-based optical coding system to increase the level of multiplexing by a factor of 100.

Theranostic nanomaterials simultaneously facilitate diagnostics including molecular sensing and active interventions required in therapies. I will discuss how our nanomaterials can produce light and interact with cells when stimulated with high energy radiation, and how this interaction can be quantified. The crossing of length scales inherent in radiotherapy combined with such nanomaterials forms powerful building blocks for innovative cancer treatments.

83

## The effect of cholesterol on Na<sup>+</sup>, K<sup>+</sup> -ATPase activity

Amy Gorman<sup>None</sup> ; Ronald Clarke<sup>None</sup> ; Alvaro Garcia<sup>None</sup> ; Flemming Cornelius<sup>None</sup>

Corresponding Author(s): amy.gorman@sydney.edu.au

The vital role of Na<sup>+</sup>, K<sup>+</sup> -ATPase is maintaining the Na<sup>+</sup> and K<sup>+</sup> electrochemical potential gradient across the plasma membrane. The significant importance, to life, of the Na<sup>+</sup>, K<sup>+</sup> -ATPase is clear when considering perturbations from the optimal function of Na<sup>+</sup>, K<sup>+</sup> -ATPase can cause many diseases; such as familial hemiplegic migraine type 2 (FHM2) and rapid onset dystonia parkinsonism (RDP). For some time, it has been known that cholesterol influences Na<sup>+</sup>, K<sup>+</sup> -ATPase activity. However, more recently, the N-terminus of Na<sup>+</sup>, K<sup>+</sup> -ATPase has become an indicative and fruitful

area of research, due to evidence the electrostatic interaction of the cytoplasmic N-terminus with the membrane is crucial to the conformational change between E1 and E2 states [1]. Here, we suggest cholesterol influences Na<sup>+</sup>, K<sup>+</sup> -ATPase activity through affecting the interaction of the N-terminus with the membrane.

Insight into cholesterol's effect on Na<sup>+</sup>, K<sup>+</sup> -ATPase activity in the native environment was possible by utilizing methyl- $\beta$ -cyclodextrin (m $\beta$ CD), for removal and reintroduction of cholesterol to Na<sup>+</sup>, K<sup>+</sup> -ATPase-containing membrane fragments. Removal of cholesterol induced Na<sup>+</sup>, K<sup>+</sup> -ATPase activity to fall to ~5% of the maximum. Reintroduction of cholesterol, via a cholesterol: m $\beta$ CD inclusion complex, recovered 100% of Na<sup>+</sup>, K<sup>+</sup> -ATPase activity for membrane fragments treated with 30mM m $\beta$ CD for cholesterol removal. However, reintroduction of cholesterol when higher concentrations of m $\beta$ CD were used, up to 60 mM, the Na<sup>+</sup>, K<sup>+</sup> -ATPase activity was only recovered to <75%. Irrespective of m $\beta$ CD concentration used, an activity increase was observed at low concentrations of cholesterol reintroduction, proceeded by an activity decrease at higher concentrations, indicative of an optimal cholesterol concentration for maximum Na<sup>+</sup>, K<sup>+</sup> -ATPase activity existing. Thus, it suggests cholesterol can distort Na<sup>+</sup>, K<sup>+</sup> -ATPase activity through affecting the plasma membrane. As recent evidence indicates the plasma membrane interacts with the protein, electrostatically, through its N-terminus, we suggest that cholesterol may be affecting this electrostatic interaction [1].

Through use of static light scattering-based assays, interactions between poly-L-lysine (PLL), which acts analogously to the lysine rich N-terminus, and vesicles of various lipid compositions have been investigated. Similarly, interactions between polyamino acid residues and Na<sup>+</sup>, K<sup>+</sup> -ATPase-containing membrane fragments were also investigated. Significant interactions were only observed between negatively charged phospholipids and positively charged polyamino acids, indicating the interaction of the cytoplasmic N-terminus with the membrane results from positively charged lysine residues and negatively charged phospholipid headgroups.

To understand cholesterol's effect on the electrostatic interaction more specifically, the next logical step is to observe cholesterol's effect on a reconstructed model of the N-terminus and membrane using negatively charged phospholipids and PLL.

[1] Q. Jiang, A. Garcia, M. Han, F. Cornelius, H.-J. Apell, H. Khandelia and R.J. Clarke, *Biophys. J.* 112, 288 (2017).

87

## The downstream signalling motifs of Akt

**Author(s):** Catheryn Gray<sup>1</sup>

**Co-author(s):** Adelle Coster<sup>2</sup>

<sup>1</sup> *University of New South Wales*

<sup>2</sup> *UNSW*

**Corresponding Author(s):** catheryn.gray@unsw.edu.au

Akt/PKB (Protein Kinase B) is a key nutrient sensor in the mammalian cell. It is known to regulate a variety of cellular processes, such as glucose metabolism, cell growth, and anti-apoptosis. The dysregulation of Akt signalling is implicated in the pathogenesis of a number of human diseases, from diabetes to cancer.

Akt derives signalling specificity from both its biochemical state and its intracellular location. Initially, Akt is synthesised in the interior of the cell. Upon receiving the insulin signal, the nascent Akt translocates to the plasma membrane (PM). Once docked at the PM, the Akt can be activated (phosphorylated) and then propagate the insulin signal to its downstream substrates. However, there is a marked lack of concordance between Akt activation and the behavior of these downstream components.

We have developed a deterministic, three-compartment, ordinary differential equation (ODE) model of Akt translocation to the PM. With this framework, we elucidate the different modes of behaviour of the Akt translocation system, the downstream signalling motifs thus generated, and explore the implications for the regulation of Akt substrates.

## The response of mechanosensitive ion channels in cardiac cell stretching stimulation

**Author(s):** Yang Guo<sup>None</sup>

**Co-author(s):** Anna-Lena Merten ; Boris Martinac<sup>1</sup> ; Charles Cox<sup>1</sup> ; Dominik Schneidereit ; Michael Feneley ; Oliver Friedrich

<sup>1</sup> *Victor Chang Cardiac Institute*

**Corresponding Author(s):** y.guo@victorchang.edu.au

It is known that cardiac pressure overload could activate certain cellular signaling pathways to induce pathological left ventricular hypertrophy (LVH). The increase in intracellular calcium has been proved to be an important signal to LVH[1]. Acting as mechanical biosensors in cardiovascular system[2], mechanosensitive ion channels (MSCs), such as Piezo1 could be possible regulators of the LVH signaling pathway through their regulation of calcium. To investigate the response of MSCs to cell stretching in pressure overload induced LVH, we applied isotropic stretching stimulation to both acutely isolated mouse ventricular cardiomyocytes and cultured HL-1 cardiac muscle cells, using PDMS stretch chamber and the IsoStrecher device[3]. The intracellular calcium fluorescence during cell stretching was recorded using epifluorescence microscopy and the Ca<sup>2+</sup>-sensitive dye Fluo-4. The intensity in cells was analysed to evaluate the calcium levels changed due to the activation of MSCs. We also used Yoda1[4] to activate Piezo1 channels to confirm their activities. In both cardiomyocytes and HL-1 cells, the calcium fluorescence level was observed to increase following application of 15% stretch for 30 seconds. Also, by adding 5 $\mu$ M Yoda1 to the chambers without stretch, increase in calcium fluorescence levels in both cardiomyocytes and HL-1 cells was noted. While the cells with Yoda1 were stretched to 15%, calcium activity increased to an even higher level compared to cells only with 15% stretch or Yoda1 alone, respectively. Moreover, a great increase in calcium fluorescence levels was observed after stretch was released from 15% to 0% in cardiomyocytes with Yoda1, which may reflect the increase of wall tension of cardiomyocytes during systole. These results show that MSCs in cardiomyocytes and HL-1 cells were activated by cell stretching stimulation applied by the IsoStrecher technology. It suggests that MSCs might be playing an important role in cardiac hypertrophy during cell stretching. It also indicates that Piezo1 is active in cardiomyocytes as a mechanically activated membrane biosensor.

[1] D.M. Bers. Annual review of physiology. 70, 23-49 (2008).

B. Martinac. Journal of cell science. 117(12), 2449-2460 (2004).

O. Friedrich, D. Schneidereit, Y.A. Nikolaev, V. Nikolova-Krstevski, S. Schürmann, A. Wirth-Hücking, A.L. Merten, D. Fatkin and B. Martinac. Progress in biophysics and molecular biology. 130, 170-191 (2017).

R. Syeda, J. Xu, A.E. Dubin, B. Coste, J. Mathur, T. Huynh, J. Matzen, J. Lao, D.C. Tully, I.H. Engels and H.M. Petrassi. Elife. 4, p.e07369 (2015).

## When Computer Meets Bio?

Sihyun Ham<sup>1</sup>

<sup>1</sup> *Sookmyung Women's University*

**Corresponding Author(s):** sihyun@sookmyung.ac.kr

Why and how a normal cell becomes a disease cell? The main research effort in my lab is to develop and apply innovative computational methods for elucidating the mechanisms and driving factors of biomolecular interactions related to human diseases and cellular functions at a molecular-level. The



fluctuating thermodynamics technology recently developed in my group offers a practical means for the thermodynamic characterizations of the folding, misfolding, and aggregation of the various proteins associated with human diseases. The use of fluctuating thermodynamics has the potential to provide a comprehensive picture of fluctuating phenomena in diverse biological processes. In this talk, I will present the detailed concepts and applications of our recent computational technologies for elucidating biological processes. These tools and new paradigm provide a unified view on how biomolecules operate and are applied to design a new function of specific interest in cellular network

- [1] Chong and Ham, *Angew. Chem. Int. Ed. Engl.*, 53, 3961 (2014).  
 Teoh et al. *J. Am. Chem. Soc.*, 137, 13503 (2015).  
 Chong and Ham, *Acc. Chem. Res.*, 48, 956 (2015).  
 Fujiwara et al. *Angew. Chem. Int. Ed. Engl.*, 55, 10612 (2016).  
 Chong, Chatterjee, and Ham, *Annu. Rev. Phys. Chem.*, 68, 117 (2017).  
 Chong and Ham, *Sci. Rep.*, 8, 7148 (2018).

162

## A study on the interaction of lubricin with different substrates

**Author(s):** Mingyu Han<sup>1</sup> ; Wren Greene<sup>1</sup>

**Co-author(s):** Weiwei Lei<sup>2</sup>

<sup>1</sup> *Institute for Frontier Materials and ARC Centre of Excellence for Electromaterials Science, Deakin University, Melbourne, Victoria, Australia.*

<sup>2</sup> *Institute for Frontier Materials, Deakin University, Geelong, Victoria, Australia.*

**Corresponding Author(s):** hanm@deakin.edu.au

Lubricin (LUB) is a mucin-like glycoprotein that plays a significant role in the boundary lubrication and wear protection system in human joints. Although most lubricin research has focused on its biotribological and biochemical properties in joints, lubricin's unique combination of self-assembly, electrochemical, and anti-adhesive, properties are now being applied to solve many problems in a diverse range of different fields including microfluidics, electrochemical sensors, contact lenses, and bionic neural interfaces. Each of these applications requires lubricin to be adsorbed via self-assembly onto a range of non-biological surfaces; however, an understanding of how lubricin adsorbs and adheres to these physically and chemically different surfaces is lacking. This research aims to bridge this knowledge gap by directly quantifying repulsion force on separation for self-assembled LUB layers on different substrates with the help of AFM. In this report, we investigate the interaction between LUB and different substrates including polystyrene, poly(methyl methacrylate), graphene, MXene, boron nitride, glass, gold, cyclic olefin copolymer (COC) and mica by measuring the adhesion energy of LUB on different substrates with the help of AFM. The results show that the adhesion energy of LUB varies with different substrates and the values for boron nitride is the highest ( $\sim 8 \times 10^{-16}$  J) which is almost 31 times higher than the value for mica that was frequently used in the LUB related studies. Meanwhile, the RMS of LUB coated substrates is incredibly low which indicates that the LUB layer on the substrate is fairly smooth. This work provides a systemic method and data prior to the potential combination of LUB with different materials for various applications such as bioimplant, anti-adhesive coating, bioimaging, biosensor and biolubricant.

186

## Structural studies of new post-translational modification erasers/readers

Quan Hao<sup>1</sup>

<sup>1</sup> *University of Hong Kong*

**Corresponding Author(s):** qhao@hku.hk

Sirtuins are NAD-dependent deacetylases that regulate important biological processes. Four mammalian sirtuins (Sirt4 to Sirt7) have no detectable or very weak deacetylase activity. Using structural and biochemical data we have discovered that Sirt5 is an efficient desuccinylase and demalonylase in vitro and in vivo, catalyzing the hydrolysis of succinyl and malonyl lysine residues. Sirt5 is the first Sirtuin demonstrated to prefer an acyl group other than acetyl, suggesting that other Sirtuins showing little or no deacetylation activity may prefer to hydrolyze different acyl groups too [1]. We have further demonstrated that Sirt6 catalyzes the removal of long chain fatty acyl groups. Sirt6 promotes the secretion of tumor necrosis factor- $\alpha$  (TNF $\alpha$ ) by removing the fatty acyl modification on this cytokine. The crystal structure of Sirt6 with a myristoyl peptide may pave a way for novel therapeutic interventions in the field of autoimmunity and inflammation [2]. We have also shown that Sirt3 is a decrotonylase in vitro and in cells. The crystal structure of Sirt3-H3K4Cr complex reveals a unique binding pocket that stabilizes the conjugated crotonyl group via  $\pi$ - $\pi$  stacking [3]. Using potent SIRT2-specific inhibitors, we have recently captured a distinct covalent catalytic intermediate (III) that is different from the previously established intermediates I and II; MALDI-TOF data further support the intermediate III formation [4]. This is the first time such an intermediate has been captured by X-ray crystallography and provides more mechanistic insights into sirtuin-catalyzed reactions. Our recent biochemical and structural studies have demonstrated that GAS41, an oncogene-coded protein, can act as the reader of succinylation on histone H3K122. This is the first time that a reader of succinyl-lysine (Ksuc) on histones has been identified [5]. This work is supported by Hong Kong RGC grants C7037-14G and AoE/P-705/16.

Du et al, *Science*, Vol. 334, 806-809 (2011).

Jiang et al, *Nature*, 496, 110-113 (2013).

Bao et al, *eLife*, 3:e02999 (2014).

Wang et al, *Cell Chem. Biol.* 24 (3), 339-345 (2017).

Wang et al, *PNAS*, 115 (10), 2365-2370 (2018).

205

## MR-PET Imaging of Neuroinflammation in the Human Brain

Ian Harding<sup>1</sup>

<sup>1</sup> *Monash Institute of Cognitive and Clinical Neurosciences, Monash University*

**Corresponding Author(s):** ian.harding@monash.edu

Immune-responsive cells of the brain – namely microglia and astrocytes – activate in response to brain injury, proteinopathy, or the influx of pathogens (e.g., infection). This activation leads to a local neuroinflammatory response that is beneficial and protective in the short-term, but becomes increasingly neurotoxic over time. Chronic inflammation may therefore actually contribute to neuronal death, which in-turn further perpetuates the neurotoxic inflammatory activity. Chronic neuroinflammation is thought to play a central role in the progressive neural morbidity that underlies neurodegenerative disorders such as Huntington's Disease (HD), Alzheimer's Disease (AD), and Parkinson's Disease (PD).

Established and emerging in vivo magnetic resonance imaging (MRI) and positron emission tomography (PET) techniques offer the opportunity to localize, quantify, and track neuroinflammatory responses in the living brain. These include PET imaging of the translocator protein (TSPO) receptor; MRI fluid mapping; MR-spectroscopy of glial osmolytes and metabolism; and quantitative susceptibility mapping (QSM). However, all available techniques suffer from limitations and varying degrees of non-specificity to neuroinflammatory activity, affecting the confidence and reliability of in vivo investigations and inference on disease mechanisms.

Multi-modal and multi-contrast imaging designs offer the potential to address these limitations by accruing convergent evidence of neuroinflammatory activity in the human brain. Simultaneous MR-PET imaging and TSPO-PET tracers suitable for use in clinical research settings allow for feasible

application of such approaches in clinical populations, and the ability to directly pair markers of neuroinflammation with indices of neurodegeneration (e.g., grey and white matter integrity). Early work using this approach is currently underway at Monash Biomedical Imaging in a number of neurodegenerative diseases, including Huntington's disease and Friedreich ataxia, to identify whether inflammation may provide a candidate marker of disease expression and progression, and/or a viable therapeutic target.

116

## Correlative Super-Resolution/AFM for Investigating Cellular Ultrastructure

**Author(s):** Riley Hargreaves<sup>1</sup>

**Co-author(s):** Toby Bell<sup>2</sup>; Donna Whelan<sup>3</sup>; Thomas McCoy<sup>2</sup>; Rico Tabor<sup>2</sup>; Ashley Rozario<sup>2</sup>

<sup>1</sup> *Monash University*

<sup>2</sup> *Monash University*

<sup>3</sup> *La Trobe University*

**Corresponding Author(s):** riley.hargreaves1@monash.edu

The cytoskeleton of cells is predominantly comprised of actin and microtubules, which both have key roles in maintaining cell shape and transporting macromolecules throughout the cytoplasm. The protein structures are difficult to visualize using conventional fluorescence microscopy and have been a key target of single molecule super-resolution (SR) microscopy techniques since their advent just over a decade ago. Utilising these up to an order of magnitude resolution increase is achievable for labelled structures [1], however, their context remains obscured. Correlative light-electron microscopy (CLEM) has been utilised to provide this information however atomic force microscopy (AFM) is also capable of providing context via topographical mapping but has been underemployed in conjunction with SR.

We have developed assays for directly correlating AFM with SR imaging of the internal ultrastructure of individual cells, including careful unroofing of cells to remove cell membrane to allow AFM imaging of the cytoskeletal ultrastructure. Multiple unroofing mechanisms were considered including the use of surfactants to dissolve lipids within the membrane [2], and sonication to peel off the membrane. The effect of dehydration and rehydration was also investigated and it was found that desiccated cytoskeletal structures could be preserved without significant artefacts.

[1] D. R. Whelan and T. D. M. Bell. *J. Phys. Chem. Lett.* 6, 374 (2015).

K. Meller and C. Theiss. *Ultramicroscopy.* 106, 320 (2006).

test / 5

## test contribution

**Corresponding Author(s):** dhatters@gmail.com

test

56

## **Abstract Investigation of multiple-dynein transport of melanosomes by non-invasive force measurement using the fluctuation theorem**

Shin Hasegawa<sup>1</sup>; Takashi Sagawa<sup>2</sup>; Kazuho Ikeda<sup>3</sup>; Yasushi Okada<sup>4</sup>; Kumiko Hayashi<sup>1</sup>

<sup>1</sup> *Tohoku University*

<sup>2</sup> *NICT*

<sup>3</sup> *RIKEN*

<sup>4</sup> *RIKEN, University of Tokyo*

### **Corresponding Author(s):**

Pigment organelles known as melanosomes disperse or aggregate in a melanophore in response to hormones. These movements are mediated by the microtubule motors kinesin-2 and cytoplasmic dynein. However, the force generation mechanism of dynein, unlike that of kinesin, is not well understood. In this study, to address this issue, we investigated the dynein-mediated aggregation of melanosomes in zebrafish melanophores. We applied the fluctuation theorem of non-equilibrium statistical mechanics [1,2,3] to estimate forces acting on melanosomes during transport by dynein, given that the energy of a system is related to its fluctuation. Our results demonstrate that multiple force-producing units cooperatively transport a single melanosome [4]. Since the force is generated by dynein, this suggests that multiple dyneins carry a single melanosome. Cooperative transport has been reported for other organelles; thus, multiple-motor transport may be a universal mechanism for moving organelles within the cell.

[1] K. Hayashi, *Biophys. Reviews*. DOI:10.1007/s12551-018-0440-5 (2018).

K. Hayashi, S. Hasegawa, T. Sagawa, S. Tasaki and S. Niwa, *Physical Chemistry Chemical Physics* 20, 3404-3410 (2018).

K. Hayashi, S. Tsuchizawa, M. Iwaki and Y. Okada, *Molecular Biology of the Cell*, in press (2018).

S. Hasegawa, T. Sagawa, K. Ikeda, Y. Okada and K. Hayashi, preprint(arxiv)  
<http://arxiv.org/abs/1808.03469>

208

## **Optogenetic control of diverse molecular and cellular processes in the mouse brain**

Won Do Heo<sup>1</sup>

<sup>1</sup> *Department of Biological Sciences, Korea Advanced Institute of Science and Technology (KAIST), Daejeon, Republic of Korea*

### **Corresponding Author(s):**

My group has been developing various bio-imaging and optogenetic tools for the study of cell signaling in live cells as well as neuronal functions in vivo. Novel optogenetic toolkit developed by my group is highly advantageous compared with conventional approaches in that it allows finely manipulated signaling pathways in a spatial and temporal resolution, thereby making it possible to dissect and analyze the transient dynamics of signaling processes within a defined period. These tools are very useful not only for imaging based researches in cell biology, but also for the studies in neuroscience. Recently developed optogenetic strategies have brought significant changes the way in which signaling in living cells is studied in neurobiology and other disciplines. Novel optogenetic toolkit my group has been developing are capable of providing what channelrhodopsins could not offer previously, contributing in a disparate perspective of neuroscience. We are applying the new technologies to the study of spatiotemporal roles of signaling proteins and second messengers in synaptic plasticity and learning and memory in normal and disease mouse models.

[1] Park H, Kim NY, Lee S, Kim N, Kim JH, Heo WD. Optogenetic protein clustering through fluorescent protein tagging and extension of CRY2. *Nature Communications*. 2017 Jun 23. doi: 10.1038/s41467-017-00060-2.

Nguyen MK, Kim CY, Kim JM, Park BO, Lee S, Park H, Heo WD. Optogenetic oligomerization of Rab GTPases regulates intracellular membrane trafficking. *Nature Chemical Biology*. 2016 Apr 11. doi: 10.1038/nchembio.2064. [Epub ahead of print].

Kyung T, Lee S, Kim JE, Cho T, Park H, Jeong YM, Kim D, Shin A, Kim S, Baek J, Kim J, Kim NY, Woo D, Chae S, Kim CH, Shin HS, Han YM#, Kim D#, Heo WD#. Optogenetic control of endogenous Ca(2+) channels in vivo. *Nature Biotechnology* (Cover Article). 2015 Sep 14. doi: 10.1038/nbt.3350.

Lee S, Park H, Kyung T, Kim NY, Kim S, Kim J, Heo WD. Reversible protein inactivation by optogenetic trapping in cells. *Nature Methods*. 2014 Jun;11(6):633-6. doi: 10.1038/nmeth.2940. Epub 2014 May 4.

Chang KY, Woo D, Jung H, Lee S, Kim S, Won J, Kyung T, Park H, Kim N, Yang HW, Park JY, Hwang EM, Kim D, Heo WD. Light-inducible receptor tyrosine kinases that regulate neurotrophin signalling. *Nature Communications*. 2014 Jun 4;5:4057. doi: 10.1038/ncomms5057.

18

## Optogenetic control of diverse molecular and cellular processes in the mouse brain

Won Do Heo<sup>None</sup>

**Corresponding Author(s):** wondo@kaist.ac.kr

My group has been developing various bio-imaging and optogenetic tools for the study of cell signaling in live cells as well as neuronal functions in vivo. Novel optogenetic toolkit developed by my group is highly advantageous compared with conventional approaches in that it allows finely manipulated signaling pathways in a spatial and temporal resolution, thereby making it possible to dissect and analyze the transient dynamics of signaling processes within a defined period. These tools are very useful not only for imaging based researches in cell biology, but also for the studies in neuroscience. Recently developed optogenetic strategies have brought significant changes the way in which signaling in living cells is studied in neurobiology and other disciplines. Novel optogenetic toolkit my group has been developing are capable of providing what channelrhodopsins could not offer previously, contributing in a disparate perspective of neuroscience. We are applying the new technologies to the study of spatiotemporal roles of signaling proteins and second messengers in synaptic plasticity and learning and memory in normal and disease mouse models.

### References

1. Park H, Kim NY, Lee S, Kim N, Kim JH, Heo WD. Optogenetic protein clustering through fluorescent protein tagging and extension of CRY2. *Nature Communications*. 2017 Jun 23. doi: 10.1038/s41467-017-00060-2.
2. Nguyen MK, Kim CY, Kim JM, Park BO, Lee S, Park H, Heo WD. Optogenetic oligomerization of Rab GTPases regulates intracellular membrane trafficking. *Nature Chemical Biology*. 2016 Apr 11. doi: 10.1038/nchembio.2064. [Epub ahead of print].
3. Kyung T, Lee S, Kim JE, Cho T, Park H, Jeong YM, Kim D, Shin A, Kim S, Baek J, Kim J, Kim NY, Woo D, Chae S, Kim CH, Shin HS, Han YM#, Kim D#, Heo WD#. Optogenetic control of endogenous Ca(2+) channels in vivo. *Nature Biotechnology* (Cover Article). 2015 Sep 14. doi: 10.1038/nbt.3350.
4. Lee S, Park H, Kyung T, Kim NY, Kim S, Kim J, Heo WD. Reversible protein inactivation by optogenetic trapping in cells. *Nature Methods*. 2014 Jun;11(6):633-6. doi: 10.1038/nmeth.2940. Epub 2014 May 4.
5. Chang KY, Woo D, Jung H, Lee S, Kim S, Won J, Kyung T, Park H, Kim N, Yang HW, Park JY, Hwang EM, Kim D, Heo WD. Light-inducible receptor tyrosine kinases that regulate neurotrophin signalling. *Nature Communications*. 2014 Jun 4;5:4057. doi: 10.1038/ncomms5057.

167

## ARTIFICIAL ASSEMBLY OF THE BACTERIAL FLAGELLA MOTOR PROTEIN FLiG ON DNA SCAFFOLDS

Sophie Hertel<sup>1</sup> ; Chu Wai Liew<sup>1</sup> ; Lawrence Lee<sup>1</sup>

<sup>1</sup> *EMBL node for Single Molecule Sciences*

**Corresponding Author(s):** s.hertel@student.unsw.edu.au

The bacterial flagella motor (BFM) is an 11 MDa protein complex, composed of ~13 different component proteins, which powers the rotation of the bacterial flagella filament. A protein called FliG forms a ring in the rotor of the BFM, which is involved in the generation of torque and rotational switching. Previous structural and biochemical data allowed us to propose a model for the self-assembly of the FliG ring. In this model, the FliG monomer exists predominantly in a compact conformation stabilised by an intramolecular interaction between two conserved armadillo-repeat motifs (ARM). However, after binding to a structural template, FliG can self-assemble into the ring shaped polymer observed in an assembled BFM, by switching to an extended domain-swapped polymer with intermolecular ARM interactions. This study aims to control FliG assembly using DNA nanostructures as an artificial template to functionally and structurally characterize interactions in the FliG ring *ex vivo*.

Rationally-designed DNA templates were used to immobilise an arbitrary number of FliG molecules in a spatial configuration similar to that in a functional motor *in vivo*, via the hybridisation of single stranded DNA that was covalently attached to the FliG. This allows us to measure the kinetics of intersubunit interactions in a FliG assembly for the first time with surface plasmon resonance (SPR). Furthermore, we will use this system to test our model for self-assembly by characterising the effect of point mutations rationally designed to disrupt the ARM-ARM interactions on the stability of FliG assemblies. Using small-angle X-ray scattering (SAXS) we demonstrated that these point mutations stabilize the extended conformation of the monomer in solution as predicted. In addition, we used disulphide crosslinking to demonstrate that the DNA template can promote the formation of assembled domain-swapped FliG polymers.

This study demonstrates the use of synthetic DNA templates to probe molecular mechanisms underlying the self-assembly of the BFM and other complex protein machinery from their component parts.

190

## Mapping DNA target search in live cell chromatin organisation by fluorescence fluctuation analysis

Elizabeth Hinde<sup>1</sup>

<sup>1</sup> *Department of Biochemistry and Molecular Biology, University of Melbourne, Australia*

**Corresponding Author(s):** elizabeth.hinde@unimelb.edu.au

Inside the nucleus at any given moment in time, thousands of molecules are diffusing throughout 3D genome organisation searching for a target DNA sequence. DNA repair machines look for sites of damage to prevent genetic mutations, and transcription factors undergo site specific DNA binding to maintain normal gene expression. The question is to what extent does nuclear architecture direct the diffusive route of molecules to a target destination? In recent work we developed a series of new fluorescence microscopy methods to track the movement of molecules around the complex DNA networks within the nuclei of live cells [1]. Based on fluorescence correlation spectroscopy, this technology has the spatiotemporal resolution to map the impact genome organisation has on nuclear traffic. From using this method, we discovered that DNA networks rearrange to create highways that facilitate repair and transcription factor recruitment to target DNA sites. This has given us the first opportunity to start understanding the biophysical rules for traversing the nuclear landscape.

125

## Probing the Interfacial Structure of Nanoemulsions

**Author(s):** Stephen Holt<sup>1</sup>

**Co-author(s):** Frank Sainsbury<sup>2</sup>; Lizhong He<sup>3</sup>; stefania Piantavigna<sup>3</sup>

<sup>1</sup> *Australian Nuclear Science and Technology Organisation*

<sup>2</sup> *AIBN*

<sup>3</sup> *Monash University*

**Corresponding Author(s):** sph@ansto.gov.au

The oil/water interface is crucial to many industrial systems, for example emulsions (food, cosmetics, drug delivery and others), chemical extraction (both aqueous to organic and the subsequent back extraction). Tailorable nanocarrier emulsions (TNEs) are a novel class of oil-in-water emulsions stabilised by molecularly-engineered biosurfactants that permit single-pot stepwise surface modification with related polypeptides that may be chemically conjugated or genetically fused to biofunctional moieties. The interfacial properties of such materials, particularly when one component is on the nanoscale, have a profound influence on biodistribution and stability as well as the effectiveness of sophisticated surface-encoded properties such as active targeting to cell surface receptors.

The target droplet size for the TNE is in the 100 - 200 nm range with low polydispersity. Molecular scale characterisation of the liquid/liquid interface in such systems is challenging. It is nonetheless of prime importance in a variety of physico-chemical-biological areas both fundamentally and practically. We have simplified the approach to this system by beginning with x-ray and neutron scattering methodologies to studying the structure and molecular conformation at planar oil/water interfaces.

I will discuss our current work on related to TNEs for drug delivery. The TNEs consist of an oil in water emulsion where the interface is stabilised by a rationally designed single alpha helix peptide (AM1). To the AM1 stabilised emulsion a related four-helix peptide (DAMP4) is added. The DAMP4 can be linked to a range of biologically functional elements including antibodies or protein resistant molecules. See figure for a schematic representation. The arrangement of the AM1 and DAMP4 at the oil/water interface and competition between the two species are important questions, the answers to which help to guide the TNE design. Furthermore, the presentation, conformation and orientation of the antibody into the aqueous phase impacts upon the TNE design and ultimately activity.

152

## Energetics of Lipid Membrane Surface Deformation

Alvaro Garcia<sup>1</sup>; Haipei Zou<sup>1</sup>; Khondker Rufaka Hossain<sup>1</sup>; Qikui Henry Xua<sup>1</sup>; Annabelle Buda<sup>1</sup>; Ronald J Clarke<sup>1</sup>

<sup>1</sup> *School of Chemistry, University of Sydney, Sydney, NSW 2006, Australia*

**Corresponding Author(s):**

The phospholipid component of biological cell membranes contains multiple dipolar residues within the headgroup region of the membrane (e.g. ester carbonyl groups, water dipoles, phosphocholine), which could via electrostatic interactions play important roles in determining membrane stability and in modulating the behavior of membrane proteins (1-3). However, the contributions of dipolar interactions to membrane function are, up to now, not well understood. To gain insight into the role of dipolar contributions to the energetics of membrane deformation, the phase behavior of dimyristoyl-phosphatidylcholine (DMPC) membranes in the presence of dipole potential,  $\psi_d$ , modifiers were investigated by differential scanning calorimetry. 7-Ketocholesterol, which weakens  $\psi_d$

and reduces membrane-perpendicular dipole-dipole repulsion, causes a discrete second peak on the high temperature side of the main transition, whereas 6-ketocholestanol, which strengthens  $\psi_d$  and increases membrane-perpendicular dipole-dipole repulsion merely produces a shoulder. Measurements on pure DMPC vesicles showed that the observed temperature profile could not be explained by a single endothermic process, i.e. breaking of van der Waals forces between hydrocarbon chains alone. Removal of NaCl from the buffer caused an increase in the main transition temperature and the appearance of an obvious shoulder, implicating electrostatic interactions. Consideration of the phosphatidylcholine headgroup dipole moment indicates direct interactions between phosphatidylcholine dipoles are unlikely to account for the additional process. It seems more likely the breaking of an in-plane hydrogen-bonded network consisting of hydrating water dipoles together with zwitterionic lipid headgroups is responsible. The evidence presented supports the idea that the breaking of van der Waals forces between lipid tails required for the main phase transition of PC membranes is coupled to partial breaking of a hydrogen-bonded network at the membrane surface.

[1] Brockman, H. *Chem. Phys. Lipids.* 73, 57-79 (1994)

Clarke, R. J.. *Adv. Colloid Interfac. Sci.* 89-90, 263-281 (2001).

O'Shea, P. *Biochem. Soc. Trans.* 31, 990-996 (2003).

94

## Membrane disrupting action of Caerin 1.1

**Author(s):** Ahmed Hourri<sup>1</sup>

**Co-author(s):** Adam Mechler<sup>2</sup>

<sup>1</sup> *Jasim*

<sup>2</sup> *La Trobe University*

**Corresponding Author(s):** 18169067@students.latrobe.edu.au

The urgent need for new antibiotics has encouraged renewed attention at the development of antimicrobial peptides (AMPs) into drugs [1, 2]. To design antimicrobial peptides for pharmacological purposes, it is important to understand their mechanism of antimicrobial action. Membrane disrupting antimicrobial peptides are of particular interest. These AMPs are believed to act as either transmembrane pore formers and surface-active peptides [3].

The caerin AMP family contains mostly broad-spectrum antibiotic peptides active against Gram-positive bacteria [2]. Of these, caerin 1.1 has been actively studied; however, its mechanism of action is still an active research area. Here quartz crystal microbalance (QCM) was used to monitor the interaction of caerin 1.1 with different lipid membranes. Plotting the QCM sensor signals  $\Delta f$  against  $\Delta D$  showed that there are changes in the viscoelastic character as a function of the concentration of the peptide, and the fingerprints are specific to each different membrane composition. Dye leakage method has been used to confirm membrane disruption. Slow dye release suggests transmembrane pore formation as the mechanism of caerin 1.1 action.

[1] Sunna, A., A. Care, and P.L. Bergquist, *Peptides and Peptide-based Biomaterials and their Biomedical Applications*. Vol. 1030. 2017: Springer.

Organization, W.H., *Antimicrobial resistance: global report on surveillance*. 2014: World Health Organization.

Pasupuleti, M., A. Schmidtchen, and M. Malmsten, *Antimicrobial peptides: key components of the innate immune system reviews*, 2012. 32(2): p. 143-171.

183

## Mechanosensitive Channels: From Osmosensing to Hearing



Pingbo Huang<sup>1</sup><sup>1</sup> *Hong Kong Univ. of Science and Technology***Corresponding Author(s):** bohaungp@ust.hk

All cell types sense and respond to mechanical stimuli, and mechanosensitive ion channels and other mechanosensitive molecules sense external or internal mechanical cues and convert them into electrical and chemical signals in the cell. Mechanosensitive ion channels govern a wide array of physiological processes, ranging from primitive osmosensing to extremely refined hearing. Cystic fibrosis transmembrane conductance regulator (CFTR) acts as a critically important anion channel in various epithelia, and this channel is long considered as a ligand-gated channel. Our studies suggest that CFTR is unexpectedly mechanosensitive and responds to mechanical stretch and cell swelling and that CFTR mechanosensitivity is involved in osmosensing in epithelial cells. The second part of my talk will discuss our more recent interest in TMC1 protein, a promising candidate for the long-sought mechanotransduction channel in hair cells in the inner ear. I will discuss the localization, physical and functional interactions of TMC1, and TMHS, another important component in the mechanotransduction complex in hair cells. The work was supported by Hong Kong RGC GRF16111616, GRF16102417, and GRF16100218.

188

## Structural definition of phospholipid-mediated oligomerization of defensins in fungal and tumour cell lysis

Marc Kvansakul<sup>1</sup> ; Mark Hulett<sup>1</sup> ; Sofia Caria<sup>1</sup> ; Ivan Poon<sup>1</sup> ; Michael Järvå<sup>1</sup> ; Kha Tran Phan<sup>1</sup> ; Fung Lay<sup>1</sup> ; Amy Baxter<sup>1</sup><sup>1</sup> *La Trobe University***Corresponding Author(s):** marc.kvansakul@gmail.com

Cationic antimicrobial peptides (CAPs) such as defensins are ubiquitously found innate immune molecules that often exhibit broad activity against microbial pathogens and mammalian tumour cells. Many CAPs act at the plasma membrane of cells leading to membrane destabilization and permeabilization. Here we describe a novel cell lysis mechanism for fungal and tumour cells by plant and human defensins that act via direct binding to the plasma membrane phospholipids phosphatidylinositol 4,5-bisphosphate (PIP2) or phosphatidic acid (PA). We have determined the crystal structures of the plant defensins NaD1 and NsD7 in complex with PIP and PA, respectively, revealing distinct oligomeric arrangements [1-3]. Both NaD1 and NsD7 form dimers that cooperatively bind the anionic head groups of PIP2 or PA via unique “cationic grip” configurations and assemble into oligomeric fibrils. Site-directed mutagenesis of NaD1 and NsD7 confirms that phospholipid binding and oligomerization are important for fungal and tumor cell permeabilization. We have shown that human beta-defensins 2 and 3 also use similar mechanisms for cell lysis [4,5]. These observations identify a conserved innate recognition system by defensins for direct binding of phospholipid that permeabilize cells via a novel membrane disrupting mechanism.

[1] I.K. Poon, A.A. Baxter, F.T. Lay, G.D. Mills, C.G. Adda, J.A. Payne, T.K. Phan, G.F. Ryan, J.A. White, P.K. Veneer, N.L. van der Weerden, M.A. Anderson, M. Kvansakul M and M.D. Hulett, *eLife* 3, e01808 (2014).

M. Kvansakul, F.T. Lay, C.G. Adda, P.K. Veneer, A.A. Baxter, T.K. Phan, I.K. Poon and M.D. Hulett. *Proc. Natl. Acad. Sci. USA* 113,11202 (2016).

M. Järvå, F.T. Lay, T.K. Phan, C. Humble, I.K. Poon, M.D. Hulett and M. Kvansakul. *Nat. Commun.* 9, 1962 (2018).

T.K. Phan, F.T. Lay, I.K. Poon, M.G. Hinds, M. Kvansakul and M.D. Hulett. *Oncotarget* 7, 2054 (2016).

M. Järvå, T.K. Phan, F.T. Lay, M. Kvansakul and M.D. Hulett. *Science Advances* 4, eaa0979 (2018)

184

## Delineation of the phenotypic heterogeneity observed in the aggregation of Cu, Zn Superoxide Dismutase1

DANISH IDREES<sup>1</sup> ; VIJAY KUMAR<sup>2</sup> ; GOURINATH SAMUDRALA<sup>3</sup><sup>1</sup> JAWAHARLAL NEHRU UNIVERSITY<sup>2</sup> Amity University<sup>3</sup> JAWHARLAL NEHRU UNIVERSITY

Corresponding Author(s): danish.idress@gmail.com

Abstract—Amyotrophic lateral sclerosis (ALS) is a neurological disease that causes the death of motor neurons with consequent muscular paralysis. ALS is caused by misfolding and aggregation of Cu, Zn Superoxide Dismutase (SOD1). In these studies, we identified the aggregation-prone sequences of the SOD1 using aggregation prediction algorithms, Zipper DB and AMYLPRED2. The six aggregation-prone peptides were synthesized from the aggregation-prone sequences of the SOD1. A combination of biophysical techniques and molecular dynamics (MD) simulation method were used to investigate the amyloid fibril forming propensities of these peptides. The peptides DS (102DSVISLS108), GQ (148GVIGIAQ154) and VE (15VQGIINFE22) showed visible aggregates in presence of Mili-Q and the aggregates were ThT positive. We also monitored the structural changes during aggregation of these peptides and showed the appearance of  $\beta$ -rich species during the aggregation. Experimental results were strongly supported by 250 ns all-atom MD simulation run of the five copies of DS and GQ. This study showed that the six aggregation-prone peptides of SOD1 have different aggregation properties that will possibly explain the heterogeneity observed in aggregation of SOD1 in vivo. The effects of these peptides on toxicity, cell proliferation of SH SY5Y cells were also studied. The results of this study would help in designing peptide based inhibitors of SOD1 aggregation.

Keywords: Amyotrophic Lateral Sclerosis; Aggregation; Amyloid Fibrils; Molecular Dynamic Simulation; Zipper DB

42

## A Thermodynamic Model of Amyloid- $\beta$ Protein Oligomerization on Negatively Charged Lipid Bilayers with High Curvatures

Keisuke Ikeda<sup>1</sup> ; Yuuki Sugiura<sup>1</sup> ; Minoru Nakano<sup>1</sup><sup>1</sup> Graduate School of Medicine and Pharmaceutical Sciences, University of Toyama

Corresponding Author(s): kiked@pha.u-toyama.ac.jp

Aggregation of amyloid- $\beta$  protein on biomembranes is a critical step for the formation of neurotoxic aggregates. In this study, the association and oligomerization of A $\beta$  on negatively charged liposomes were investigated by spectroscopic techniques and calorimetry. The A $\beta$ -(1-40)[Y10W] mutant exhibited the three-state transition from a monomer with random coil structure to  $\beta$ -sheet-rich or  $\alpha$ -helix-rich conformations along with the titration of lipid vesicles with a high curvature [1]. Each conformer of A $\beta$  was estimated by the spectral decomposition analysis of tryptophan fluorescence. The helix-to-sheet transition is well explained by a thermodynamic model of micelle formation (Fig. 1). The Gibbs free energy, enthalpy, and entropy changes of the oligomerization were determined (Fig. 2). We have found that the oligomerization is driven by entropic forces such as hydrophobic interactions.

[1] Y, Sugiura, K. Ikeda, M. Nakano, *Langmuir* 31, 11549 (2015).

197

## Ferritin Assembly Mechanism Studied by Time-resolved Small-angle X-ray Scattering

Daisuke Sato<sup>1</sup>; Takumi Kuwata<sup>1</sup>; Kazuo Fujiwara<sup>1</sup>; Masamichi Ikeguchi<sup>1</sup><sup>1</sup> Soka University

Corresponding Author(s): ikeguchi@soka.ac.jp

The assembly reactions of *Escherichia coli* ferritin A (EcFtnA) and its mutants were studied using time-resolved small-angle X-ray scattering (TR-SAXS). EcFtnA forms a cage-like structure that consists of 24 identical subunits and dissociates into dimers at acidic pH. The dimer maintains native-like secondary and tertiary structures and is able to reassemble into a 24-mer when the pH is increased. The reassembly reaction was induced by pH jump and reassembly was followed by TR-SAXS. Time-dependent changes in the forward scattering intensity and in the gyration radius suggested the existence of a significant population of intermediate oligomers during the assembly reaction. The initial reaction was a mixture of second- and third-order reactions (formation of tetramers and hexamers) from the protein-concentration dependence of the initial velocity. The time-dependent change in SAXS profile was roughly explained by a simple model in which only tetramers, hexamers, and dodecamers were considered as intermediate [1].

To understand how electrostatic interaction influences the assembly reaction, the dependence of the process on ionic strength and pH was investigated. The rate of assembly increased with increasing ionic strength and decreased with increasing pH from 6 to 8. These dependences were thought to originate from repulsion between assembly units (dimer in the case of EcFtnA) with the same net charge sign; therefore, to test this assumption, mutants with different net charges (net-charge mutants) were prepared. In buffers with low ionic strength, the rate of assembly increased with decreasing net charge. Thus, repulsion between the assembly unit net charges was demonstrated to be an important factor determining the rate of assembly. However, the difference in the assembly rate among net-charge mutants was not significant in buffers with an ionic strength higher than 0.1. Notably, under such high ionic strength conditions, the assembly rate increased with increasing ionic strength, suggesting that local electrostatic interactions are also responsible for the ionic-strength dependence of the rate of assembly and are repulsive on average [2].

The role of local electrostatic interactions was addressed as to several mutant proteins, in which intersubunit charge pair may be repulsive or attractive. Because Asp63 is close to Glu129 and Glu131 in the neighbor subunit dimer, the assembly kinetics of D63N and D63A mutants was investigated. The assembly rates of these mutants were similar to that of wild-type proteins, indicating that the electrostatic repulsion between Asp63 and Glu129/131 did not significantly affect the assembly rate. Because Asp63 may also interact with His128, the replacement of D63N or D63A may disrupt this interaction and retard the assembly. This effect may be cancelled out by the acceleration produced by elimination of the repulsion between Asp63 and Glu129/131. To test this possibility, we made H128A and H128V mutants. The assembly rates of H128A and H128V were slower than the wild-type protein, leaving the possibility of repulsive interaction between Asp63 and Glu129/131.

[1] D. Sato, H. Ohtomo, Y. Yamada, T. Hikima, A. Kurobe, K. Fujiwara and M. Ikeguchi, *Biochemistry*. 55, 287 (2016).

D. Sato, S. Takebe, A. Kurobe, H. Ohtomo, K. Fujiwara and M. Ikeguchi, *Biochemistry*. 55, 482 (2016).

50

## Oligomer formation of Abeta(29-42) by Coulomb replica-permutation molecular dynamics simulations

Satoru Itoh<sup>None</sup>; Hisashi Okumura<sup>None</sup>

Corresponding Author(s): itoh@ims.ac.jp

The amyloid- $\beta$  peptides ( $A\beta$ ) form amyloid fibrils which are associated with Alzheimer's disease. It is necessary to clarify the oligomerization process of  $A\beta$  in order to understand the amyloid fibril formation process and to find a remedy for Alzheimer's disease. To investigate the oligomerization process of  $A\beta$ , we applied the Hamiltonian replica-permutation method (HRPM) [1–3] to  $A\beta$  fragments,  $A\beta$  (29–42) peptides, in explicit water solvent.  $A\beta$  (29–42) consists of the residues 29 to 42, which correspond to the transmembrane domain of  $A\beta$ . The length of  $A\beta$  after residue 29 is a critical determinant of the amyloid formation rate. Moreover, this fragment forms amyloid fibrils by itself.

HRPM combines the advantages of RPM and the Hamiltonian replica-exchange method (HREM). RPM is a better alternative to REM. In RPM, temperature permutations among more than two replicas are performed with the Suwa-Todo algorithm. In HREM, by exchanging the parameters that are related only to limited degrees of freedom, the number of replicas can be decreased in comparison with REM.

I will introduce HRPM and show the oligomerization process of  $A\beta$  (29–42) [4] in my presentation.

[1] S. G. Itoh and H. Okumura, *J. Chem. Theory Comput.* 9, 570 (2013).

S. G. Itoh and H. Okumura, *J. Comput. Chem.* 34, 2493 (2013).

S. G. Itoh and H. Okumura, *J. Phys. Chem. B* 118, 11428 (2014).

S. G. Itoh and H. Okumura, *J. Phys. Chem. B* 120, 6555 (2016).

44

## Dynamic behaviour of DNA-binding proteins characterized by single-molecule fluorescence microscopy

**Author(s):** Yuji Itoh<sup>1</sup>

**Co-author(s):** Agato Murata<sup>1</sup>; Sridhar Mandali<sup>2</sup>; Satoshi Takahashi<sup>1</sup>; Reid Johnson<sup>2</sup>; Kiyoto Kamagata<sup>1</sup>

<sup>1</sup> *Tohoku University*

<sup>2</sup> *University of California, Los Angeles*

**Corresponding Author(s):** y.itoh@mail.tagen.tohoku.ac.jp

A variety of DNA-binding proteins (DBPs) are working in cells to sustain life. For instance, transcription factors such as bacterial CRP and eukaryotic p53 search and bind to their specific target DNA sites to regulate the transcription of mRNA. Architectural DBPs such as Fis and HU in bacteria contact DNA and modulate the functions of other DBPs. To clarify when, where and how DBPs work is important both for understanding of the different mechanistic properties of DBPs and for medical and pharmaceutical applications. In this study, we aimed to reveal the dynamics of DBPs in vitro and in vivo by applying single-molecule fluorescence microscopy.

First, we observed the process by which p53 transfers from one DNA strand to another to understand its target search mechanism. We constructed crisscrossed DNA molecules on the coverslip and observed the mobility of p53 labelled with a fluorescent dye along the DNA strands at the single-molecule level. We visualized intermolecular transfer of the pseudo-WT p53 at the contact point of the two DNA molecules (Fig. 1). By contrast, a mutant of p53 lacking the C-terminal domain did not exhibit transfer. Our results indicate that p53 can directly transfer from one DNA molecule to another in a reaction that requires the C-terminal domain. Intermolecular transfer may enable p53 to avoid roadblocks on DNA and facilitate the efficient target search in chromatin [1].

Second, we constructed eGFP-tagged DBPs and tracked them in *E. coli* to reveal their dynamics in vivo. We found that a large fraction of the CRP transcription factor diffuses fast whereas others are immobile. The averaged diffusion coefficient ( $D$ ) of CRP was  $0.330 \mu\text{m}^2 \text{s}^{-1}$  (Fig. 2). By contrast, most Fis molecules in *E. coli* did not exhibit apparent diffusion having the small averaged  $D$  value of  $0.019 \mu\text{m}^2 \text{s}^{-1}$  (Fig. 2). Our data suggest that CRP searches for its target by diffusing in cells but

that Fis is always associated with DNA. The results were consistent with our recent work on the in vitro single-molecule imaging of Fis [2] and CRP (unpublished).

[1] Y. Itoh, A. Murata, S. Takahashi and K. Kamagata, *Nucleic Acids Res.* 46, 14 (2018).

K. Kamagata, E. Mano, K. Ouchi, S. Kanbayashi and R. C. Johnson, *J. Mol. Biol.* 430, 5 (2018).

39

## Study of Breast Cancer Metabolism by MRI and in-vivo MR Spectroscopy

Naranamangalam Jagannathan<sup>1</sup>

<sup>1</sup> *All India Institute of Medical Sciences*

**Corresponding Author(s):** jagan1954@hotmail.com

During malignancy metabolic alterations occur in cells and tissues and thus the study of cancer metabolism involves identification, characterization and quantification of metabolites using advanced technologies like magnetic resonance (MR). Various MR methodologies like routine, diffusion, perfusion and dynamic contrast MRI monitors the tumor morphology and various physiological functions during progression of cancer as well as during therapy in vivo. Tumor volume, apparent diffusion coefficient, kinetic parameters like volume transfer coefficient, etc are estimated and these provide information on the tumor microstructure, microenvironment, abnormal vasculature etc. Such changes are associated with the alterations in the tumor metabolism, leading to changes in the cell architecture. While in vivo MR spectroscopy is used to study and monitor cancer metabolism by detection of various biochemicals or metabolites involved in various metabolic pathways. Several in vivo NMR studies using <sup>1</sup>H and <sup>31</sup>P MRS have demonstrated increased levels of total choline containing compounds, phosphomonoesters and phosphodiester in human breast cancer. These are indicative of altered choline and phospholipid metabolism. These levels get reversed on successful treatment. This talk will highlight the role of in vivo MR methodologies in breast cancer metabolism.

214

## Precision Medicine Approaches in Metabolic Disease

David James<sup>None</sup>

**Corresponding Author(s):**

The future in diabetes care promises to move from a more generic form of care to treatment that is better tailored toward the individual. To achieve this it is essential to begin to define the principles that govern individual responsiveness to the environment (i.e. food and exercise) as well as to drugs so that health practitioners can better match optimized treatments with improved long term health. This will require analysis of multiple layers of metabolic systems such as the genome, the transcriptome, the proteome and the environment using a range of model systems as well as interdisciplinary approaches to define the underlying features that determine key biological outcomes. These novel approaches will be aided by advances in accurate data acquisition, better ways of integrating data from different labs/centres and across different omic platforms and advances in data analysis and visualization. I will describe our efforts to map individual diversity in response to diet using different genetic strains of flies, mice and humans. I will describe omics analysis in both *Drosophila* and mice of different genetic backgrounds that clearly highlight the immense complexity of the gene-diet interaction. By marrying these data with longitudinal analysis of humans it should be feasible to develop a suite of biomarkers that predict future health outcomes and optimal prevention strategies for individuals. Such a venture will necessitate a move toward 'big data' medical care where individuals are empowered with personalized data that provides them with better options for long term health.



This enhancement results from a specific increase in the formation of integrin  $\alpha\text{IIb}\beta\text{3}$ -fibrinogen adhesion contacts. Strikingly, the enhancing effect of diabetes on discoid platelet adhesion is red blood cell dependent. Using a Biomembrane Force Probe (BFP), we demonstrate that compression force activates integrin  $\alpha\text{IIb}\beta\text{3}$  to increase its association rate for fibrinogen, leading to a greater stability of adhesive contacts. This compression force-induced integrin activation is calcium and PI 3-kinase dependent and is dysregulated in diabetes, resulting in enhanced integrin affinity maturation and enhanced platelet adhesion. Analysis of discoid platelet adhesion and aggregation in the mesenteric circulation of mice confirmed that diabetes leads to a marked enhancement in the formation and stability of discoid platelet aggregates, via a mechanism that is not inhibited by therapeutic doses of aspirin and clopidogrel, but is eliminated by PI 3-kinase inhibition. These studies demonstrate the existence of a compression force sensing mechanism regulating integrin adhesive function. Dysregulation of this compression force sensing mechanism is likely to represent a distinct diabetic prothrombotic phenotype that is resistant to commonly employed antiplatelet therapies [1].

#### References:

Ju L, McFadyen JD, Al-Daher S, Alwis I, Chen Y, Tønnesen LL, Maiocchi S, Coulter B, Calkin A, Felner EI, Cohen N, Yuan Y, Schoenwaelder SM, Cooper ME, Zhu C, and Jackson SP. (2018) Compression force sensing regulates integrin  $\alpha\text{IIb}\beta\text{3}$  adhesive function on diabetic platelets. *Nature Communications* 9: 1084. doi: 10.1038/s41467-018-03430-6

107

## Tracking phosphorylation induced conformational change in cardiac Troponin: an EPR and PRE-NMR study

Ehsan Kachoei<sup>1</sup> ; Phani Potluri<sup>1</sup> ; Joanna Guse<sup>2</sup> ; Dane McCamey<sup>2</sup> ; Louise Brown<sup>1</sup>

<sup>1</sup> *Department of Molecular Sciences, Macquarie University, Sydney, New South Wales 2109, Australia*

<sup>2</sup> *School of Physics, University of New South Wales, Sydney, New South Wales 2052, Australia*

**Corresponding Author(s):** ehsan.kachoei@students.mq.edu.au

Troponin (Tn) is a large heterotrimeric protein complex which acts as the 'switch' element in striated muscle contraction. The three subunits of Tn are: TnC - an 18 kDa dumbbell shape protein which binds  $\text{Ca}^{2+}$  to initiate contraction; TnI - a 24 kDa regulatory subunit which inhibits the myosin binding site on actin; and TnT - a 36 kDa flexible anchoring protein which adheres the whole complex to the muscle thin filament. Interestingly, the cardiac isoform of Tn has an additional 32 residue N-terminal extension (N-extension) region on the TnI subunit. This N-extension region can be phosphorylated (Ser 23 & 24) by protein kinase A (PKA) in response to  $\beta$ -adrenergic stimuli. The TnI N-extension is believed to play a secondary role in the Tn switch mechanism in cardiac muscle. Therefore, understanding the interaction between different subunits of cardiac Tn, especially the regulatory elements, in response to phosphorylation is important. Although several structural models have been proposed, to date, there are still no high-resolution structures for this region in the intact cardiac Troponin complex.

In this study, we have employed site directed spin labeling (SDSL) methods to introduce nitroxide spin labels (MTSL) on several sites on the N-domain of TnC, and on the TnI N-extension and regulatory regions. The distances between two spin labels in the reconstituted Tn complex was then measured using electron paramagnetic resonance (EPR) with two approach: continuous wave (CW) and double electron-electron resonance (DEER). CW and DEER were performed for both the phosphorylated and de-phosphorylated states of Tn. CW is sensitive to interspin distances in the range of 8 to 25 Å, and DEER in the range of 20 to 80 Å. Paramagnetic Relaxation Enhancement (PRE)-NMR was also used to measure distances between a single spin-labeled residue on TnI and all residues on N15-TnC within the sensitivity range of 10 to 25 Å. Together, our EPR and PRE-NMR results demonstrate the disruption of the interaction between TnC-TnI upon phosphorylation. We found that, upon phosphorylation, the interaction between the TnI N-extension region with the TnC N-domain becomes destabilized in the region close to the TnC  $\text{Ca}^{2+}$  binding site. In light of these findings, we conclude that phosphorylation alters the structural dynamic of Tn, leading to an increase in the relaxation rate.

9

## Binding Mechanism of Synthesized 5 $\beta$ -dihydrocortisol and 5 $\beta$ -dihydrocortisol acetate with Human Serum Albumin to understand their Role in Breast Cancer

Monika Kallubai<sup>1</sup><sup>1</sup> *Rayalaseema University***Corresponding Author(s):** monikasku.7@gmail.com

Our study is all about the biological interactions of synthesized 5 $\beta$ -dihydrocortisol (Dhc) and 5 $\beta$ -dihydrocortisol acetate (DhcA) molecules with carrier protein Human Serum Albumin (HSA). The cytotoxic study was performed on breast cancer cell line (MCF-7) normal human embryonic kidney cell line (HEK293), the IC<sub>50</sub> values for MCF-7 cells were 28 and 25  $\mu$ M, respectively, whereas no toxicity in terms of cell viability was observed with HEK293 cell line. Further experiment proved that Dhc and DhcA induced 35.6% and 37.7% early apoptotic cells and 2.5%, 2.9% late apoptotic cells respectively, morphological observation of cell death through TUNEL assay revealed that Dhc and DhcA induced apoptosis in MCF-7 cells. The complexes of HSA–Dhc and HSA–DhcA were observed as static quenching, and the binding constants (K) was  $4.7 \pm 0.03 \times 10^4$  M<sup>-1</sup> and  $3.9 \pm 0.05 \times 10^4$  M<sup>-1</sup>, and their binding free energies were found to be -6.4 and -6.16 kcal/mol, respectively. The displacement studies confirmed that lidocaine  $1.4 \pm 0.05 \times 10^4$  M<sup>-1</sup> replaced Dhc, and phenylbutazone  $1.5 \pm 0.05 \times 10^4$  M<sup>-1</sup> replaced by DhcA, which explains domain I and domain II are the binding sites for Dhc and DhcA. Further, CD results revealed that the secondary structure of HSA was altered in the presence of Dhc and DhcA. Furthermore, the atomic force microscopy and transmission electron microscopy showed that the dimensions like height and molecular size of the HSA–Dhc and HSA–DhcA complex were larger compared to HSA alone. Detailed analysis through molecular dynamics simulations also supported greater stability of HSA–Dhc and HSA–DhcA complexes, and root-mean-square-fluctuation interpreted the binding site of Dhc as domain IB and domain IIA for DhcA. This information is valuable for further development of steroid derivatives with improved pharmacological significance as novel anti-cancer drugs

13

## Binding Mechanism of Synthesized 5 $\beta$ -dihydrocortisol and 5 $\beta$ -dihydrocortisol acetate with Human Serum Albumin to understand their Role in Breast Cancer

Monika Kallubai<sup>1</sup><sup>1</sup> *Rayalaseema University***Corresponding Author(s):** monikasku.7@gmail.com

Our study is all about the biological interactions of synthesized 5 $\beta$ -dihydrocortisol (Dhc) and 5 $\beta$ -dihydrocortisol acetate (DhcA) molecules with carrier protein Human Serum Albumin (HSA). The cytotoxic study was performed on breast cancer cell line (MCF-7) normal human embryonic kidney cell line (HEK293), the IC<sub>50</sub> values for MCF-7 cells were 28 and 25  $\mu$ M, respectively, whereas no toxicity in terms of cell viability was observed with HEK293 cell line. Further experiment proved that Dhc and DhcA induced 35.6% and 37.7% early apoptotic cells and 2.5%, 2.9% late apoptotic cells respectively, morphological observation of cell death through TUNEL assay revealed that Dhc and DhcA induced apoptosis in MCF-7 cells. The complexes of HSA–Dhc and HSA–DhcA were observed as static quenching, and the binding constants (K) was  $4.7 \pm 0.03 \times 10^4$  M<sup>-1</sup> and  $3.9 \pm 0.05 \times 10^4$  M<sup>-1</sup>, and their binding free energies were found to be -6.4 and -6.16 kcal/mol, respectively. The displacement studies confirmed that lidocaine  $1.4 \pm 0.05 \times 10^4$  M<sup>-1</sup> replaced Dhc, and phenylbutazone  $1.5 \pm 0.05 \times 10^4$  M<sup>-1</sup> replaced by DhcA, which explains domain I and domain II are the binding sites for Dhc and DhcA. Further, CD results revealed that the secondary structure of HSA was altered in the presence of Dhc and DhcA. Furthermore, the atomic force microscopy and transmission electron microscopy showed that the dimensions like height and molecular size of the HSA–Dhc and HSA–DhcA complex were



larger compared to HSA alone. Detailed analysis through molecular dynamics simulations also supported greater stability of HSA–Dhc and HSA–DhcA complexes, and root-mean-square-fluctuation interpreted the binding site of Dhc as domain IB and domain IIA for DhcA. This information is valuable for further development of steroid derivatives with improved pharmacological significance as novel anti-cancer drugs

98

## Physicochemical and Computational Analysis for S100A4-MetAP2 peptide Interaction

**Author(s):** Naohiro Katagiri<sup>1</sup>

**Co-author(s):** Satoru Nagatoishi<sup>1</sup>; Hideya Endo<sup>1</sup>; Kouhei Tsumoto<sup>1</sup>

<sup>1</sup> *The University of Tokyo*

**Corresponding Author(s):** n-katagiri@protein.t.u-tokyo.ac.jp

Protein-protein interactions (PPIs) play a critical role in cellular signalling pathways, and are considered as potential therapeutic targets. In various drug screenings against PPIs, one of the representative screening methods is to divide one protein of PPI into some fragments and evaluate the inhibitory activity in a phenotypic cell-based assay. Although it has been expected to obtain the specific binder, the inhibition mechanism remains unclear, and therefore, the development of inhibitor is difficult due to lack of the information about the interaction mechanism at the molecular level. In this research, PPI between S100A4 and MetAP2 was selected as a model PPI. In the previous in vitro binding study, 170-208aa of MetAP2 has been already reported as the binding site, and the fragment peptide of 170-208aa named NBD has inhibited this PPI [1]. However, the interaction mechanism is unknown, and there is no guideline for the design of higher potential inhibitor.

NBD has the characteristic secondary structure, Helix-Turn-Helix (HTH), in an X-ray crystallographic structure of MetAP2 (PDB-ID: 5JFR). Therefore, HTH motif might be important for the inhibitory potential of NBD suggesting that this motif is a novel motif for inhibitory peptides against S100A4. Herein, to reveal the correlation between the inhibitory activity and the characteristic secondary structure, competitive Surface Plasmon Resonance (SPR) assay and Circular Dichroism (CD) measurement were performed. In addition, through combining computational prediction of the interaction manner with these physicochemical analyses, we suggest a novel methodology for developing the PPI inhibitor based on a fragment peptide of one protein of the target PPI.

First, we showed that the helices have a critical role in the inhibitory activity by competitive SPR assay, and that NBD had the solid secondary structure by CD. We further designed and examined the each N/C or both terminal deficient fragment peptides. As a result, only N-terminal deficient peptide maintained the inhibitory activity. We did the Rosetta docking simulation between NBD and S100A4. The most energetically stable complex structure of 20000 predicted structures is well correlated with the result of in vitro physicochemical analysis. From the predicted complex structure, we designed a new peptide named NBD-ΔN10 and demonstrated that NBD-ΔN10 maintained the inhibitory activity as expected.

[1] T. Ochiya, H. Endo, et. al., *Mol. Ther.* 2, 15008 (2015).

106

## Spectroscopic study of UV-absorbing microbial rhodopsin

**Author(s):** Chihiro Kataoka<sup>1</sup>

**Co-author(s):** Keiichi Inoue<sup>2</sup>; Kota Katayama<sup>1</sup>; Oded Béjà<sup>3</sup>; Hideki Kandori<sup>1</sup>

<sup>1</sup> Department of Life Science and Applied Chemistry, Nagoya Institute of Technology

<sup>2</sup> The Institute for Solid State Physics, The University of Tokyo

<sup>3</sup> Faculty of Biology, Technion Israel Institute of Technology

**Corresponding Author(s):** 29411052@stn.nitech.ac.jp

SAR11 TAT rhodopsin is a new member of microbial rhodopsin, which was recently identified in SAR11 HIMB114 strain through genomic analysis[1]. To investigate its photoreaction, we expressed SAR11 TAT in *E. coli* and purified the protein. Interestingly, the pKa of the retinal Schiff base of SAR11 TAT is close to physiological pH (~pH 8), suggesting the presence of both of protonated and unprotonated states under physiological environment (Fig. 1).

For the visible-absorbing protonated state, TAT showed neither ion transport activity nor transient absorption change representing the accumulation of photo-intermediate at  $t > 40 \mu\text{s}$ . The low-temperature UV-visible and FTIR spectroscopy at 77 K showed that retinal photoisomerization occurs similarly with that of other microbial rhodopsins[2], though the following structural changes do not occur due to rapid reversion to the original state. Thus, it is unlikely that the protonated state is the functional state of TAT.

In contrast, we observed transient absorption change upon excitation of the UV-absorbing deprotonated state in micro-second to several-tens-second time region (Fig. 2). The positive peak at 381 nm corresponds to the M intermediate state. In addition, low-temperature UV-visible spectroscopy showed formation of a visible-absorbing intermediate at 77 K, monitoring proton transfer reaction from protein moiety to retinal Schiff base. Proton transfer at such low temperatures was never reported before, and we analysed the mechanism by means of FTIR spectroscopy.

On the basis of present experimental results, we will discuss the unique photoreaction mechanism of SAR11 TAT.

[1] Philosof and Béjà. *Environ. Microbiol. Rep.* 5, 475 (2013)

Ernst. et al. *Chem. Rev.* 114, 126 (2014).

103

## Nonlinear Optical Assay for Sensitive Detection of Cell Membrane Damage

Noritaka Kato<sup>1</sup>

<sup>1</sup> Department of Electronics and Bioinformatics, Meiji University

**Corresponding Author(s):** nkato@meiji.ac.jp

Cytotoxic materials damage cell membranes and the cytotoxicity can be tested by detecting a membrane leakage or a metabolic activity of the cell. Here, I report that the second harmonic generation (SHG), whose intensity is sensitive to the lipid ordering in the membranes [1], can be utilized to analyze the damage of the cell membrane. In this method, cell membranes were stained by the amphiphilic polar dye molecules (Fig. 1, RH237). The amphiphilic nature of RH237 let the dyes intercalate parallel to the lipid molecules in the outer leaflet of membranes and align their polar axis, resulting in the SHG-active membranes. The SHG intensity (ISHG) and the two-photon excited fluorescence (TPF) intensity (ITPF) of the dyes were observed simultaneously by microscope using the excitation wavelength of 850nm. Since the polycation damages the cell membrane, poly(ethyleneimine) (PEI) was used as the model toxicant [2].

Fig. 2 shows the bright-field and SHG images of the stained HeLa cells. The cells incubated in the medium with PEI (Fig. 2d) exhibit lower ISHG than those incubated without PEI (Fig. 2b). Because the ITPF is proportional to the number of the dye molecules, the ISHG was normalized by ITPF to compensate the fluctuation of staining intensity among batches and the ISHG/ITPF value as a function of the PEI concentration in the culture medium was investigated. The lactate dehydrogenase release assay and the cell counting assay were also performed. By comparing these conventional

assays with the proposed assay, it will be represented that how sensitive detection of the membrane damage had been made by the nonlinear optical assay.

[1] D. Fischer, T. Bieber, Y. Li, H.-P. Elsässer, and T. Kissel, *Pharm. Res.* 16, 1273 (1999).  
L. Sacconi, I. M. Tolic-Nørrelykke, M. D'Amico, F. Vanzi, M. Olivetto, R. Antolini, and F.S. Pavone, *Cell Biochem. Biophys.* 45, 289 (2006).

161

## Experimental and Theoretical Spectroscopic Study of the Tyrosine Kinase Inhibitor PD-153035

**Author(s):** Muhammad Khattab<sup>1</sup>

**Co-author(s):** Daryll Knowles<sup>2</sup>; Feng Wang<sup>1</sup>; Andrew Clayton<sup>1</sup>

<sup>1</sup> *Swinburne University of Technology*

<sup>2</sup> *Australian Custom Pharmaceuticals*

**Corresponding Author(s):** mkhattab@swin.edu.au

Our study revolves around investigating the spectroscopic properties of the tyrosine kinase inhibitor, PD-153035, both experimentally and theoretically. The UV-Vis absorption spectrum of PD-153035 exhibited four absorption peaks at ca. 220, 250, 330, and 340 nm. The position and relative optical density of the two lowest energy bands at 330 and 340 nm were significantly altered depending on solvent used in UV-Vis measurements. We therefore prompted to computationally examine PD-153035 structures. The potential energy surface scan revealed four energetically stable conformers of PD-153035 calculated through rotation of the dihedral angle between the anilino and quinazolinyl moieties. Two structures have planar conformations while the other two have twisted conformations. The energy difference between the global minimum structure and the highest energy conformer was estimated at 2.12 kcal/mol. The HOMO-LUMO energy gap was calculated at  $(4.3140 \pm 0.0196)$  eV for the four conformers. The time-dependant Density Functional Theory (td-DFT) calculations employing B3LYP/6-311++G\*\* level of theory revealed that the 330 nm peak can be attributed to the planar conformers while the 340 nm peak can be due to the twisted conformers. The computed oscillator strength of the planar isomers in various solvents had values double that of the twisted isomers. Taken together, these results showed how the absorption spectrum is sensitive to PD-153035 conformation. Hence, our findings assume relevance in understanding the structure and environment of PD-153035 in the ATP binding pocket of its target proteins. Our future work is to identify the fluorescence spectra of PD-153035 in different solvents and when it bounds to its target proteins.

**Acknowledgment:** Authors acknowledge with gratitude the financial support from Excellerate Australia and iMOVE.

206

## Diffusion tensor MR imaging of treatment-induced white matter injury in childhood cancer survivors: clinical and translational studies

Pek-Lan Khong<sup>1</sup>

<sup>1</sup> *Department of Diagnostic Radiology, The University of Hong Kong*

**Corresponding Author(s):**

Diffusion tensor MR imaging (DTI) is based on the diffusion of water molecules in the brain, and advantageous for evaluating white matter pathology as the diffusion process in white matter is highly directional (anisotropic) due to axonal fibers running in parallel. We evaluated its novel role as a marker for treatment-induced neurotoxicity in childhood cancer (medulloblastoma and acute lymphoblastic leukemia) survivors, and then performed translational studies using an animal model of radiation-induced white matter injury to elucidate the histological correlates of the diffusion tensor indices. We found DTI indices to be associated with known neurotoxicity risk factors, and neurocognitive scores in children. In translational studies, the longitudinal changes of DTI indices reflected the histopathological changes of myelination, axonal damage, astrogliosis and necrosis. Hence, our results support the use of DTI to probe white matter microstructure, and as a biomarker to monitor radiation-induced white matter damage.

101

## Modulation of APC expression in mesenchymal stem cell during nomadic culture on heterogeneous field of elasticity

Satoru Kidoaki<sup>None</sup> ; Kousuke Moriyama<sup>None</sup> ; Thasaneeya Kuboki<sup>None</sup> ; Rumi Sawada<sup>1</sup> ; Yuki Tsuji<sup>None</sup> ; Hiroyuki Ebata<sup>None</sup> ; Saori Sasaki<sup>None</sup> ; Aki Yamamoto<sup>None</sup> ; Ken Kono<sup>None</sup> ; Kazusa Tanaka<sup>None</sup>

<sup>1</sup> Division of Cell-Based Therapeutic Products, National Institute of Health Sciences,

**Corresponding Author(s):** kidoaki@ms.ifoc.kyushu-u.ac.jp

Mesenchymal stem cell (MSC) is one of the most potent stem cells, and is a strong cell-resource closest to the clinical application for regenerative medicine. However, standardization and quality assurance of the MSC are essential issues because the quality of MSC is easily varied depending on collection method, individual differences, and changes in stemness during culture. Therefore, to establish the evaluation criteria and culture techniques for assuring the quality of MSC has been strongly required.

As an important factor to cause quality change of MSC during culture, involvement of memory of MSC on mechanical conditions of culture environment has recently been reported [1]. Precise definition of mechanics of the culture substrate that can preserve quality of MSC is a problem. For this problem, we try to establish the design of micro-mechanical field of cell culture hydrogel that can maintain undifferentiated state of MSC. The main strategy is to regulate the mechanical signals input to the cells from local mechanical field during spontaneously migration of MSCs, i.e., when MSCs are cultured in a periodically-designed elastic field such as alternating patterns of stiff and soft regions, a kind of vibrating mechanical signal input to MSCs from each of stiff and soft region are generated especially in the nomadic mode of movement between those two regions. We have observed before that the MSCs after the nomadic movement keep the undifferentiated state due to inhibition of fixation of mechanical memory (we call this phenomenon as “frustrated differentiation”[2]).

In this project, we aim to fully prove the phenomenon and concept of the frustrated differentiation, and to apply the culture methodology for finding standardized MSCs because the MSC culture in nomadic mode of movement on heterogeneous mechanical field always initialize mechanical memory from culture substrate in principle. Recently, we have established complete design of the microelastically-patterned gelatinous gels to realize the nomadic movement of MSCs and quasi-oscillatory input of mechanosignals to the MSCs, which employs the triangular elasticity patterns to induce both forward and reverse durotaxis [3]. After culture of MSCs on the gels for 4days, the highest up-regulation of APC gene was first found from comprehensive analysis for gene expression with DNA microarray, which is deeply related to Wnt signaling and cell motility. We will discuss the effect of forced nomadic movement of MSCs across the elasticity boundaries on the maintenance of stemness through modulating APC expression and resulted regulation of Wnt signaling.

[1] C. Yang, M. W. Tibbitt, L. Basta, K.S. Anseth, *Nat. Mater.* 13, 645-652 (2014).

S. Kidoaki, S. Jinnouch, *Biophys. J.*, 102, Suppl.1, p716a (2012).

A. Ueki, S. Kidoaki, *Biomaterials*, 41, 45-52 (2015).

130

## Subcellular Localization Factors of Type II Membrane Proteins

Tatsuki Kikegawa<sup>1</sup> ; Yuri Mukai<sup>None</sup><sup>1</sup> *Meiji university, japan*

Corresponding Author(s): kikegawa@meiji.ac.jp

Type II membrane proteins are inserted into endoplasmic reticulum (ER) at the early stage of protein subcellular localization due to the recognition of the signal-anchors by ER translocons. However, the evidential transport mechanisms of transmembrane protein localization from ER to the Golgi or plasma membrane have not been elucidated.

In this study, to elucidate transport mechanisms of transmembrane proteins, the discrimination accuracy of each subcellular localization was estimated using the amino acid propensities around the signal-anchor and C-terminus regions. The transmembrane protein dataset was classified into three groups: plasma membrane proteins, ER membrane proteins and Golgi membrane proteins. Furthermore, the trans-Golgi membrane protein dataset was extracted from the Golgi group. The Golgi and plasma membrane proteins could be discriminated with high accuracy (> 90%) using the position-specific scoring matrix (PSSM) created by the signal-anchor sequences [1]. The trans-Golgi membrane proteins are well distinguished from plasma membrane proteins using the PSSM created by the C-terminal sequences. These results suggested that the amino acid propensities around signal-anchor were related to the Golgi to plasma membrane localization mechanism. The C-terminal sequence was considered to related to the trans-Golgi-plasma membrane transport.

To verify this presumption by experimental methods, the GFP fusion proteins with signal-anchors of the representative proteins selected from each group were designed. The subcellular localization of these GFP fusion proteins expressed in HeLa cells were observed by confocal laser fluorescence microscope. As a result, GFP fusion proteins with the transmembrane region (TMR) of ER and cis-Golgi located proteins were localized to ER and cis-Golgi region, respectively. Thus, TMR was thought to be a determinant of ER and cis-Golgi localization. On the other hand, GFP fusion protein with the TMR of plasma membrane located protein was localized to trans-Golgi region. Therefore, type II membrane proteins were suggested to be transported by another mechanism such as C-terminal sequences from trans-Golgi to plasma membrane.

[1] K. Kikegawa, T. Yamaguchi, R. Nambu, K. Etchuya, M. Ikeda and Y. Mukai, *Biosci. Biotech. Biochem.* 82, 1708-1714 (2018).

172

## Structural features determining cardiotonic steroid-induced Na<sup>+</sup>-K<sup>+</sup> pump stimulation – a journey back to the future in the management of new-onset atrial fibrillation?

Yeon Jae Kim<sup>1</sup> ; Elisha Hamilton<sup>1</sup> ; William Hannam<sup>1</sup> ; Chia-Chi Liu<sup>2</sup> ; Helge Rasmussen<sup>3</sup> ; Alvaro Garcia<sup>4</sup><sup>1</sup> *Kolling Institute, University of Sydney and Royal North Shore Hospital*<sup>2</sup> *University of Sydney*<sup>3</sup> *University of Sydney and Royal North Shore Hospital*<sup>4</sup> *University of Technology, Sydney*

Corresponding Author(s): ykim8883@uni.sydney.edu.au

Background: Simple pharmacological approaches in the treatment of atrial fibrillation (AF) must address the raised myocyte cytosolic Ca<sup>2+</sup> concentration ([Ca<sub>i</sub>]), important for the electrophysiological

substrate.  $[Ca_i]$  is expected to be raised in AF due to increased systolic  $Ca^{2+}$  influx during action potentials with the rapid asynchronous atrial myocyte contraction rates.  $Ca_i$  efflux will be reduced because  $[Na_i]$  also must increase with the frequent myocyte action potentials in AF, decreasing export through the main export route for  $Ca_i$ : membrane  $Na^+-Ca^{2+}$  exchange, which is dependent on a low  $[Na_i]$  maintained by the  $Na^+-K^+$  pump (NKP). While cardiotonic steroids (CTSs) inhibit the NKP, stimulation at low concentrations has been sporadically reported, mostly with ouabain. Such stimulation is expected to reduce  $[Ca_i]$ . We have ascertained CTS-induced NKP stimulation can occur, and identified key features of the CTS's steroid core, sugar moiety, and lactone ring required for stimulation. Methods: Voltage clamped rabbit cardiac myocytes were exposed to experimental solutions, which blocked non-NKP currents. NKP current ( $I_p$ , normalised to membrane capacitance) was measured as the inward shift in holding current following elimination of extracellular  $K^+$ , with or without prior exposure to CTSs, for ~1 min at a range of different low concentrations. Results: Exposure to 1-30nM ouabain maximally increased  $I_p$  at 5nM to  $0.69 \pm 0.09$  pA/pF,  $N=6$  vs.  $0.46 \pm 0.03$  pA/pF, in 25 controls ( $p < 0.01$ ). Stimulation was similar in the absence of extracellular  $Na^+$ , ruling out stimulation secondary to  $Na^+$  influx. Rostafuroxin, a putative ouabain antagonist, abolished this stimulation ( $I_p = 0.40 \pm 0.04$  pA/pF,  $N=7$ ). NKP activity is regulated by glutathionylation, a reversible oxidative modification that inhibits the NKP at baseline; and inclusion of a peptide in patch pipette solutions that selectively prevented de-glutathionylation abolished the ouabain-induced NKP stimulation. Exposure to 1-50nM dihydroouabain, differing from ouabain by only having a saturated lactone ring, increased  $I_p$  at 1nM to  $0.65 \pm 0.02$  pA/pF,  $N=6$  ( $p < 0.01$ ). However ouabagenin, that lacks the rhamnose sugar moiety of ouabain, did not increase  $I_p$  at concentrations between 10-500nM, nor did exposure to 5-30nM digoxin that differs from ouabain by possessing a digitose sugar moiety rather than rhamnose, and has an absence of hydroxyl groups on the  $\beta$  surface of its steroid core. Steady-state binding of ouabain will not occur with the ~1 min exposures. Ouabain pre-exposure for 1 hour to achieve near steady state binding reduced  $I_p$  ( $p < 0.05$ ) at 10nM. Conclusions: Some CTSs can induce transient NKP stimulation. A sugar moiety and possibly hydroxyl groups on the steroid core are important for the stimulation to occur. The mechanism for NKP stimulation is reversal of the inhibitory oxidative modification of glutathionylation, a pathway not previously implicated in effects of CTSs on NKP activity. Implications: The ~50% ouabain-induced NKP stimulation shown here can realistically be expected to improve the pathophysiological substrate in acute management of new-onset AF. Ouabain was previously used in heart failure, but lost to digoxin in the marketplace because of its poor oral absorption. A human trial of intravenous ouabain vs. digoxin should be considered. "Bringing ouabain back" would face significantly fewer regulatory hurdles than introducing a new drug candidate due to its previously established human safety record.

86

## Structure-Property-Energetics Relationships in Deriving Guidelines for Rational Drug Design: Thermodynamic Approach

Nand Kishore<sup>1</sup><sup>1</sup> Indian Institute of Technology Bombay

Corresponding Author(s): nandk@chem.iitb.ac.in

Oral bioavailability and effective delivery of a drug molecule to the target site are interrelated to each other. Suitable delivery vehicles are required for effective delivery of new molecular entities which usually have high hydrophobic character, and hence low bioavailability. Self-assemblies of micelles, niosomes, and liposomes offer interesting partitioning abilities to the drug molecules, therefore have been used as effective delivery vehicles. Most of the information available in literature is qualitative in nature. We have quantitatively investigated the partitioning of antibiotic drugs streptomycin, lincomycin, neomycin, tetracyclin, and others having different functionalities into cationic, non-ionic, mixture of cationic and nonionic surfactant micelles, and niosomes. Their interaction with the transport protein serum albumin upon subsequent delivery when released from self-assemblies has been studied. A combination of isothermal titration calorimetry, differential scanning calorimetry, spectroscopy and microscopy has been used to obtain the thermodynamic signatures associated with partitioning along with interaction with the protein and the resulting conformational changes. A comparison of thermodynamic signatures for partitioning of several antibiotic drugs have permitted an understanding of the role of molecular features which are effective in the partitioning process. These studies are important in understanding biophysics of partitioning of a variety of

existing drug molecules and new molecular entities into suitable delivery vehicles and hence establishing structure–property–energetics relationships. Attempts have been made to derive guidelines towards a broader goal of rational drug design based on such structure-property-energetics relationships in these systems.

191

## Unveiling the molecular mechanism of RNA interference by single molecule approaches

Hye Ran Koh<sup>1</sup>

<sup>1</sup> *Chung-Ang University*

**Corresponding Author(s):** hrkoh@cau.ac.kr

RNA interference (RNAi) is a gene regulation pathway induced by small RNA molecules, microRNA (miRNA) and small interfering RNA (siRNA). It is a multi-step process consisting of the small RNA genesis by Dicer/TRBP, guide strand selection and the guide strand-mediated gene silencing by RNA-induced silencing complex (RISC). Despite of the well-characterized RNAi pathway, it still remains unclear how the structural features of small RNAs contribute to dicing and subsequent gene silencing efficiency. Here, we incorporated single-molecule fluorescence resonance energy transfer (smFRET) to investigate the molecular interaction between RNA and the components of RISC and discovered that TRBP diffuses specifically on dsRNA, which contributed to enhancing miRNA and siRNA processing by Dicer. Also, with single-molecule fluorescence in situ hybridization (smFISH) to count mRNA at single-cell level, we quantified the RNAi efficiency by screening various structures of small RNAs. We found that dicing rate and silencing efficiency both increase as a function of the loop length of the small RNAs in a correlated manner. In contrast, mismatches in the stem drastically diminish the silencing efficiency without impacting the dicing rate. Our results imply that the stem structures prevalent in cellular miRNAs are intended for suboptimal silencing efficiency. The quantitative analysis of RNAi using smFISH together with smFRET would be a powerful platform to study RNAi and other gene-regulating system.

49

## Molecular dynamics study on the mechanism of voltage dependent inactivation in a mutant of the voltage-gated potassium channel

Hiroko X. Kondo<sup>1</sup> ; Norio Yoshida<sup>2</sup> ; Matsuyuki Shirota<sup>3</sup> ; Yu Takano<sup>4</sup> ; Kengo Kinoshita<sup>3</sup>

<sup>1</sup> *Kitami Institute of Technology*

<sup>2</sup> *Kyushu University*

<sup>3</sup> *Tohoku University*

<sup>4</sup> *Hiroshima City University*

**Corresponding Author(s):** h\_kondo@mail.kitami-it.ac.jp

Voltage-gated potassium (Kv) channels conduct K<sup>+</sup> ions selectively in response to membrane depolarization and regulate the amplitude and duration of action potentials. Their gating processes are regulated by several mechanisms [1]. “C-type” inactivation is one of well-defined inactivation processes in the voltage-gated potassium channels [2-4]. This inactivation is primarily caused by conformational changes around the selectivity filter (SF) and/or outer mouth of the channels. The W434F-mutated Shaker channel is known as a nonconducting mutant and is in a C-type inactivation state at a depolarizing membrane potential [5,6]. To clarify the structural properties of C-type inactivated protein, we performed molecular dynamics

simulations of the wild-type and W366F (corresponding to W434F in Shaker) mutant of the Kv1.2-2.1 chimera channel. The W366F mutant was in a nearly nonconducting state with a depolarizing voltage and recovered from inactivation with a reverse voltage. The result of the principal component analysis for SF structures shows a conformational difference at V375 and G376 between channels in the 'active' and 'inactive' states. For the molecular mechanism of C-type inactivation, we hypothesized that the local conformational change in SF correlated with a change in SF occupancy by K<sup>+</sup> ions and the restriction of ion permeation. To evaluate this hypothesis, we analyzed the probability distributions of K<sup>+</sup> ions in SF of the WT and W366F mutant by using the three-dimensional reference interaction site model (3D-RISM) theory [7-9]. Our simulations and 3D-RISM analysis suggested that structural changes in the SF upon membrane depolarization trap K<sup>+</sup> ions around the inner mouth of the selectivity filter and prevent ion permeation. This pore restriction is involved in the molecular mechanism of C-type inactivation.

G. Yellen, *Q. Rev. Biophys.* 31, 239 (1998).

K. L. Choi, R. W. Aldrich, and G. Yellen, *Proc. Natl. Acad. Sci.* 88, 5092 (1991).

G. Yellen, D. Sodickson, T. Y. Chen, and M. E. Jurman, *Biophys. J.* 66, 1068 (1994).

G. Panyi, Z. Sheng, and C. Deutsch, *Biophys. J.* 69, 896 (1995).

E. Perozo, R. MacKinnon, F. Bezanilla, and E. Stefani, *Neuron* 11, 353 (1993).

J. F. Cordero-Morales, V. Jogini, S. Chakrapani, E. and Perozo, *Biophys. J.* 00, 2387 (2011).

Molecular Theory of Solvation, F. Hirata, Ed., *Understanding Chemical Reactivity* (Kluwer Academic Publishers, 2003)

D. Beglov and B. Roux, *J. Phys. Chem. B* 101, 7821 (1997)

A. Kovalenko and F. Hirata, *Chem. Phys. Lett.* 290, 237 (1998)

79

## Analysis of functional and structural properties of a neuroferritinopathy-related ferritin light chain variant A96T

**Author(s):** Takumi Kuwata<sup>None</sup>

**Co-author(s):** Yuta Okada ; Tomoki Yamamoto ; Daisuke Sato ; Kazuo Fujiwara ; Masamichi Ikeguchi <sup>1</sup>

<sup>1</sup> *Soka University*

**Corresponding Author(s):** e18m5608@soka-u.jp

Neuroferritinopathy is a disease caused by mutations in the ferritin light chain 1 (FTL1) gene leading to abnormal excessive iron accumulation in the brain, predominantly in the basal ganglia [1]. To date, nine types of mutations relating to neuroferritinopathy have been identified. Eight of them are frameshift mutations in the exon 4 and produce mutants with different amino acid sequence and extension from 4 to 16 residues at the C-terminal region [1]. Some of these mutants have been investigated in detail, so that the information of their properties and the crystal structures gave us an insight into the mechanism of neuroferritinopathy caused by these mutations [2,3]. In contrast to the frameshift mutants, structural information on the point mutant A96T has not yet been obtained (Fig1). Thus, we expressed A96T mutant in *E. coli*, purified it, and characterized its structure by circular dichroism (CD) spectroscopy, analytical ultracentrifugation (AUC) and small-angle X-ray scattering (SAXS). The structure of A96T was revealed to be essentially identical to that of the ferritin light chain wild type (HuFTL). It was also shown that A96T bears the normal iron-incorporation activity. The stability of A96T is lower than that of HuFTL, but the structure of A96T is enough stable to function under the physiological conditions. The refolding efficiently of A96T is significantly lower than that of HuFTL (Fig2). These results suggest that the A96T molecule may aggregate due to its misfolding in the cell, and this aggregation may induce neuroferritinopathy.

[1] Levi, S., Rovida, E., *Neurobiol. Dis.* 81, 134-143 (2015).

Baraibar, M. A., Barbeito, A. G., Muhoberac, B. B., Vidal, R., *J. Biol. Chem.* 283, 31679-31689 (2008).



Baraibar, M. A., Muhoberac, B. B., Garringer, H. J., Hurley, T. D., Vidal, R., J. Biol. Chem. 285, 11948-11957 (2010).

124

## Structure and Assembly Mechanism of the Type III Secretion System Needle Tip Complex

Wunna Kyaw<sup>1</sup> ; Andrew Tuckwell<sup>1</sup> ; Stephanie Xu<sup>1</sup> ; Lawrence Lee<sup>1</sup>

<sup>1</sup> UNSW

Corresponding Author(s): blugyblug@gmail.com

The assembly of macromolecular complexes, which gives rise to biological structure, follows strict temporal and spatial control to result in well-ordered superstructures. This is exemplified in the Type 3 Secretion System, a 3.5 MDa syringe shaped protein superstructure consisting of hundreds of subunits which injects virulence factors into host cells. The most distal substructure, the needle tip complex (NTC), is the most surface exposed and could be a strong candidate for epitope engineering and structure guided vaccine design towards bacterial infection. Current cryo-EM reconstructions of assembled NTC's are incompatible with high resolution crystal structures of the disassembled monomers, and an atomic resolution model of the assembled NTC is not yet available. We predict that NTC assembly is spatially controlled by pre-existing structures scaffolding its construction in vivo. Here, we combine Rosetta de novo protein designs with molecular dynamics simulations of scaffolded NTCs to gain insight into the mechanism of spatially localized, scaffolded protein assembly. We then use data from cross linking mass spectrometry and solution X-ray scattering to design stabilized assemblies on synthetic DNA scaffolds for structure guided vaccine design.

96

## In vitro reconstitution of HIV capsid lattices as interaction platforms to study host protein binding dynamics

Derrick Lau<sup>1</sup> ; Wang Peng<sup>1</sup> ; James Walsh<sup>1</sup> ; Till Böcking<sup>1</sup>

<sup>1</sup> UNSW Single Molecule Science

Corresponding Author(s): derrick.lau@student.unsw.edu.au

The HIV capsid is a fragile fullerene cone shell composed of ~1500 individual CA proteins arranged into ~240 hexamers and exactly 12 pentamers, which are required for closure of the capsid. This structure protects the viral genetic material from detection and degradation on its journey to the nucleus and must undergo controlled disassembly in a process known as "uncoating". The capsid lattice is a binding platform for competing sets of host cell proteins that determine the fate of the capsid and its cargo. On one hand, the virus has evolved to hijack the functions of a series of host cell proteins to move towards the nucleus, to "cloak" its capsid from being detected and to coordinate capsid uncoating. On the other hand, the cell has evolved pattern recognition proteins that bind to the viral capsid and reroute it for degradation. A dissection of this molecular arms race between virus and host requires tools to measure the binding of host cell proteins to the capsid lattice.

Here, we self-assembled recombinant CA protein with engineered cysteines to form fluorescently labelled, cross-linked lattices with different architectures as binding platforms to study the binding of host cell proteins. Depending on the positions of the engineered cysteines [1], CA protein self-assembled into open tubes (diameters of 67 nm and several  $\mu\text{m}$  long), which aggregated into bundles, or into soluble spheres (38 nm diameter) as shown by negative staining electron microscopy. These

structures were immobilised via antibodies on the modified surface of a glass coverslip for observation using total internal reflection fluorescence (TIRF) microscopy. Tubes were grown from mutant CA proteins directly on the surface to minimise aggregation and appeared as lines in the fluorescence image. Spheres were pre-assembled and then captured onto the modified surface, appearing as diffraction-limited spots. A solution with host cell proteins labelled with a different fluorophore was then added via microfluidics to visualise their dynamic interactions with individual CA structures on the surface at the single-molecule level using time-lapse TIRF imaging. Binding kinetics and stoichiometries from the fluorescence movies were extracted using automated image analysis scripts. Our data show that the known capsid-binding protein cyclophilin A (CypA) bound to our cross-linked CA tubes with a dissociation constant in the low  $\mu\text{M}$  range and at sub-stoichiometric ratio, consistent with structural models of its binding to the CA lattice [2]. The technique developed here can be used to identify and estimate binding kinetics of novel binders to the capsid lattice at a single molecule level, whereby the different architectures recapitulate different structural features found in the authentic conical capsid.

[1] O. Pornillos, B.K. Ganser-Pornillos, S. Banumathi, Y. Hua and M. Yeager, *J. Mol. Biol.* 401, 5 (2010)  
C. Liu, J. R. Perilla, J. Ning, M. Lu, G. Hou, R. Ramalho, B.A. Himes, G. Zhao, G.J. Bedwell, I. Byeon, J. Ahn, A.M. Gronenborn, P.E. Prevelige, I. Rouso, C. Aiken, T. Polenova, K. Shulten and P. Zhang, *Nat. Commun.* 7, Article number: 10714 (2016)

21

## Using Neutron Reflectometry to Understand Antibiotic Resistance in Gram-negative Bacteria at the Outer Membrane

Meiling Han<sup>1</sup> ; Anton Le Brun<sup>2</sup> ; Seong Hoong Chow<sup>1</sup> ; Hsin-Hui Shen<sup>1</sup> ; Tony Velkov<sup>1</sup> ; Jian Li<sup>1</sup>

<sup>1</sup> Monash University

<sup>2</sup> ANSTO

**Corresponding Author(s):** abn@ansto.gov.au

With bacteria increasingly becoming resistant to common antibiotics, we are currently heading for a post-antibiotic world, where treatable common ailments are suddenly untreatable. This means that there is now considerable research effort in understanding how antibiotic resistance arises, and in creating a new generation antibiotics. The outer membrane is the first line of defence against antibiotics for Gram-negative bacteria. Being able to penetrate the outer membrane is essential to designing effective antibiotics and antimicrobial peptides. The outer membrane is an asymmetric bilayer consisting of phospholipids on its lower leaflet and lipopolysaccharides on its environment-facing outer leaflet. This work will present on creating model outer membranes from *Pseudomonas aeruginosa*, a bacterium that is normally harmless, but infections from which can prove to be problematic for those that are immunocompromised. Worryingly, *P. aeruginosa* is showing increasing signs of becoming resistant to Polymixin B, an antibiotic of last resort. Certain biochemical modifications to lipid A (a component of lipopolysaccharides) can confer resistance to Polymixin B in *P. aeruginosa* strains. Model *P. aeruginosa* outer membranes using lipid A with different modifications were created on silica surfaces using Langmuir-Blodgett and Langmuir-Schaeffer deposition techniques. Model outer membranes created this way are ideal tools for studying the binding antimicrobial peptides because: a) they reflect the lipid composition of the membrane, b) reflect the fluidity of the membrane, and c) maintain the asymmetric nature of the outer membrane. The nanoscale structures of the membranes were determined using neutron reflectometry and it was observed that Polymixin B was unable to penetrate into bilayers that consist of de-acylated lipid A. New drug targets Octapeptin A3 [1], and modified Polymixins FADDI-019 and FADDI-020 [2] were tested and found to disrupt membranes composed of modified lipid A which confer resistance to Polymixin B.

[1] M.-L. Han et al., *ACS Infect. Dis.* 3, 606 (2017)  
M.-L. Han et al., *ACS Chem. Biol.* 13, 121 (2018)

32

## Computational Study on the Amyloid-beta peptides in Explicit Water

**Author(s):** THI DIEM LE<sup>1</sup>

**Co-author(s):** Sihyun Ham<sup>1</sup>

<sup>1</sup> *Sookmyung Women's university*

**Corresponding Author(s):** lethidiem3495@gmail.com

The self-assembly of the amyloid- $\beta$  (A $\beta$ ) peptides is strongly related to the pathogenesis of Alzheimer's disease. Among A $\beta$  peptide alloforms, amyloid- $\beta$ 1-40 (A $\beta$ 40) and amyloid- $\beta$ 1-42 (A $\beta$ 42) are the most abundant ones in the human body. Although A $\beta$ 42 differs only by the additional I41A42 residues in the C-terminus, it exhibits a greater tendency to aggregate and much higher toxicity to neurons than A $\beta$ 40. Here, we investigated the molecular factors that influence the aggregation propensity of A $\beta$ 42 and A $\beta$ 40 based on molecular dynamics simulations combined with solvation thermodynamic analyses. Although the two variants display structurally similar topologies, a slightly enhanced  $\beta$ -structure forming tendency is observed in the C-terminal region of A $\beta$ 42 as compared to A $\beta$ 40. The thermodynamic decomposition analysis indicates that the further dehydration of C-terminal region due to its enhanced formation of  $\beta$ -structure, together with two additional hydrophobic residues (I41A42), leads to the higher solvation free energy of A $\beta$ 42 relative to A $\beta$ 40. This result implies a larger water-mediated attraction between A $\beta$ 42 monomers for its self-assembly. Our results provide structural and thermodynamic understanding on the role of the C-terminal region in increasing the aggregation propensity of A $\beta$ 42 relative to A $\beta$ 40 in aqueous solution.

31

## Computational Drug Design to Target Human MDM2 Protein

**Author(s):** THI DIEM LE<sup>1</sup>

**Co-author(s):** Sihyun Ham<sup>1</sup>

<sup>1</sup> *Sookmyung Women's university*

**Corresponding Author(s):** lethidiem3495@gmail.com

Inhibitor design to target intracellular protein-protein interaction (PPI) is quite challenging in chemical biology and drug discovery. Herein, we attempted to design inhibitors for an intracellular PPI, p53-HDM2 (human MDM2), based on the modified peptide scaffold. The tumor suppressor protein p53 is a transcription factor which regulates a major pathway for protecting cells from malignant transformation. Under non-stressed conditions, p53 binds with HDM2 to be inactivated. In many human tumor cells, HDM2 is overproduced to impair the p53 level. Recently, inhibitors mimicking the  $\alpha$ -helix part of the p53 protein have been designed and found to exhibit high binding affinity with HDM2 protein, and hydrocarbon stapled peptides have found to make up a promising class of protein-protein interaction regulators. We report the comparative study on the structural and thermodynamic characteristics for the binding complex of the stapled p53/HDM2 and unstapled p53/HDM2. We performed molecular dynamics simulations to investigate the structural information of the complexes. The binding free energy calculation was executed to elucidate the molecular factors contributing to the binding affinity. We found that the binding affinity of the stapled p53 peptide was higher than that for the corresponding unstapled peptide. We demonstrated structurally and thermodynamically that the hydrocarbon linker contributes significantly to the high binding affinity of the stapled p53/HDM2.

111

## Biomembrane Dynamics at Cell-Surface Interfaces: A Role in Multi-Drug Resistance Mechanism

Tzong-Hsien Lee<sup>None</sup>

**Corresponding Author(s):** john.lee@monash.edu

Biomembranes are highly complex in the chemical composition, structural properties and physical dynamics. The bactericidal action of antimicrobial peptides (AMPs) rely on the direct interaction with bacterial membrane lipids. Thus, changes in the lipid composition of bacterial membranes can have profound effects on lowering the activity of AMPs. In order to understand the effect of biomembrane dynamics in bilayer thickness and molecular order on the activity of AMPs, the interaction of maculatin 1.1 (Mac1.1) with various phosphatidylcholine (PC) model membranes composed of monounsaturated acyl chain length between 14-22 carbons was studied by dual polarisation interferometry (DPI) and <sup>31</sup>P and <sup>1</sup>H solid-state NMR techniques [1]. The thickness and bilayer order of each PC bilayer determined by DPI showed a linear dependence on the acyl chain length and the thickness values correlated well with those obtained from X-ray and neutron scattering data. At low peptide concentration, the Mac1.1 bound with highest mass to DPOPC (di-(16:1)-PC) while the lowest membrane-bound Mac1.1 mass was obtained with DEPC (di-(22:1)-PC). Higher Mac1.1 concentration and higher membrane-bound peptide mass are required to induce bilayer disorder in higher ordered PC bilayer. No significant perturbation of <sup>31</sup>P chemical shift anisotropy (CSA) values was observed for DMOPC (di-(14:1)-PC) and DPOPC, while a small and larger increase in <sup>31</sup>P CSA values was observed for DOPC (di-(18:1)-PC) and DEPC, respectively. In the case of DEPC, the greater range in CSA indicates different DEPC headgroup conformations or environments in the presence of Mac1.1. Furthermore, a greater change in bilayer birefringence was observed by DPI for DEPC with smaller amount of Mac1.1, indicating a larger extent of bilayer disorder. Overall, an optimum bilayer thickness and lipid order may be required for effective membrane perturbation by Mac1.1 and increasing the bilayer thickness and order may counteract the activity of Mac1.1 and impose antimicrobial resistance.

[1] T.H. Lee, M-A. Sani, S. Overall, F. Separovic and M.I. Aguilar, *Biochim. Biophys. Acta Biomembr.* 1860, 300 (2018).

65

## General anaesthetic modulation of pentameric ligand-gated ion channel fu

Bogdan Lev<sup>1</sup> ; Brett Cromer<sup>2</sup> ; Marc Delarue<sup>3</sup> ; Toby W Allen<sup>1</sup>

<sup>1</sup> *School of Science, RMIT University, Melbourne, VIC 3001, Australia*

<sup>2</sup> *Department of Chemistry and Biotechnology, Swinburne University of Technology, John Street, Hawthorn, VIC, 3122, Australia*

<sup>3</sup> *Department of Structural Biology and Chemistry, Institut Pasteur and UMR 3528 du CNRS, F-75015 Paris, France*

**Corresponding Author(s):** bogdan.lev@rmit.edu.au

General anaesthetics work by blocking “on” switches and enhancing “off” switches in the brain, leading to loss of sensation and the ability to feel pain. These switches, called pentameric ligand-gated ion channels, control synaptic neurotransmission via an allosteric mechanism, where agonist binding induces global conformational changes that open an ion-conducting pore. These proteins are targets for general anaesthetics, with GABAA receptors identified as the key determinants of anaesthetic sensitivity. Using atomic-resolution structures for a related channel, GLIC, from bacteria, we aim to understand how general anaesthetics affect channel function by binding to disparate excitatory and inhibitory sites in the protein. We use flooding simulations to target propofol binding sites and employ an atomistic molecular dynamics string method to solve for the minimum free energy gating pathways for activation in the presence of general anaesthetic propofol. We employ transition analysis to compute free energy surfaces from millions of short ‘swarm’ simulations. Through direct

comparison to recently uncovered activation mechanisms and energetics in the absence of propofol [1], we attempt to explain the mechanisms of allosteric modulation of the receptor. These results provide molecular-level insight into the effects of general anaesthetics on pentameric ligand-gated channels, allowing for the design of more effective anaesthetics that are safer, both immediately and for long-term brain function.

[1] Lev et al., PNAS, (2017), 114, 21, E4158–E4167

132

## **N-linked glycosylation determines the membrane trafficking of human Piezo1 ion channels**

Jinyuan Li<sup>1</sup>

<sup>1</sup> VCCRI

**Corresponding Author(s):** j.li2@victorchang.edu.au

Mechanosensitive (MS) channels are essential integral membrane proteins that sense mechanical stimuli. The Piezo family of ion channels are a relatively new class of MS channels that are ubiquitously expressed and important in both physiology and pathophysiology. Like all membrane proteins they must go through quality control processes in the golgi and endoplasmic reticulum that results in them reaching their final destination at the plasma membrane. Here we show that N-linked glycosylation of two highly conserved asparagine residues in the cap of human Piezo1 is necessary for the mature protein to reach the plasma membrane. Both mutation of these asparagines (N2294Q & N2331Q) and treatment with PNGaseF abolish the fully glycosylated mature protein. Consistent with this HEK293T cells over-expressing the double mutant (N2294Q & N2331Q) exhibit almost no stretch activated currents. These findings may help in the study of loss of function mutations (caused by aberrations in protein trafficking) of human Piezo1, which cause diseases such as generalized lymphatic dysplasia, where the upper fully glycosylated version represents the major component of the surface protein.

218

## **Principles Governing Biological Processes**

Carmay Lim<sup>1</sup>

<sup>1</sup> *Institute of Biomedical Sciences Academia Sinica, Taiwan*

**Corresponding Author(s):**

105

## **Investigating apical constriction force of Madin-Darby Canine Kidney cells by laser ablation**

Keng-hui Lin<sup>1</sup>

<sup>1</sup> *Institute of Physics, Academia Sinica*

**Corresponding Author(s):** kenghui@gate.sinica.edu.tw

Tight junctions locate at the sub-apical region on the lateral plane. It serves a convenient marker to indicate apical area. The study of tight junction functions is usually performed on confluent Madin-Darby Canine Kidney (MDCK) cells or Caco cells grown on filter paper. It has been shown that the actomyosin contractility is linked to the morphology of tight junctions and its paracellular transport. The change is always accompanied with the morphological change of tight junctions. Under high tension, the tight junctions become tortuous. When actomyosin contractility is disrupted by drug treatment, the tight junctions morphology become straighter. There was proposed mechanism as actomyosin cable as a purse-string connecting to the tight junctions [1] but the observed phenomena which can not fully be explained by this model. In this work, we propose the tight junctions in mature and polarized MDCK cells are linked to the actomyosin network on the apical surface exerting non-negligible medio-apical tension on the apical surface. We used femto-second laser to ablate the apical surface of MDCK cells. Through quantitative image analysis, we found that cell area increase accompanied with the straightening of the tight junctions. The apical area expansion rate is positively correlated with the cell area and tortuosity. Our findings support our hypothesis. Contrary to the conventional thinking, the mechanism of MDCK apical constriction force is from the actomyosin-network on the apical surface, instead of the circumferential actomyosin cable. Our finding is not only important for understanding how actomyosin contractility regulate paracellular transport but also in tissue morphogenesis such as MDCK cystogenesis.

[1] J. R. Turner, *Semin. Cell Dev. Biol.*, 11, 301 (2000).

57

## Tuning the antimicrobial properties of biomimetic microstructured titanium surfaces towards efficient killing of *Staphylococcus aureus*

Elena Ivanova<sup>1</sup> ; Russell Crawford<sup>1</sup> ; Saulius Juodkazis<sup>2</sup> ; Denver Linklater<sup>2</sup>

<sup>1</sup> RMIT

<sup>2</sup> Swinburne University of Technology

**Corresponding Author(s):** dlinklater@swin.edu.au

Although titanium is the material of choice for the manufacture of orthopaedic and dental implants because of excellent corrosion resistance and proven biocompatibility, the occurrence of premature implant failure due to implant-associated infections remains a prominent concern for clinicians [1]. In this study we examine the evolution of surface microarchitecture following mask-less plasma etching of bulk titanium for 5, 10, 20, 30 and 40 minutes based on 2D-FFT, SEM and AFM characterisation, highlighting the formation of a two-tier pillared surface topology at the maximum etch period. Each separate surface topography was assessed for its antibacterial efficiency against two common human pathogens, *Pseudomonas aeruginosa* and *Staphylococcus aureus*, achieving maximum antibacterial efficiencies of  $87.2 \pm 2\%$  and  $72.5 \pm 13\%$ , respectively. Using a range of microscopic techniques, this work highlights the influence of change in microscale topology on bactericidal activity based on changes to height, spacing and density. Significantly, the formation of 3D hierarchical features was found to minimise attachment of *S. aureus*, trapping the cells inside the micron size pillars and killing by the second tier of pillars (Figure 1).

[1] M. Ribeiro, F.J. Monteiro, M.P. Ferraz, Infection of orthopedic implants with emphasis on bacterial adhesion process and techniques used in studying bacterial-material interactions, *Biomatter* 2(4) (2012) 176-194.

52

## Entropic Contribution to Enhanced Thermal Stability in the Thermostable P450 CYP119

Zhuo Liu<sup>1</sup> ; Sara Lemmonds<sup>None</sup> ; Juan Huang<sup>None</sup> ; Madhusudan Tyagi<sup>None</sup> ; Liang Hong<sup>1</sup> ; Nitin Jain<sup>None</sup>

<sup>1</sup> *Shanghai Jiao Tong University*

**Corresponding Author(s):** liuzhuo-chirality@hotmail.com

The enhanced thermostability of thermophilic proteins with respect to their mesophilic counterparts is often attributed to the enthalpy effect, arising from strong interactions between protein residues. Intuitively, these strong inter-residue inter-actions will rigidify the biomolecules. However, the present work utilizing Neutron Scattering and solution NMR spectroscopy measurements demonstrates a contrary example that the thermophilic cytochrome P450, CYP119, is much more flexible than its mesophilic counterpart, CYP101A1, something which is not apparent just from structural comparison of the two proteins. A mechanism to explain this apparent contradiction is that higher flexibility in the folded state of CYP119 increases its conformational entropy and thereby reduces the entropy gain during denaturation, which will increase the free energy needed for unfolding and thus stabilize the protein. This scenario is supported by thermodynamic data on the temperature dependence of unfolding free energy, which shows a significant entropic contribution to the thermostability of CYP119 and lends a new dimension to enhanced stability, previously attributed only to presence of aromatic stacking interactions and salt-bridge networks. Our experimental data also supports the notion that highly thermophilic P450s such as CYP119 may use a mechanism that partitions flexibility differently from mesophilic P450s between ligand binding and thermal stability.

51

## Direct characterization of contributions of self-motion of hydrogen and interatomic motion of heavy atoms to protein anharmonicity

Zhuo Liu<sup>1</sup> ; Chenxing Yang<sup>None</sup> ; Juan Huang<sup>None</sup> ; Gaia Ciampalini<sup>None</sup> ; Jun Li<sup>None</sup> ; Victoria García Sakai<sup>None</sup> ; Madhusudan Tyagi<sup>None</sup> ; Hugh O'Neill<sup>None</sup> ; Qiu Zhang<sup>None</sup> ; Simone Capaccioli<sup>None</sup> ; Kai Ling Ngai<sup>None</sup> ; Liang Hong<sup>1</sup>

<sup>1</sup> *Shanghai Jiao Tong University*

**Corresponding Author(s):** liuzhuo-chirality@hotmail.com

One of the fundamental challenges in biophysics and biochemistry is to understand the connection between protein dynamics and its function. This challenge partially arises from the fact that protein molecules often present a variety of local atomic motions and collective dynamics on the same time scales, and this has rendered difficulty on the experimental identification and quantification of different dynamic modes. Here, by performing neutron scattering on lyophilized hydrogenated proteins and their perdeuterated counterparts using instruments of different time resolutions, the self-motion of hydrogen atoms and the collective interatomic motion of heavy atoms (C, O, N) in proteins were characterized separately over a wide temperature range on the pico-to-nanosecond time scales. It is found that the self-motions of protein hydrogen atoms present a resolution-time-dependent anharmonic onset, which can be ascribed to the thermal activation of local side-group motions, mostly the methyl rotations with an energy barrier of ~3 kcal/mol, while the collective dynamics of protein heavy atoms exhibit a resolution-time-independent anharmonicity around 200 K. Further dielectric spectroscopy and Brillouin light scattering results suggest that the anharmonicity of the heavy atoms results from the unfreezing of the relaxation of the protein structures within the laboratory equilibrium time (100-1000 s), which softens the entire bio-macromolecules.

17

## Phasor analysis and image correlation spectroscopy of histone

## FLIM/FRET reveals spatiotemporal regulation of chromatin organization by the DNA damage response.

Jieqiong Lou<sup>1</sup> ; Lorenzo Scipioni<sup>2</sup> ; Belinda Wright<sup>3</sup> ; Tara Bartolec<sup>4</sup> ; Jessie Zhang<sup>4</sup> ; Katharina Gaus<sup>3</sup> ; Enrico Gratton<sup>2</sup> ; Anthony Cesare<sup>4</sup> ; Elizabeth Hinde<sup>5</sup>

<sup>1</sup> *1Department of Biochemistry and Molecular Biology, Bio21 Institute, University of Melbourne, Victoria 3010, Australia.*

<sup>2</sup> *2Laboratory for Fluorescence Dynamics, Biomedical Engineering, University of California, Irvine, California 92697-2715, USA.*

<sup>3</sup> *3EMBL Australia Node in Single Molecule Science, School of Medical Sciences, University of New South Wales, New South Wales 2052, Australia.*

<sup>4</sup> *4Genome Integrity Unit, Children's Medical Research Institute, University of Sydney, Westmead, New South Wales 2145, Australia.*

<sup>5</sup> *1Department of Biochemistry and Molecular Biology, Bio21 Institute, University of Melbourne, Victoria 3010, Australia. 3EMBL Australia Node in Single Molecule Science, School of Medical Sciences, University of New South Wales, New South Wales 2052, Australia. 5ARC Centre of Excellence in Advanced Molecular Imaging, University of New South Wales, Sydney, NSW 2052, Australia.*

**Corresponding Author(s):** jieqiong.lou@unimelb.edu.au

Here we describe a biophysical method to measure chromatin organisation in live cells with nucleosome level resolution. The method is based on a localised phasor image correlation analysis (ICS) of FLIM-FRET microscopy data acquired in human cells co-expressing H2B-eGFP and H2B-mCherry. This multiplexed approach produces spatiotemporal maps of nuclear wide chromatin compaction and quantifies the stability, size and spacing between detected chromatin foci. We used this method in cells where double strand breaks (DSBs) were induced by near-infrared laser micro irradiation to assay chromatin dynamics during the DNA damage response (DDR). These experiments revealed that ATM- and RNF8 directed rapid local chromatin decompaction at DSBs, coupled with formation of a stable ring of compact chromatin surrounding the repair locus. ATM and RNF8 also directed reorganization of global chromatin into compact chromatin domains over hours. Based on these data we built a longevity map of sites with high FRET indicating the time scale of large scale compaction events. Then by use of a phasor-based ICS analysis we identified the locations where the DDR shapes local and global chromatin dynamics and demonstrate the utility of phasor-based ICS analysis of FLIM-FRET for the study of chromatin biology.

141

## Regulatory effect of the N-terminus in Na,K-ATPase

Caitlin MacKintosh<sup>None</sup> ; Ron Clarke<sup>None</sup>

**Corresponding Author(s):**

P-type ATPases are essential to life. They all use energy from ATP to pump ions or lipids across membranes. A prime example is the Na<sup>+</sup>,K<sup>+</sup>-ATPase, which plays a crucial role in maintaining the volume of all animal cells (1). Several P-type ATPases possess extra-membrane lysine-rich segments at either the N- or C-termini of their catalytic subunits. These segments are often referred to as R-domains, where R = regulatory, but the mechanism by which they might regulate ATPase activity is still unclear. Recent investigations on the Na<sup>+</sup>,K<sup>+</sup>-ATPase suggest that its N-terminal tail may be interacting electrostatically with the neighbouring membrane, thus influencing the relative stabilities of different protein conformational states (2).

In order to study the details of this possible interaction three different enzymes were investigated: the Na<sup>+</sup>,K<sup>+</sup>-ATPase, the gastric H<sup>+</sup>,K<sup>+</sup>-ATPase and the sarcoplasmic reticulum Ca<sup>2+</sup>-ATPase. Both the Na<sup>+</sup>,K<sup>+</sup>-ATPase and the H<sup>+</sup>,K<sup>+</sup>-ATPase have lysine-rich N-termini, whereas the extra-membrane N-terminus of the Ca<sup>2+</sup>-ATPase is significantly shorter and is not particularly rich in lysines. Poly-L-lysine (PLL) was used as a model for the Na<sup>+</sup>,K<sup>+</sup>- or H<sup>+</sup>,K<sup>+</sup>-ATPase N-terminus. It was found that PLL produced a significant inhibition of Na<sup>+</sup>,K<sup>+</sup>-ATPase activity, which could possibly be explained



by PLL binding to the membrane surface, displacing the enzyme's own N-terminus. Ca<sup>2+</sup>-ATPase in contrast, showed no substantial decrease in activity when in the presence of PLL using similar assays.

Discovering the mechanism of these ATPases could lead to life changing medical advances for illnesses which up to now are incurable. Mutations in isoforms of the Na<sup>+</sup>,K<sup>+</sup>-ATPase's catalytic subunit result in a number of severe hereditary neurological diseases such as rapid-onset dystonia Parkinsonism (RDP) which drastically lowers a sufferer's quality of life. It is believed to be caused by a reduction in the ability of the enzyme to discriminate between Na<sup>+</sup> and K<sup>+</sup> ions in its E1 state (3). Understanding the interactions determining the protein's conformational transitions could, therefore, aid in the search for possible therapeutic interventions.

1. Q. Jiang, A. Garcia, M. Han, F. Cornelius, H.-J. Apell, H. Khandelia and R.J. Clarke, *Biophys. J.* 112, 288 (2017).
2. A. Garcia, P.R. Pratap, C. Lüpfer, F. Cornelius, D. Jacquemin, B. Lev, T. W. Allen and R.J. Clarke, *Biochim. Biophys. Acta - Biomem.* 1859, 813 (2017).
3. Einholm AP, Toustrup-Jensen MS, Holm R. Anderson JP, Vilsen B (2010) *J Biol Chem* 285:26245-54

63

## Antibody Interactions of Disordered Malaria Antigens

Chris MacRaid<sup>1</sup>; Bankala Krishnarjuna<sup>1</sup>; Jeffrey Seow<sup>1</sup>; Rodrigo Morales<sup>None</sup>; Jack Richards<sup>None</sup>; Robin Anders<sup>None</sup>; Ray Norton<sup>None</sup>

<sup>1</sup> Monash University

**Corresponding Author(s):** chris.macrauld@monash.edu

Disordered proteins are important targets of the immune response to a range of infectious diseases. However, the molecular basis for their recognition by antibodies is unclear. Indeed, it is widely speculated that disordered proteins may be ineffective targets of the antibody response, owing to their lack of defined structure. Using a large dataset of protein antigens we show that disordered antigens are in fact common targets for recognition by high-affinity antibodies, but that the molecular interactions underpinning that recognition differ in important ways from those of ordered antigens [1]. These differences have implications for the specificity of antibody recognition of this important class of antigens, and for the effectiveness of disordered proteins as vaccine antigens.

We are exploring these implications in the specific cases of the disordered malaria vaccine antigens MSP2 and CSP. Using NMR spectroscopy, we have identified structural features of both antigens that account for the immunodominance of certain epitopes within these antigens [2]. Moreover we have identified interactions made by the antigens in situ on the parasite surface which determine important antigenic differences between the native antigens and their respective vaccine formulations. Finally, we have revealed unexpected strain-specificity in the recognition of conserved epitopes within disordered antigens, and characterised the atypical and transient antibody-antigen interactions that are responsible for this specificity [3]. Collectively, these insights are informing the design of new vaccine formulations based on disordered antigens.

[1] MacRaid, C. A., Richards, J. S., Anders, R. F. & Norton, R. S. Antibody recognition of disordered antigens. *Structure* 24, 148-157 (2016).

MacRaid, C. A. et al. Conformational dynamics and antigenicity in the disordered malaria antigen merozoite surface protein 2. *PLOS One* 10, e0119899 (2015).

Krishnarjuna, B. et al Transient antibody-antigen interactions mediate the strain-specific recognition of a conserved malaria epitope. *Commun Biol* 1, 58 (2018)

189

## Ordered and Disordered Segments of Amyloid- $\beta$ Drive Sequential Steps of the Toxic Pathway

sudipta maiti<sup>1</sup>

<sup>1</sup> *Tata Institute of Fundamental Research*

**Corresponding Author(s):** maiti@tifr.res.in

The mechanisms of toxicity of disease-causing disordered peptides, such as Alzheimer's disease (AD) associated amyloid beta (A $\beta$ ), remain poorly understood. A $\beta$  oligomers are highly toxic partially structured peptide assemblies with a distinct ordered (residues ~10-40) and a shorter disordered region (residues 1-9), which offer an opportunity to probe the role of disorder in toxicity. We probe the interactions of an array of A $\beta$  fragments with lipid membranes and cultured neurons, using the techniques of confocal imaging, lattice light sheet imaging, fluorescence lifetime imaging, and fluorescence correlation spectroscopy (FCS). Remarkably, we find that neither part (A $\beta$ 10-40 or A $\beta$ 1-9) is toxic in absence of the other. The ordered part (A $\beta$ 10-40) is the major determinant of how A $\beta$  attaches to lipid bilayers, enters neuronal cells, and localizes in the late endosomal compartments. The absence of the disordered part to some extent reduces cellular entry and increases the level of endosomal localization. Once it enters the cell, the disordered N-terminal part (only when it is a part of the full length peptide) has a strong interaction with an unknown cellular component. This interaction, coupled with the increased ability to escape endosomal localization, divert A $\beta$  to the toxic pathway. These findings correlate well with A $\beta$  sites of familial AD mutations. Our results suggest that while the required steps of membrane attachment and cellular entry are dictated by the ordered region, the key to toxicity lies in the intracellular interactions of the disordered N-terminal of A $\beta$ .

108

## Multi-scale molecular dynamics simulation of spheroidal high-density lipoprotein subpopulations

**Author(s):** Chris Malajczuk<sup>1</sup>

**Co-author(s):** Ricardo Mancera <sup>1</sup>

<sup>1</sup> *Curtin University*

**Corresponding Author(s):** c.malajczuk@postgrad.curtin.edu.au

Circulating high-density lipoprotein (HDL) particles are integral for mediating intravascular lipid and protein trafficking to regulate cardiovascular health and thus reduce vascular-related disease risk [1]. Developing a molecular understanding of HDLs is critical towards evaluating and elucidating their diverse vasoprotective functionality [2]. However, HDLs are structurally and functionally heterogeneous, as well as being very small and soft in nature. Taken together, these inherent features of HDL make them poor candidates for high-resolution structural characterisation via the currently available experimental techniques. Alternatively, over the past two decades a range of computational molecular simulation approaches have been successfully utilised to develop and investigate the molecular structure and dynamics of representative HDL models. This research expands on the progress made towards characterising HDL models via computational techniques [3], by employing a multi-scale molecular dynamics (MD) simulation approach to develop and characterise HDL models that reflect the average molecular compositions and physical properties (size, geometry and hydrated density) of the five major subtypes in plasma circulation (HDL3c, HDL3b, HDL3a, HDL2a and HDL2b). The effect of particle size and density due to lipid composition has been investigated to provide a unique description of core, interstitial and surface lipid distributions and interactions for each major subpopulation. This study has also investigated and scrutinised apoA-I in trefoil, quatrefoil and pentafoil arrangements across the surface of individual HDL particles, focussing on key structural differences observed for corresponding HDL subclasses. These findings provide insight towards understanding how different HDL subpopulations might exhibit distinct functional associations depending on particle size, density and composition.

[1] K.-A. Rye, P.J. Barter, Cardioprotective functions of HDLs, *Journal of lipid research*, 55 (2014) 168-179.

A.M.O. Cukier, P. Therond, S.A. Didichenko, I. Guillas, M.J. Chapman, S.D. Wright, A. Kontush, Structure-function relationships in reconstituted HDL: Focus on antioxidative activity and cholesterol efflux capacity, *Biochimica et Biophysica Acta (BBA) - Molecular and Cell Biology of Lipids*, 1862 (2017) 890-900.

L. Pan, J.P. Segrest, Computational studies of plasma lipoprotein lipids, *Biochimica et Biophysica Acta (BBA)-Biomembranes*, (2016).

104

## A new, flexible enhanced sampling method to predict binding free energy of small molecules – membrane systems

**Author(s):** Carlo Martinotti<sup>1</sup>

**Co-author(s):** Evelyne Deplazes<sup>1</sup>; Ricardo Mancera<sup>1</sup>

<sup>1</sup> Curtin University

**Corresponding Author(s):** carlo.martinotti@postgrad.curtin.edu.au

Understanding the interactions of small, drug-like molecule and a biological membrane is important to fields such as pharmacology, toxicology and rational drug design. Molecular dynamics (MD) is a computational method that can complement experimental techniques to study small molecule-membrane interactions (SMMIs) with atomic level resolution, providing information on both structural and dynamical properties as well as the ability to predict the binding free energy ( $\Delta G_b$ ). However, the accurate prediction of  $\Delta G_b$  is still one of the most challenging tasks in computational biophysics. Several techniques have been developed to calculate  $\Delta G_b$  for molecule-membrane systems, the most popular of which is umbrella sampling. Most of these approaches though are well known to suffer from insufficient sampling of the rotational motion of the molecule resulting in the system to become trapped in local energy minima for long times, sometimes for hundreds of nanoseconds. This results in inaccurate  $\Delta G_b$  and/or prohibitively long simulations to reach convergence.

To address this, we have developed a flexible implementation of replica exchange with solute tempering [1] within GROMACS 4.6.7 that allows the selective scaling of non-bonded interactions between any pairs of components in the system as well as separate modulation of electrostatic and van der Waals interactions. For example, to calculate  $\Delta G_b$  for a small molecule-membrane system the non-bonded interactions for solute-membrane and solute-water are scaled while leaving the solute-solute and membrane-membrane interactions unscaled to ensure the integrity of the membrane. The method was tested by simulating the interactions of both a charged and an uncharged terpene molecule (DPAC and LIM, respectively) with a POPC phospholipid bilayer. These replica-exchange simulations with selective scaling were then combined with umbrella sampling to calculate the free energy profiles (potential of mean force, PMF) from which an estimate of  $\Delta G_b$  can be obtained. Umbrella sampling simulations with and without enhanced sampling were conducted and compared for their ability to predict  $\Delta G_b$  of DPAC and LIM for POPC and to assess the accuracy of the new method with respect to previously reported simulation and experimental data of the same system [2]. The method can be used for other types of small molecules and is currently being tested on larger molecules such as peptides.

[1] L. Wang, R. A. Friesner, and B. J. Berne, "Replica Exchange with Solute Scaling: A More Efficient Version of Replica Exchange with Solute Tempering (REST2)," *J. Phys. Chem. B*, vol. 115, no. 30, pp. 9431–9438, Aug. 2011.

S. Witzke, L. Duelund, J. Kongsted, M. Petersen, O. G. Mouritsen, and H. Khandelia, "Inclusion of terpenoid plant extracts in lipid bilayers investigated by molecular dynamics simulations," *J. Phys. Chem. B*, vol. 114, no. 48, pp. 15825–15831, 2010.

171

## Migration of Endoderm and Mesoderm Derived from Human Induced Pluripotent Stem Cells during Human Gastrulation Stage

**Author(s):** Kenshiro Maruyama<sup>1</sup>

**Co-author(s):** Ryo Kobayashi<sup>2</sup>; Kiyoshi Ohnuma<sup>2</sup>

<sup>1</sup> *Nagaoka university of technology*

<sup>2</sup> *Nagaoka University of Technology*

**Corresponding Author(s):** s143361@stn.nagaokaut.ac.jp

Gastrulation is the initial systematic deformation of the embryo, hence is a critical stage for forming the human body. Although the morphology of human gastrulation is known to follow the pattern observed in birds, the dynamics are unknown because of ethical and technical limitations. Here we used human induced pluripotent stem cells (hiPSCs) to study the migration during human gastrulation in vitro. Human iPSCs correspond to epiblasts, differentiate into mesoderm and endoderm cells, and undergo epithelial-mesenchymal transition (EMT) within a few days through the activation of activin/nodal and Wnt/ $\beta$ -catenin signaling pathways.

Previous Report [1], hiPSCs differentiated into mesendodermal cells and that EMT occurred through the activation of nodal and Wnt pathways. Single-cell time-lapse imaging showed that mesendodermal differentiation resulted in the dissociation of cells and increased their migration speed, thus confirming the occurrence of EMT. Results of random walk analysis showed the random migration of both undifferentiated hiPSCs and differentiated mesendodermal cells. In this report, hiPSCs was differentiated into endoderm and mesoderm respectively. In zebrafish, Endoderm cells move linear and Mesoderm cells move randomly in gastrulation stage [2].

In results, Immunostaining showed that hiPSCs differentiated into mesoderm and endoderm through the activation of Wnt or nodal pathways respectively. Flow cytometry showed that positive cells of endoderm and mesoderm marker were over 80%. Single-cell time-lapse imaging showed that mesoderm and endoderm differentiation increased their migration speed. The speed of endodermal cells accelerated rapidly at 24 hours from differentiation, peaked at 48 hours and thereafter gradually decelerated. Mesodermal cells continued to accelerate steadily up to 72 hours. Brown motion analysis showed the random migration of both mesodermal and endodermal cells. However, the change of motion angle in a short period around 15 minutes had autocorrelation.

These results suggest that the shape in development is formed using each cell movement. Endodermal cells move faster at 48 hours suggesting the cells travel longer. Endodermal cells move slower at 72 hours suggesting forming bottom layer sheet. Random motion can create a homogeneous cell distribution.

[1] Y. Yamamoto, S. Miyazaki, K. Maruyama, R. Kobayashi, M.N.T. Le, A. Kano, A. Kondow, S. Fujii, K. Ohnuma, PLoS One. 13, 9 (2018)

L. Solnica-Krezel, D.S. Sepich, Annu. Rev. Cell Dev. Biol. 28 (2012)

64

## Run-time and velocity distributions of human KIF1A mutants in hippocampal neurons in relation to hereditary spastic paraplegia

Shiori Matsumoto<sup>1</sup>; Kyoko Chiba<sup>2</sup>; Shinsuke Niwa<sup>1</sup>; Kumiko Hayashi<sup>1</sup>

<sup>1</sup> *Tohoku University*

<sup>2</sup> *UC Davis, Hokkaido University*

**Corresponding Author(s):** mtmts@xd6.so-net.ne.jp

The kinesin 3 family member KIF1A is a molecular motor that transports synaptic vesicle precursors (SVPs) in the axons. In this study, we investigated the SVPs in mouse hippocampal neurons, carried by human KIF1A mutants, which cause hereditary spastic paraplegia[1,2]. The genes of mutant KIF1A – GFP were transfected into the hippocampal neurons: the motion of SVPs was observed by fluorescence microscopy. We found that run-time (the time for a SVP vesicle to keep moving) for the mutants was longer than that for the wild-type, and that velocity for the mutants was smaller than that for the wild-type. The reason of this increased run-time and decreased velocity was clarified by physical quantities such as force and number of motors involved in the SVP transport. Finally, the behaviors of the physical quantities were explained from deficits of the autoinhibition mechanism of KIF1A previously studied [3].

[1] S. Klebe, A. Lossos, H. Azzedine, E. Mundwiller, R. Sheffer, M. Gausen, C. Marelli, M. Nawara, W. Carpentier, V. Mayer, A. Rastetter, E. Martin, D. Bouteiller, L. Orlando, G. Gyapay, K. H. El-Hachimi, B. Zimmerman, M. Gamliel, A. Misk, I. Lerer, A. Brince, A. Durr and G. stevanin, *Eur. J. Human Gen.*, 20, 645 (2012).

Z. Iqbal, S. L. Rydning, I. M. Wedding, J. Koht, L. Pihlstrøm, A. H. Rengmark, S. P. Henriksen, C. M. E. Tallaksen and M. Toft, *PLOS ONE*,  
DOI : 10.1371/journal.pone.0174667, (2017).

S. Niwa, D. M. Lipton, M. Morikawa, C. Zhao, N. Hirokawa and H. Lu, *Cell Reports*, 16, 2129 (2016).

74

## Kinetic regulation of a transcription factor complex

Jacqui Matthews<sup>1</sup> ; Neil Robertson<sup>None</sup> ; Ngaio Smith<sup>None</sup> ; Athina Manakas<sup>None</sup> ; Ann Kwan<sup>None</sup>

<sup>1</sup> *The University of Sydney*

**Corresponding Author(s):** jacqui.matthews@sydney.edu.au

Nuclear LIM proteins and their partners take part in a transcriptional code that regulates cell specification in many tissues including the central nervous system. The LIM domains in these proteins bind short intrinsically disordered regions (IDRs) in their partner proteins which undergo disorder-to-order transitions on binding. The establishment of cell specific transcriptional complexes involves multiple competing IDR-LIM protein interactions, while DNA binding is mediated directly through homeodomains or through binding to DNA-binding proteins. We have been evaluating the IDR-LIM and protein-DNA interactions that govern cell specific transcription factor formation that drive different cell fates using a range of binding and structural studies [1,2]. Our data indicate that the interactions made by closely related proteins can have surprisingly different binding properties in terms of affinities, kinetics and or mechanisms of binding. For example, where multiple homeodomains contribute to DNA-binding, one homeodomain is the major contributor to binding, while a second homeodomain can stabilise binding. Modelling the population distributions of complexes based on these data reveals an important role for binding kinetics on transcriptional complex formation, where complexes dominated by weaker interactions with surprisingly slow off rates predominate over stronger, faster interactions [3].

[1] Robertson NO, Shah M, Matthews JM., *Angew Chem* 55, 13236 (2016).

Matthews JM., Potts JR, *FEBS Lett* 587, 1164 (2013).

Robertson NO, Smith NC, Manakas A, Mahjoub M, McDonald G, Kwan AH, Matthews JM., *Proc. Natl. Acad. Sci.* 115, 4643 (2018).

25

## The Aminopeptidase N: domain motions and species complexity in the M1 family

Sheena McGowan<sup>1</sup>; Wei Yang<sup>2</sup>; Nyssa Drinkwater<sup>2</sup>; Isaac Kresse<sup>3</sup>; Komagal Kannan Sivaraman<sup>2</sup>; Tess R Malcolm<sup>2</sup>; Ganesh Anand<sup>3</sup>

<sup>1</sup> Monash University

<sup>2</sup> Department of Microbiology, Monash University

<sup>3</sup> National University of Singapore

**Corresponding Author(s):** sheena.mcgowan@monash.edu

The M1 or aminopeptidase N (APN) family of the MA clan proteases are found in all kingdoms of life and encode drug targets for both chronic and infectious diseases. Successfully targeting the enzyme for drug discovery platforms requires knowledge of their action and specificity. The mammalian M1 aminopeptidase enzymes undergo a remarkable conformational change from a closed, catalytically competent conformation to an inactive 'open' conformation that exposes the active site to the external environment. A similar conformational change is present in the archetypal aminopeptidase N, the archaeon tricorner interacting factor 3 (TIF3), however, no conformational change has ever been observed in lower species, including the bacteria or unicellular eukaryotes. Here, we use a combination of molecular dynamic (MD) simulation and experimental data to show that the M1 aminopeptidase from the protozoan parasite *Plasmodium falciparum* can undergo the closed to open transition. MD simulation data from seven representative APN structures indicates that dynamics are inherent to the molecular mechanism of all APNs, regardless of their origin, and that the relationship between sequence, structure and dynamics will be critical to the design of selective APN inhibitors.

45

## The role of the C-terminal chemistry in the membrane disrupting activity of the antimicrobial peptide aurein 1.2

Adam Mechler<sup>1</sup>; mahdi shahmiri<sup>2</sup>

<sup>1</sup> La Trobe University

<sup>2</sup> La Trobe

**Corresponding Author(s):** a.mechler@latrobe.edu.au

C-terminal amidation is a common feature of wild type membrane disrupting antimicrobial peptides (AMPs). Empirical evidence suggests that this modification increases antimicrobial efficacy. However, the actual role of C-terminal amidation in the mechanism of action of AMPs is not fully understood. Amidation alters two key properties simultaneously: the net charge and helicity of the peptide, both of which are implicated in the mechanism of action. Here the membrane disrupting activity of two aurein 1.2 mutants is compared: one with a free C terminus and one in which a secondary amide was formed with a terminal methyl group, instead of the primary amide as in the wild type peptide. Results of quartz crystal microbalance, dye leakage and circular dichroism experiments show that the activity of each mutant is substantially reduced compared to the wild type peptide; in particular, the modified peptides exhibited a much reduced ability to bind to the membrane. Thus, the primary amide at the C-terminus is required to bind to the membrane, and a secondary amide cannot serve the same purpose. Therefore our results suggests that the role of the C-terminal amidation is not to increase helicity or net charge of the peptide, rather it is a feature required for initial membrane binding; we hypothesize that this function is exerted by controlling the hydration state of the terminus.

119

## Super-resolution imaging of DNA at low damage levels

**Author(s):** Esther Miriklis<sup>1</sup>

**Co-author(s):** Ashley Rozario<sup>1</sup>; Riley Hargreaves<sup>2</sup>; Donna Whelan<sup>3</sup>; Toby Bell<sup>1</sup>

<sup>1</sup> *Monash University*

<sup>2</sup> *Monash Univeristy*

<sup>3</sup> *La Trobe University*

**Corresponding Author(s):** elmir1@student.monash.edu

Estimates to the amount of spontaneous DNA damage sustained in mammalian cells are as high as 105 lesions per replicating cell per day [1]. Many of these lesions are relatively easily repaired and generally well tolerated by the cell. The most toxic lesion and the greatest threat to genomic integrity is the DNA double strand break (DSB) [2]. Although researched widely, studies have focussed on long term damage induction and responses, usually at high damage levels.

We have developed single molecule localisation microscopy (SMLM) assays to investigate the immediate cellular responses following low level DSB induction by camptothecin (CPT) treatment. Replication forks and nascent DNA were pulse labelled using the DNA base analogue 5-ethynyl-2'-deoxyuridine (EdU) enabling direct visualisation of DNA. DNA damage response proteins were costained alongside pulsed DNA to visualise sites of DNA damage (Fig. 1). The developed assay was then used to quantify overall replication levels at low CPT concentrations revealing complex cellular responses to damage approaching endogenous levels.

[1] J. H. J. Hoeijmakers, *N Engl. J. Med.* 361, 1475 (2009).

K. K. Khanna and S. P. Jackson, *Nature Genet.* 27, 247 (2001).

59

## Stability of Fatty Acid Binding Protein by Molecular Simulation

Kazuhiisa Miyazawa<sup>1</sup>; Satoru Itoh<sup>None</sup>; Hisashi Okumura<sup>2</sup>

<sup>1</sup> *Shinshu University*

<sup>2</sup> *ExCELLS, IMS, SOKENDAI*

**Corresponding Author(s):** miyazawa@ims.ac.jp

Fatty acids are used to synthesize adenosine triphosphate in a mitochondrion. The delivery of fatty acids is done by a fatty acid binding protein (FABP). FABP forms a  $\beta$  barrel structure (see, for example, Fig. 1). The fatty acid binds to the inside of the beta barrel. While FABPs usually exist in the cytoplasm, a part of organisms have extracellular FABPs. A secretory abundant heat-soluble (SAHS) protein is one of them [2]. Function and stability of the SAHS protein are not cleared. Then, we investigated the stability of the apo-SAHS protein, which does not include the fatty acid, using all-atom molecular dynamics (MD) simulations. We also performed MD simulations of a human liver FABP for comparison. In our poster presentation, we will show results of the simulations and differences between two FABPs.

[1] Ashwani Sharma and Amit Sharma, *J. Biol. Chem.* 286, 31924-31928 (2011)

Y Fukuda, Y Miura, E Mizohata and T Inoue, *FEBS Letters.* 591, 2458-2469 (2017).

160

## A biosensor based FLIM-FRET phasor approach to measure proteostasis capacity in cells

Nagaraj Moily<sup>1</sup> ; Elizabeth Hinde<sup>1</sup> ; Danny Hatters<sup>2</sup>

<sup>1</sup> *Department of Biochemistry and Molecular Biology, University of Melbourne, Australia*

<sup>2</sup> *elizabeth.hinde@unimelb.edu.au*

**Corresponding Author(s):** *nagaraj.moily@unimelb.edu.au*

The pool of quality control proteins that maintain protein-folding (proteostasis) is dynamic but can become quickly depleted in cellular stress and disease. The ability of these quality control chaperones to maintain the proteome in a folded state in health and response to stressors is not yet defined quantitatively. We have developed a family of barnase FRET-based biosensors with differing folding stabilities that engage primarily with HSP70 and HSP90 family proteins and modify its foldedness and aggregation[1]. Here we quantify the ability of these critical cellular chaperones to bind to the barnase biosensor using the phasor approach to FLIM analysis of FRET in a living cell. The phasor method is a fit free approach to fluorescence lifetime analysis that has the capacity to quantify the FRET efficiency of the barnase sensor in each pixel of a FLIM image and therefore spatially map protein foldedness in a living cell[2]. Using phasor FLIM-FRET analysis we are able to calculate the chaperone occupancy rates in folded and unfolded barnase biosensors fractions, thereby quantifying their holdase abilities in baseline conditions and when challenged through stress. By multiplexing this technology with image correlation spectroscopy, we also hope to understand the stickiness of unfolded proteins in cells by measuring barnase diffusion rates and predict how cells reacts to excess unfolded protein load and aggregate formation.

[1] Wood, R.J., et al., A biosensor-based framework to measure latent proteostasis capacity. *Nature Communications*, 2018. 9(1): p. 287.

Hinde, E., et al., Biosensor FRET detection by the phasor approach to fluorescence lifetime imaging microscopy (FLIM).

148

## **N-acyl amino acid analgesics bind at an allosteric site to selectively inhibit the glycine transporter, GlyT2**

**Author(s):** Shannon Mostyn<sup>1</sup>

**Co-author(s):** Alexandra Schumann-Gillett<sup>2</sup> ; Subhdeep Sarker<sup>1</sup> ; Zachary Frangos<sup>1</sup> ; Susan Shimmon<sup>3</sup> ; Sarasa Mohammadi<sup>1</sup> ; Macdonald Christie<sup>1</sup> ; Renae Ryan<sup>1</sup> ; Megan O'Mara<sup>2</sup> ; Tristan Rawling<sup>3</sup> ; Robert Vandenberg<sup>1</sup>

<sup>1</sup> *University of Sydney*

<sup>2</sup> *Australian National University*

<sup>3</sup> *University of Technology, Sydney*

**Corresponding Author(s):** *shannon.mostyn@sydney.edu.au*

There is a great need to develop new therapeutics and explore new targets in the treatment of chronic pain as many cases are refractory to conventional treatment, and current analgesics can cause adverse side effects and have the potential for abuse. There is evidence that abnormal inhibitory neurotransmission in the spinal cord dorsal horn can contribute to the pathology of neuropathic pain, thus targeting the inhibitory glycine transporter, GlyT2, may restore normal inhibitory control of pain signalling and be an effective strategy to treat pain.

N-arachidonyl glycine (NAGly) is a bioactive lipid that is found in highest concentrations within the spinal cord and may play an important role in endogenous regulation of glycine neurotransmission and pain perception. In addition to NAGly, a number of lipid inhibitors of the glycine transporter, GlyT2, have been identified. These compounds are comprised of a long flexible lipid tail and a polar or charged head group. The aims of my study were two-fold; first to identify new, more potent, lipid inhibitors and develop a structure activity relationship for these compounds; and second, to elucidate the molecular mechanisms of inhibition.



A library of 60 lipid compounds with varying head and tail groups were synthesised and tested at both GlyT2 and the closely related glycine transporter, GlyT1, using two-electrode voltage clamp electrophysiology. Majority of analogues were found to be selective GlyT2 inhibitors with varying maximal levels of inhibition and rates of reversibility. There was an ideal chain length, with an order of potency C18 > C16 > C14, and a preferred defined double bond conformation and position. N-acyl amino acids containing an aromatic or positively charged side chain conferred the highest apparent affinity, with C16  $\omega$ 3 L-Lys possessing the highest potency (10.7 nM). 13 compounds inhibited GlyT2 < 100 nM, and one of these inhibitors, oleoyl D-Lys, was also tested for metabolic stability and ability to produce analgesia in a nerve ligation rat model of neuropathic pain.

Mutagenesis of extracellular loop 4 (EL4), and transmembrane helices TM5 and TM8 suggest that the binding site is comprised of a cluster of aromatic residues which may strongly coordinate the positively charged or aromatic head group. Additionally, a membrane facing residue, when mutated, alters the washout of these compounds. From these results, in addition to preliminary docking studies, we propose that the compounds first diffuse into the lipid bilayer where they interact with a membrane exposed cavity. The lipid compounds then snorkel between TM5 and TM7 and into the binding site formed by aliphatic and aromatic residues from TM8 and EL4. The combination of structure-activity studies with molecular insights provides key information on the mechanism of inhibition which will drive the second generation of GlyT2 inhibitors for the treatment of neuropathic pain.

168

## Structure of the photo-activated acid-meta state of squid rhodopsin

Midori Murakami<sup>1</sup><sup>1</sup> Nagoya University

Corresponding Author(s): midori@bio.phys.nagoya-u.ac.jp

Rhodopsin is the photoreceptor protein in retina of vertebrate and invertebrate eyes and a member of the class A GPCRs. Upon absorption of light, the retinal chromophore in rhodopsin isomerizes from the 11-cis to all-trans configuration, initiating a photoreaction cycle. In contrast to vertebrate rhodopsins, invertebrate metarhodopsins are thermally stable (bi-stability) and hit back to rhodopsin by absorption of a second photon (photo-regeneration). We have been performing crystallographic studies of squid rhodopsin. A series of photoreaction intermediates were trapped by illumination of the dark state crystal at cryogenic temperatures and determined the structures of Rh -> Batho -> Lumi -> LM (and Iso) states. When the illuminated crystal was warmed >240 K, the crystal quality was severely lowered, suggesting large helix rearrangements of rhodopsin could occur in the crystal to destroy the crystal lattice upon formation of metarhodopsin.

To investigate the mechanism of two-photon absorption in invertebrate rhodopsins we have performed crystallographic studies of squid rhodopsin in meta states. Using a sample of 100 % meta state of squid rhodopsin, we obtained new crystals which diffracted up to 3.6 Å. The structure suggests that helix architecture is in a partially open form with unlocked salt bridge of the DRY motif at the cytoplasmic side. In addition, some aromatic rings of residues near the retinal are moved to enlarge the active site. Based on these results, we will discuss structural insights into the activation mechanism of bistable invertebrate rhodopsin.

91

## “Force-From-Lipids” gating of *Corynebacterium glutamicum* mechanosensitive channels specialized in glutamate export

Author(s): Yoshitaka Nakayama<sup>1</sup>

**Co-author(s):** Boris Martinac <sup>2</sup> ; Hisashi Kawasaki <sup>3</sup> ; Ken-ichi Hashimoto <sup>3</sup> ; Kosuke Komazawa <sup>4</sup> ; Navid Bavi <sup>5</sup>

<sup>1</sup> *Victor Chang Cardiac Research Institute*

<sup>2</sup> *Victor Chang Cardiac Research Institute*

<sup>3</sup> *University of Tokyo*

<sup>4</sup> *Tokyo Denki university*

<sup>5</sup> *University of Chicago*

**Corresponding Author(s):** y.nakayama@victorchang.edu.au

*Corynebacterium glutamicum* has been utilized for industrial amino acid production, especially for monosodium glutamate (MSG). The glutamate secretion in this bacterium is triggered by increased membrane tension. Recently, the opening of the mechanosensitive channel MscCG, one of the MscS-like channels, has been identified as the main pathway for glutamate secretion. In addition to MscCG, two other mechanosensitive channels, CgMscL and MscCG2, have recently been found and characterized in giant spheroplasts of *C. glutamicum*. Unlike in other bacteria, *C. glutamicum* MscCG and MscCG2, but not CgMscL, release glutamate when either total membrane lipid amount, or cell-wall is removed [1]. Here we show that all three different types of *C. glutamicum* mechanosensitive channels in the native membrane of giant spheroplasts can be activated by membrane tension [2]. These mechanosensitive channels are activated by increased membrane tension indicating that the “Force-From-Lipids” gating paradigm known to control the gating of MscL and MscS bacterial mechanosensitive channels can also be applied to MscCG channels. Significantly, the bacterial types of mechanosensitive channels have been found in all cell-walled organisms from bacteria to land plants, where their physiological functions have specialized beyond their basic function in bacterial osmoregulation. This seems also to be the case for the *C. glutamicum* MscCG channel, whose specialized function is of a glutamate exporter mechanosensitive channel.

[1] Y. Nakayama et al, *Biophys. Rev.* (2018) doi: 10.1007/s12551-018-0452-1

Y. Nakayama et al, *Sci. Rep.* (2018) doi: 10.1038/s41598-018-31219-6.

163

## Prediction of cancer-associated hotspot mutations that affect GPCR oligomerization

Wataru Nemoto<sup>1</sup> ; Sakie Shimamura<sup>1</sup> ; Limviphuvadh Vachiranee<sup>2</sup> ; Sebastian Maurer-Stroh<sup>2</sup> ; Yoshihiro Yamanishi<sup>3</sup> ; Toh Hiroyuki<sup>4</sup>

<sup>1</sup> *Department of Science and Technology, Tokyo Denki University, Saitama, Japan.*

<sup>2</sup> *Bioinformatics Institute, Agency for Science, Technology and Research, Singapore.*

<sup>3</sup> *Medical Institute of Bioregulation, Kyushu University, Japan.*

<sup>4</sup> *School of Science and Technology, Kwansai Gakuin University, Japan.*

**Corresponding Author(s):** w.nemoto@mail.dendai.ac.jp

We developed a high-performance method to predict interacting pairs for G-Protein Coupled Receptors (GPCRs) oligomerization, GPCR-GPCR Interaction Pair predictor (GGIP), by integrating the structure and sequence information [1]. In addition, we launched a prediction server, which is available at our website [2].

A recent study reported that somatic mutations in GPCR-encoding genes are frequently found in various types of cancer. Among the somatic mutations, hotspot mutations are defined as recurrent amino acid changes occurring in coding sequences. It has been revealed that many GPCRs have hotspot mutations in the same types of cancer tissues. However, most of the hotspot mutations have not been characterized yet, and their effects on the cancer pathways remain unknown. Some of the hotspot mutations may be related to cancers through modifying GPCR oligomerization, since they are considered to be present on the surface of transmembrane helices. Hence, we examined

the predicted interacting pairs including the GPCRs with hotspot mutations. We will discuss the characteristics of these mutations and introduce several examples.

[1] Nemoto et al. *Proteins*. 84, 1224-33 (2016).  
GGIP ([http://protein.b.dendai.ac.jp/GGIP/.](http://protein.b.dendai.ac.jp/GGIP/))

70

## Looking for dominant-negative effect of hERG channel mutations

Chai Ng<sup>1</sup>; Matthew Perry<sup>1</sup>; Jamie Vandenberg<sup>1</sup>

<sup>1</sup> VCCRI

**Corresponding Author(s):** c.ng@victorchang.edu.au

The expression of hERG potassium channels at the plasma membrane of cardiac myocytes is critical for the coordinated propagation of the electrical signals that regulate the rhythm of the heartbeat. Reduced hERG function due to mutations cause long QT syndrome type 2 (LQTS2), which increases the risk of sudden cardiac arrest and death. Mutations may affect mRNA or protein subunit synthesis, assembly of subunits into the functional tetrameric channel, trafficking and/or gating and ion permeation of the channels once they have reached the plasma membrane. HERG mutations have been found throughout the channel with mutations in the pore domain found to have a higher clinical risk than mutations from either the N or C-terminus of hERG [1]. It is postulated that most pore-domain mutants result in a dominant negative suppression of channel function. However, not all pore mutations result in a dominant negative phenotype [2].

The aim of this study was to develop a high throughput assay that could determine whether mutants result in a dominant negative phenotype or not. In order to investigate the dominant-negative effect of hERG mutations, the mutant hERG needs to be co-expressed with WT hERG in a heterozygote setting. Accordingly, we have generated stable flpin HEK293 cell lines that co-express mutant with WT hERG. Further, we have expressed a range of mutants that we anticipate would have a dominant negative phenotype as well as a range of mutants expected to have a simple haploinsufficient trafficking phenotype. As negative control, we have also generated a polymorphism of hERG (K897T) with WT hERG. We have assayed channel expression using an ELISA assay and current density using a SyncroPatch 384 automated patch-clamp system.

Preliminary result shows our in-vitro phenotyping assays are capable of distinguishing dominant-negative hERG mutations from mutations that are simply haploinsufficient. In the era of precision medicine, large numbers of hERG mutations with unknown significance are going to be identified. Our high-throughput phenotyping assays will not only allow identification of high impact mutations it can also be used to filter out non-pathogenic mutations. In future work we aim to validate our assays by correlating the results from our in-vitro phenotyping with clinical data for different hERG mutations.

[1] Moss et al. *Circulation*. 105 (7), 794-799 (2002).  
Zhao et al. *J Cardiac Electrophysiol*. 20 (8), 923-3 (2009).

143

## Influence of wrinkled surface topologies on the colonisation of *Pseudomonas aeruginosa*

**Author(s):** Duy H K Nguyen<sup>1</sup>

**Co-author(s):** James Wang<sup>1</sup>; Igor Sbarski<sup>1</sup>; Saulius Juodkazis<sup>1</sup>; Russell Crawford<sup>2</sup>; Elena Ivanova<sup>2</sup>

<sup>1</sup> *Swinburne University of Technology*<sup>2</sup> *RMIT***Corresponding Author(s):** huukhuongduynguyen@swin.edu.au

Surface wrinkling is a natural phenomenon that has inspired an emerging technology in surface patterning with tunable, self-organized topographical features providing advantageous properties compared to their flat counterparts. In this study, we demonstrate the significance of air entrapments and their corresponding distributions that influence the colonization of Gram-negative rod-shape *Pseudomonas aeruginosa* ATCC 9721 bacterial cells on wrinkled gold-coated and amorphous graphite-like carbon coated polystyrene surfaces possessing topologies at microscale. Together with corresponding film-coated planar surfaces as controls, surface feature heights covered 2 order of magnitude from 15 nm to 1.5 micron. The wrinkled amorphous graphite-like coated surface topology has demonstrated an incapability of trapping air at the interfacial area unlike the wrinkled gold-coated polystyrene surface. Through confocal laser scanning microscopic, Raman spectroscopic, scanning electron microscopic and atomic force microscopic image analysis it is shown that air-water interfaces control the bacterial attachment. Imposition of microscale topology on amorphous graphite-like coated wrinkles facilitated a nine-fold increase in *P. aeruginosa* attachment compared to its flat equivalent surface due to the absence of air entrapments. Hence the surface topology and surface chemistry of wrinkled gold-coated polystyrene surface are both attributable to the long term stable entrapment of air. This study provides a useful insight towards facile, tunable and low cost microfabrication approaches in anti-biofouling surfaces design.

89

## Insights into the mechanism of archaellar motor rotation from observation of unexpectedly high torque

Takayuki Nishizaka<sup>1</sup> ; Seiji Iwata<sup>None</sup> ; Daisuke Nakane<sup>None</sup><sup>1</sup> *Gakushuin University***Corresponding Author(s):** takayuki.nishizaka@gakushuin.ac.jp

It is unknown how the archaellum—the rotary propeller used by Archaea for motility—works. The archaellum is a helical filament that generates thrust when rotated by a membrane-embedded, ATP-driven archaellar motor. The only energy-transducing archaellar motor protein is the hexameric ATPase FlaI that powers both assembly and rotation, yet the mechanism of torque generation by FlaI is unknown. We previously characterized motor function in the model organism *Halobacterium salinarum* using advanced fluorescent microscopy [1], but challenges manipulating motor load prevented us from measuring torque. To gain insights into the molecular mechanism underlying how FlaI drives rotation, here we describe determination of motor torque through imposition of various loads on archaella using markers of different sizes, trajectory quantification using three-dimensional tracking [2], and high-speed recording. We show that rotation slows as the viscous drag of markers increases, and torque remains constant at 160 pN·nm, independent of rotation speeds between 0.5 and 30 Hz. Notably, the estimated work done in a single rotation is twice the expected energy that would come from hydrolysis of six ATP molecules, indicating that 12 ATP molecules are required for a single rotation, and suggesting a model for the mechanism of archaellar motor rotation.

[1] Y. Kinoshita, N. Uchida, D. Nakane, T. Nishizaka, *Nature Microbiology* 1, 16148 (2016).J. Yajima, K. Mizutani, T. Nishizaka, *Nature Structural & Molecular Biology* 15, 1119-1121 (2008).

113

## Intrinsic diversities of catalytic activity among single enzyme molecules and virus particles revealed with femtoliter reactor array

Hiroyuki Noji<sup>1</sup>

<sup>1</sup> *The University of Tokyo*

**Corresponding Author(s):** hnoji@appchem.t.u-tokyo.ac.jp

Digital bioassay has emerged as a promising analytical approach for the quantification of target molecules with extremely high sensitivity [1]. The most typical protocols of digital bioassays utilize femtoliter reactor array in which target molecules, typically enzymes or molecules tagged with enzyme-conjugated antibody, are stochastically entrapped into individual reactors with fluorogenic substrate [2, 3]. Reactors encapsulating a single molecule enzyme show strong fluorescence signal due to the production of fluorescence dyes upon catalytic activity. The resultant fluorescence signal is distinctive from that of dark empty reactors, allowing the accurate and very sensitive quantification of target molecules after the binarization of the signal.

In this study, we conducted quantitative analysis of catalytic activities of single molecules of an enzyme and single particles of influenza virus, in order to evaluate the intrinsic diversity of the catalytic activities of them. As a model enzyme, dimeric alkaline phosphatase (ALP) was measured. Histogram of single molecule catalytic activity of ALP showed that ALP molecules have distinctive subpopulation with 50% activity compared with fully active population. Single-molecule analysis of ALP prepared from *in vitro* gene expression with a molecular chaperon a disulfide bond enhancer suggests that incorporation of immature monomer of which disulfide bond is not formed into the dimer complex of ALP halves activity of ALP, resulting in the subpopulation with lower activity.

We also tested the diversity of neuraminidase activity of influenza virus particle, by encapsulating virus particles into reactors with a fluorogenic substrate for virus neuraminidase. Virus samples irrespective of the type (A or B) showed very broad distribution compared with enzymes such as ALP or beta-glucosidase. The coefficient of variance was over 30%, significantly larger than the systematic measurement error (less than 5-7%) and that of other enzymes (typically 10%). The broad diversity of influenza virus particles was attributable to the diversity of particle size of influenza virus that we previously observed [4]. Surprisingly, the diversity to the sensitivity to a specific inhibitor of the influenza neuraminidase was also observed, suggesting that a very small fraction of influenza particle population has intrinsic resistance or tolerance against the anti-virus inhibitor.

[1] Y. Zhang and H. Noji, *Anal. Chem.* 89, 13675 (2017).

Y. Rondelez, et al., *Nat. Biotech.* 433, 773 (2005).

S. H. Kim and et al., *Lab Chip.* 12, 3923 (2012).

S. Enoki and et al., *PLoS One.* 7, 49208 (2012).

136

## Gene expression from a single large DNA encapsulated in artificial cell device

**Author(s):** Yuto Ochiai<sup>1</sup>

**Co-author(s):** Hiroshi Ueno<sup>2</sup>; Masayuki Su'etsugu<sup>3</sup>; Hiroyuki Noji<sup>1</sup>

<sup>1</sup> *The University of Tokyo*

<sup>2</sup> *The University Tokyo*

<sup>3</sup> *Rikkyo University*

**Corresponding Author(s):** ochiai.y17@nojilab.t.u-tokyo.ac.jp

Reconstitution of autonomous artificial cells requires encapsulation of a large DNA and components for gene expression and replication into cell-sized reactors. In this work, we developed the artificial cell device having millions of water-in-oil droplet reactors, which implements cell-free transcription-translation reactions from 200 kbp DNA.

In order to test the transcription and translation activities from a large DNA, we prepared the 200 kbp plasmid DNA encoding a fluorescent protein, Venus. Before encapsulation in a micro reactor,

we confirmed the in vitro synthesis of Venus from the 200 kbp DNA, and found that Venus was synthesized from the 200 kbp DNA with comparable yields of that from the 3kbp DNA encoding Venus [Fig.1]. Then, we attempted to encapsulate the 200 kbp DNA with a hydrodynamic diameter of about 1  $\mu\text{m}$  in cell-sized reactors (5  $\mu\text{m}$  of diameter). However, initial experiments were unsuccessful; DNA was hardly encapsulated. Supposing that it is due to the electrostatic repulsion between DNA and reactors, the surface of the micro reactors were modified with cationic polymer. This modification has led successful encapsulation of the 200 kbp DNA in cell-sized reactors. We visualized a single 200 kbp DNA encapsulated in reactors by using the oil pre-equilibrated with the fluorescent DNA dye for sealing the reactors [Fig.2]. Moreover, we quantified the efficiency of gene expression with various concentration of the cationic polymer, and determined the optimized condition for in vitro gene expression from the 200 kbp DNA [Fig.3].

33

## Interaction of RecA proteins and DNA-wrapped carbon nanotubes using various carbon nanotube powders

Shusuke Ohura<sup>1</sup> ; Daisuke Miyashiro<sup>1</sup> ; Kazuo Umemura<sup>1</sup>

<sup>1</sup> Department of Physics, Graduate school of Science, Tokyo University of Science

Corresponding Author(s): 1216704@ed.tus.ac.jp

Single-walled carbon nanotubes (SWNTs) and single-stranded DNA (ssDNA) can form ssDNA-SWNT hybrids by performing sonication. Since discovering ssDNA-SWNT hybrids, the hybrids have been regarded as a potential materials for the medical application in terms of unique optical properties of SWNTs. In our previous study, we used SWNTs synthesized by high-pressure carbon monoxide decomposition (HiPCO) method, and found that the ssDNA molecules on SWNT surfaces could be recognized by DNA-binding protein RecA [1]. In this study, we investigated the interaction between RecA proteins and ssDNA-SWNT hybrids using (6,5) or (7,6) rich SWNT powders which are both prepared by CoMoCAT catalytic chemical vapor deposition method.

For the sample, (6,5) or (7,6) rich SWNT powders were mixed with ssDNA solution, respectively. The base-sequence of ssDNA is 30-mers of thymine (T30), and the ssDNA solution is adjusted to be 1mg/mL using Tris-HCl buffer solution (pH 7.5). RecA proteins with T30-(6,5) or (7,6) rich SWNT solution incubated at 37 °C for 60 minutes [2].

The microscopic images by atomic force microscopy, we found a lot of thick SWNTs in the sample of T30-(6,5) rich SWNT with RecA (Fig. (b)). The mean height of SWNT hybrids for (6,5) rich SWNT with RecA sample was  $3.58 \pm 0.86$  nm, which is approximately 1.8 nm higher than that of T30-(6,5) rich SWNT without RecA (Fig.(e),(f)). On the other hand, there were few attachments on T30-(7,6) rich SWNT surfaces (Fig.(c),(d)). Furthermore, the average height of T30-(7,6) rich SWNT with RecA was similar to that of T30-(7,6) rich SWNT (Fig.(e),(f)). Our results suggest that the chirality composition of the SWNTs in the carbon nanotube powders affect to the interaction between RecA proteins and ssDNA-SWNT hybrids, because (6,5) or (7,6) rich SWNT powders in this study were synthesized by identical process.

### References

- [1] S. Oura, M. Ito, D. Nii, Y. Homma and K. Umemura, *Colloids Surf. B* 126, 496 (2015).  
S. Oura and K. Umemura: *Jpn. J. Appl. Phys.* 55, 03DF04 (2016).

149

## Difference in structural and fluctuation difference between two ends of A $\beta$ amyloid fibril revealed by molecular dynamics simulations

HISASHI OKUMURA<sup>None</sup> ; Satoru G. ITOH<sup>None</sup>

**Corresponding Author(s):**

A $\beta$  amyloid fibrils, which are related to Alzheimer's disease, have a cross- $\beta$  structure consisting of two  $\beta$ -sheets:  $\beta$ 1 and  $\beta$ 2. The A $\beta$  peptides are thought to be serially arranged in the same molecular conformation along the fibril axis. However, to understand the amyloid extension mechanism, we must understand the amyloid fibril structure and fluctuation at the fibril end, which has not been revealed to date.

Here, we reveal these features by all-atom molecular dynamics (MD) simulations of A $\beta$ 42 and A $\beta$ 40 fibrils in explicit water [1]. MD simulations were performed by the Generalized-Ensemble Molecular Biophysics program developed by one of the authors (H.O.) [2]. This program has been applied to several biomolecules [3-5].

The structure and fluctuation were observed to differ between the two ends. At the even end, the A $\beta$  peptide always took a closed form wherein  $\beta$ 1 and  $\beta$ 2 were closely spaced. The A $\beta$  peptide fluctuated more at the odd end and took an open form wherein the two  $\beta$ -sheets were well separated. The differences are attributed to the stronger  $\beta$ -sheet formation by the  $\beta$ 1 exposed at the even end than the  $\beta$ 2 exposed at the odd end. Along with the small fluctuations at the even end, these results explain why the fibril extends from one end only, as observed in experiments. Our MD results agree well with recent observations by high-speed atomic force microscopy.

**References:**

- H. Okumura and S. G. Itoh, *Sci. Rep.* 6 (2016) 38422.  
 H. Okumura, *Proteins* 80 (2012) 2397.  
 H. Okumura and S. G. Itoh, *J. Am. Chem. Soc.* 136 (2014) 10549.  
 H. Okumura and S. G. Itoh, *Phys. Chem. Chem. Phys.* 15 (2013) 13852.  
 M. Yamauchi and H. Okumura, *J. Chem. Phys.* 147 (2017) 184107.

61

**Membrane bound states of melittin form distinct phases in DMPC**

Sara Pandidan<sup>None</sup> ; Adam Mechler<sup>1</sup>

<sup>1</sup> *La Trobe University*

**Corresponding Author(s):** sarapandidan@yahoo.com

Antimicrobial peptides (AMPs) serve as an effective weapon against bacteria, viruses and fungi. They are secreted by all complex organisms including plants, insects, animals and humans [1]. Due to their distinct mode of action, AMPs represent a potential solution for the global health threat of antibiotic resistance [2]. Melittin, the main component of bee venom, is one of the most thoroughly characterized AMPs. It is  $\alpha$ -helical, cationic and amphiphilic peptide consisting of 26 amino acids [3], believed to act via disrupting the plasma membrane of cells by forming toroidal pores [4]. However the confirmation of the mechanism of action, in particular the stages of the membrane disrupting process have proven challenging for the existing methodology.

An unorthodox way to characterize peptide-membrane interactions is by using phase transition measurements. It was noted that peptides and proteins can influence the phase transition temperature of phospholipid membranes [5, 6]. A calorimetry study in 1997 suggested that melittin can reduce the pre-transition temperature of DPPC membranes, without noticeable change of the main transition temperature [7]. Following on this lead, we have performed nano-viscosimetry based phase transition measurements on melittin-exposed DMPC membranes at different peptide concentrations. We found that melittin leads to the separation of at least three different domains in DMPC membrane. These domains can be correlated to the membrane bound states of melittin. Of the three domains, one can be clearly identified as the main phase transition of DMPC; the other two domains likely represent monomeric and aggregated states of the peptide in the membrane.

[1] Zasloff M. Antimicrobial peptides of multicellular organisms. *nature* 2002;415:389.

Matsuzaki K. Why and how are peptide–lipid interactions utilized for self-defense? Magainins and tachyplesins as archetypes. *Biochimica et Biophysica Acta (BBA)-Biomembranes* 1999;1462:1-10.

Raghuraman H, Chattopadhyay A. Melittin: a membrane-active peptide with diverse functions. *Bio-science reports* 2007;27:189-223.

Mihajlovic M, Lazaridis T. Antimicrobial peptides in toroidal and cylindrical pores. *Biochimica et Biophysica Acta (BBA)-Biomembranes* 2010;1798:1485-93.

Chapman D, Urbina J, Keough KM. Biomembrane phase transitions studies of lipid-water systems using differential scanning calorimetry. *Journal of Biological Chemistry* 1974;249:2512-21.

Sharma VK, Mamontov E, Anunciado DB, O'Neill H, Urban VS. Effect of antimicrobial peptide on the dynamics of phosphocholine membrane: role of cholesterol and physical state of bilayer. *Soft matter* 2015;11:6755-67.

Lohner K, Latal A, Lehrer RI, Ganz T. Differential scanning microcalorimetry indicates that human defensin, HNP-2, interacts specifically with biomembrane mimetic systems. *Biochemistry* 1997;36:1525-31.

112

## Response of pheochromocytoma (PC 12) cells following exposure to electromagnetic fields of 18 GHz

**Author(s):** Tharushi Perera<sup>1</sup> ; Elena Ivanova<sup>2</sup>

**Co-author(s):** The Hong Phong Nguyen<sup>1</sup> ; Chaitali Dekiwadia<sup>2</sup> ; Jason Wandiyanto<sup>1</sup> ; Igor Sbarski<sup>1</sup> ; Olha Bazaka<sup>2</sup> ; Kateryna Bazaka<sup>3</sup> ; Russell Crawford<sup>2</sup> ; Rodney Croft<sup>4</sup>

<sup>1</sup> *Swinburne University of Technology*

<sup>2</sup> *RMIT University*

<sup>3</sup> *Queensland University of Technology*

<sup>4</sup> *University of Wollongong*

**Corresponding Author(s):** pgperera@swin.edu.au

Effects of man-made electromagnetic fields (EMF) on living organisms potentially include transient and permanent changes in cell behaviour, physiology and morphology. At present, these EMF-induced effects are poorly defined, yet their understanding may provide important insights into consequences of uncontrolled (e.g. environmental) as well as intentional (e.g. therapeutic or diagnostic) exposure of biota to EMFs. In this work, for the first time, we study mechanisms by which a high frequency (18 GHz) EMF radiation affects the physiology of membrane transport in pheochromocytoma PC 12, a convenient model system for neurotoxicological and membrane transport studies. Suspensions of the PC 12 cells were subjected to three consecutive cycles of 30s EMF treatment with a specific absorption rate (SAR) of 1.17 kW kg<sup>-1</sup>, with cells cooled between exposures to reduce bulk dielectric heating. The EMF exposure resulted in a transient increase in membrane permeability in up to 90 % of the treated cells, as demonstrated by rapid internalisation of silica nanospheres (diameter  $d \approx 23.5$  nm) and their clusters ( $d \approx 63$  nm). In contrast, the PC12 cells that received an equivalent bulk heat treatment behaved similar to the untreated controls, showing minimal nanosphere uptake of approximately 1-2 %. Morphology and growth of the EMF treated cells were not altered, indicating that the PC 12 cells were able to remain viable after the EMF exposure. The metabolic activity of EMF treated PC 12 cells was similar to that of the heat treated and control samples, with no difference in the total protein concentration and lactate dehydrogenase (LDH) release between these groups. These results provide new insights into the mechanisms of EMF-induced biological activity in mammalian cells, suggesting a possible use of EMFs to facilitate efficient transport of biomolecules, dyes and tracers, and genetic material across cell membrane in drug delivery and gene therapy, where permanent permeabilisation or cell death is undesirable.

23



## Conformational switching of the MLKL pseudokinase domain controls cell death by necroptosis.

**Author(s):** Emma Petrie<sup>1</sup>

**Co-author(s):** Jarrod Sandow<sup>1</sup>; Annette Jacobsen<sup>1</sup>; Lung-Yu Liang<sup>1</sup>; Willamus Kersten<sup>1</sup>; Michael Griffin<sup>2</sup>; Brian Smith<sup>3</sup>; Diane Coursier<sup>4</sup>; Cheree Fitzgibbon<sup>4</sup>; Katherine Davies<sup>4</sup>; Samuel Young<sup>4</sup>; Ahmad Wardak<sup>4</sup>; Guillaume Lessene<sup>4</sup>; John Silke<sup>4</sup>; Peter Czabotar<sup>4</sup>; Gerrard Manning<sup>5</sup>; Isabelle Lucet<sup>4</sup>; James Murphy<sup>4</sup>

<sup>1</sup> *The Walter and Eliza Hall Institute*

<sup>2</sup> *Department of Biochemistry & Molecular Biology, The University of Melbourne*

<sup>3</sup> *LaTrobe University*

<sup>4</sup> *Walter and Eliza Hall Institute*

<sup>5</sup> *Genentech*

**Corresponding Author(s):** petrie.e@wehi.edu.au

The Mixed-Linage Kinase-domain Like (MLKL) protein is essential to the programmed cell death mechanism of necroptosis. During necroptosis the inner plasma membrane is compromised, leading to cell swelling and release of intracellular contents, inviting an inflammatory response.

MLKL is the most terminal protein in the kinase signalling cascade that leads to necroptosis, which is well-characterised downstream of the TNF receptor. Phosphorylation of the C-terminal pseudokinase domain (PsKD) of MLKL by RIPK3 is thought to release the N-terminal 4-helical bundle (4HB), which is the killing domain, and promote oligomer formation.

The detection of phosphorylated MLKL oligomers at the plasma membrane is a hallmark of necroptosis. While recombinant protein can disrupt liposomes *in vitro*, little is known about the mechanism of action, including how MLKL transitions from an inert cytosolic protein to a killer assembly and the arrangement of MLKL subunits within the oligomer.

This talk will describe how the PsKD of MLKL controls the activation state of the protein. Through combining cross-linking-, hydrogen deuterium exchange- and native- mass spectrometry with Small Angle X-ray Scattering we characterised the conformation of the basal cytosolic monomer and the structural changes that occur as MLKL transitions to a tetrameric assembly that kills cells. We characterised PsKD mutants associated with some cancers that stabilise the basal state of MLKL. When reconstituted into MLKL<sup>-/-</sup> cells these mutations impacted the kinetics of tetramer formation and delayed cell death. This suggests that a delay in necroptosis may give some tumours a growth advantage.

This work also highlighted species-specific differences in RIPK3-mediated activation of MLKL. We have identified viral MLKL-like proteins that target the RIPK3-MLKL interaction and block necroptosis. Characterisation of this interaction provides insights into the evolution of the proteins involved in the necroptotic pathway and therapeutic potential of blocking necroptosis.

198

## Spin resonance at the quantum limit using superconducting microwave resonators

Jarryd Pla<sup>1</sup>

<sup>1</sup> *UNSW Sydney*

**Corresponding Author(s):** jarryd@unsw.edu.au

The characterisation of materials by electron paramagnetic resonance (EPR) spectroscopy is widely used throughout Chemistry, Biology and Materials Science, from *in vivo* imaging to distance measurements in spin-labelled proteins. Most EPR spectrometers typically rely on the inductive detection of microwave signals emitted by the spins into a coupled microwave resonator during their

Larmor precession - however, such signals can be very small, prohibiting the application of EPR to micro and nanoscale samples.

Recently, we demonstrated that by exploiting two modern quantum technologies, namely circuit-based superconducting resonators and noiseless quantum microwave amplifiers, we were able to achieve record EPR sensitivities down to 65 spins [1,2]. Our experiments were performed in a dilution refrigerator at a temperature of 20 mK, where spin relaxation times are expected to be prohibitively long. We were able to utilise the enhanced coupling of the spins with the circuit resonators to demonstrate a new way [3] of inducing spin relaxation (on-demand) via spontaneous emission of microwave photons into the resonator. In this presentation I will discuss the quantum-limited spectrometer technology and its application to measurements in Biology. In particular, I will show that this system might be used to extend the range and drastically reduce the time required for long distance (> 6 nm) EPR measurements in spin-labelled proteins.

[1] A. Bienfait, J.J. Pla, et al., *Nature Nano.* 11, 253-257 (2015)

S. Probst et al., *Appl. Phys. Lett.* 111, 202604 (2017)

A. Bienfait, J.J. Pla, et al., *Nature* 531, 74-77 (2016)

75

## Effect of Lipid Diversity on Membrane and Protein Functions

David Poger<sup>1</sup> ; Michael Corbett<sup>1</sup> ; Alan Mark<sup>1</sup>

<sup>1</sup> *The University of Queensland*

**Corresponding Author(s):** d.poger@uq.edu.au

Biological membranes regulate a myriad of cellular processes through the modulation of essential properties such as membrane fluidity and the formation of lipid microdomains. Such differences in turn affect the function of membranes and membrane proteins. The chemical and structural diversity of lipids is only being uncovered. For example, the repertoire of lipids in bacterial membranes is much broader than in eukaryotic membranes. In many if not most bacteria, membrane lipids include branched-chain fatty acids. Hopanoids have been identified in a range of bacteria. Branched-chain fatty acids have been proposed to protect membranes against hostile conditions and hopanoids have long been hypothesised to be surrogates of sterols, but, in fact, little is known about their actual effect on membranes. Using atomistic simulations, I showed that the different types of branching and hopanoids have specific effects on membrane fluidity and structure that allow bacteria to finely tune the sensitivity of their membranes to the environment. Furthermore, branched-chain lipids could affect the effect of commonly used disinfectants such as triclosan and para-chloroxylenol on membranes by modulating the interaction of the biocides with lipids. The membrane composition also plays a critical role in the function of proteins. In simulations of the type-I cytokine receptors for growth hormone (GHR), prolactin (PRLR) and erythropoietin (EPOR) embedded in membranes, the presence of cholesterol altered the behaviour of the transmembrane domains, suggesting a key role of cholesterol in the mechanical coupling of the receptors through the plasma membrane upon receptor activation. The lipid composition is thus critical in the function of membrane and membrane proteins.

216

## Mechanoelectrical transduction at the cell-substrate interface

**Author(s):** Kate Poole<sup>1</sup>

**Co-author(s):** Jessica Richardson ; Setareh Sianati ; Navid Bavi

<sup>1</sup> *EMBL Node in Single Molecule Science, School of Medical Sciences, University of New South Wales, NSW 2052, Australia*

**Corresponding Author(s):**

The ability of cells to sense and respond to their physical environment is fundamental to a broad spectrum of biological processes. Cells express an array of force sensors that can transduce mechanical inputs into biochemical signals, including mechanically activated (MA) ion channels. These ion channels form pores in the plasma membrane and their open probability increases with increasing mechanical input. Several tools have been developed to evoke mechanically-activated currents in order to study MA channel function and regulation. MA channels have traditionally been activated by membrane stretch (using high-speed pressure clamp) or cellular indentation (using a glass probe). More recently we have established a technique to apply deflection stimuli at the interface between cells and their substrate (using elastomeric pillar arrays as force transducers). Studying the activation of MA channels using this array of different techniques has highlighted how important context is in understanding MA channel activation: the PIEZO1 channel is activated by stretch, indentation and deflection and TRPV4 by deflection alone. As such, TRPV4 is only activated by mechanical stimuli when it is integrated into the cell-substrate interface. In addition, the mechanical properties of the substrate to which cells are bound can regulate the sensitivity of PIEZO1 and TRPV4, in a fashion dependent on cytoskeletal elements within the cell. We propose that the integration of transduction via multiple MA channels could engender cells with a tuneable and diverse repertoire of mechanical sensing.

121

## **The arginine-rich dipeptide repeats proteins of C9ORF72-associated Motor Neuron Disease cause the ribosome to stall during synthesis**

**Author(s):** Mona Radwan<sup>1</sup>

**Co-author(s):** Bradley J. Turner<sup>2</sup>; Gavin E. Reid<sup>3</sup>; Danny Hatters

<sup>1</sup> *Department of Biochemistry and Molecular Biology, Bio21 Molecular Science and Biotechnology Institute, University of Melbourne, Victoria 3010, Australia*

<sup>2</sup> *Florey Institute of Neuroscience and Mental Health, University of Melbourne, Victoria, Australia; Centre for Neuroscience, University of Melbourne, Victoria, Australia.*

<sup>3</sup> *Department of Chemistry, Bio21 Molecular Science and Biotechnology Institute, University of Melbourne, Victoria 3010, Australia*

**Corresponding Author(s):** monar@student.unimelb.edu.au

A mutation in intron 1 of C9ORF72 gene is a major cause of familial Motor neuron disease (MND) and frontotemporal dementia (FTD). The GGGGCC repeat expansion undergoes unconventional repeat-associated non-AUG (RAN) translation of the sense and antisense transcripts of the repeats generating five different dipeptide repeat (DPR) proteins. These DPRs accumulate in human brain and are candidates as the major cause of dysfunction in disease. Of the 5 DPRs, the positively-charged PR and GR DPRs are the most profoundly toxic, which has been proposed previously from experiments that added exogenous DPRs to cells to arise due to the poisoning of ribosome biogenesis [1]. Here we used quantitative proteomics to explore in more detail which proteins are associated with transiently expressed short (10x) and long (100x) repeat lengths of the DPRs, in a neuroblastoma cell culture model of disease. The PR and GR 'interactomes' were found to selectively include ribosomal proteins, translation initiation factors and translation elongation factors. Of note, the ribosome stalling factor ABCE1, was uniquely identified in the interactome of the long PR DPR, suggesting that translation of this protein induces ribosome stalling, rather than impairing ribosome biogenesis as previously reported. To test this hypothesis, we employed an assay of ribosome stalling, which involved monitoring the expression of two fluorescent proteins from a single mRNA sequence separated by the DPR sequences. The PR- and GR-containing long DPRs were found to selectively and robustly stall the ribosome. We therefore conclude that the predominant effect of Arg-rich DPRs expressed in cells is the stalling of ribosome synthesis rather than poisoning of ribosome biogenesis. We propose that the long stretch of positive charges of arginine electrostatically interact with negatively charged residues of the ribosomal exit tunnel and hence provide a mechanism to broadly

collapse ribosome activity. This revised mechanism is consistent with previously reported global protein translation inhibition induced by the expression of arginine-rich DPRs [2].

[1] I. Kwon, et al. (2014). *Science*. 345, 1139 (2014).

K. Kanekura, et al., *Human Molecular Genetics*. 25, 803 (2016).

196

## Insights on the impact of mitochondrial organisation on bioenergetics in high-resolution computational models of cardiac cell architecture

Shouryadipta Ghosh<sup>1</sup> ; Kenneth Tran<sup>2</sup> ; Eric Hanssen<sup>3</sup> ; Edmund Crampin<sup>1</sup> ; Vijay Rajagopal<sup>1</sup>

<sup>1</sup> *University of Melbourne*

<sup>2</sup> *University of Auckland*

<sup>3</sup> *Bio21 Molecular Science and Biotechnology Institute, The University of Melbourne, Parkville 3052, Australia*

**Corresponding Author(s):** vrajagopal.home@gmail.com

The organization of mitochondria in cardiac myocytes is not homogenous with significant spatial variation in mitochondrial distribution. The main objective of the study is to determine how mitochondrial arrangement affects metabolite distributions within cardiomyocytes and their impact on force dynamics.

We used 2D cross-sections from serial block-face imaging data to develop 2D finite element (FE) models of cardiac bioenergetics with a detailed description of mitochondrial oxidative phosphorylation. We used these models to simulate two different conditions – normoxia and hypoxia.

Our models predict that (A) non-uniform mitochondrial distribution in cardiomyocytes can lead to large gradients in the concentration of inorganic phosphate (Pi), creatine phosphate (PCr) and creatine (Cr) at high workloads when exposed to normal oxygen supply (normoxia) from the capillaries. These large concentration gradients exist over the entire cross-section of the cell between areas with high and low localised mitochondrial density. However, the gradients in ATP and ADP are negligible due to the rapid diffusion of PCr and Cr coupled with the activity of CK enzymes; (B) regional variation in intracellular oxygen supply can impact the metabolite distribution under hypoxic conditions; (C) and finally, by computing the distribution of peak force and twitch duration using our simulated metabolite distributions as input, we find that the peak force distribution and twitch duration is insensitive to a heterogeneous distribution of phosphagens under normoxic conditions. However, the twitch duration can vary by as much as 30 ms between different parts of the cell under hypoxic conditions. The results suggest that the PCr shuttle, and associated enzymatic reactions, act to maintain uniform force dynamics in the cell despite an observed heterogeneous mitochondrial organization. However, our model also predicts that under hypoxia - activity of mitochondrial CK enzyme and diffusion of high-energy phosphate compounds

156

## Interactions of cryoprotectants with model membranes- The Langmuir monolayer study

**Author(s):** Rekha Raju<sup>1</sup>

**Co-author(s):** Gary Bryant<sup>2</sup> ; Juan Torrent Burgues<sup>3</sup>

<sup>1</sup> *PhD Research scholar*

<sup>2</sup> *Professor*

<sup>3</sup> Full Professor**Corresponding Author(s):** rekha.raju@rmit.edu.au

Artificial cryoprotectants such as Dimethyl sulphoxide (DMSO) and Glycerol act by penetrating cell membranes so they can perform their essential functions inside cells. However, these molecules are toxic to cell membranes, and cryopreservation involves balancing these two effects[1, 2]. Despite their importance, the interaction between cryoprotectants and membranes is poorly understood, in contrast with natural cryoprotectants such as sugars whose mechanisms of action have been extensively studied [3, 4]. In order to better understand this interaction, the Langmuir monolayer technique, the principles of which can be found elsewhere[5, 6], has been used to investigate the effect of several penetrating cryoprotectants on 1,2-dioleoyl-sn-glycero-3-phosphocholine (DOPC) isotherms. Two cryobiologically relevant concentrations (5% and 10% by volume) were investigated. We find that the isotherms are significantly affected by the presence of the molecules, with effects on the area per lipid molecule, collapse pressure, compressibility modulus and phase transition pressures. Interestingly, the two most widely used cryoprotectants (DMSO and Glycerol) have very different effects. We discuss these findings in terms of the mechanisms of cryopreservation.

J. Wolfe, G. Bryant, *Cryobiology and anhydrobiology of cells*, Sydney, 2004.

J. Wolfe, G. Bryant, *Cellular cryobiology: thermodynamic and mechanical effects*, *International Journal of Refrigeration-Revue Internationale Du Froid*, 24 (2001) 438-450.

G. Bryant, K.L. Koster, J. Wolfe, *Membrane behaviour in seeds and other systems at low water content: the various effects of solutes*, *Seed Science Research*, 11 (2001) 17-25.

C.J. Garvey, T. Lenne, K.L. Koster, B. Kent, G. Bryant, *Phospholipid membrane protection by sugar molecules during dehydration-insights into molecular mechanisms using scattering techniques*, *Int J Mol Sci*, 14 (2013) 8148-8163.

G.L. Gaines, *Insoluble monolayers at liquid-gas interfaces*, DOI (1966).

J. Torrent-Burgués, *Langmuir films study on lipid-containing artificial tears*, *Colloids and Surfaces B: Biointerfaces*, 140 (2016) 185-188.

194

## Broken Force Dispersal Network in Tip-links induces Hearing-Loss

Jagadish Hazra<sup>1</sup> ; Amin Sagar<sup>1</sup> ; Sabyasachi Rakshit<sup>1</sup>

<sup>1</sup> *Indian Institute of Science Education and Research Mohali*

**Corresponding Author(s):** srakshit@iisermohali.ac.in

Mechanical force is transduced into an electrical signal in hearing. The molecular-spring, tip-links, senses the input-force, maintains its integrity against force-induced rupture, and conveys the force to ion-channels. This delicate balance between integrity-maintenance and force-conveying is maintained in a low-Ca<sup>2+</sup> environment (~50  $\mu$ M) of endolymph in inner-ear. Interestingly, the majority of mutations in tip-links are at the Ca<sup>2+</sup>-binding residues leading to syndromic diseases along with non-syndromic deafness, as if nature has identified the Ca<sup>2+</sup>-binding residues as hotspots to mutate which can reliably alter the function of cadherins. However, the mechanism by which the function is altered is not understood. Crystal Structures resolved at high Ca<sup>2+</sup> also failed to highlight the differences between wild-type (WT) and mutant tip-links.

We found that the Ca<sup>2+</sup>-binding hotspot residues are critical for propagating the input-force through the complex for the force-conveying in mechanotransduction. Simultaneously, these particular residues adequately dissipate the input-force through orthogonal force-dispersal pathways, such that the integrity of the tip-link is maintained even under tension. Mutations on these residues induce conformational changes in the tip-links at the low-Ca<sup>2+</sup> endolymph-like environment, which eventually break the force-dissipating orthogonal components in the propagation-network and make tip-links vulnerable to external input-force. Thus the mutant tip-links complex becomes the victim of input-force and dissociates readily instead of conveying the input-force further.

222

## Tracking missing human olfactory receptors

Shoba Ranganathan<sup>1</sup><sup>1</sup> *Department of Molecular Sciences, Macquarie University, Sydney.***Corresponding Author(s):**

211

## Structures of the Herpes simplex virus type 2 B-capsid & C-capsid with capsid-vertex-specific component

Zihe Rao<sup>1</sup><sup>1</sup> *Tsinghua University Beijing, China***Corresponding Author(s):**

Herpes simplex viruses (HSVs) cause human oral and genital ulcer diseases. Patients with HSV-2 have a higher risk of acquiring a human immunodeficiency virus infection. HSV-2 is a member of the  $\alpha$ -herpesvirinae subfamily that together with the  $\beta$ - and  $\gamma$ -herpesvirinae subfamilies forms the Herpesviridae family. Structurally and genetically, human herpesviruses are amongst the largest and most complex of viruses. Using an optimized reconstruction strategy, we report the structures of HSV-2 B-capsid at 3.1 Å resolutions and C-capsid at 3.75 Å resolution which includes, 28,138 residues in the asymmetric unit, belonging to 46 different conformers of 4 capsid proteins (VP5, VP23, VP19C, VP26) making up 4 types of capsomers (C-Hex, E-Hex, P-Hex, Pen) and triplexes. Acting as core organizers, VP5s exhibit striking differences in configuration and mode of assembly to form extensive intermolecular networks, involving VP26s and triplexes via covalent (25 disulfide bonds per asymmetric unit) and non-covalent interactions, that underpin capsid stability and assembly. Conformational adaptations of these proteins induced by their microenvironments lead to the assembly of a massive quasi-symmetric shell, exemplifying the structural and functional complexity of HSV. We also present atomic models of multiple conformers for the C-capsid proteins (VP5, VP23, VP19C and VP26) and CVSC. Comparison of the HSV-2 homologues yields information about structural similarities and differences between the three herpesviruses sub-families and we identify  $\alpha$ -herpesvirus-specific structural features. The hetero-pentameric CVSC, consisting of a UL17 monomer, a UL25 dimer and a UL36 dimer, is bound tightly by a five-helix bundle that forms extensive networks of subunit contacts with surrounding capsid proteins, which reinforce capsid stability. The portal structures of HSV2 B-capsid and C-capsid also discussed.

[1] Yuan S, et al. *Science*. 2018 Apr 6;360(6384).Wang J et al *Nature Commun*. 2018 9: 3668.

145

## PIEZO1 Can be Modulated by Substrate Mechanics Alone

**Author(s):** Jessica Richardson<sup>1</sup>**Co-author(s):** Kate Poole<sup>1</sup> ; Navid Bavi<sup>2</sup><sup>1</sup> *UNSW Sydney*<sup>2</sup> *UNSW Sydney, University of Chicago*

**Corresponding Author(s):** jessica.richardson@unsw.edu.au

Cells must respond to a wide variety of mechanical stimuli. Mechanically-activated (MA) ion channels play a pivotal role in sensing these stimuli by facilitating a flux of ions across the lipid bilayer in response to both internally and externally applied mechanical stimuli. MA channels are the fastest mechanotransducers and are involved in many physiological processes including vascular development, touch, hearing and osmoregulation. The mammalian protein, PIEZO1 is a MA channel which responds to membrane stretch, cell indentation and substrate deflection, which in turns may activate downstream signalling pathways. PIEZO1 has been implicated in providing instructive cues to cells in response to substrate mechanics. However, few studies have directly investigated the interaction between the mechanical properties of the substrate and PIEZO1 signalling. We have utilised elastomeric pillar arrays to apply molecular-scale deflections directly at the cell-substrate interface in conjunction with patch-clamp electrophysiology. By using pillar arrays of varying stiffness and array density, we show that PIEZO1-mediated currents are significantly modulated by these parameters, which suggests a role for PIEZO1 in stiffness and topography sensing. Furthermore, we have found that forces arising from actin contractility significantly contribute to the sensitisation of PIEZO1-mediated currents during substrate topography sensing.

71

## Cholesterol-dependent PIEZO1 clusters are essential for efficient cellular mechanotransduction

Pietro Ridone<sup>1</sup>

<sup>1</sup> *The Victor Chang Cardiac Research Institute*

**Corresponding Author(s):** p.ridone@victorchang.edu.au

The human mechanosensitive ion channel PIEZO1 is gated by membrane tension and regulates essential biological processes such as vascular development and erythrocyte volume homeostasis [1,2,3]. Currently, little is known about PIEZO1 plasma membrane localization and organization. Using a PIEZO1-GFP fusion protein, we investigated whether cholesterol enrichment, depletion (methyl- $\beta$ -Cyclodextrin; MBCD) and the disruption of membrane cholesterol organization (Dynasore) affects PIEZO1's response to mechanical force. STORM super-resolution imaging revealed that, at the nano-scale, PIEZO1 channels in the membrane associate as clusters which increase in number upon cholesterol addition. Both cluster size and diffusion rates were profoundly affected by treatment with MBCD (5 mM). In addition, electrophysiological recordings in the cell-attached configuration revealed that MBCD caused a rightward shift in the PIEZO1 pressure-response curve and increased channel latency in response to mechanical stimuli. Our results indicate that PIEZO1 function is directly dependent on the amount and lateral organization of membrane cholesterol which is crucial for the concerted inactivation of PIEZO1 clusters.

[1] Cahalan SM, et al. Piezo1 links mechanical forces to red blood cell volume. *eLife*. 2015;4.

Rode B, et al. Piezo1 channels sense whole body physical activity to reset cardiovascular homeostasis and enhance performance. *Nat Commun*. 2017;8.

Li J, et al. Piezo1 integration of vascular architecture with physiological force. *Nature*, 2014.

131

## Separately Measuring Photosynthesis of Oxygenic and Anoxygenic Photosynthetic Organisms using Pulse Amplitude Modulation (PAM) Fluorometry

Raymond J. RITCHIE<sup>1</sup> ; Piamsook CHANDARAVITHOON<sup>1</sup> ; John W. RUNCIE<sup>2</sup>

<sup>1</sup> Prince of Songkla University-Phuket

<sup>2</sup> Aquation Pty Ltd, Umina Beach, NSW 2257, Australia.

**Corresponding Author(s):** raymond.ritchie@uni.sydney.edu.au

Oxygenic photosynthesis can easily be measured using O<sub>2</sub> or CO<sub>2</sub> gas exchange, oxygen electrodes, Winkler titration and <sup>14</sup>CO<sub>2</sub>-fixation and by PAM (Pulse Amplitude Modulation) fluorometry. PAM estimates the photosynthetic electron transport rate (ETR) by measuring fluorescence of chlorophyll (Chl) a (> 700 nm) induced by blue (Soret, QX) band or red light (QY) band. Photosynthetic rates are much less readily measurable in anoxygenic photosynthesis. Anoxygenic photosynthetic bacteria (APB) do not use water as an electron source and are typically photoheterotrophic rather than photoautotrophic and so <sup>14</sup>CO<sub>2</sub> fixation is a misleading estimate of photosynthetic electron transport in APB photosynthesis. Most use bacteriochlorophyll (BChl) a as their primary photosynthetic pigment. In vivo BChl a has a Soret band similar to Chl a but its QY bands are in the infrared and fluorescence is at > 800 nm. Blue-diode-based PAM can be used measure the ETR in purple non-sulphur anoxygenic photobacteria: *Aifella marina* (1) and *Rhodospseudomonas palustris* (2) and purple sulphur bacteria: *Thermochromatium tepidum* (3) because their RC-2 type BChl a complexes fluoresce similarly to PSII. Conventional blue-diode PAM cannot readily distinguish oxygenic and RC-2 type anoxygenic photosynthesis in situations such as sewage ponds which contain both types of photosynthetic organisms (4). PAM cannot measure ETR of RC-1 type photosynthetic bacteria. We describe the development of two new types of PAM machines: one supposedly would only measure oxygenic photosynthesis and the other supposedly only measure RC-2 type anoxygenic photosynthesis. The oxygenic PAM uses a 695-750 nm bandpass filter to measure Chl a fluorescence from PS-II, the anoxygenic PAM uses a highpass filter (>780 nm) to measure BChl a fluorescence. It was found that the fluorescence bands of Chl a and BChl a were too wide to unambiguously distinguish between oxygenic and anoxygenic photosynthesis purely by fluorometry. Treatment with the specific PS-II inhibitor DCMU (Diuron) did enable discrimination of the two types of photosynthesis in a mixture of oxygenic and anoxygenic organisms. Experience with the oxygenic and anoxygenic PAMs leads to the conclusion that the approach is viable and a better choice of fluorescence filters would improve the discrimination between the two types of photosynthesis. Ecologies made up both oxygenic and anoxygenic organisms such as microbial mats and hypereutrophic environments are much more common than often realized. Anoxygenic photosynthesis in such systems is largely unquantified.

References:

Ritchie RJ, Runcie JW (2013). *Photochem Photobiol* 89: 370-383

Ritchie RJ (2013). *Photochem Photobiol* 89: 1143-1162.

Ritchie RJ, Mekjinda N (2015). *Photochem Photobiol* 91: 350-358.

Chandaravithoon P, Nakphet S, Ritchie RJ (2018). *J Appl Phycol* DOI: 10.1007/s10811-018-1423-3

220

## Study of Membrane Proteins by Single Particle Cryo-Electron Microscopy

Isabelle Rouiller<sup>1</sup>

<sup>1</sup> Department of Biochemistry and Molecular Biology & Bio21 Institute, University of Melbourne, Victoria 3010, Australia.

**Corresponding Author(s):**

126

## Subdiffraction Imaging to Characterize Live-Cell Dynamics of Microtubule-Affecting Anticancer Compounds

Ashley Rozario<sup>1</sup> ; Toby Bell<sup>2</sup> ; Donna Whelan<sup>3</sup> ; Sam Duwe<sup>4</sup> ; Peter Dedecker<sup>4</sup>



<sup>1</sup> School of Chemistry, Monash University, Victoria 3800, Australia

<sup>2</sup> Monash University

<sup>3</sup> La Trobe University

<sup>4</sup> Department of Chemistry, University of Leuven, Belgium

**Corresponding Author(s):** ashley.rozario1@monash.edu

The microtubule cytoskeleton is a vital structure to cellular health and function, most notably in cell division. As such, microtubule-affecting agents are found in almost 60% of anticancer therapies. Colcemid (COL) is a synthetic analogue of prospective anticancer agent Colchicine that acts by depolymerizing microtubule filaments and disrupting genetic segregation during mitosis. Thus far, the agent's physiological effects have been promising in reducing tumour cell proliferation in mice models [1]. However, its mode of action at the subcellular level has not been characterized in vivo at acceptable clinical concentrations (~5 ng/ml). This is in part because conventional diffraction-limited fluorescence microscopy does not have the resolving power to visualize substructural changes to microtubules.

We have used super-resolution fluorescence imaging techniques to investigate the effects of low concentrations of COL on the microtubule network in HeLa cells. Single molecule localization (dSTORM) achieves imaging resolution as good as 20 nm, a 10-fold improvement beyond the diffraction limit of light (200 nm), providing enhanced visualization of individual microtubule filaments and drug-induced alterations in fixed cells (Figure 1). We have also employed fluorescence intensity correlation imaging (SOFI) [2] that achieves ~2 – 4-fold improved resolution to monitor subdiffraction microtubule dynamics in living cells.

[1] C.C. Wu, Z.Y. Lin, C.H. Kuoc, W.L. Chuang, Kaohsiung J. Med. Sci. 31 (2015).

P. Dedecker, G.C.H. Mo, T. Dertinger, J. Zhang, PNAS, 109 (2012).

97

## FTIR study of hydrogen bonding environment in different FAD redox states of photolyase/cryptochrome family

**Author(s):** Yui Sakai<sup>1</sup>

**Co-author(s):** Daichi Yamada <sup>1</sup>; Tatsuya Iwata <sup>2</sup>; Hideki Kandori <sup>1</sup>

<sup>1</sup> Nagoya Institute of Technology

<sup>2</sup> Toho University

**Corresponding Author(s):** yblueorange@gmail.com

Photolyase (PHR)/Cryptochrome (CRY) family proteins are the flavin adenine dinucleotide (FAD)-containing flavoproteins. They perform different functions in different organisms, despite structural homology. Photolyases repair two types of UV-induced DNA lesion (CPD and (6-4) photoproducts). Cryptochromes function as photoreceptor for regulation of plant growth. Their different functions are related to FAD redox states. The FAD chromophore of PHR/CRY family proteins have four different redox states: oxidized (FADox), anion radical (FAD<sup>•-</sup>), neutral radical (FADH<sup>•</sup>) and fully reduced (FADH<sup>-</sup>) forms. The functionally active states of PHR and CRY have FADH<sup>-</sup> and FADH<sup>•</sup>, respectively. We focus on how each FAD redox state is formed at molecular level by using FTIR measurement with isotope labeling. Our previous FTIR study of CPD photolyase from *E. coli* showed the hydrogen bond between FAD N5-H and the proximal Asn (Figure 1) is strongest in FADH<sup>•</sup> [1].

In this study, we performed FTIR spectroscopy for two types of PHR/CRY family proteins, CRY-DASH and (6-4) PHR from *Xenopus laevis*. They have different functions, (6-4) PHRs repair (6-4) photoproduct and CRY-DASHs repair single-strand CPD. In addition, they have different FAD redox states in aerobic condition. By using isotope labelling, we assigned C=O band of Asn among all FAD redox states. The obtained comprehensive FTIR results showed that the hydrogen bonding environment in four redox states is similar among PHR/CRY family (Figure 2), despite different functions.

[1] Wijaya et. al., J. Am. Chem. Soc. 138, 4368-4376 (2016).  
Iwata et. al., Biochemistry 49,8882-8891 (2010).

200

## Hitting the dimensionality limit in single cell characterisation using fluorescence and Genomic Cytometry.

Rob Salomon<sup>None</sup> ; Wenyan Li<sup>1</sup> ; Andrew Lim<sup>2</sup> ; John Wotherspoon<sup>3</sup> ; Nona Farbehi<sup>1</sup> ; Dominik Kaczorowski<sup>1</sup> ; Fatima Valdes-Mora<sup>4</sup> ; David Gallego-ortega<sup>5</sup>

<sup>1</sup> *Garvan-Weizmann Centre for Cellular Genomics. Garvan Institute of Medical Research. Sydney, NSW. Australia.*

<sup>2</sup> *BD Bioscience, Sydney Australia*

<sup>3</sup> *Wotherspoon Consulting, Sydney Australia*

<sup>4</sup> *Histone Variants Lab, Genomics and Epigenetics Division. Garvan Institute of Medical Research. Sydney, NSW. Australia.*

<sup>5</sup> *Tumour Development, The Kinghorn Cancer Centre. Garvan Institute of Medical Research. Sydney NSW Australia.*

**Corresponding Author(s):** rob@rob-salomon.com

Whilst flow cytometry remains the gold standard tool for single cell characterisation, recent advances are increasing our ability to delve deeper into cellular heterogeneity. These advances are allowing us to characterise cells using more than just fluorescence or mass detection and we are now entering the world of Genomic Cytometry.

Advances in the application of droplet microfluidics to the study of biology through systems such as the Chromium 10x, Indrop, DropSeq and DroNCSeq systems are allowing us to compartmentalise single cells into reaction volume in the sub nanolitre range using water-in-oil reaction chambers whilst emerging systems such as a BD Rhapsody are allowing us to do this using non-droplet based techniques. Importantly we are able to do this at levels of throughput previously thought to be impossible and can now be leveraged to allow the detection of antibody binding through the use of barcoded oligos attached to the antibody.

By discussing our experience with the droplet based SCRNAseq systems above, as well as the development of high dimensional Fluorescent panels for the Symphony A5, we will highlight some of the major changes that have occurred in the cytometry field over the past few years and describe the emergence of what we are calling Genomic Cytometry. That is, the measurement of cells using nucleic acid sequencing. As we will show, Genomic Cytometry not only allows the detection of cell intrinsic nucleic acids but through smart molecular approaches nucleic acid sequence can be used as a surrogate measure for many other cell characteristics, including high dimensional epitope detection.

To illustrate the power of genomic cytometry we will present cytometry data obtained using high throughput whole transcriptome (dropseq and Indrop) and targeted (BD Rhapsody) single cell RNASeq profiling tools in the context of breast cancer. Additionally we will also show data for high dimensional (25 plus colour) fluorescent panels and discuss how oligo labelled antibodies are set to push the dimensionality barrier for epitope detection well beyond what we currently think is possible.

99

## Aggregation kinetics in the presence of brain lipids of A $\beta$ 40) peptides cleaved from a soluble fusion protein

Miriam Kael<sup>1</sup> ; Frances Separovic<sup>1</sup> ; Marc-Antoine Sani<sup>1</sup>

<sup>1</sup> *The University of Melbourne*

**Corresponding Author(s):** msani@unimelb.edu.au

The cleavage of the amyloid precursor protein by  $\beta$ - and  $\gamma$ -secretases leading to the production of amyloid beta ( $A\beta$ ) peptides is a key event associated with Alzheimer's disease (AD). A fusion protein was constructed to investigate how the cleavage rate impacts on the aggregation kinetics of amyloid-beta (1-40) ( $A\beta$ 40WT) [1] and the early AD onset A2V mutant ( $A\beta$ 40A2V) peptide. The native peptide was expressed with a Small Ubiquitin-Like Modifier (SUMO) on the N-terminus and cleaved by a SUMO protease, Ulp1. The time course of the cleavage reaction followed by SDS-PAGE gel showed faster cleavage kinetics for SUMO- $A\beta$ 40A2V compared to SUMO- $A\beta$ 40WT. Interestingly, fibril formation monitored by ThT fluorescence indicated that the faster SUMO- $A\beta$ 40A2V cleavage led to significant longer lag time and decrease in fibril formation. The presence of unilamellar vesicles comprised of brain total lipid extract had no significant effect on the cleavage rate but slightly shortened the lag time in ThT assays. However, a slower cleavage of the SUMO- $A\beta$ 40A2V induced a significantly shorter lag time for fibril formation. Overall, the fusion protein SUMO- $A\beta$  was shown to be a means by which to study the cleavage and aggregation of native amyloid peptides and that peptide cleavage rate and the presence of lipids strongly modulate the aggregation of  $A\beta$ (1-40) peptides.

M. A. Kael, D. K. Weber, F. Separovic and M.-A. Sani, *BBA-biomembranes* 1860(9), 1681-1686 (2018)

137

## DNA amplification from single molecule in micro-sized droplet

**Author(s):** Hiroki Sawada<sup>1</sup>

**Co-author(s):** Naoki Soga<sup>1</sup>; Seia Nara<sup>2</sup>; Masayuki Su'etsugu<sup>2</sup>; Kazuhito Tabata<sup>1</sup>; Hiroyuki Noji<sup>1</sup>

<sup>1</sup> *University of Tokyo*

<sup>2</sup> *Rikkyo University*

**Corresponding Author(s):** sawada.h17@nojilab.t.u-tokyo.ac.jp

There is a huge demand for analysing genome of microorganisms in fields such as searching antibiotics or ecosystem. For analysing specific genome, it is important to obtain a large amount of homogeneous genome. However, microorganisms exist heterogeneously in nature, so it is necessary to extract and multiply genome from single cell. In order to achieve this purpose, DNA amplification from single molecule is a key method. Despite the development of various methods for DNA amplification, conventional methods have limitations of DNA length or difficulties in amplifying DNA as intact molecules. In recent years, replication-cycle reaction (RCR) which enables isothermal amplification of large circular DNA in vitro has been developed. RCR makes it possible to amplify up to 0.2Mb large circular DNA as intact covalently closed molecules with high fidelity (10<sup>-8</sup> error per base) [1]. To investigate the feasibility for DNA amplification from single molecule, we demonstrated the amplification of large circular DNA from single molecule using micro-sized droplets.

We encapsulated a template DNA in the micro-sized droplet containing the RCR components. By encapsulating DNA in micro-sized droplets at low concentration, each droplet contained 0 or 1 template DNA. After reaction, we introduced intercalator dye into droplets through oil to judge whether single DNA was amplified. As a result, some droplets showed fluorescence. Other droplets kept the base line that is the intensity of droplets in which DNA or RCR enzyme was not encapsulated [Fig. 1]. It suggests that DNA amplification was occurred by RCR in micro-sized droplets. The reaction ratio of amplified DNA was similar to the theoretical values. These results show that template DNA was amplified from single molecule by RCR in micro-sized droplet. According to the calibration curve using DNA fragments, it is estimated that template DNA was amplified up to 2000-fold from single DNA.

We demonstrate that DNA can be amplified from single molecule by RCR in micro-sized droplet. It would be extended for use in the application of in vitro single cell genomics.

[1] M. Su'etsugu, et al., *Nucleic. Acids. Res.* 45, 11525-11534 (2017).

215

## An atlas of protein-protein interactions across mouse tissues

**Author(s):** Nichollas Scott<sup>1</sup>

**Co-author(s):** Michael A. Skinnider<sup>2</sup>; Anna Prodova<sup>2</sup>; Craig H. Kerr<sup>2</sup>; Nikolay Stoynov<sup>2</sup>; R. Greg Stacey<sup>2</sup>; Joerg Gsponer<sup>3</sup>; Leonard J. Foster<sup>3</sup>

<sup>1</sup> *Michael Smith Laboratories, University of British Columbia, Vancouver, V6T 1Z4, Canada* *bPeter Doherty Institute, Department of Microbiology and Immunology, The University of Melbourne, Melbourne, 3000, Australia*

<sup>2</sup> *Michael Smith Laboratories, University of British Columbia, Vancouver, V6T 1Z4, Canada*

<sup>3</sup> *Michael Smith Laboratories, University of British Columbia, Vancouver, V6T 1Z4, Canada and Department of Biochemistry & Molecular Biology, University of British Columbia, Vancouver, V6T 1Z3, Canada*

### Corresponding Author(s):

Cellular processes arise from the dynamic organization of proteins in networks of physical interactions. Mapping the complete network of biologically relevant protein-protein interactions, the interactome, has therefore been a central objective of high-throughput biology [1, 2]. However, the dynamics of protein interactions across physiological contexts are poorly understood. With recent improvements in proteomics technologies the distribution and relative abundances of proteins can now be characterized in unprecedented detail providing an ideal means to explore the interactome of previously recalcitrant systems.

Using a quantitative proteomic approach combining protein correlation profiling [3] with stable isotope labelling of mammals (PCP-SILAM) we have mapped the interactomes of seven mouse tissues, revealing 51,665 protein interactions with an accuracy comparable to the highest-quality human screens. This resource provides the first global view of protein-protein interactions in a mammalian tissue-specific context. This systematic interactome map expands the known mouse interactome by almost 50% and revealing over 35,000 novel interactions.

The richness of this dataset provides the first resource to explore differences in the organisation of proteins interactions across mammalian tissues. Examination of the tissue interactomes reveal systematic suppression of cross-talk between the evolutionarily ancient housekeeping interactome and younger, tissue-specific modules. Rewiring of protein interactions across tissues is widespread, and rewired proteins are tightly regulated by multiple cellular mechanisms and implicated in disease. The observation of rewiring of protein interactions across physiological contexts reveal it is not simply the presence of proteins which define differences between tissues but how proteins interaction in the context of the tissue.

1. Rolland, T., et al., A proteome-scale map of the human interactome network. *Cell*, 2014. 159(5): p. 1212-1226.
2. Huttlin, E.L., et al., Architecture of the human interactome defines protein communities and disease networks. *Nature*, 2017. 545(7655): p. 505-509.
3. Kristensen, A.R., J. Gsponer, and L.J. Foster, A high-throughput approach for measuring temporal changes in the interactome. *Nat Methods*, 2012. 9(9): p. 907-9.

154

## The role of amyloid formation in human necroptosis cascade and its modulation by viruses

**Author(s):** Nirukshan Shanmugam<sup>None</sup>

**Co-author(s):** Chi L.L Pham<sup>1</sup> ; Max O.D.G Baker ; Yann Gambin ; Emma Sierecki ; Margaret Sunde<sup>2</sup>

<sup>1</sup> *University of Sydney*

<sup>2</sup> *The University of Sydney*

**Corresponding Author(s):** nsha6072@uni.sydney.edu.au

Recent insights into cell death pathways have uncovered a new form of programmed cell death, called necroptosis. The key adapter proteins needed for necroptosis activation are receptor interacting protein kinase 1 (RIPK1) and the Z-DNA binding protein 1 (ZBP1). Both interact with receptor interacting protein kinase 3 (RIPK3) through amino acid sequences called RIP homotypic interaction motifs (RHIMs), to form hetero-oligomeric amyloid fibrils<sup>1</sup>. Viral infection can trigger host cell death when activation of RIPK3 results in phosphorylation of MLKL and lytic cell death.

Viruses such as murine cytomegalovirus (MCMV) and herpes simplex virus 1 (HSV-1) encode RHIM-containing proteins, M45 and ICP6, respectively that are involved in inhibition of necroptosis in hosts to ensure viral survival<sup>2</sup>. The molecular mechanisms underpinning the viral modulation of necroptosis are the focus of this study. We hypothesise that the viral proteins form alternative structures with the host RHIM-containing protein/s that are incompatible with downstream signalling.

We have produced multiple fluorescently-tagged RHIM-containing fusion proteins to study the interaction between host and viral proteins and to distinguish between the formation of homo-oligomeric and hetero-oligomeric amyloid fibrils. Amyloid assembly by the RHIM-containing proteins has been studied by thioflavin T fluorescence assays, single molecule confocal spectroscopy and SDS agarose gel electrophoresis. The effect of mutations within the RHIMs of these proteins, on self-assembly and interactions with other RHIM-containing proteins, have been determined. The large fibrillar complexes formed by the viral and host proteins have been imaged by fluorescence and electron microscopy to gain insight into the mechanism of viral modulation of necroptosis.

[1] Li et al., *Cell*. 150, 339-50 (2012).

Mocarski et al., *Virology*. 479-480, 160-6 (2015)

60

## Control of glycine receptor activation by glycine transporters co-expressed in *Xenopus* oocytes

**Author(s):** Diba Sheipouri<sup>1</sup>

**Co-author(s):** Renae Ryan<sup>1</sup> ; Robert Vandenberg<sup>1</sup>

<sup>1</sup> *University of Sydney*

**Corresponding Author(s):** dshe4741@uni.sydney.edu.au

Inhibitory glycinergic neurotransmission in the dorsal horn of the spinal cord is essential in regulation of nociceptive signalling, through reduction of neuronal excitability. Failure of glycinergic transmission in the dorsal horn causes normally innocuous stimuli to become painful (allodynia) and increases sensitivity to noxious stimuli (hyperalgesia). The development of chronic, pathological pain is thought to be attributed to the loss of inhibitory signalling [1]. In studies assessing compounds which increase glycinergic signalling by potentiating glycine receptor activity or inhibiting transporter activity, this system has shown potential for therapeutic targeting [2-5]. The spatially restricted expression of glycine receptors and transporters is an advantage for targeting specific pathologies such as pain .

In this work we present a co-expression model in *Xenopus* oocytes consisting of the GlyT1 or GlyT2 co-expressed with either GlyR $\alpha$ 1 or GlyR $\alpha$ 1 $\beta$ , where transporters remove glycine from the vicinity of the membrane, reducing glycine-gated receptor currents. We show that increases in co-expressed

transporter density subsequently diminish receptor currents. Reductions in receptor mediated currents are not observed when non-transportable agonists are applied or when Na<sup>+</sup> is not available. The transporters remove glycine across different concentration ranges, corresponding with their ion-coupling stoichiometry, and full receptor currents can be restored when the transporters are blocked with selective inhibitors. We show that due to diffusion barriers in the vicinity of the extracellular membrane [6], the actual glycine concentration sensed at the membrane by receptors can be greatly reduced. Finally, we show that the GlyR competitive antagonist, picrotoxin, which has ~17 fold greater sensitivity for  $\alpha\beta$  GlyR heteromers compared to  $\alpha$  homomers [7], can only act as a partial inhibitor at  $\alpha\beta$  subtypes when transporters are present.

1. von Hehn, C.A., R. Baron, and C.J. Woolf, Deconstructing the neuropathic pain phenotype to reveal neural mechanisms. *Neuron*, 2012. 73(4): p. 638-52.
2. Vandenberg, R.J., et al., Glycine transport inhibitors for the treatment of pain. *Trends Pharmacol Sci*, 2014. 35(8): p. 423-30.
3. Dohi, T., et al., Glycine transporter inhibitors as a novel drug discovery strategy for neuropathic pain. *Pharmacology & Therapeutics*, 2009. 123(1): p. 54-79.
4. Harvey, R.J., et al., GlyR alpha3: an essential target for spinal PGE2-mediated inflammatory pain sensitization. *Science*, 2004. 304(5672): p. 884-7.
5. Lu, J.P., et al., Involvement of glycine receptor alpha 1 subunits in cannabinoid-induced analgesia. *Neuropharmacology*, 2018. 133: p. 224-232.
6. Barry, P.H. and J.M. Diamond, Effects of unstirred layers on membrane phenomena. *Physiological reviews*, 1984. 64(3): p. 763-872.
7. Pribilla, I., et al., The atypical M2 segment of the beta subunit confers picrotoxinin resistance to inhibitory glycine receptor channels. *EMBO J*, 1994. 13(6): p. 1493.

187

## Function-related Dynamics of High Molecular Proteins

Ichio Shimada<sup>1</sup>

<sup>1</sup> *The Univ of Tokyo*

**Corresponding Author(s):** shimada@iw-nmr.f.u-tokyo.ac.jp

High molecular proteins, such as membrane proteins, play fundamental roles in many physiological processes and are target proteins for drug development. For better understanding of the functions of the proteins, not only precise static three-dimensional structures determined by X-ray crystallography and cryo-electron microscopy methodologies, but also dynamical nature are required. NMR (nuclear magnetic resonance spectroscopy) provides us information about proteins dynamics, including conformation equilibrium related to functions. However, it is frequently difficult to obtain information about the protein dynamics related to the functions, due to the molecular weight limitation in NMR. We have recently developed novel NMR methods for characterizing protein dynamics utilizing multiple quantum relaxation rates of side-chain methyl groups, which can be sensitively observed in high molecular weight proteins. In this paper, we will show our recent results of function-related dynamics of high molecular proteins.

213

## Tracking of Single Nanoparticles in Living Cells

**Author(s):** Olga Shimoni<sup>None</sup>

**Co-author(s):** Fan Wang ; Shihui Wen ; Hao He ; Baoming Wang ; Zhiguang Zhou ; Dayong Jin

**Corresponding Author(s):**

3

## Testing

John Smith<sup>1</sup>

<sup>1</sup> *Uni of Melbourne*

**Corresponding Author(s):** dhatters@gmail.com

174

## Active Mechanosensing at Cell-Substrate and Cell-Cell Adhesions

**Author(s):** Masahiro Sokabe<sup>1</sup>

**Co-author(s):** Takeshi Kobayashi <sup>1</sup> ; Hiroaki Hirata <sup>1</sup>

<sup>1</sup> *Nagoya University Graduate School of Medicine*

**Corresponding Author(s):** msokabe@med.nagoya-u.ac.jp

Mechanosensitive ion channels (MSCs) are the major player in cell mechanosensing. Among them, the bacterial MSCs, MscL and MscS, are the best studied ones owing to their resolved 3D crystal structure of the closed channel and successful reconstitution in the lipid bilayer. They are activated exclusively by tension in the membrane, contributing to the cell volume control against hypo-osmotic challenge. By contrast, eukaryotic MSCs are known to be activated also by tension in the actin cytoskeletons, including the stress fibre (SF) anchoring at the focal adhesion (FA), by which eukaryotic cells have obtained new functions such as direction- and local-sensing of forces. In the case of Ca<sup>2+</sup>-permeable MSCs in endothelial cells, forces conducting along the SF/FA complex can activate MSCs existing in or adjacent to FAs to increase the intracellular Ca<sup>2+</sup> concentration [Ca<sup>2+</sup>]<sub>i</sub>. Surprisingly, this system has an ultra-high sensitivity to tension as low as 1 pN [1].

The SF/FA/MSC complex has another important function called “active-touch sensing”, in which contractile forces of SFs pull the cell substrate via FAs to activate MSCs. As changes in strain or stress in the SF/FA in response to the contractile force depend on the substrate stiffness, the MSCs can transduce substrate stiffness into the amount of Ca<sup>2+</sup> influx across the MSCs [2]. Actually we observed spontaneous [Ca<sup>2+</sup>]<sub>i</sub> increases (Ca<sup>2+</sup> sparks) mediated by SF contraction in a variety of cultured cells including mesenchymal stem cells, in which amplitude and frequency of the Ca<sup>2+</sup> sparks strictly depended on the substrate stiffness. The Ca<sup>2+</sup> sparks were nearly perfectly inhibited by extracellular Ca<sup>2+</sup> depletion, GsMTx4, a generic MSC inhibitor, or a ROCK inhibitor. Furthermore, a TRPV4-antagonist or TRPV4-knockdown strongly inhibited the Ca<sup>2+</sup> sparks, suggesting that SF/FA/TRP complex as well as talin-integrin complex [3] acts as a mechanosensor to detect substrate stiffness.

Confluence-dependent arrest of cell proliferation, termed ‘contact inhibition’ (CI), is crucial for epithelium homeostasis; loss of CI is a typical hallmark of cancer cells. We found that CI was provoked by an active mechanosensing at the E-cadherin mediated cell-cell junction, adherens junction (AJ), in confluent keratinocytes [4]. Actomyosin cables developed underneath the apical surface of confluent keratinocytes connect to E-cadherin via  $\alpha$ - and  $\beta$ -catenins, applying traction force onto AJs. Actomyosin inhibition by blebbistatin significantly reduced the CI, suggesting that traction force onto AJs (E-cadherin) contributes to provoking CI. Application of pulling force to AJs using magnetic beads attenuated cell proliferation, further supporting the idea that tensile force acting on AJs inhibits keratinocyte proliferation, thus provoking CI. This is surprising because stretching cells is

generally reported to promote cell proliferation. Using a skin cancer mouse model, we found that cell proliferation was upregulated while actomyosin activity was reduced in the epidermoid carcinoma tissue compared with in the normal epidermis tissue. Notably, exogenous activation of the actomyosin regulator RhoA led to reduction in the proliferation of epidermoid carcinoma, giving a novel clue for skin cancer therapy.

[1] H. Hayakawa, H. Tatsumi and M. Sokabe, *J Cell Sci.* 121(4):496 (2008)

T. Kobayashi and M.Sokabe, *Curr Opin Cell Biol.* 22(5):669 (2010).

H. Hirata, K. Chiam, CT. Lim and M. Sokabe. *J R Soc Interface*, 11(99): 20140734 (2014)

H. Hirata, M. Samsonov and M.Sokabe, *Sci Rep.* 7:46326 (2017).

179

## Optogenetic activation of the Enteric Nervous System and induction of colonic transit in conscious mice

Tim Hibberd<sup>1</sup> ; Feng Jing <sup>2</sup> ; Yang Pu<sup>2</sup> ; Vijay Samineni<sup>2</sup> ; Vijay Gereau<sup>2</sup> ; Nigel Kelly<sup>3</sup> ; Hongzhen Hu<sup>2</sup> ; Nick Spencer<sup>4</sup>

<sup>1</sup> Flinders University

<sup>2</sup> Washington University in St.Louis

<sup>3</sup> Flinders Medical Center, South Australia

<sup>4</sup> Flinders University in South Australia

**Corresponding Author(s):** nicholas.spencer@flinders.edu.au

**Background and aims:** Optogenetics is a powerful technique to successfully control the activity of the central nervous system. But no studies have demonstrated optogenetics can control activity in the Enteric Nervous System in the wall of the gastrointestinal (GI) tract. There is significant interest in new technologies to improve GI-transit without using conventional drugs that act on multiple organs. The aim of this study was to determine if optogenetics could be used to stimulate the Enteric Nervous System and induce propagating neurogenic contractions leading to changes in colonic transit. **Methods:** Calretinin-expressing colonic enteric neurons are predominantly cholinergic excitatory neurons. Therefore, we generated transgenic mice with Cre-driven expression of light-sensitive channelrhodopsin-2 (ChR2) in calretinin neurons. **Results:** In the isolated colon, in vitro, focal light stimulation of calretinin enteric neurons evoked classic polarized motor reflexes (latency  $3.4 \pm 0.3$  seconds, 50/58 stimulations), typically followed by premature anterogradely-propagating contractions (latency  $34 \pm 2$  seconds, 39/58 stimulations). These effects could be evoked by light stimulation at points along the entire length of the colon; were abolished by neural blockade with tetrodotoxin ( $n = 2$ ); and did not occur in control mice ( $n = 5$ ). Light stimulation of the proximal colon in vitro, increased the proportion of natural fecal pellets expelled over 15 minutes compared to controls ( $75 \pm 17\%$  vs  $32 \pm 8\%$   $P < 0.05$ ). In vivo, activation of wireless light emitting diodes implanted onto the colon wall significantly increased hourly fecal pellet output in conscious, freely moving mice ( $4.17 \pm 0.4$  versus  $1.3 \pm 0.3$  in controls,  $P < 0.001$ ). **Conclusion:** The findings show that focal activation of a subset of enteric neurons can enhance whole colonic motility in vitro, and fecal output, in vivo. This is the first demonstration that optogenetic control of enteric neurons can be used to modify gut motility.

68

## Single-Molecule and Super-Resolution Microscopy for Intracellular Membrane Dynamics

Qian Su<sup>1</sup>

<sup>1</sup> IBMD, University of Technology Sydney



**Corresponding Author(s):** qian.su@uts.edu.au

We have established in vitro single-molecule reconstitution assays and in vivo super-resolution microscopy systems for the study of intracellular membrane dynamics, especially for autolysosome tubulation and mitochondrial network formation.

The recent development of single-molecule and super-resolution microscopy, which were awarded the Nobel Prize in 2014, drives our understanding of the mechanisms of intracellular processes with spatial resolution down to tens of nanometers scale and dynamic information in the milliseconds level.

Intracellular membrane nanotube formation and its dynamics play important roles for cargo transportation and organelle biogenesis, which are mainly driven by motor proteins. The formation and dynamics of nanotubes are increasingly recognized to play important roles in a multitude of biological progresses. We recently demonstrated the role of nanotube dynamics in autophagic lysosome reformation (ALR) during autophagy[1,2] and mitochondrial network remodeling[3] with single-molecule in vitro reconstitution assay and super-resolution fluorescent microscopy.

During autophagy, lysosomes fuse with autophagosomes to create autolysosomes. Lysosomes are later regenerated via a process involving autolysosome tubulation. We show that the KIF5B kinesin, through direct interactions with PtdIns(4,5)P<sub>2</sub>, drives tubulation by pulling on the autolysosome membrane, revealing a motor-based membrane deformation process that helps maintain lysosomal homeostasis.

Formation of mitochondrial networks is important for maintaining mitochondrial DNA integrity and interchanging mitochondrial material, whereas disruption of the mitochondrial network affects mitochondrial functions. We report a new mechanism for formation of mitochondrial networks through KIF5B-mediated dynamic tubulation of mitochondria. We found that KIF5B pulls thin, highly dynamic tubules out of mitochondria. Fusion of these dynamic tubules, which is mediated by mitofusins, gives rise to the mitochondrial network. We further demonstrated that dynamic tubulation and fusion is sufficient for mitochondrial network formation in vitro.

[1] Du, W., Qian Peter Su, Y. Chen, Y. Zhu, D. Jiang, Y. Sun, and L. Yu. 2016. *Kinesin-1 Drives Autolysosome Tubulation. Developmental Cell* 37: p. 326-336.

Su Qian Peter, W. Du, Q. Ji, B. Xue, Y. Zhu, D. Jiang, J. Lou, L. Yu, and Y. Sun. 2016. *Vesicle Size Regulates Nanotube Formation in the Cell. Scientific Reports* 6:24002.

Wang, C., W. Du, Qian Peter Su, M. Zhu, P. Feng, Y. Li, Y. Zhou, N. Mi, Y. Zhu, D. Jiang, S. Zhang, Z. Zhang, Y. Sun, and L. Yu. 2015. *Dynamic tubulation of mitochondria drives mitochondrial network formation. Cell Research* 25(10): p. 1108-1120.

221

## **Bayesian PET reconstruction using a joint PET-MR patch based dictionary prior**

**Author(s):** Viswanath P. Sudarshan<sup>1</sup>

**Co-author(s):** Gary F. Egan ; Zhaolin Chen ; Suyash P. Awate

<sup>1</sup> *Indian Institute of Technology Bombay, Maharashtra, India. b Monash University, Victoria, Australia. c Monash Biomedical Imaging, Victoria, Australia*

**Corresponding Author(s):**

146

## **Effect of Magnetic Field on Stimulation of Young Para Rubber Trees (*Hevea brasiliensis* Müll. Arg.)**

Chadapust Sudsiri<sup>1</sup>

<sup>1</sup> Prince of Songkla University, Suratthani Campust

**Corresponding Author(s):** chadapust.s@psu.ac.th

Para rubber trees (*Hevea brasiliensis* Müll.Arg.) are an important tree crop in Southern Thailand not only for latex. The trees are widely be used for manufacturing furniture and for making plywood. Unfortunately, young para rubber trees need a planting time of more than six years to become adult. Budding is normally used for propagation (about 2 months) followed by about 6 months in a nursery to become young trees. After planting, the first to the third year is very important for successful establishment. Attention has to be paid to nutrition and water. The trees are partially deciduous during the dry season and are prone to dying from drought stress. Tree growth accelerates after the third year. In this work, we used a magnetic field [1,2] to stimulate para rubber sprouting of cuttings. The cuttings were separated into two groups. The first group was exposed to magnetic field with a field intensity ranging from 2 mT to 9 mT for times ranging from 1-5 hours prior to attempting to grow the cuttings. The second group acted as control. All groups were daily watered using magnetically treated water. We found the experimental group which was exposed to a magnetic field with field intensity of 2 mT for 4 hours grew with a 100% percent sprouting rate within 2 weeks, whereas no sprouting was observed for the control group over this time. After 2 months, the magnetically treated group trees had an average height of 60 cm whereas the control had just begun sprouting. Hence, magnetic treatment of the cuttings was very effective but simply watering with magnetically treated waters was not effective in stimulating sprouting. We concluded that the magnetic field treatment can stimulate Para rubber trees to growth faster than normal and decreased mortality.

[1] Ch. (J). Sudsiri, N. Jampa, P. Kongchana, and R.J Ritchie, *Seed Science and Technology* 44, 267-280 (2016).

Ch. (J). Sudsiri, N. Jampa, P. Kongchana, and R.J. Ritchie, *Scientia Horticulturae* 220, 66-77.

53

## Quantitative analysis of Sec14-mediated lipid transfer by using small-angle neutron scattering

**Author(s):** Taichi Sugiura<sup>1</sup> ; Minoru Nakano<sup>1</sup>

**Co-author(s):** Ukyo Yoshida <sup>1</sup> ; Hiroyuki Nakao <sup>1</sup> ; Keisuke Ikeda <sup>1</sup>

<sup>1</sup> *Grad. Sch. Med. Pharm. Sci., Univ. Toyama*

**Corresponding Author(s):** d1661307@ems.u-toyama.ac.jp

Sec14 is the major phosphatidylinositol (PI)/phosphatidylcholine (PC) transfer protein in yeast, which facilitates vesicle budding from trans-Golgi membrane. Through PI/PC exchange, Sec14 activates PI kinase (Pik1), which generates PI 4-phosphate (PI4P), a target for some proteins related to vesicle formation [1]. Sec14 has a hydrophobic pocket and an amphipathic helix (gate) that covers a phospholipid captured into the pocket [2]. The Sec14 lipid transfer is thought to be in three steps: binding to membrane with inserting the gate helix, exchange of lipids on the membrane, and dissociation from the membrane with closing the gate. However, how the Sec14 lipid transfer activity is regulated remains unclear. Here, we focused on the lipid-membrane environments (lipid composition and membrane curvature) and evaluated their effect on the Sec14 lipid transfer.

We measured the lipid transfer by using small-angle neutron scattering (SANS) which allows quantitative analysis of the lipid transfer. We prepared deuterated PC (d-PC) vesicle (D-vesicle) and hydrogenated PC (h-PC) vesicle (H-vesicle), and then mixed them in H<sub>2</sub>O/D<sub>2</sub>O mixed solvent. Initially, both vesicles exhibit strong scattering intensity because scattering length density (SLD) of each vesicle is quite different from that of the solvent. The exchange of d-PC and h-PC between D- and H-vesicle reduces the difference in the SLD between the solvent and the vesicles, so that a decrease in the scattering intensity is observed.

When we used d-PC and h-PC vesicles, we could observe the Sec14 lipid transfer activity from the reduction in the neutron scattering intensity. Next, we examined the effect of PI, another ligand of Sec14, on the lipid transfer activity. In the 10 mol% PI containing system, the scattering intensity decay was accelerated, showing that PI promotes the Sec14 lipid transfer. Because PI has a negative charge at its headgroup, we next examined the effect of phosphatidylserine (PS) to focus on the charge. The data showed that PS also accelerated the lipid transfer, indicating that acidic phospholipids promote the Sec14 lipid transfer. In order to evaluate the lipid transfer in detail, we plotted initial rates against Sec14 concentrations and calculated apparent dissociation constant (KD). As a result, KD value was not reduced by PI and PS, indicating that the Sec14 binding to membrane is not enhanced by the acidic phospholipids. Next, we examined the effect of membrane curvature on the lipid transfer. Compared with the case when we used large unilamellar vesicles (LUVs, low curvature membrane), Sec14 exhibited faster lipid transfer between small unilamellar vesicles (SUVs, high curvature membrane). In addition, in the mixture of d-PC LUV and h-PC SUV, Sec14 exhibited very slow lipid transfer between LUV and SUV. These results imply that Sec14 has higher affinity for SUV than for LUV, and Sec14 preferentially transfers lipids between SUVs and hardly accesses the LUV.

[1] Schaaf G., Ortlund E. A., Tyeryar K. R., Mousley C. J., et al., *Mol. Cell* 29, 191-206 (2008).  
Sha B., Phillips S. E., Bankaitis V. A., Luo M., *Nature* 391, 506-510 (1998).

62

## The impact of proteostasis imbalance on proteome solubility

Xiaojing Sui<sup>1</sup> ; Gavin Reid<sup>1</sup> ; Danny Hatters<sup>1</sup>

<sup>1</sup> *The University of Melbourne*

**Corresponding Author(s):** suix@student.unimelb.edu.au

A hallmark of neurodegenerative diseases is that certain proteins abnormally aggregate into insoluble deposits. A leading hypothesis is that a breakdown in protein folding quality control mechanisms leads to the accumulation of unfolded or misfolded proteins that are prone to aggregation. We hypothesized there would be a metastable subproteome vulnerable to aggregation when protein quality control is stressed by any mechanism. However, a systematic understanding of the proteins that are affected remains poorly understood. Here we performed extensive quantitative proteomic studies to measure the changes in proteome solubility (as determined by 100,000 g pelleting for 20 min) arising from inhibition of three hubs of the protein quality control network. We compared the subproteomes affected when cells were subjected to two stresses that are observed in many neurodegenerative disease settings, as well as a Huntington's Disease cell model that is characterized by aggregation of mutant Huntingtin protein. Unexpectedly, all stresses (except the Huntington Disease model where we could not collect this information) resulted in no net increase in aggregated protein suggesting that the proteome is robustly buffered against the accumulation of misfolded protein. At the individual level there were many changes both upwards and downwards for all stresses, indicative of a pleiotropic combination of protein complex remodelling, protein misfolding induced aggregation and protein complex disassembly and other possible factors. Further unexpected was that each treatment unmasked a surprisingly distinct subproteome signature for changes in aggregation state with the only common pattern being proteins that comprise the nuclear pore complex. Overall the similarities in the stress signatures with the Huntington Disease cell model were: Hsp90 inhibition (4.2%), oxidative stress (3.7%), ER stress (2.8%), proteasome inhibition (2.2%) and Hsp70 inhibition (0.7%), as represented by proteins that changed solubility in the same direction in common out of all proteins that changed solubility and were detected in both datasets.

210

## Super-resolution study of nuclear structure and dynamics

Yujie Sun<sup>1</sup><sup>1</sup> *State Key Laboratory of Membrane Biology, Biodynamic Optical Imaging Center (BIOPIC), School of Life Sciences, Peking University, Beijing 100871, China***Corresponding Author(s):**

Cell nucleus is a highly crowded yet organized world. Essential biological processes, such as replication and transcription, are tightly regulated in time and space. We apply single molecule and super-resolution imaging techniques to understand the spatial-temporal regulation of nuclear structure and dynamics by combining both in vitro and in vivo assays. Using in vitro single molecule assays, we confirmed that double stranded DNA has allosteric effects which regulate protein binding. Using in vivo super-resolution imaging, we proved that the spatial organization of chromatin DNA is a key factor to define the efficiency of replication origins as well as transcription, promoting the concept that chromatin structure is an important epigenetic code. In order to study chromatin dynamics, we also developed a new approach to realize multicolor chromosomal loci imaging based on a modified single-guide RNA (sgRNA) of the CRISPR/Cas9 system. We demonstrated that the new approach is easy to implement and enables robust multicolor labeling of genomic elements with superior counter-bleaching capacity for continuous, long term tracking of chromosomal dynamics.

73

## Near-infrared spectroscopy of DNA wrapped single-walled carbon nanotubes with fluorescent dyes

**Author(s):** Hiroaki Tada<sup>1</sup>**Co-author(s):** Shusuke Oura<sup>1</sup>; Kazuo Umemura<sup>1</sup><sup>1</sup> *Tokyo University of Science***Corresponding Author(s):** 1217624@ed.tus.ac.jp

Single-walled carbon nanotubes (SWNTs) has physically and chemically superior properties. Although SWNTs are generally hydrophobic, SWNTs can be dispersed in aqueous solution by forming complexes with DNA (DNA-SWNTs) [1]. Nanobiosensors using optical responses of DNA-SWNT complexes such as near-infrared photoluminescence (PL) of SWNTs have been proposed by many research groups. On the other hand, it is known that the optical responses of SWNTs are affected by chirality of SWNTs although the chirality effects in the nanobiosensing with DNA-SWNT complexes have not been well understood. If we understand and regulate the chirality effects, it is expected that more sophisticated nanobiosensing techniques can be established. In this study, we investigated the chirality effects on PL from DNA-SWNT surfaces in absence and presence of fluorescent dyes. We previously reported attachments of fluorescent dyes to DNA-SWNT surfaces for functionalization [2].

SWNTs were dispersed with single stranded DNA (ssDNA) or double stranded DNA (dsDNA). Excitation wavelengths for PL measurements were 550 to 750 nm. PL of SWNTs were measured from 850 to 1600 nm (every 1 nm). When rhodamine B solution (RB) or uranine solution (UR) was added to DNA-SWNT suspension as fluorescent dyes, molar ratio of the fluorescent dyes to carbon atom in the samples were adjusted to 1:200. Normalized PL intensities before and after addition of dyes were plotted for several different chiralities of SWNTs. For normalization, PL of (9, 4) chirality was defined as 1. The data indicated average values of independent three experiments.

PL intensity was decreased in all the chiralities when RB or UR were added to the DNA-SWNT suspension, however, quenching ratios were different due to chirality of SWNTs and combinations of types of DNA and dyes. In the case of ssDNA-SWNT complexes with RB, quenching ratios of (8,6), (8,3), (8,4), (7,5), (7,6), and (9,4) were 5%, 3%, 4%, 10%, 10%, and 10%, respectively (Fig. 1). Based on this result, we propose categorization of the six chiralities. In group (a) ((8,6), (8,3), and (8,4)), the quenching ratios were low (average quenching ratios of the three chiralities = 4%). In the groups (b) ((7,5), (7,6), and (9,4)), those were relatively higher (average quenching ratios of the three chiralities

= 10%).

In ssDNA-SWNT with UR, average quenching ratios of groups (a) and (b) were 3% and 3%, respectively (Fig. 1). In the case of dsDNA-SWNT with RB, the ratios of (a) and (b) were 3% and 3%, respectively (Fig. 2). In these samples, there was no difference between groups (a) and (b). In dsDNA-SWNT with UR, the ratios of (a) and (b) were 2% and 0%, respectively. In this combination, group (a) indicated slightly higher quenching ratios. Our results revealed that each chirality of SWNTs involves its specific optical responses. The different responses originated from chirality are probably useful to establish nanobiosensing techniques using DNA-SWNT complexes.

[1] Zheng et al., *Nat. Mater.*, 2, 338-342(2003).

Tomura et al., *Anal. Biochem.*, 547, 1-6(2018).

48

## Statistical and quantum-chemical analysis of the effect of heme porphyrin distortion in heme proteins: differences between oxidoreductases and oxygen carrier proteins

Yusuke Kanematsu<sup>1</sup> ; Hiroko Kondo<sup>2</sup> ; Yasuhiro Imada<sup>3</sup> ; Yu Takano<sup>1</sup>

<sup>1</sup> *Hiroshima City University*

<sup>2</sup> *Kitami Institute of Technology*

<sup>3</sup> *Osaka University*

**Corresponding Author(s):** ytakano@hiroshima-cu.ac.jp

Heme proteins are involved in various biochemical functions. About 5000 heme protein structures have been reported and deposited in Protein Data Bank (PDB). Given the recent accelerating increase of the available data, the statistical approach on heme proteins will pave the way to seek how they make excellent use of their hemes to control their functions. Recently, the protein-induced distortions of a heme porphyrin ring have also attracted great attention [1, 2]. It has been demonstrated that some out-of-plane distortions are conserved in functionally related proteins in spite of the energetic preference for the planar structure, implying their biological significance.

We report a study of the effect of heme distortions on chemical properties in two protein classes, oxidoreductases and oxygen carrier proteins, with the combination of statistical analysis and quantum chemical calculation [3]. Principal component analysis (PCA) of the distribution of heme distortion showed that the oxidoreductases frequently utilized the ruffling distortion for the fine tuning of their redox potentials. In contrast, a preference of a planar structure of heme was found in oxygen carrier proteins. We also performed linear discriminant analysis (LDA) on the distribution of heme distortion. It provided a feature vector, which reasonably classifies the structural distributions in these heme proteins. The redox potentials and the oxygen affinities of heme with distortions were calculated along the feature vector by using density functional theory. We found different dependences of these properties on the feature vector. This implies that LDA captured the structural bias imposed by the protein environment for the enhancement of their functions of oxidoreductases and oxygen carrier proteins. These implied that heme proteins utilize these distortions to enhance their functionalities. The combination of statistical analysis and quantum chemical calculation is useful for the elucidation of structure-function relationship.

[1] W. Jentzen, J.-G. Ma, J. A. Shelnut, *Biophys. J.* 74, 753 (1998).

Y. Imada, H. Nakamura, Y. Takano, *J. Comput. Chem.* 39, 143 (2018).

Kanematsu, Y.; Kondo, H. X.; Imada, Y.; Takano, Y. *Chem. Phys. Lett.* 710, 108 (2018).

129

## A Potent Inhibitor for Mitotic Kinesin Eg5

Miyanishi Takayuki<sup>1</sup> ; Tomisin Happy Ogunwa<sup>1</sup> ; Yuka Kawata<sup>1</sup> ; Kei Sadakane<sup>2</sup> ; Shinsaku Maruta<sup>2</sup>

<sup>1</sup> Nagasaki University

<sup>2</sup> Soka University

**Corresponding Author(s):** miyanish@nagasaki-u.ac.jp

Searching for promising natural compounds with inhibitory potential against the mitotic protein, Eg5, we used in silico tools to screen forty (40) plant-derived biflavonoids. Our selection of potential inhibitor was based on parameters such as their binding modes, molecular interactions, binding energies and functional groups which may participate in the Eg5 interaction. The results predicted morelloflavone as a potential inhibitor which might bind the putative allosteric pocket of Eg5, being embedded in silico within the cavity of Eg5, L5/ $\alpha$ 2/ $\alpha$ 3 allosteric site, with binding energy value of -8.4 kcal/mol and with a single hydrogen bond. Subsequent in vitro biochemical analysis confirmed that morelloflavone inhibited both basal and microtubule - activated ATPase activity of Eg5 in a non-competitive manner, probably binding at an allosteric site to affect the structure of ATP binding site on Eg5. Morelloflavone also suppressed the Eg5 gliding along microtubules. These results suggest that morelloflavone may bind the allosteric binding site of Eg5 and inhibit the ATPase activity and motor function of Eg5.

[1] H. El-Nassan, Eur. J. Med. Chem. 62, 614-631 (2013).

K. Sadakane, M. Takaichi, and S. Maruta, J. Biochem. 164(3), 239-246 (2018).

Z. Maliga, T.M. Kapoor and T.J. Mitchison, Chem. Biol. 9(9), 989-96 (2002)

55

## Molecular dynamics study of structural fluctuations in CDR-H3 of anti-HIV antibodies PG9 and PG16

**Author(s):** Naoki Tanabe<sup>1</sup>

**Co-author(s):** Akimitsu Kugimiya<sup>1</sup> ; Daisuke Kuroda<sup>2</sup> ; Hiroko.X Kondo<sup>3</sup> ; Jiro Kohda<sup>1</sup> ; Kohei Tsumoto<sup>2</sup> ; Ryo Kiribayashi<sup>1</sup> ; Toru Saito<sup>1</sup> ; Yasuhisa Nakano<sup>1</sup> ; Yu Takano<sup>1</sup>

<sup>1</sup> Hiroshima city university

<sup>2</sup> The university of tokyo

<sup>3</sup> Kitami institute of technology

**Corresponding Author(s):**

Monoclonal antibodies PG9 and PG16 neutralize 70 to 80% of circulating human immunodeficiency virus 1 (HIV-1) isolates. X-ray crystallographic studies of these antibodies have suggested their structural similarity. Both PG9 and PG16 have a 28-residue third complementarity-determining region of the heavy chain (CDR-H3), which forms a unique subdomain referred to as “hammerhead” [1]. In this study we compared the structural fluctuations of the CDR-H3s of these antibodies by using molecular dynamics simulations. Principal component analysis (PCA) of each CDR-H3 revealed that the difference in the structural fluctuation between them (Fig. 1). The “hammerhead” tended to bend at the root of CDR-H3 in PG9, while the CDR-H3 of PG16 showed a partial bending of “hammerhead.” The number of hydrogen bonds are associated to these dynamics.

[1] M. Pancera et al., J. Virol. 84, 8098-8110 (2010).

150

## DNA-Templated Assembly of the Type III Secretion System Tip Complex

**Author(s):** Andrew Tuckwell<sup>1</sup>

**Co-author(s):** Steph Xu <sup>1</sup> ; Wunna Kyaw <sup>1</sup> ; Lawrence Lee <sup>1</sup>

<sup>1</sup> *EMBL Australia Node for Single Molecule Sciences, UNSW, Sydney, Australia.*

**Corresponding Author(s):** a.tuckwell@unsw.edu.au

The Type III Secretion System (T3SS) is a protein superstructure, consisting of hundreds of subunits, which self-assemble into a molecular syringe that allows bacteria to inject virulence factors directly into a host cell. The tip complex caps an extracellular needle filament and is involved in the regulation of a pore-forming complex that is secreted upon host-cell contact.

High resolution crystal structures of tip complex subunits have been determined from several species, however their monomeric conformations appear to be incompatible with in situ electron microscopy (EM) micrographs. While these also provide information on stoichiometry, the resolution of EM micrographs are at present too low to determine the arrangement of subunits in an intact tip complex, this is in part because the tip complex can currently only be studied as part of the entire T3SS superstructure.

Using synthetic DNA nanostructures and covalent DNA-protein conjugation we demonstrate the ability to artificially template the tip complex subunits with tuneable dimensions and stoichiometry and use EM to directly visualise these DNA-templated assemblies. Chemical crosslinking of monomeric or templated subunits in combination with mass spectroscopy was used to provide a set of distance-restrained residue pairs that are specific to DNA-templated assemblies. Combining the distance restraint data from DNA templates and crosslinked proteins with rigid body modelling and molecular dynamics of subunit crystal structures, we generated structural models of DNA-templated T3SS tip complexes that resemble published low-resolution EM images of tip complexes in situ.

These structural models of DNA-templated assemblies may further be validated by the design of mutations for crosslinking in situ and furthermore presents the exciting prospect of detailed structural characterization of T3SS tip complexes in isolation.

120

## **Lipids can disperse clusters of BAK dimers after formation of the apoptotic pore**

**Author(s):** Rachel Uren<sup>1</sup>

**Co-author(s):** Martin O'Hely <sup>1</sup> ; Sweta Iyer <sup>1</sup> ; Ray Bartolo <sup>1</sup> ; Melissa Shi <sup>1</sup> ; Jason Brouwer <sup>1</sup> ; Amber Alsop <sup>1</sup> ; Grant Dewson <sup>1</sup> ; Ruth Kluck <sup>1</sup>

<sup>1</sup> *Walter and Eliza Hall Institute of Medical Research*

**Corresponding Author(s):** uren.r@wehi.edu.au

During apoptosis, BAK and BAX change shape and initially assemble as symmetric homodimers. The dimers then form clusters, which are thought to be precursors to apoptotic pores that perforate the mitochondrial outer membrane. The topology of BAK dimers can be divided into three regions: N-termini that are flexible and solvent exposed; a highly structured core domain; and C-termini that are flexible but in contact with the membrane [1,2]. Using our knowledge of BAK dimer topology, we can precisely monitor the aggregation of BAK dimers in cells and show that the clusters form without a dominant interface. Critically, cluster formation without a dominant interface provides a molecular explanation for the wide variety of rings, arcs, lines and clusters of BAK and BAX visualised in cells undergoing apoptosis. We propose that both the clustering of dimers and subsequent pore formation require changes in the lipid membrane.

To interrogate the role of lipids in pore formation, we applied exogenous lipids to mitochondria expressing human BAK. We first triggered BAK dimer clustering and pore formation (by the addition

of BID) and then applied soluble cholesterol. While soluble cholesterol could not dissociate BAK dimers into monomers, it could disperse clusters of BAK dimers. We are also testing for changes in lipid order in the mitochondrial outer membrane that might correspond to BAK and BAX function.

[1] Uren RT, O'Hely M, Iyer S, Bartolo R, Shi MX, Brouwer JM, Alsop AE, Dewson G, Kluck RM. Disordered clusters of Bak dimers rupture mitochondria during apoptosis. *eLife* 2017 Feb 6;6. Pii: e19944.

Uren RT, Iyer S, Kluck RM. Pore formation by dimeric Bak and Bax: an unusual pore? *Phil. Trans. R. Soc. B* 2017 372: 20160218.

193

## Allosteric Inhibitors of Glycine Transport for the Treatment of Pain

**Author(s):** Robert Vandenberg<sup>1</sup>

**Co-author(s):** Shannon Mostyn<sup>1</sup>; Tristan Rawling<sup>2</sup>; Zachary Frangos<sup>1</sup>; Alexandra Schumann-Gillett<sup>3</sup>; Renae Ryan<sup>1</sup>; Megan O'Mara<sup>3</sup>

<sup>1</sup> *University of Sydney*

<sup>2</sup> *University of Technology, Sydney*

<sup>3</sup> *Australian National University*

**Corresponding Author(s):** robert.vandenberg@sydney.edu.au

The glycine transporter, GlyT2, is the target for a number of drugs that can alleviate neuropathic and inflammatory pain. We have developed a series of N-acyl amino acid analogues that inhibit GlyT2 and also show promise as leads for the development of a novel class of lipid-based analgesics. ~60 new N-acyl amino acids with varying head and acyl-tail groups were synthesised and found to be potent, selective GlyT2 inhibitors, 13 of which possess an IC<sub>50</sub> < 100 nM, and provide analgesia in rat models of neuropathic pain. We have used site-directed mutagenesis combined with quantitative structure activity analysis to identify potential allosteric lipid binding sites and to understand communication between the lipid binding site and inhibition of transport. Mutations in four distinct regions of the protein influence the potency and extent of inhibition. Extracellular loop 4 undergoes considerable conformational changes in the transport cycle, and mutations in the loop (I545L, Y550L) disrupt inhibition by all lipids. A reverse mutation in EL4 of GlyT1 (L425I) introduces lipid sensitivity, which further reinforces the critical role of this domain in lipid binding and mechanism of inhibition. We reasoned that transmembrane domains that flank EL4 may also influence lipid inhibition. Mutations on the membrane-exposed external surface of TM8 (P561S, W563L) differentially reduce the potency of selected N-acyl amino acids and suggest potential lipid head group interactions with the transporter. Mutations of additional residues in TM8 (L569F) and TM5 (F428A, V432A) also reduce the potency of lipid inhibition in an acyl-tail specific manner, suggesting that this region binds the lipid tail. Finally, mutations in the middle of TM7 (eg. F515W) enhance the potency and also speed up the rate of recovery from inhibition, which suggest a role of TM7 in influencing accessibility of the lipids for their binding site. Coarse grain molecular dynamics simulations of lipids associating with GlyT2 suggest that the N-acyl amino acids enter the membrane and first associate with TM7 (near F515) and then intercalate between the transmembrane domains before reaching a stable binding site formed by EL4 and the extracellular halves of TM8 and TM5. A lipid-based inhibitor bound at this site is likely to restrict conformational changes in the transporter and thereby prevent the transport mechanism. We are currently using this information to further develop novel N-acyl amino acid GlyT2 inhibitors that may have therapeutic value in treating chronic pain.

192

## A fluorescent protein-tagged peptide toxin as a tool for KV1.3 visualisation



Dorothy Wai<sup>None</sup> ; Raymond Norton<sup>1</sup><sup>1</sup> Monash University**Corresponding Author(s):** dorothy.wai@monash.edu

Voltage-gated potassium channels play an important role in immunity, in particular T-cell activation [1]. Homotetrameric KV1.3 channels are specifically upregulated in effector memory T-cells (TEM), which have been implicated in autoimmune diseases including rheumatoid arthritis, psoriasis, multiple sclerosis and type I diabetes [2]. It is therefore of interest to be able to identify such KV1.3-expressing cells. However, fluorescent conjugates of antibodies or small molecules are unable to distinguish homotetrameric KV1.3 channels from heterotetrameric KV1.3/KV1.x channels. In contrast, a number of animal-derived peptide toxins that bind the extracellular vestibule of the channel exhibit selectivity for KV1.3 homotetramers [3]. One example is HsTX1[R14A], an analogue of a 34-residue peptide toxin from the scorpion *Heterometrus spinifer* that binds KV1.3 with an IC<sub>50</sub> of 45 pM and displays a 2000-fold selectivity for KV1.3 over KV1.1 [4].

Although it is possible to label peptide toxins with small-molecule fluorophores, this is often costly and synthetically challenging as residues commonly used for fluorophore attachment are also critical for toxin folding and function [5]. Earlier work has demonstrated the feasibility of tagging peptide toxins with fluorescent proteins by recombinant expression [6]. A possible limitation is that many peptide toxins, including HsTX1[R14A], require oxidising conditions to form disulfide bonds that are essential for correct folding.

To address this issue, we have developed a construct comprising HsTX1[R14A] and an N-terminal GFP tag. The GFP variant used [7] was selected for its brightness, monomeric form and Cys-to-Ser mutations that are compatible with an oxidising expression environment. The fusion protein was successfully produced using a periplasmic expression system in *E. coli*, purified by nickel affinity and size-exclusion chromatography, and assessed by UV-Vis spectroscopy and <sup>1</sup>H 1D NMR. Further work will be undertaken to evaluate KV1.3 binding by GFP-HsTX1[R14A] using electrophysiology assays and microscopy. Once validated, GFP-HsTX1[R14A] would be a readily accessible and cost-effective tool for studying KV1.3-expressing cells in applications requiring fluorescently-labelled ligands, such as confocal imaging and fluorescence-activated cell sorting.

[1] E.Y. Chiang, et al., *Nature Commun.* 8, 14644 (2017).

J. Lam and H. Wulff, *Drug Develop. Res.* 72, 573-584 (2011).

R.S. Norton and K.G. Chandy, *Neuropharmacology.* 127, 124-138 (2017).

M.H. Rashid, et al., *Sci Rep-UK.* 4, 4509 (2014).

A.I. Kuzmenkov and A.A. Vassilevski, *Neurosci Lett.* 679, 15-23 (2018).

A.I. Kuzmenkov, et al., *Sci Rep-UK.* 6, 33314 (2016).

L.M. Costantini, et al., *Nature Commun.* 6, 7670 (2015).

58

## The apo structure of Dehydroqualene Desaturase and the co-crystal structure with inhibitors

Wenjin WAN<sup>None</sup>**Corresponding Author(s):** u3005155@connect.hku.hk

In recent years, an increasing number of people have been infected by *Staphylococcus aureus* from community and hospital along with the appearance of antibiotic-resistant *S. aureus*, particularly methicillin-resistant strain. The infection causes many kinds of diseases, from a minor illness like pimples to a lethal disease, such as pneumonia and septic arthritis. [1] Staphyloxanthin, a golden colored membrane-bound pigment in *S. aureus*, was found to be an important contributor to the survival of *S. aureus* in human bodies. [2] Dehydroqualene desaturase (CrtN) is a crucial enzyme in staphyloxanthin biosynthesis pathway.[3] So a collaborative lab of mine synthesized four inhibitors

that could inhibit CrtN and pigment production. And my job is to purify CrtN, and then try to get the crystal of CrtN and the co-crystal with inhibitors to see the binding mode between them and provide information to design better drugs.

[1] Baorto, E. P., D. B., & Romero, J. R. (2017, November 01). Staphylococcus Aureus Infection (M. L. Windle, L. I. Lutwick, & R. W. Steele, Eds.). Retrieved November 6, 2017, from <https://emedicine.medscape.com/article/9/overview>

Clauditz, A., Resch, A., Wieland, K., Peschel, A., & Gotz, F. (2006). Staphyloxanthin Plays a Role in the Fitness of Staphylococcus aureus and Its Ability To Cope with Oxidative Stress. *Infection and Immunity*, 74(8), 4950-4953. doi:10.1128/iai.00204-06

Gao, P., Davies, J., & Kao, R. Y. (2017). Dehydrosqualene Desaturase as a Novel Target for Anti-Virulence Therapy against Staphylococcus aureus. *MBio*, 8(5). doi:10.1128/mbio.01224-17

84

## Comparison of biomolecular force fields on simulation P-glycoprotein

**Author(s):** Lily Wang<sup>1</sup>

**Co-author(s):** Megan O'Mara<sup>2</sup>

<sup>1</sup> *The Australian National University*

<sup>2</sup> *The Australian National University*

**Corresponding Author(s):** lily.wang@anu.edu.au

The semi-empirical nature of molecular dynamics requires force fields to balance their general applicability with the ability to produce accurate simulations of their targets. Force fields are generally benchmarked and validated to experimental or high-level quantum mechanical data of small molecules, and comparing the performance of different force fields on a particular system or class thereof is a popular study. However, it is uncommon to conduct these investigations on proteins larger than a couple hundred residues, likely to due to the significant computational cost required. As protein molecular dynamics continues to flourish with ever more efficient hardware, it becomes both reasonable and necessary to check the performance of different force fields and consider whether a body of literature that includes studies across a range of force fields can be considered a unified corpus of data or whether some methods yield different results.

Membrane transporter P-glycoprotein is an efflux pump infamous for its broad substrate specificity and role in conferring multidrug resistance. Despite over forty years of biochemical investigation, the particular molecular mechanism of its promiscuity remains to be elucidated. It is a common target of molecular dynamics investigations, many of which are conducted using very different methods and different force fields. This study compares the conformational distribution of P-glycoprotein across five major biomolecular force fields: GROMOS 54A7, AMBER 99SB-ILDN, CHARMM 36, OPLS-AA/L, and MARTINI. Each force field characterised markedly different areas of conformational space within the first 200 ns of simulation. Simulations expanded to 500 ns displayed a degree of convergence, although clustered structures were still largely aligned along force field differences and different secondary structures were present in each force field. Simulations for all trajectories surprisingly agreed to experimental data to very similar, if minor, extents. Longer simulations were more likely to sample conformations agreeing with experimental data and to remain in that region of conformational space longer. This suggests that the major bottleneck in such studies of large biomolecular systems remains the challenge of sufficient sampling of the conformational distribution within the limits of computational hardware and resources.

7

## Structure of a prokaryotic SEFIR domain reveals two novel SEFIR-SEFIR interaction modes

Min Wang<sup>None</sup>**Corresponding Author(s):** minwang2009@126.com

SEFIR domain-containing proteins are crucial for mammalian adaptive immunity. As a unique intracellular signaling domain, the SEFIR-SEFIR interactions mediate physical protein-protein interactions in the immune signaling network, especially the IL-17- and IL-25-mediated pathways. However, due to the lack of structural information, the detailed molecular mechanism for SEFIR-SEFIR assembly remains unclear. In the present study, we solved the crystal structures of a prokaryotic SEFIR domain from *Bacillus cereus* F65185 (BcSEFIR), where the SEFIR domain is located at the N terminus. The structure of BcSEFIR revealed two radically distinct SEFIR-SEFIR interaction modes. In the asymmetric form, the C-terminal tail of one SEFIR binds to the helix  $\alpha$ A and  $\beta$ B- $\alpha$ B' segment of the other one, while in the symmetric form, the helices  $\eta$ C and  $\alpha$ E and the DE-segment compose the inter-protomer interface. The C-terminal tail of BcSEFIR, critical for asymmetric interaction, is highly conserved among the SEFIR domains of Act1 orthologs from different species, in particular three absolutely conserved residues that constitute an EXXXPP motif. In the symmetric interaction mode, the most significant contacts made by residues on helix  $\alpha$ E are highly conserved in Act1 SEFIR domains, constituted an RLI/LXE motif. The two novel SEFIR-SEFIR interaction modes might explain the structural basis for SEFIR domain-mediated complex assembly in signaling pathways

[1] Yang H, Zhu Y, Chen X, Li X, Ye S, Zhang R. 2018. *J Struct Biol*.

41

## The Effect of DNA Backbone on The Triplet Mechanism of UV-Induced Thymine-Thymine (6-4) Dimer Formation

Xingyong Wang<sup>1</sup> ; Haibo Yu<sup>1</sup><sup>1</sup> *University of Wollongong***Corresponding Author(s):** xingyong@uow.edu.au

UV radiation may initiate the formation of two classes of DNA lesions: cyclobutane pyrimidine dimers (CPDs) and pyrimidine-pyrimidone (6-4) photoproducts ((6-4)PPs), and their Dewar valence isomers (DewarPPs) (Scheme 1), which are considered to be the main causes of skin cancer [1]. While the mechanism of CPD formation has been intensively studied, the reaction pathway for the formation of (6-4)PP or DewarPP remains elusive. Based on a model containing two thymines connected by a truncated sugar-phosphate backbone, density functional theory (DFT) calculations have been carried out to investigate the formation mechanism of the thymine-thymine (6-4) dimer ((6-4)TT). The DNA backbone was found to have non-negligible effects on the triplet reaction pathway, particularly the reaction steps involving substantial base rotations. The mechanism for the isomerisation from (6-4)TT to its Dewar valence isomer (DewarTT) was also explored, confirming the necessity of absorbing a second photon. In addition, the solvation effects were examined and showed considerable influence on the potential energy surface.

[1] J. S. Taylor, *Acc. Chem. Res.* 27, 76 (1994).

173

## Detecting DNA Damage Using Correlative Synchrotron Infrared Spectroscopy and Super-Resolution Fluorescence Microscopy

Donna Whelan<sup>1</sup> ; Esther Miriklis<sup>None</sup> ; Ashley Rozario<sup>2</sup> ; Toby Bell<sup>3</sup> ; Eli Rothenberg<sup>4</sup><sup>1</sup> *Department of Pharmacy and Applied Science, La Trobe University, Bendigo, Victoria 3552, Australia*

<sup>2</sup> Monash University

<sup>3</sup> School of Chemistry, Monash University, Victoria 3800, Australia

<sup>4</sup> Department of Biochemistry and Molecular Pharmacology

#### Corresponding Author(s):

Single molecule localization microscopy (SMLM) and Synchrotron Fourier transform infrared (S-FTIR) spectroscopy are two techniques capable of elucidating unique and valuable detail and are especially suited for interrogation of biological samples. SMLM provides images of targeted biomolecules at spatial resolutions an order of magnitude better than the diffraction limit [1], whereas S-FTIR objectively measures the holistic biochemistry of a sample revealing variations in overall composition [2]. Previously, we reported the successful correlation of these techniques at the single cell level to investigate the effects of chemical fixation [3].

Here, we use this correlative approach to probe the cellular response to low levels of DNA replicative stress. In this study we analysed S-FTIR spectra of drugged live and fixed cells using multivariate statistics alongside colocalization studies of SMLM super resolution cell images which enabled visualization of the DNA damage sites and their associated repair proteins [4]. The complementary nature of these techniques allowed detection of subtle changes to cellular metabolism as well as chromatin structure. Remarkably, we were able to differentiate undamaged cells from those treated with drug dosages that cannot be detected using conventional imaging and biochemical methods. These studies strikingly demonstrate the potential sensitivity of these combined techniques for characterizing biochemical changes and offers new insights into the complex mechanisms involved in DNA damage and repair.

[1] D.R. Whelan and T.D.M. Bell, *J. Phys. Chem. Letts.* 6, 374 (2015).

D.R. Whelan, et. al. *Analyst* 138, 3891 (2013).

D.R. Whelan and T.D.M. Bell, *ACS Chem. Biol.* 10, 2874 (2015).

D.R. Whelan, et. al. *Nat. Commun.* 9, 3882 (2018).

177

## Molecular mechanisms of lipid transfer by ORP family

Jiang-Qing Dong<sup>1</sup>; Huan Wang<sup>1</sup>; Ximing Du<sup>2</sup>; Qianli Ma<sup>2</sup>; Hongyuan Yang<sup>3</sup>; Jia-Wei Wu<sup>1</sup>

<sup>1</sup> Tsinghua University

<sup>2</sup> the University of New South Wales

<sup>3</sup> the University of New South Wales

**Corresponding Author(s):** jiaweiwu@mail.tsinghua.edu.cn

Cellular compartmentalization into membranous organelles requires precise spatio-temporal distribution of certain lipids and proteins, and the intracellular trafficking of lipids is central to normal cellular homeostasis. Recent studies show that specific non-vesicular lipid transfer pathways play crucial roles in the maintenance of membrane lipid composition. The oxysterol-binding protein (OSBP) and its related proteins (ORP, for OSBP-related protein) have emerged as central regulators of sterol/lipid transport in a nonvesicular manner. OSBP and its homologs are conserved among species from yeast (Osh family) to mammals (ORP family). These proteins all share a conserved ligand-binding domain (ORD, for OSBP-related domain), and many family members possess additional functional domains including a FFAT motif for ER targeting, a PH domain for targeting other membranes and an ANK domain for regulator protein binding. Here we showed in vitro that ORP1 can transport sterols between membranes in the presence of certain phosphoinositides, but can't transport any PIPs backwards. In cells, both ORP1L and PIP2 were required for the efficient removal of cholesterol from LELs. The crystal structures of ORP1-ORD in complex with cholesterol or phosphoinositide revealed similar, yet different, binding modes of two lipids, and strikingly, the ORP1 structures adopt 'open' conformations, distinct from the 'closed' conformations observed in yeast Osh structures. Further biochemical and cell biological analyses demonstrated that phosphoinositide was required for the physiological function of ORP1 by promoting membrane targeting and pushing

the ORD lid open. Thus, our work unveils a distinct mechanism by which PIPs may allosterically enhance OSBP/ORPs-mediated transport of major lipid species such as cholesterol.

77

## Characterisation of Mutations in the Excitatory Amino Acid Transporter SLC1A3 Linked to Episodic Ataxia Type 6 (EA6)

**Author(s):** Qianyi Wu<sup>1</sup>

**Co-author(s):** Jeffrey Setiadi<sup>1</sup>; Serdar Kuyucak<sup>1</sup>; Robert Vandenberg<sup>1</sup>; Renae Ryan<sup>1</sup>

<sup>1</sup> *University of Sydney*

**Corresponding Author(s):** qiwu3835@uni.sydney.edu.au

Glutamate is the predominant excitatory neurotransmitter in the mammalian central nervous system, the extracellular concentration of which has to be tightly regulated to avoid neurotoxicity. This role is carried out by Excitatory Amino Acid Transporters (EAATs). In addition to their primary role of clearing glutamate from the synaptic cleft, the EAATs also possess a thermodynamically uncoupled Cl<sup>-</sup> conductance. Dysfunction of these transporters has been implicated in diseases including episodic ataxia. Episodic ataxias (EA) are a group of rare genetic disorders caused by inherited channelopathies, clinically characterised by progressive, and recurrent episodes of ataxia. EA6 was firstly identified in a child with early onset episodic ataxia with a single point mutation in the gene SLC1A3 that encodes membrane protein EAAT1. It has been demonstrated that a large increase in the Cl<sup>-</sup> channel function of this transporter contributes to the pathology of EA6 [1,2]. Recently, several more mutations in SLC1A3 have been identified in EA6 patients. We have introduced these mutations into the EAAT1 transporter and characterised them using electrophysiology, radiolabelled glutamate uptake, confocal microscopy and molecular dynamics simulation to investigate the effects of these mutations on glutamate transporter activity.

[1] Parinejad N, Peco E, Ferreira T, Stacey SM, & van Meyel DJ (2016). Disruption of an EAAT-mediated chloride channel in a *Drosophila* model of ataxia. *Journal of Neuroscience* 36: 7640-7647.  
 Winter N, Kovermann P, & Fahlke C (2012). A point mutation associated with episodic ataxia 6 increases glutamate transporter anion currents. *Brain* 135: 3416-3425.

69

## NDM-1 with cadmium substitution reveals initiate state of beta-lactam hydrolysis

Yuan Wu<sup>1</sup>

<sup>1</sup> *HKU*

**Corresponding Author(s):** yuanwu1993@hotmail.com

Antibiotic resistant bacterial infections pose an increasing threat to the global public health. New Delhi metallo-beta-lactamase 1 (NDM-1) belonged to metallo-beta-lactamases (MBLs) family which can hydrolyze  $\beta$ -lactam antibiotics is a newly identified enzyme in *Klebsiella pneumoniae* [1]. NDM-1 hydrolyzes and inactivates nearly all the  $\beta$ -lactam-based antibiotics and performs tight binding with penicillin as well as cephalosporins. Rapid spread of NDM-1 among clinically related bacteria becomes a great concern. However, there are no efficient NDM-1 inhibitors applied in clinical therapy due to little known about the catalytic mechanism of this enzyme. Additionally, different metal co-factors in NDM-1 may provide an alternative reaction mechanism to NDM-1 with  $\beta$ -lactamases.

Previous studies have acquired enzymatic product (hydrolyzed ampicillin) and intermediate (partially hydrolyzed ampicillin) in NDM-1-catalyzed ampicillin reaction process [2][3]. However, initial state of the catalytic reaction is unknown. Here we report the X-ray crystal structure of NDM-1 whose zinc ions in the active site are substituted by cadmium ions in complex with an un-hydrolyzed ampicillin at 1.4-Å resolution. This is the first time such initial un-hydrolyzed ampicillin has been captured by X-ray crystallography and provides more mechanistic insights into NDM-1 catalyzed reactions.

[1] Sauvage, E., F. Kerff, M. Terrak, J. A. Ayala and P. Charlier (2008). "The penicillin-binding proteins: structure and role in peptidoglycan biosynthesis." *FEMS Microbiol Rev* 32(2): 234-258.

Zhang, H. and Q. Hao (2011). "Crystal structure of NDM-1 reveals a common beta-lactam hydrolysis mechanism." *FASEB J* 25(8): 2574-2582.

Kim, Y., Cunningham, M. A., Mire, J., Tesar, C., Sacchettini, J., & Joachimiak, A. (2013). NDM-1, the ultimate promiscuous enzyme: substrate recognition and catalytic mechanism. *The FASEB Journal*, 27(5), 1917-1927.

170

## Building biology: a new method for understanding subunit interactions in protein superstructures

Stephanie Xu<sup>1</sup> ; Andrew Tuckwell<sup>1</sup> ; Sophie Hertel<sup>1</sup> ; Chu Wai Liew<sup>1</sup> ; Lawrence Lee<sup>1</sup>

<sup>1</sup> *EMBL Australia Node for Single Molecule Sciences, UNSW, Sydney, Australia.*

**Corresponding Author(s):** stephanie.xu@student.unsw.edu.au

The bacterial Type 3 Secretion System (T3SS) and the HIV-1 viral capsid are two protein systems that have been heavily studied over recent years, due to their central role in the pathogenesis of Gram-negative bacteria species and the human immunodeficiency virus respectively. Many studies have focused on the structure of the systems and their components, in order to understand how they function. However, most approaches centralise on either the individual subunits - where they are able to establish high-resolution models of the proteins but potentially lose biologically relevant information - or the entire superstructure - where they can gain an overview of the system but lose important details at low resolution. Furthermore, the assembly of the individual subunits into the complete structure is inexplicably linked to the function of the system and its parts. But current methods tend to use a top-down approach, preventing the visualisation of this crucial step, and hindering our progress in understanding these biological machines.

Therefore, we have developed a new method which allows us to observe the assembly process of multiple protein subunits and measure the strength of their interactions. This allows us to pull out information about the biological assembly of the whole structure. We have done this by using rationally designed DNA nanostructures as structural scaffolds to template protein subunits for assembly. The reliability and tunability of DNA base-pairing enables us to build precise DNA scaffolds which can orient protein subunits in close proximity to each other, in order to probe for potential weak biologically relevant protein-protein interactions. We can measure them using surface plasmon resonance, providing us with information on the kinetics of the protein interactions. These will then be applied to mathematical models for biological assembly. We can also use our templates as a stabilising unit for further crosslinking studies and generation of discrete substructures for study and imaging.

Not only has our method allowed us to potentially initiate and measure weak biologically relevant interactions, but recent publications have suggested that Nature may also utilise scaffolds to control protein self-assembly. This has already been observed in the assembly of the basal rings of the bacterial flagella motor, and is also suspected to be the case for the tip complex of the Type 3 Secretion System.

181

## Membrane stiffness is a key determinant of EcMscS activity

Feng Xue<sup>1</sup> ; Charles Cox<sup>1</sup> ; Paul Rohde<sup>1</sup> ; Pietro Ridone<sup>1</sup> ; Yoshitaka Nakayama<sup>1</sup> ; Boris Martinac<sup>1</sup><sup>1</sup> victorchang's cardiac research institute

Corresponding Author(s): fexxue@victorchang.edu.au

The E. coli mechanosensitive channel of small conductance (EcMscS) is one of the bacterial membrane tension sensors necessary for osmoregulation. Reconstitution of purified EcMscS into lipid bilayers of known composition shows that its gating is based on the force-from-lipids concept. Here we aim to quantify the effect of lipid composition on tension sensitivity of EcMscS. Using patch fluorometry we have measured the tension sensitivity of EcMscS reconstituted in liposomes containing increasing amounts (0 to 60%) of phosphatidylethanolamine (PE). Our data shows that increasing PE, the major lipid component of E. coli membranes, results in higher tensions being required to open EcMscS, whereas less tension is required in the presence of equivalent amounts of PC. Considering the differences in mechanical properties between PE and PC containing membranes, our data suggests that EcMscS senses membrane stiffness.

46

## Nano-ZnO interface stimulates the insulin fibrillation and cytotoxicity at physiological pH

Kanti Yadav<sup>1</sup> ; suman jha <sup>2</sup><sup>1</sup> National Institute of Technology, Rourkela<sup>2</sup> National Institute of Technology, Rourkela, Odisha

Corresponding Author(s): kantibt@gmail.com

Due to its vast biomedical applications ZnONPs come in contact with various biological molecules including proteins and can modulate their structure and stability, thus implicating their role in accelerating or inhibiting protein fibrillation. The process of aggregation and amyloid formation of proteins is considered as one of the most fundamental cause of the onset of numerous neurodegenerative diseases. Insulin is a well-studied model amyloid protein and is associated with a clinical syndrome, injection-localized amyloidosis which is expected to occur at physiological pH only. Hence, in the present study, we have synthesized spherical ZnONPs (30nm) and performed a systematic investigation on the effect of ZnONP interface induced structural perturbations on the mechanism of fibrillation of insulin, at physiological pH 7.4.

The fibrillation kinetics as monitored by Thioflavin-T (ThT) assay showed a dose-dependent acceleration of fibrillar amyloid growth of insulin with no lag phase in presence of ZnONP interface. From the data derived from CD and ANS fluorescence and other spectroscopic measurements, such increase in fibrillation was observed to be associated with a decrease in  $\alpha$ -helical content, increase in surface hydrophobicity and formation of partially unfolded intermediates. The long lag phase of insulin at pH 7.4 observed can be attributed to the presence of oligomeric (hexamer/trimer/dimer) units which in the presence of ZnONP interface, got dissociated into monomer and caused the formation of nuclei necessary for the induction of amyloidosis. TEM analysis observed a large network of long fibrils (10-14nm diameter) in presence of ZnONP interface, indicating a loosely packed  $\beta$ -sheet structure in insulin fibrils formed at pH7.4. Such fibrils formed in the presence of ZnONP showed profound cellular toxicity as compared to the insulin in absence of ZnONP interface. Overall; our work throws a light on the potential for ZnONPs interface to accelerate protein fibrillation and may lead to the better understanding of utilization of ZnONPs in therapeutics and other medical applications.

118

## The (6-4) Photolyase Reaction ~Role of the Important Residues in Active Center~

**Author(s):** Daichi Yamada<sup>1</sup>

**Co-author(s):** Hisham M. Dokainish<sup>2</sup>; Junpei Yamamoto<sup>3</sup>; Tatsuya Iwata<sup>4</sup>; Elizabeth D. Getzoff<sup>5</sup>; Akio Kitao<sup>6</sup>; Hideki Kandori<sup>7</sup>

<sup>1</sup> Nagoya Institute of Technology

<sup>2</sup> RIKEN

<sup>3</sup> Osaka Univ.

<sup>4</sup> Toho Univ.

<sup>5</sup> Scripps Res. Inst.

<sup>6</sup> Tokyo Inst. Tech.

<sup>7</sup> Nagoya Inst. Tech.

**Corresponding Author(s):** yamada.daichi@nitech.ac.jp

(6-4) photolyases ((6-4) PHRs) are DNA repair flavoenzymes that specifically revert UV-induced photoproducts, (6-4) photoproducts ((6-4) PPs), into normal bases to maintain genetic integrity. (6-4) PHRs repair (6-4) PPs by electron transfer from fully reduced form of flavin adenine dinucleotide chromophore in a light dependent manner. So far, (6-4) PP repair mechanism of (6-4) PHRs have been studied [1], and His354 residue in the active center has been regarded as the most important function (Figure). However, we reported that (6-4) PP can be repaired by another His (H358), even if His354 is mutated to Ala [2,3]. Recently we proposed a new (6-4) PP repair mechanism with the important role of Lys in the active center, based on the quantum chemical/molecular mechanical calculation [3].

In this study, to investigate the role of the Lys residue (Figure) experimentally, we performed Fourier transform infrared (FTIR) spectroscopy and molecular dynamics (MD) simulation for the Lys mutants. As results of FTIR measurement, (6-4) PP repair signal was not observed for K236A and K236H, indicating complete loss of the DNA repair ability. In addition, K236R and K236Q retained the function of (6-4) PP repair, though the (6-4) PP repair efficiency was decreased from WT. We then performed MD simulation of each mutant, which showed that the hydrogen bonding networks of the active center differ between the mutants with and without (6-4) PP repair activity. These results implicate that Lys at the active center stabilizes the hydrogen bonding network including the position of His354, which is necessary for the (6-4) PP repair. From these experimental and theoretical observations, we will discuss the role of Lys reaction model in the (6-4) PHR.

[1] J. Yamamoto, et al., *Photochem. Photobiol.* 93, 51 (2017).

D. Yamada, et al., *Biophys. Physicobiol.* 22, 139 (2015).

H. M. Dokainish, et al., *ACS Catal.* 7, 4835 (2017).

157

## Single particle analysis for membrane fusion of liposomes

Masato Yamada<sup>1</sup>; Kazuhiro Abe<sup>2</sup>; Naoki Soga<sup>1</sup>; Hiroyuki Noji<sup>1</sup>; Rikiya Watanabe<sup>3</sup>

<sup>1</sup> The University of Tokyo

<sup>2</sup> Nagoya University

<sup>3</sup> Molecular physiology laboratory RIKEN

**Corresponding Author(s):** yamada.m17@nojilab.t.u-tokyo.ac.jp

Membrane vesicles mediate various physiological functions upon fusion with biological membranes. Despite the physiological importance, biophysical features of membrane fusion remain elusive due to the technical difficulties to quantitatively measure fusion events in high throughput manner. To



address this issue, we here attempted to elucidate various biophysical features of membrane fusion by developing a novel microsystem, enabling single particle analysis of membrane fusion in quantitative manner.

The fusion events were visualized by using micro-chamber array sealed with bio-membrane. In this setup, fluorescent lipids are provided into a membrane on chamber upon the fusion of fluorescent liposome [Fig. 1a], and therefore, single fusion event is detectable as a stepwise fluorescent increase on chamber [Fig. 1b].

Then, we measured the fusion efficiency by counting the number of chambers with membrane fusion. As shown in Fig. 2, the efficiency was extremely low ( $\approx 0.1\%$ ) without any additives and increased more than 30-folds by fusion promoters, i.e.,  $\text{Ca}^{2+}$  and PEG, as expected from previous studies. Interestingly, the efficiency was decreased 8-folds by FoF1, a membrane protein with large hydrophilic domains. This result suggested that steric hindrance of membrane proteins would hamper membrane fusion.

In this study, we succeeded in developing a novel microsystem to visualize membrane fusion at single particle level, and moreover, quantitatively evaluating the effect of fusion promoter and inhibitor on membrane fusion. For further understating, we would like to measure the membrane fusion events in more physiological conditions.

54

## Development of isothermal-isobaric replica-permutation method and its application to the $\beta$ -hairpin mini protein

**Author(s):** Masataka Yamauchi<sup>1</sup>

**Co-author(s):** Hisashi Okumura<sup>2</sup>

<sup>1</sup> SOKENDAI, ExCELLS, IMS

<sup>2</sup> ExCELLS, IMS, SOKENDAI

**Corresponding Author(s):** yamauchi@ims.ac.jp

We developed a two-dimensional replica-permutation molecular dynamics method in the isothermal-isobaric ensemble [1]. The replica-permutation method [2] is a improved alternative to the replica-exchange method. It was originally developed in the canonical ensemble. This method employs the Suwa-Todo algorithm [3], instead of the Metropolis algorithm, to perform permutations of temperatures and pressures so that the rejection ratio can be minimized. The isothermal-isobaric replica-permutation method performs better sampling efficiency than the isothermal-isobaric replica-exchange method [4, 5, 6].

We applied this method to a  $\beta$ -hairpin mini protein, chignolin. Chignolin is an artificially designed peptide consist of ten amino-acid residues (1GYDPETGTWG10) and has unique folded and misfolded structures. In our simulation, not only the folding event but also the misfolding event were observed. We calculated the temperature and pressure dependence of the fraction on the folded, misfolded, and unfolded states. Thermodynamic quantities such as differences in partial molar enthalpy, partial molar volume, and heat capacity were also determined and in good agreement with experimental data.

We also found unusual behavior that the misfolded chignolin becomes more stable under high pressure conditions while the folded chignolin is denatured. We revealed the mechanism of the stability as follows: In the folded state, the hydrogen bond that form  $\beta$ -hairpin structure is exposed to the solvent. As the pressure increase, water molecules approach the hydrogen bond and break the hydrogen bond. Thus, the folded chignolin changes to the unfolded state. On the other hand, the hydrogen bonds that form a  $\beta$ -hairpin structure in the misfolded state are covered with Tyr2 and Trp9 side chains and protected. Thus, the hydrogen bonds do not break even when the water molecules approach the chignolin in the high-pressure conditions.

References:

- M. Yamauchi and H. Okumura, *J. Chem. Phys.* 147 (2017) 184107.  
 S. G. Itoh and H. Okumura, *J. Chem. Theory Comput.* 9 (2013) 570.  
 H. Suwa and S. Todo, *Phys. Rev. Lett.* 105 (2010) 12060.  
 K. Hukushima and K. Nemoto, *J. Phys. Soc. Jpn.* 65 (1999) 1604.  
 Y. Sugita and Y. Okamoto, *Chem. Phys. Lett.* 314 (1999) 141.  
 T. Okabe, M. Kawata, Y. Okamoto and M. Mikami, *Chem. Phys. Lett.* 335 (2001) 435.

35

## Single GUV Studies on Mode of Action of Antimicrobial Peptides and Cell-Penetrating Peptides

**Author(s):** Masahito Yamazaki<sup>1</sup>

**Co-author(s):** Moynul Hasan<sup>1</sup>; Md. Zahidul Islam<sup>1</sup>

<sup>1</sup> *Shizuoka University*

**Corresponding Author(s):** yamazaki.masahito@shizuoka.ac.jp

For antimicrobial peptides (AMPs) with bactericidal activity and cell-penetrating peptides (CPPs) with activity of translocation across plasma membranes, their interactions with lipid bilayers play important roles in these functions. However, the elementary processes and mechanisms of the functions of AMPs and CPPs have not been clearly revealed. We have recently developed the single giant unilamellar vesicle (GUV) method for investigation on the interaction of peptides/proteins with lipid bilayers [1,2]. In this method, changes in physical quantities of a single GUV that are induced by interactions with peptides/proteins are observed as a function of time and spatial coordinates. The same experiments are then carried out using many “single GUVs” and their results of the changes in the physical quantities of single GUVs are statistically analyzed over many “single GUVs”. Thereby, the single GUV method can reveal the details of elementary processes of individual events, and allow calculation of their kinetic constants. Here, we show new information on the mode of action of AMPs such as magainin 2 and CPPs such as transportan 10 (TP10), revealed by the single GUV methods.

Our recent results indicate that the binding of magainin 2 to the outer leaflet of a GUV increases the area of the GUV bilayer, a change that strongly correlates with the rate constant of magainin 2-induced pore formation,  $k_p$ . Moreover, an increase in the tension on a GUV membrane (e.g., by imposition of an external force) also increases the  $k_p$ . These results indicate that a magainin 2-induced pore is a stretch-activated pore [3]. Recently, we have developed a method to prepare GUVs with transbilayer asymmetric lipid packing [4]. Using these GUVs, we found that the  $k_p$  decreased with increasing in lipid packing of the inner leaflet, which indicates the role of stretching of inner leaflet in the magainin 2-induced pore formation.

Using the single GUV method for CPPs, we can obtain the relationship between the entry of CPPs into GUV lumen and pore formation, the rate of the entry of the CPPs into GUV lumen, and the time course of CPP concentration in the GUV membrane [5]. The application of mechanical tension by an external force on the lipid bilayers increased the rate of entry of CF-TP10 into the GUVs without pore formation [6]. High concentration of cholesterol suppressed the translocation of CF-TP10 from the outer to the inner leaflet [6]. These results suggest that transient pre-pores in lipid bilayers formed by their thermal fluctuations play an important role in the translocation of CF-TP10 from the outer to the inner leaflet [6].

- [1] M.Z. Islam, M. Yamazaki, et al. *Phys. Chem. Chem. Phys. (Perspective)* 16, 15752 (2014)  
 M. Hasan, and M. Yamazaki, *Antimicrobial Peptides; Basics for Clinical Application* (Springer, 2018), in press.  
 M.A.S. Karal, J.M. Alam, T. Takahashi, M. Yamazaki, et al. *Langmuir* 31, 3391 (2015).  
 M. Hasan, M.A.S. Karal, V. Levadnyy, M. Yamazaki, et al. *Langmuir* 34, 3349 (2018).

M.Z. Islam, M. Yamazaki, et al. *Appl. Microbiol. Biotechnol.* (Mini-review) 102, 3879 (2018).

M.Z. Islam, S. Sharmin, V. Levadnyy, M. Yamazaki, et al. *Langmuir* 33, 2433 (2017).

37

## Thermotropic Phase Transition Behavior and Structural Properties of Partially Fluorinated Dipalmitoylphosphatidylcholine Bilayer

**Author(s):** Tamami Yanagi<sup>1</sup>

**Co-author(s):** Hiroshi Takahashi<sup>1</sup>; Toshiyuki Takagi<sup>2</sup>; Hideki Amii<sup>1</sup>; Toshinori Motegi<sup>1</sup>; Takeshi Hasegawa<sup>3</sup>; Toshiyuki Kanamori<sup>2</sup>; Masashi Sonoyama<sup>1</sup>

<sup>1</sup> *Gunma University*

<sup>2</sup> *AIST*

<sup>3</sup> *Kyoto University*

**Corresponding Author(s):** t13301154@gunma-u.ac.jp

Perfluoroalkyl (Rf, CnF2n+1) compounds show unique properties, such as water/oil repellency, high melting point and low electric permittivity. In this study, thermotropic behavior and structural properties of Rf-containing dipalmitoylphosphatidylcholine (Fn-DPPC; n = 4, 6 and 8; Fig. 1) hydrated bilayers were investigated by differential scanning calorimetry (DSC) and X-ray diffraction to clarify effects of Rf groups on membrane properties of Fn-DPPC.

In DSC thermograms of Fn-DPPC suspensions, endothermic peaks appeared at 24.1 °C, 37.5 °C and 69.9 °C for n = 4, 6 and 8, respectively. Judging from temperature-dependent changes in wide-angle X-ray diffraction (WAXD) patterns, the endothermic peaks are attributable to the gel to liquid-crystalline phase transition. WAXD peaks appeared at  $Q = 12.63$  and  $13.73$  nm<sup>-1</sup> for F4-DPPC at 15 °C. These corresponding spacings (d) are 0.50 and 0.46 nm, respectively, being larger than DPPC. Owing to the difference of molecular area between ordered hydrocarbon chains and Rf chains, F4-DPPC would form loosed-packed gel phase as compared with DPPC, which leads to the marked drop in the phase transition temperature (Tm) of F4-DPPC compared to DPPC. In F6-DPPC, sharp WAXD peaks appeared at  $Q = 12.98$  nm<sup>-1</sup> (d = 0.48 nm) and  $13.76$  nm<sup>-1</sup> (d = 0.46 nm) at 25 °C, showing that the chain packing density of F6-DPPC is higher than F4-DPPC. A single sharp WAXD peak of F8-DPPC observed at  $Q = 12.93$  nm<sup>-1</sup> (d = 0.49 nm) at 30 °C indicates hexagonal chain packing with much higher density than others. The most plausible origin of the higher chain packing density of F8-DPPC is the combination of the Rf-specific helical conformation and the dipole-dipole interaction cooperativity proposed as the stratified dipole arrays (SDA) theory [1,2]. The stabilizing effect in F8-DPPC bilayer due to the SDA of Rf groups is suggested by the significant rise in Tm of F8-DPPC compared to others.

One-dimensional electron density profiles of Fn-DPPC were calculated from small-angle X-ray diffraction (SAXD) data. In F4-DPPC, the profiles of the Rf moiety as well as the hydrocarbon segment changed dramatically in association with the phase transition, indicating the phase-transition-induced melting of the overall acyl chain. In contrast, little electron density profiles of the Rf moiety of F6-DPPC and F8-DPPC changed in spite that the phase transition occurred. It is likely that the conformations of Rf groups of F6-DPPC and F8-DPPC even in the liquid-crystalline phase are restricted.

[1] T. Hasegawa et al., *ChemPlusChem* 79, 1421 (2014).

T. Hasegawa, *Chem. Rec.* 17, 903 (2017).

## Nanosystems for Food, Drug and Biomedical Applications

Jackie Ying<sup>None</sup>

### Corresponding Author(s):

Nanotechnology allows for the unique design and functionalization of materials and devices at the nanometer scale for a variety of applications. Our laboratory has fabricated nanosystems for drug screening, in vitro toxicology, sample preparation, diagnostic, and food pathogen detection. The miniaturized devices allow for the rapid and automated processing of drug candidates, clinical and food samples in tiny volumes, greatly facilitating drug testing, genotyping assays, infectious disease detection, cancer diagnosis, point-of-care monitoring, and food testing.

For example, we have designed plasmonic nanocrystals for single nucleotide polymorphism (SNP) genotyping. The platform involves polymerase chain reaction (PCR) for target sequence amplification and colorimetric detection with nanoprobe for pharmacogenomics applications. We have also established polymer-based lab-on-a-cartridge for automated sample preparation and PCR detection. The integrated all-in-one system, termed MicroKit, allows for the rapid and accurate typing and subtyping of influenza and other viral infections within 2 hours. We have further developed sophisticated lab-on-a-chip system that enables us to achieve multiplexed detection of drug-resistant bacteria and food pathogens.

We have created the silicon-based Microsieve system for the rapid and selective isolation of circulating tumor cells (CTCs) from peripheral blood. This non-invasive, near real-time, inexpensive liquid biopsy approach allows for the enumeration and biomarker analysis of CTCs for cancer diagnosis, prognosis and monitoring. We have also established paper-based assays for the rapid detection of various diseases, such as Dengue, Zika, hepatitis and sexually transmitted diseases. In addition, these inexpensive test kits can be used for food pathogen detection and meat speciation.

144

## Structural insights into mitochondrial DNA maintenance by nucleases

Hanna S. Yuan<sup>1</sup>

<sup>1</sup> *Academia Sinica*

**Corresponding Author(s):** mbyuan@gate.sinica.edu.tw

Mitochondria are important organelles providing cellular energy in the form of ATP through oxidative phosphorylation. Defects in mitochondrial DNA (mtDNA) replication and maintenance, including mutations in the nuclear genes that affect the stability of mtDNA, are thus linked to a wide spectrum of mitochondrial disorder and diseases. Two nuclear-encoded mitochondrial nucleases, EndoG and ExoG, play crucial roles in accurate processing, maintenance and replication of mtDNA. Our crystal structures of EndoG in complex with DNA provide the molecular basis of how EndoG binds and cleaves DNA as a dimeric endonuclease and why its dimeric conformation is disrupted and its activity is diminished under oxidative stress in mitochondria. On the other hand, ExoG is a 5'-3' exonuclease that prefers to remove RNA dinucleotide in RNA-DNA chimeric duplexes and processes the 5' end of the nascent DNA strands during mtDNA replication. We suggest that ExoG participates in the RNA primer removal process during mitochondrial DNA replication to maintain mitochondrial genome integrity. As depletion of these two nucleases are linked to mitochondria dysfunction and high levels of ROS, modulation of the dimer conformation and nuclease activity of EndoG and ExoG could present an avenue for improving mitochondrial functions under oxidative stresses.

182

## Evolutionary and Taxonomic Analyses of Luciferases, Photoproteins and Luciferins

**Author(s):** Kei Yura<sup>1</sup>

**Co-author(s):** Misato Funahashi<sup>1</sup>

<sup>1</sup> *Ochanomizu University*

**Corresponding Author(s):** yura.kei@ocha.ac.jp

Light emitting organisms have attracted great attention. Based on literature search, organisms in 117 different families which belong to 12 different phyla have been known to emit light. These organisms are luminous and are not fluorescent, hence have an organ for light generation. In the organ, a chemical reaction, taken place on a small molecule called luciferin, is catalysed by an enzyme named luciferase or photoprotein. The chemical reactions catalysed by either luciferase or photoprotein is considered to be different. The amino acid sequences and protein structures of luciferases and photoproteins from different organisms are mostly different, so that luminescent mechanisms should evolved independently. The idea of independent and convergent evolution of the luciferase and photoprotein is further supported by the scattered distribution of light emitting species over the phylogenetic tree of life.

After establishing the idea of independent evolution of luciferases and photoproteins, bioinformatics method has been improved and many luminous organisms have been discovered. We, therefore, have started collecting data of luminous organisms, including species, habitats, organelles, proteins, ligands and chemical reactions, and revisiting the evolution of luminescent systems in organisms. Out of 117 families, the habitat of 103 families (88%) were found in ocean, of 13 families were on land (11%) and of only one family was in freshwater (1%). The dominance of marine organisms turned out apparent. The light emitting mechanism of each organism can be divided into two. One is by utilising proteins encoded in its own genome, and the other is by the proteins encoded in the genome of symbiotic bacterium. The proteins can be classified into ten groups, based on their sequence similarity, hence they were not derived from a complete independent evolution. Luciferin, the light emitting ligand, can be classified into nine groups, based on their backbone structures. No systematic combination of luciferin and luciferase was found. The cases, such as the same luciferins bind to evolutionary different luciferases in different organisms and the evolutionary related luciferases bind different luciferins, were found. The intriguing independent evolution was found in the luciferases of the marine organisms. Different organisms used the protein derived from a common ancestor as an enzyme for the same catalytic reaction with completely different residues involved. Molecular phylogeny of the proteins apparently showed that the evolution of the enzymes was separated by non-luminous proteins, indicating that they have evolved independently and invented different catalytic mechanisms. We also found that the evolutionary unrelated proteins used the similar local structure to catalyse the chemical reaction of luciferin in different organisms. These data are in the process of compilation and are going to be on a web database. The database will be used for evolutionary analyses as well as a platform for the modification of luciferase/photoprotein for a marker material of wetlab experiments.

36

## Using cryo-electron microscopy maps for X-ray structure determination

**Author(s):** Lingxiao Zeng<sup>None</sup>

**Co-author(s):** Wei Ding ; Quan Hao

**Corresponding Author(s):** zenglingxiao@gmail.com

X-ray crystallography and cryo-electron microscopy (cryo-EM) are complementary techniques for structure determination. Crystallography usually reveals more detailed information, while cryo-EM is an extremely useful technique for studying large-sized macromolecules. As the gap between the resolution of crystallography and cryo-EM data narrows, the cryo-EM map of a macromolecule could

serve as an initial model to solve the phase problem of crystal diffraction for high-resolution structure determination. FSEARCH is a procedure to utilize the low-resolution molecular shape for crystallographic phasing [1]. The IPCAS (Iterative Protein Crystal structure Automatic Solution) pipeline is an automatic direct-methods-aided dual-space iterative phasing and model-building procedure [2]. When only an electron-density map is available as the starting point, IPCAS is capable of generating a completed model from the phases of the input map automatically, without the requirement of an initial model. In this study, a hybrid method integrating X-ray crystallography with cryo-EM to help with structure determination is presented. With a cryo-EM map as the starting point, the workflow of the method involves three steps. (a) Cryo-EM map replacement: FSEARCH is utilized to find the correct translation and orientation of the cryo-EM map in the crystallographic unit cell and generates the initial low-resolution map. (b) Phase extension: the phases calculated from the correctly placed cryo-EM map are extended to high-resolution X-ray data by non-crystallographic symmetry averaging with phenix.resolve. (c) Model building: IPCAS is used to generate an initial model using the phase-extended map and perform model completion by iteration. Four cases (the lowest cryo-EM map resolution being 6.9 Å) have been tested for the general applicability of the hybrid method, and almost complete models have been generated for all test cases with reasonable R<sub>work</sub>/R<sub>free</sub>. The hybrid method therefore provides an automated tool for X-ray structure determination using a cryo-EM map as the starting point.

[1] Q. Hao, Acta Cryst. D62, 909 (2006).

T. Zhang, L.J. Wu, Y.X. Gu, C.D. Zheng and H.F. Fan, Chin. Phys. B, 19, 096101 (2010).

122

## In Vivo Immuno-Optical Imaging the Behaviour and Function of Immunocytes in the Complex Microenvironment

Zhihong Zhang<sup>None</sup>; Fei Yang<sup>None</sup>; Deqiang Deng<sup>None</sup>; Xiang Yu<sup>None</sup>; Qiaoya Lin<sup>None</sup>; Qingming Luo<sup>None</sup>

**Corresponding Author(s):** cyyzzh@mail.hust.edu.cn

Immune system provides defense, surveillance and self-stabilizing functions for lives, the major challenge for researchers is to consider immune system as a system to investigate. Optical imaging is the most promising tools for investigating the function and motility of multiple immune cells in the complex physiological and pathological microenvironment [1]. The combination of optical imaging with high spatio-temporal resolution (e.g., multi-photon excitation microscopy and photoacoustic tomography) and in vivo labelling methods (e.g., fluorescent proteins, NIR dye, nanocarrier) have shown great charm on the visualization of immune system, which immuno-optical imaging becomes as a new interdisciplinary research area. Here, I would like to share our recent works on immune-optical imaging. First, we developed a fluorescent antigen model system based on a tetrameric far-red fluorescent protein (tFRFP). The visualization results by intravital microscopy clearly show that strong and specific immune response against tFRFP-expressing B16 melanoma (tFRFP-B16) cells is occurred in the tFRFP-immunized mice after the implantation of tFRFP-B16 cells [2]. Second, in vivo photoacoustic (PA) and fluorescence imaging reveal the strategic arrangement of KCs in liver. The 3D structure information of hepatic sinusoids and crisscrossing arrayed hepatic lobules were clearly reconstructed according to the PA signal of hemoglobin. Dual wavelength-PA imaging showed that the PA signal of KCs was located in red area contrasted by PA signal of hemoglobin. 3D images visually displayed that the KCs were inclined to distribute at the portal triad area rather than at central vein area of hepatic lobules. Third, we establish an approach to specifically target and modulate liver sinusoidal endothelial cells (LSECs) in vivo. Intravital imaging showed that LSECs fluoresced within 20 s after intravenous injection of peptide-lipid nanoparticles (X-NPs). Our research demonstrates that breaking LSEC-mediated immunologic tolerance successful control liver metastasis through the immune modulation of LSECs.

[1] Shuhong Qi, Hui Li, Lisen Lu, Zhongyang Qi, Lei Liu, Lu Chen, Guanxin Shen, Ling Fu, Qingming Luo, *Zhihong Zhang*. Long-term intravital imaging of the multicolor-coded tumor microenvironment during combination immunotherapy. *eLife*, 5: e14756 (2016)

Fei Yang, Shun Liu, Xiuli Liu, Lei Liu, Meijie Luo, Shuhong Qi, Guoqiang Xu, Sha Qiao, Xiaohua Lv, Xiangning Li, Ling Fu, Qingming Luo, *Zhihong Zhang*. In Vivo Visualization of Tumor

Antigen-containing Microparticles Generated in Fluorescent-protein-elicited Immunity. *Theranostics*. 6(9):1453-1466 (2016)

8

## Castration modulates electrophysiological properties of HVC neurons in adult male zebra finches

Dongfeng LI<sup>None</sup> ; Wenli ZHOU<sup>None</sup>

### Corresponding Author(s):

The nucleus HVC (high vocal center) within the avian motor cortex is the initial part of two song control pathways, which are vocal motor and anterior forebrain pathway. HVC also receive the feedback of the auditory signal. Androgens (testosterone) play an important role in control birdsong. Castration can decrease levels of plasma testosterone and change song stability. In this study, we investigated the effect of castration on electrophysiological properties of neurons in the HVC of adult male zebra finches. The bird was castrated and HVC neurons were electrophysiological recorded using patch clamp recording. We found that membrane time constants, and input resistance of HVC projection neurons (HVCRA and HVCX) in the castration group were lower than those of the control group. Afterhyperpolarization(AHP) time to peak and amplitude of action potential was prolonged after castration. These findings suggest that castration decreases excitability of HVC projection neurons and song stability in male zebra finches.

In conclusion, androgen can enhance the excitability of HVC projection neurons. Androgens can activate the VMP pathway and inhibit the AFP pathway to maintain the stability of the song.

30

## G-quadruplex Structures Formed by Human Telomeric DNA and C9orf72 Hexanucleotide Repeats

Author(s): Guang Zhu<sup>1</sup>

Co-author(s): changdong Liu<sup>2</sup>

<sup>1</sup> Division of Life Science, The Hong Kong University of Science and Technology

<sup>2</sup> Division of Life Science, The Hong Kong University of Science and Technology,

Corresponding Author(s): gzhu@ust.hk

G-quadruplex, a tetra-helical structure formed by guanine-rich sequence, is a non-canonical structure of nucleic acids consisting of stacked G-tetrad planes connected by Hoogsteen hydrogen bonds and stabilized by monovalent cations such as Na<sup>+</sup> and K<sup>+</sup>. Guanine tracts of human telomeric DNA sequences are known to fold into eight different four-stranded G-quadruplexes that vary by the conformation of guanine nucleotides arranged in the stack of G-tetrads in their core and by different kind and order of connecting loops. Here, we present a novel G-quadruplex fold formed in K<sup>+</sup> solution by a human telomeric variant d[(GGGTTA)<sub>2</sub>GGGTTGGG], htel21T18. This variant DNA is located in subtelomeric regions of human chromosomes 8, 11, 17, and 19 as well as in the DNase hypersensitive region and in subcentromeric region of chromosome 5. Interestingly, htel21T18 forms a three-layer chair-type G-quadruplex with two loops interacting through reverse Watson-Crick A6•T18 base pair. The loops are edgewise; glycosidic conformation of guanines is syn•anti•syn•anti around each tetrad, and each strand of the core has two antiparallel adjacent strands [1].

In addition, the large expansion of human GGGGCC (G4C2) repeats of the C9orf72 gene have been found to lead to the pathogenesis of devastating neurological diseases, amyotrophic lateral sclerosis (ALS) and frontotemporal dementia (FTD). The structural polymorphisms of C9orf72 HRE DNA and RNA may cause aberrant transcription and contribute to the development of ALS and FTD. Here we

showed that the two-repeat G4C2 DNA, d(G4C2)<sub>2</sub>, simultaneously formed parallel and antiparallel G-quadruplex conformations in the potassium solution. We separated different folds of d(G4C2)<sub>2</sub> by anion exchange chromatography, followed with characterizations by circular dichroism and nuclear magnetic resonance spectroscopy. The parallel d(G4C2)<sub>2</sub> G-quadruplex folded as a symmetric tetramer, while the antiparallel d(G4C2)<sub>2</sub> adopted the topology of an asymmetric dimer. These folds are distinct from the antiparallel chair-type conformation we previously identified for the d(G4C2)<sub>4</sub> G-quadruplex. Our findings have demonstrated the conformational heterogeneity of the C9orf72 HRE DNA, and provided new insights into the d(G4C2)<sub>n</sub> folding. [2,3].

Our results described above expand the repertoire of known G-quadruplex folding topologies and may provide potential targets for structure-based anticancer and anti-ALS/FTD drug design. These works were supported by GRF (16103714, 16104315, and 16103717), VPRGO17SC07PG, 1419-281-0091-41000 and AoE/M-403-16.

[1] CD. Liu, et al, Chemical Science, (2018) accepted

B. Zhou, et al, Sci. Rep. 8:2366(2018)

B. Zhou, et al, Sci. Rep. 5:16673(2015)

40

## DNP-NMR studies of the antimicrobial peptide maculatin in bacteria

**Author(s):** Shiyong Zhu<sup>1</sup>

**Co-author(s):** Frances Separovic<sup>1</sup>; Marc Antoine Sani<sup>1</sup>

<sup>1</sup> *University of Melbourne*

**Corresponding Author(s):** shiyongz2@student.unimelb.edu.au

Maculatin 1.1 (Mac1) is a 21 residue antimicrobial peptide (AMP) isolated from the skin glands of the Australian tree frog *Litoria genimaculata* with low micromolar activity against Gram-positive bacteria. The cationic peptide is membrane-active and adopts an  $\alpha$ -helical conformation in model membrane environments<sup>1</sup>. In an attempt to further understand the mode of action of Mac1 in intact bacteria, we designed mono-radical and bi-radical spin labelled peptides, TOAC-MacW and TOAC-TOAC-MacW, to allow implementation of in-cell dynamic nuclear polarization (DNP) solid-state NMR experiments. In comparison to the glycerol-protected hydrophilic radical sources used for DNP to date, our radical-tagged peptide approach serves the purpose to anchor the free-electron source within the lipid membrane of bacteria and thereby increase signal enhancement and decrease the background signal. Circular dichroism and solution NMR spectroscopy revealed that the spin-labelled peptides kept a helical conformation in the presence of lipid environments. Finally, an expression method was designed to obtain Mac1 in good yield and with the potential for C-amidation, to facilitate a series of isotopic enrichment schemes. Significant <sup>13</sup>C and <sup>15</sup>N DNP-NMR signal enhancement was obtained in model membranes and live bacteria, with the biradical performing better than the single radical label. Preliminary structural in-cell DNP-NMR results show that Mac1 retained a helical structure and is unlikely to self-assemble in an anti-parallel fashion in bacterial membranes.

[1] M.-A Sani, F. Separovic, Acc. Chem. Res. 49, 1130-1138 (2016).

6

## Rational improvement of gp41-targeting HIV-1 fusion inhibitors

Yun Zhu<sup>1</sup>



<sup>1</sup> *IBP,CAS***Corresponding Author(s):** zhuyun@moon.ibp.ac.cn

Peptides derived from the C-terminal heptad repeat (CHR) of HIV gp41 have been developed as effective fusion inhibitors against HIV-1, but facing the challenges of enhancing potency and stability. Here, we report a rationally designed novel HIV-1 fusion inhibitor derived from CHR-derived peptide (Trp628~Gln653, named CP), but with an innovative Ile-Asp-Leu tail (IDL) that dramatically increased the inhibitory activity by up to 100 folds. We also determined the crystal structures of artificial fusion peptides N36- and N43-L6-CP-IDL. Although the overall structures of both fusion peptides share the canonical six-helix bundle (6-HB) configuration, their IDL tails adopt two different conformations: a one-turn helix with the N36, and a hook-like structure with the longer N43. Structural comparison showed that the hook-like IDL tail possesses a larger interaction interface with NHR than the helical one. Further molecular dynamics simulations of the two 6-HBs and isolated CP-IDL peptides suggested that hook-like form of IDL tail can be stabilized by its binding to NHR trimer. Therefore, CP-IDL has potential for further development as a new HIV fusion inhibitor, and this strategy could be widely used in developing artificial fusion inhibitors against HIV and other enveloped viruses.

[1] Zhu Y, Su S, Qin L, Wang Q, Shi L, Ma Z, Tang J, Jiang S, Lu L, Ye S, Zhang R. 2016. *Sci Rep* 6:31983.

Su S, Zhu Y, Ye S, Qi Q, Xia S, Ma Z, Yu F, Wang Q, Zhang R, Jiang S, Lu L. 2017. *J Virol* 91.